Dynamic aalysis of a small weaving loom

Gülen, Serdar

Dynamic Analysis of a Small Weaving Loom

by

Serdar Gülen B.Sc.

Thesis submitted for the degree of Master of Science in the University of Durham.

August, 1976

ABSTRACT

The project deals with an investigation to determine experimentally the axial and bending strains (normal to the plane of the mechanism) in the two connecting rods of the weaving mechanism of a small textile loom. A complete theoretical, kinematic, force and stress analysis has been made on the six-bar chain constituting the mechanism. The peak to peak strain values have been measured at various different crank speeds. The nature of the bending strains in a direction normal to the plane of the mechanism have been further examined by static tests which have been performed on the mechanism. Measured dynamic strain data for the connecting rods is presented and comparison is made between calculated and measured values. Experimental results for axial peak to peak and cyclic strain variation showed good agreement with the calculated values.

ACKNOWLEDGMENTS

I wish to express my sincere gratitude to Professor G.R. Higginson and Dr. P.A.T. Gill for their guidance, advice and continuous encouragement during the preparation of this work.

I would also like to express my thanks to Mr. T. Sweeting for his constant help during the experimental stage of the project and to Miss J. Campbell for typing this thesis.

I am indebted to my parents for providing me with financial support.

CONTENTS

List of Figures, Tables and Plates

Nomenclature

ψ = psi	crank angle in degrees - in a direction counterclockwise from the horizontal
β = Beta	angle in degrees between link 3 and the horizontal, in a counterclockwise direction from the horizontal
γ = gama	angle in degrees between the side O_2C of the rigid triangular link 4 and the horizontal in a direction counterclockwise from the horizontal
$x\lambda$ = xlamb	angle in degrees between link 5 and the horizontal in a direction counterclockwise from the horizontal
upa	angle in degrees between link 6 and the horizontal in a direction clockwise from the horizontal
A_A^t = AAT	Tangential acceleration component of A-m/s^2
A_A^r = AAR	Radial acceleration component of A-m/s^2
A_B^t = ABT	Tangential acceleration component of B-m/s^2
A_B^r = ABR	Radial acceleration component of B-m/s^2
A_{BA}^t = ABAT	Tangential acceleration component of B with respect to A-m/s^2
A_{BA}^r = ABAR	Radial acceleration component of B with respect to A-m/s^2
A_D^r = ADR	Radial acceleration component of D-m/s^2
A_D^t = ADT	Tangential acceleration component of D-m/s^2
A_{DC}^r = ADCR	Radial acceleration component of D with respect to C-m/s^2
A_{DC}^t = ADCT	Tangential acceleration component of D with respect to C-m/s^2
α_2	Angular acceleration of link 2 - rad/s^2
α_3 = ANGC3	Angular acceleration of link 3 - rad/s^2
α_4 = ANGC4	Angular acceleration of link 4 - rad/s^2
α_5 = ANGC5	Angular acceleration of link 5 - rad/s^2
α_6 = ANGC6	Angular acceleration of link 6 - rad/s^2

V_A	velocity of A-m/s^2
V_B = VB	velocity of B-m/s
V_{BA} = VBA	velocity of B with respect to A-m/s
V_D = VD	velocity of D-m/s
V_{DC} = VDC	velocity of D with respect to C-m/s
ω_2 = OMEGA2	angular velocity of link 2-rad/s
ω_3 = OMEGA3	angular velocity of link 3-rad/s
ω_4 = OMEGA4	angular velocity of rigid triangular link 4-rad/s
ω_5 = OMEGA5	angular velocity of link 5-rad/s
ω_6 = OMEGA6	angular velocity of link 6-rad/s
I_n	Mass moment of inertia of the corresponding links about their mass centres - kg - m^2
where n =	2,3,4,5,6
I_{on}	Mass moment of inertia of the corresponding shafts - kg - m^2
where n =	1,2,3
EN1	Kinetic energy due to rotation - link 4 - kgm^2/s^2
EN2	Kinetic energy due to rotation - shaft O_3 - kgm^2/s^2
EN3	Kinetic energy due to rotation - shaft O_2 - kgm^2/s^2
EN4	Kinetic energy due to rotation - link 3 - kgm^2/s^2
EN5	Kinetic energy due to rotation - link 5 - kgm^2/s^2
EN6	Kinetic energy due to rotation - link 6 - kgm^2/s^2
RT1	(Angular velocity of link 3)/(angular velocity of crank arm)
RT2	(Angular velocity of link 4)/(angular velocity of crank arm)
RT3	(Angular velocity of link 5)/(angular velocity of crank arm)
RT4	(Angular velocity of link 6)/(angular velocity of crank arm)
CAL	Angle of transmission in degrees - angle ABO_2
YUM	Angle of transmission in degrees - angle CDO_3

Introduction

1 Stages encountered during the development of the Project

The primary objective was to determine both theoretically and experimentally the axial forces and the corresponding stresses in two of the linkage members of the mechanism. For this purpose pairs of strain gauges were placed on opposing faces of the rods in a configuration capable of measuring axial strains as well as bending strains in a direction normal to the plane of the links. Bending strains in the plane of the linkage could not be measured because of space limitations and the complex shape of the connecting rods which prohibited alternative placing of the gauges. Two different $\frac{1}{2}$ bridge 120 Ω strain-gauge circuits were available to measure axial and bending strains independently. The bending strains were expected to be zero. However in the course of the measurements it became apparent that substantial bending stesses were present in these members. To confirm the dynamic strain measurement results and to determine the nature and cause of the bending strains a set of static tests was carried out on the mechanism. The steps taken to achieve these objectives were:

1 - A detailed examination and description of the machine

2 - A complete theoretical kinematic, force and stress analysis

3 - Preparation of the experimental set-up

4 - Determination of basic material properties for the two connecting rods

5 - Measurement of dynamic strains

6 - Static tests on the mechanism aiming to find out the nature and cause of bending strains in a direction normal to the plane of the mechanism

7 - Comparison and discussion of experimental and calculated results.

2 Historical background to the Investigation

Bonas Machine Company Ltd., of Sunderland, England,have started to manufacture a high-speed weaving loom that weaves ribbon or tape. The loom was hoped to operate at 4000 r.p.m. but it was found that some of the moving parts fractured below this speed. By the increase of speed stoppages due to component fracture occurred more frequently. At the time of the initiation of this project the loom ran commercially at just over 2000 r.p.m. The basic problem was the short term fatigue failures of weft needle arms and the reeds. There were also failures of the connecting rods and links. Although dynamic stresses in the needle arms and reeds have been measured experimentally and calculated analytically in a previous study (24), no investigation had been made on the link mechanism driving the components. To improve the operating characteristics of the machine, the designer suggested that the following major points should be considered in further projects;

- a Measuring the strain of the components under investigation under various conditions
- b Interpreting the results
- c Suggesting possible design changes which would increase the maximum speed of the loom

In order to be able to suggest solid changes in design, the driving mechanism, weaving components, lubrication system and power transmission mechanism should be studied in great detail analytically and experimentally involving fatigue, material, structural, dynamic and economical analyses with different models.

3 Plane Mechanisms in General, current research and short bibliographical review

If all points of the curves of motion of all the links of a mechanism lie in one and on the same plane, the mechanism is called a plane mechanism. A mechanicsm can simply be defined as a combination of machine elements arranged to achieve a certain motion. Since it deals with the composition of members of a machine into an assemblage to perform a task, to produce a new and unusual result, mechanisms are one of the most fascinating topics in the field of mechanical engineering. Machine design is a creative art involving the possession of careful analytical ability, good judgement and a broad experience. The basic factors which must be taken into consideration in general machine design are: utility, safety, cost, strength, rigidity, deflection, friction, lubrication, wear, heat, noise, flexibility, control and appearance. A tremendous amount of work has been published on various aspects of mechanisms especially in the last two decades. The introduction of computers into design work has accelerated the research a great deal. Numerous new methods have been developed. Today the techniques for studying the dynamics of mechanisms can be classified as kineto-static or time response approaches (4). Current research topics in the field are concentrated on:

(a) Optimum mechanism design combining kinematic and dynamic force considerations.

(b) Synthesis of linkage function generators by means of mathematical methods, models and computers.

(c) Shaking and bearing force optimization.

(d) Experimental and theoretical study of connection forces and frequency response characteristics.

Dynamic effects in mechanisms become important as operating speeds increase and as light low power consuming economical designs are sought. In the design and experimental examination of the strength of mechanism links the state of stress and strain has to be investigated. Strength may be checked both theoretically and experimentally, however it is usually impossible to calculate stresses theoretically. Theoretical calculations are sometimes too inaccurate because a number of premises and assumptions have to be made. Most components and members are stressed three-dimensionally but with the existing methods of measurement only stresses at the surface can be determined and these do not give an overall picture of the stress distribution. The most expedient way of studying strength problems for mechanism links is to supplement theoretical calculation by experimental data and coefficients.

The efficiency of linkages is greater than that of any gear or cam due to their small frictional losses and high power transmitting ability. The four-bar linkage due to its simplicity has been used for transmission of motion in general. Although it is the simplest possible lower-paired mechanism, since more complex mechanisms have four-bar linkages as elements, the theory of the four-bar linkage is useful in designing of these mechanisms. The recent major contribution in this field can be found in (1), (25) and (4). Mechanism dynamics deals with the motion of a mechanism in response to actuating forces, torques and also the forces and torques produced by a given mechanism motion. Controlling force and torque levels is an important concern in avoiding problems of fatigue, vibration and noise. Most of the present dynamic design procedures start with a mechanism skeleton, distribute the mass of the members, and add springs or dampers to meet dynamic performance criteria associated with shaking moment, input torque balancing, and dynamic time response synthesis (25), (10). Elasticity in the links of mechanisms has a substantial effect on the dynamic behaviour of the mechanisms. The introduction of clearances in mechanisms causes a substantial increase in the connection forces resulting in degradation of life and performance (16). In mechanisms axial loads are induced in the links by impacts at bearing surfaces and by operating loads. Impact-induced axial loads are highly transient in nature (16). Kineto-elastodynamic analysis, which is the kinematic and dynamic study of mechanisms in motion including the effects of elasticity and mass distribution has recently been given increased attention(25). Imam and Sandor divide the complete mechanism design process into the following three steps:

(1) Selection of the type of mechanism

(2) Selection of the design parameters to satisfy kinematic requirements

(3) Selection of the design parameters to satisfy dynamic and kineto-elastodynamic requirements - mass distribution, inertia and reaction forces at the joints and bearings, transient and steady state vibrations, frequency and time response, elastic deformation of the components, dynamic stress in the links, impact, dynamic stability and balancing.

The basic criteria in designing and optimizing the areas of cross section of mechanism links are (4)

1 - The deviation (elastic deflections) from the ideal performance (rigid body motion) must be within the prescribed tolerances

2 - The mass of the linkage is to be minimized

3 - The stresses in any of the links are not be exceed the endurance limits

4 - Various combinations of the criteria such as mass, deformation and stress are to be minimized

A new method of kineto-elastodynamic design of high-speed mechanisms, which is general for all planar linkages including multi-loop and multi-degree-of-freedom mechanisms has recently been presented (25). Of special interest to this work is (15) which is considered and discussed in Chapter 5.

Chapter 1.

Description of the Machine.

The machine is a small variable high-speed weaving loom designed to manufacture ribbon or tape. The main body consists of a rigid steel case enclosing the sump and lubricating mechanism above which is mounted an H-shaped mechanism unit box. The whole complex is mounted on a π - shaped, box section steel platform. The main control box is mounted on the right side of the body while the opposing face is reserved for the power transmission. An inspection cover is fitted to the front of the main body. The important weaving components are mounted externally to the rear and top of the mechanism unit box. The main body and basic features are shown in Fig. (1.1) and Plate (1.1)

1.1 Power Transmission System

Originally an "Elektrim 1410 r.p.m., 1.1 kw, 1.5 HP, 415 V. 2.5 amp" constant speed electric motor was fitted to the rear of the main body. The replacement was a 3 phase, 2 HP variable speed (480-4320 output r.p.m.) electric motor. The motor was mounted on the rear end of the π -shaped platform, complete with an adjustable carriage which enabled belt adjustment to be carried out. AC current is taken directly from the floor by an insulated cable fed into the switch box. A "Fenner B 1800 B69" V-belt was used to transmit the power to the intermediate shaft. Fitted to the intermediate shaft was a 40 tooth pulley driving via a timing belt the 20 tooth pulley fitted to the main drive shaft. The timing belt used was "Fenner 240 L 100". The V-belt also drove the oil-pump shaft end disc. (Fig. 1.1). A handwheel/ flywheel was attached to the main drive shaft. The intermediate V-belt pulley was manufactured to suit the available belt. All pulleys were fitted to their respective shafts using "taper-lock" drive device. The two intermediate pulleys were first screwed together before fitting to the shaft.

Fig. 1.1

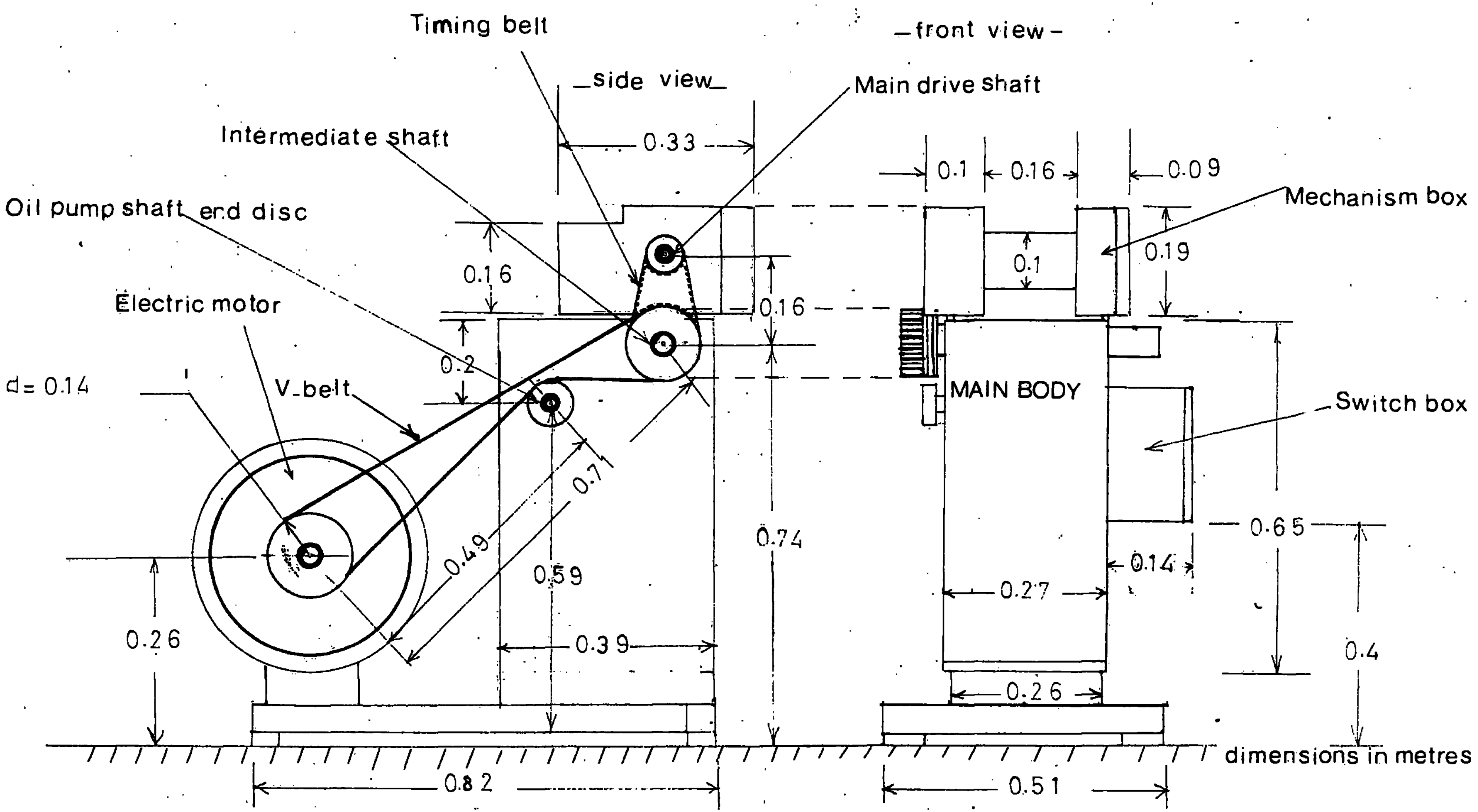
Timing belt
– front view –
– side view –
Main drive shaft
Intermediate shaft
Oil pump shaft end disc
Mechanism box
Electric motor
MAIN BODY
Switch box
V-belt
d = 0.14
0.33
0.1
0.16
0.09
0.19
0.2
0.71
0.49
0.59
0.74
0.39
0.26
0.65
0.14
0.27
0.4
0.82
0.51
dimensions in metres

At speeds in excess of 2500 r.p.m. (main drive shaft speed) slip was detected between "taper-lock" device and the main drive shaft. Due to vertical eccentricity in the axes of the motor pulley, intermediate shaft and main drive shaft excess wear was observed on the v-belt and on the timing belt.

1.2 Mechanism Unit box.

The left(drive) and right (output) end sections of the mechanism unit box, with covers removed, are shown in Plates (1.2) and (1.3). Plate (1.4) shows the right end section complete with connecting rods. In figures (1.2) and (1.3) the mechanism is shown as actual shafts and links and as pin jointed rods respectively. The main drive shaft goes through O_1 causing the crank arm O_1A to rotate with constant angular velocity. The rotary motion of the crank arm is transmitted to the rigid triangular link 4 via the coupler (link 3). The crank arm, coupler and rigid link 4 represent an offset crank-rocker mechanism. The oscillatory motion of link 4 is transmitted to shaft O_3 via the connecting rod link 5 and link 6. The connecting rods, rigid link 4 and link 6 are shown in Plate (1.5). The specification of the links are given in the following table:

Table 1.1

Link No.	Material	Experimental Location of Mass centres	Experimental Moment of inertia about mass centre: kg - m^2	Experimental BHN
3	Phosphor Bronze alloy	12 mm from A	5.84×10^{-5}	117
4	Carbon Steel	7.5 mm from O_2 30° from O_2C	4.35×10^{-5}	-
5	Phosphor Bronze alloy	1.45 mm from C	7.5×10^{-6}	142
6	Carbon steel	1 mm from O_3	2.26×10^{-5}	-

MECHANISM

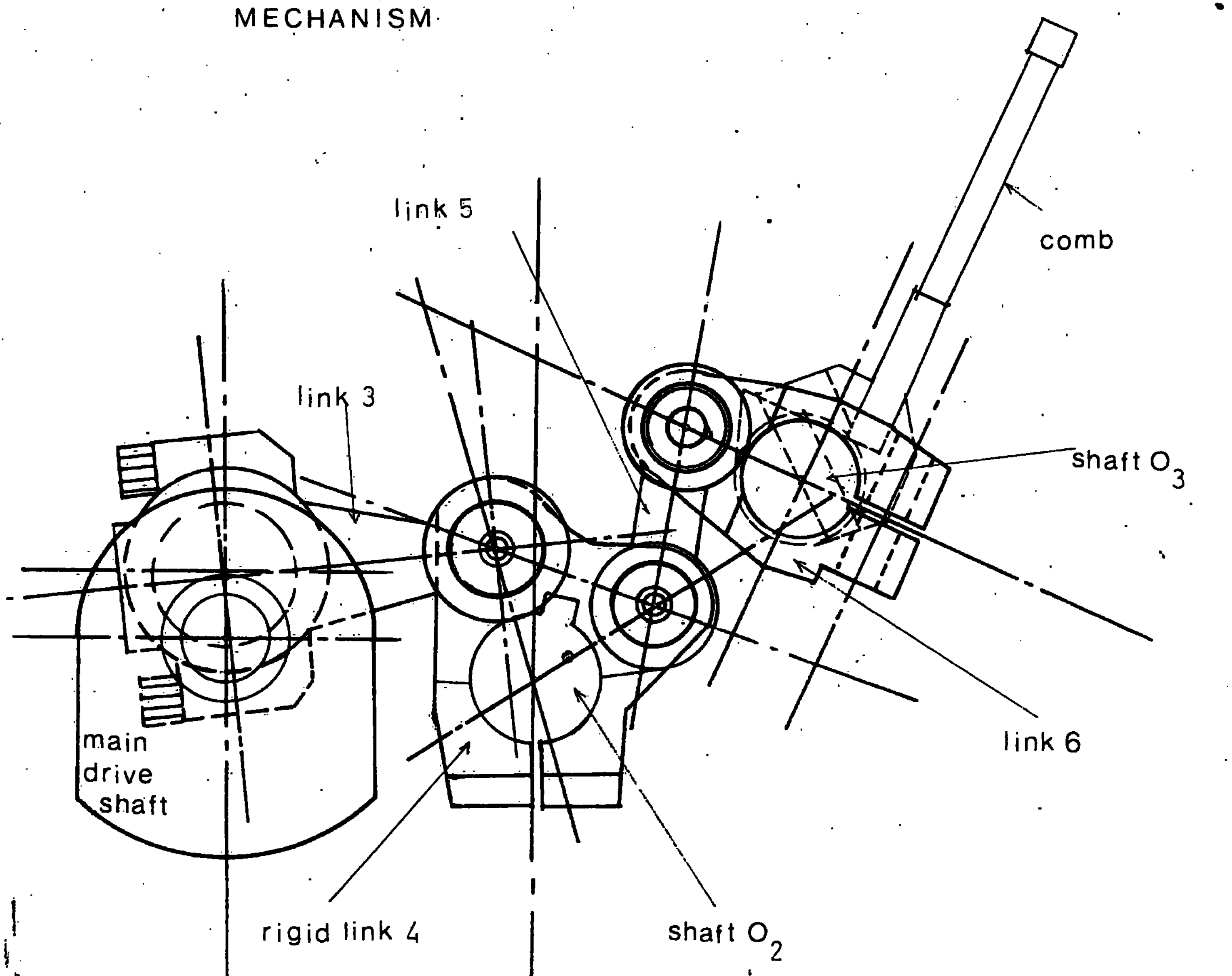

scale 1:1

Fig. (1.2)

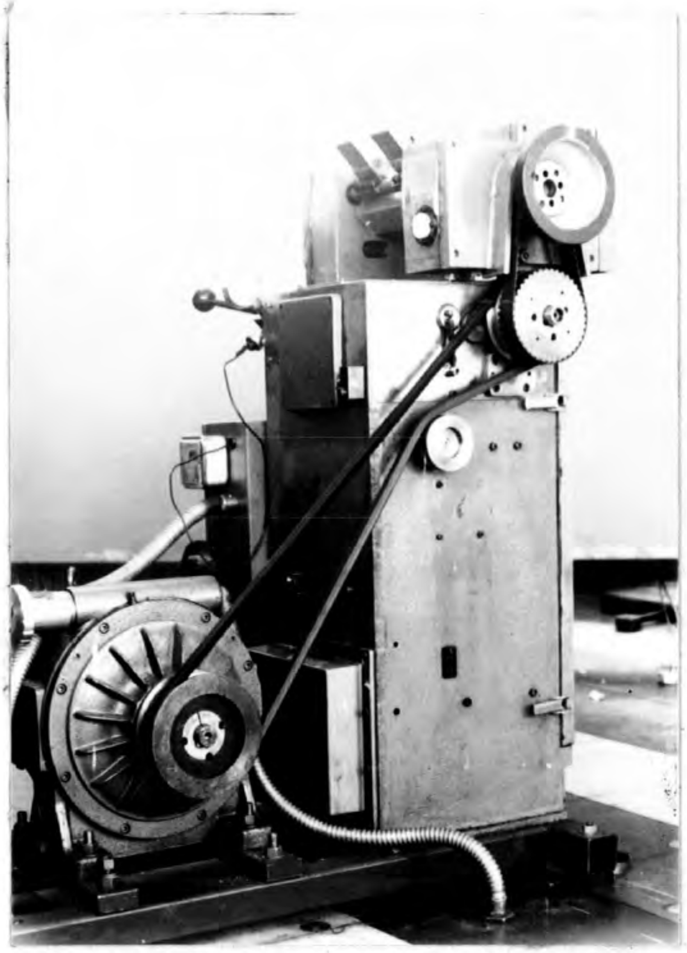

Plate (1.1) Power transmission system

Plate 1.2 Mechanism box left end. From left to right. Bearings for shafts O_3, O_2 and O_1

mechanism shown as pin jointed rods

$O_1A = 11$ mm.
$AB = 42$ mm.
$BO_2 = O_2C = 22$ mm.
$CD = 29$ mm.
$DO_3 = 20$ mm.

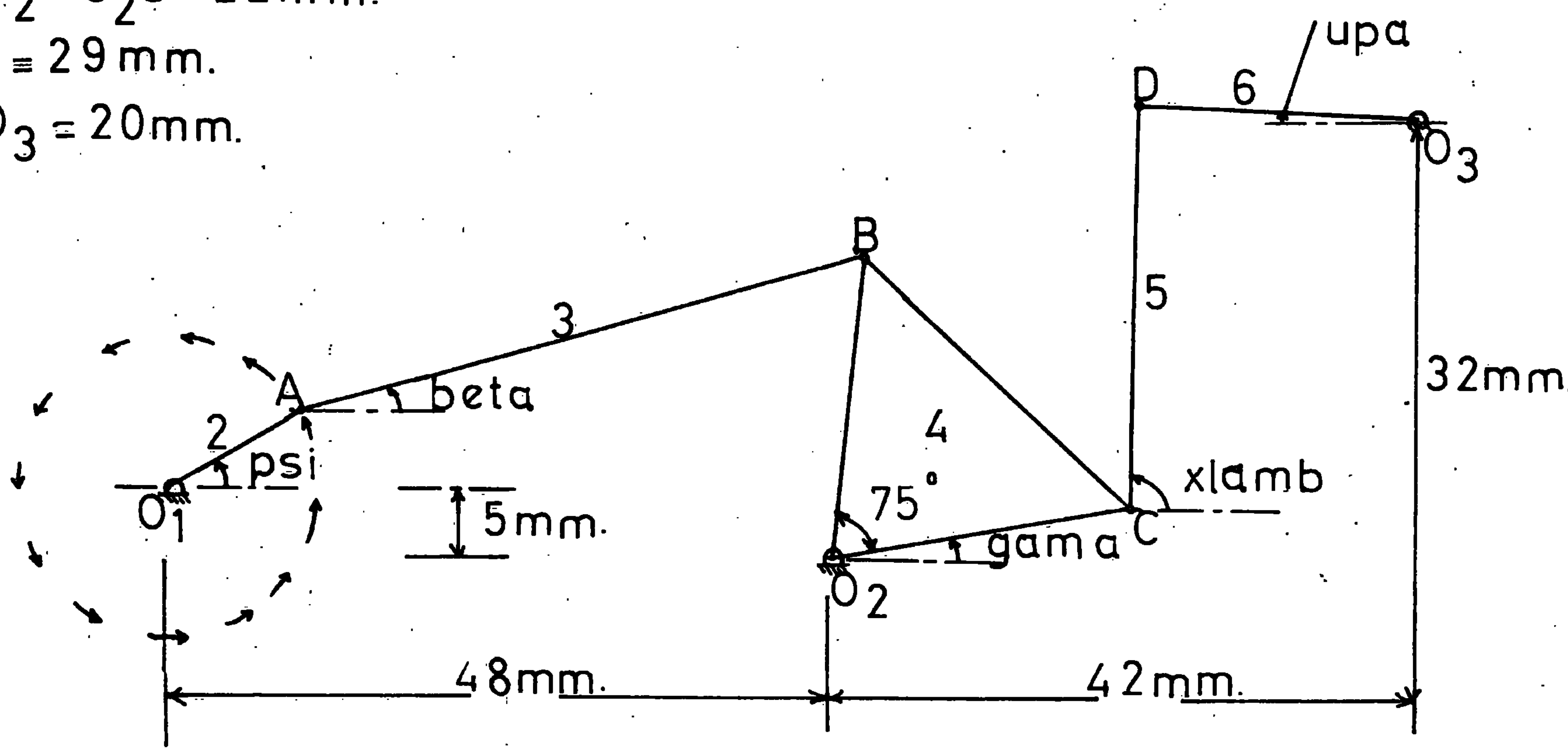

Fig. (1.3)

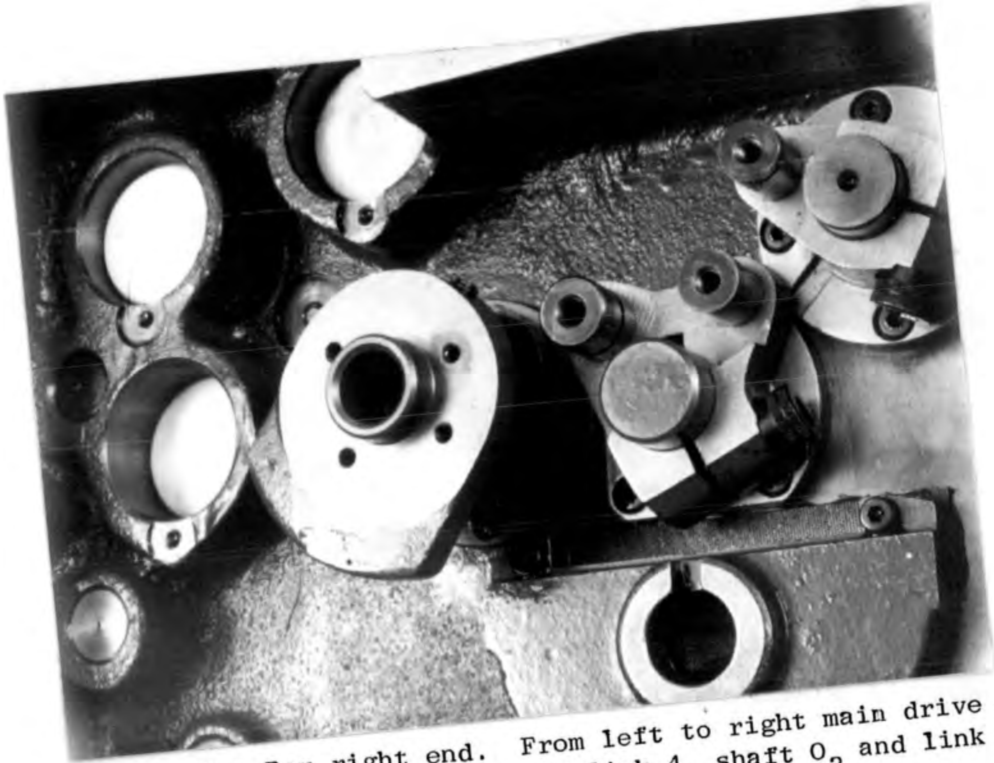

Plate 1.3 Mechanism Box right end. From left to right main drive shaft (O_1) crank arm, shaft O_2 and rigid link 4, shaft O_3 and link 6

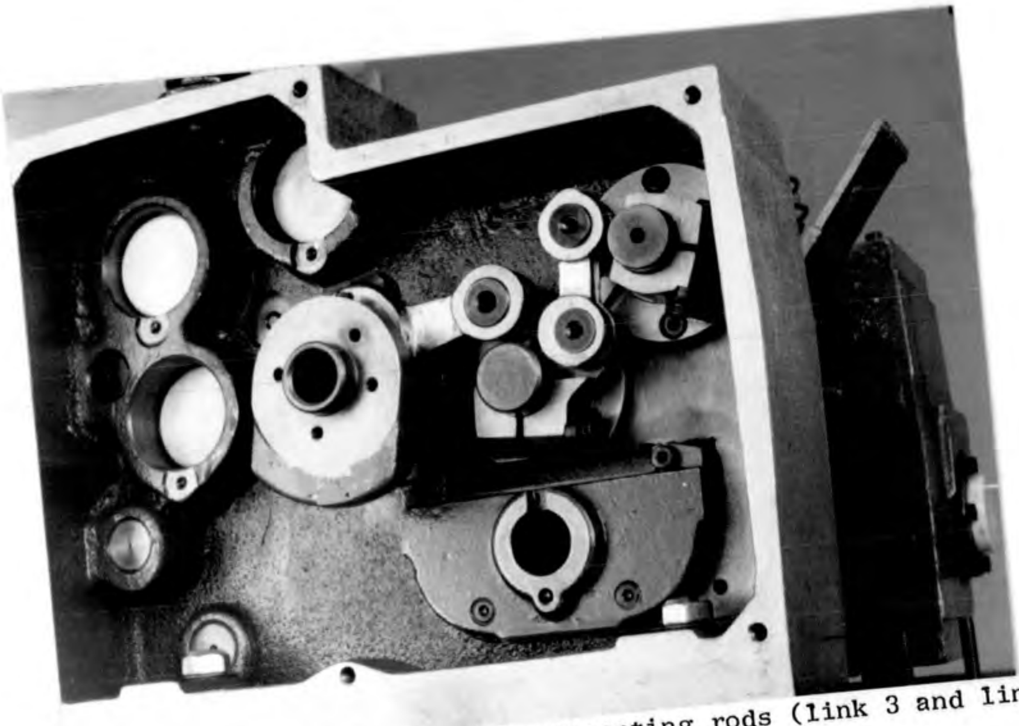

Plate 1.4 Mechanism, complete with connecting rods (link 3 and link 5)

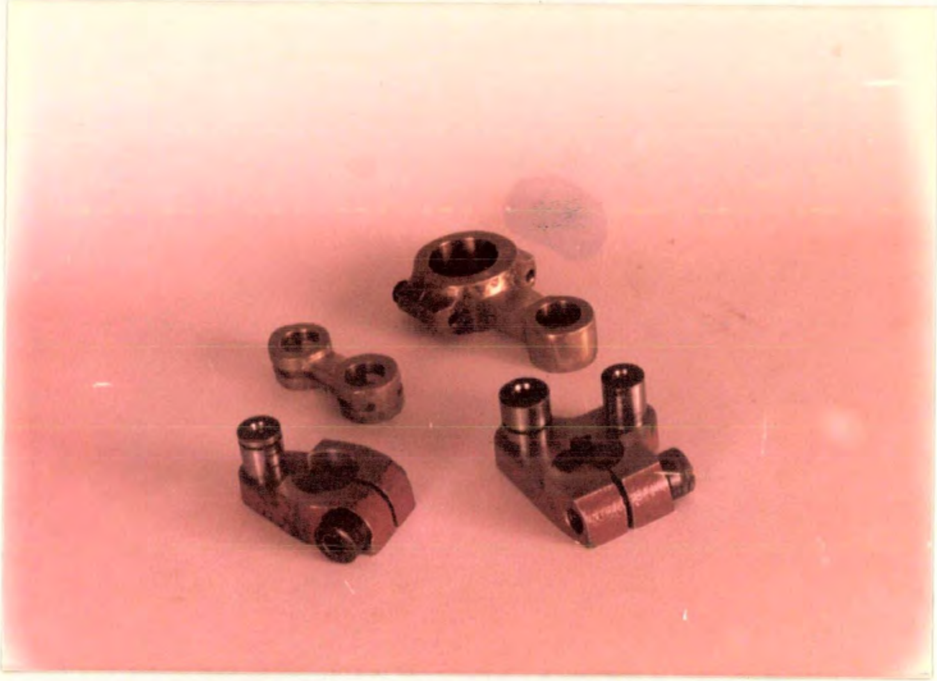

Plate 1.5 Connecting rods (links 3 and 5), rigid triangular link 4 and link 6

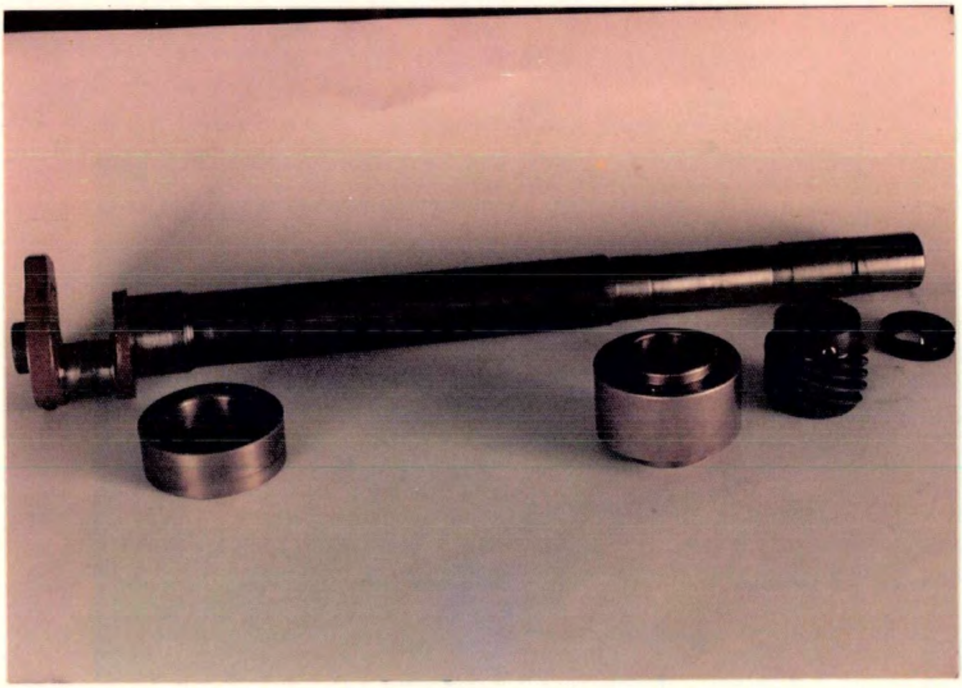

Plate 1.6 Main drive shaft (shaft O_1)

The main drive shaft, which was manufactured hollow to allow for lubrication, is shown in Plate (1.6). The diameter varies from point to point. A detailed crank-arm end drawing is shown in Fig. (1.4). The rigid triangular link 4 is attached to shaft O_2 by a clamp mechanism and secured with a key, while link 6 is attached by a similar clamp mechanism but without a key. At high crank arm speeds (approaching to 2500 r.p.m.) slip between link 6 and shaft O_3 caused stoppages and mechanical damage. Lubrication was hydrodynamic in the shaft bearings. Lubricant enters the bearings via converging channels to support the shafts without shaft to bearing contact. Hollow head cap screws were used to fit the bearings to the frame. The shafts were not secured against movement in a direction perpendicular to the plane of the mechanism. At right angles to the axis of the shaft O_2 is the rotation of the needle arms produced by pairs of bevel gears on the needle arm base and shaft O_2.

Detailed drawings of link 6 and shaft O_3 with the comb, are shown in Fig. (1.5) and (1.6). The horizontal positioning of the shafts are shown in Fig. (1.7) The specification of shafts O_1, O_2 and O_3 are presented in Table 1.2.

Table 1.2

shaft no.	mass kg.	Exp. moment of inertia about mass centres $kg\text{-}m^2$	Function
O_1	1.409	8.72×10^{-4} (with the hand wheel)	Main drive shaft delivers power to the system
O_2	0.699	9.22×10^{-5} (with the bevel gears)	Carries a pair of partial bevel gears to rotate the needle arms
O_3	0.805	3.06×10^{-4} (with the combs)	Carries a pair of combs for weaving

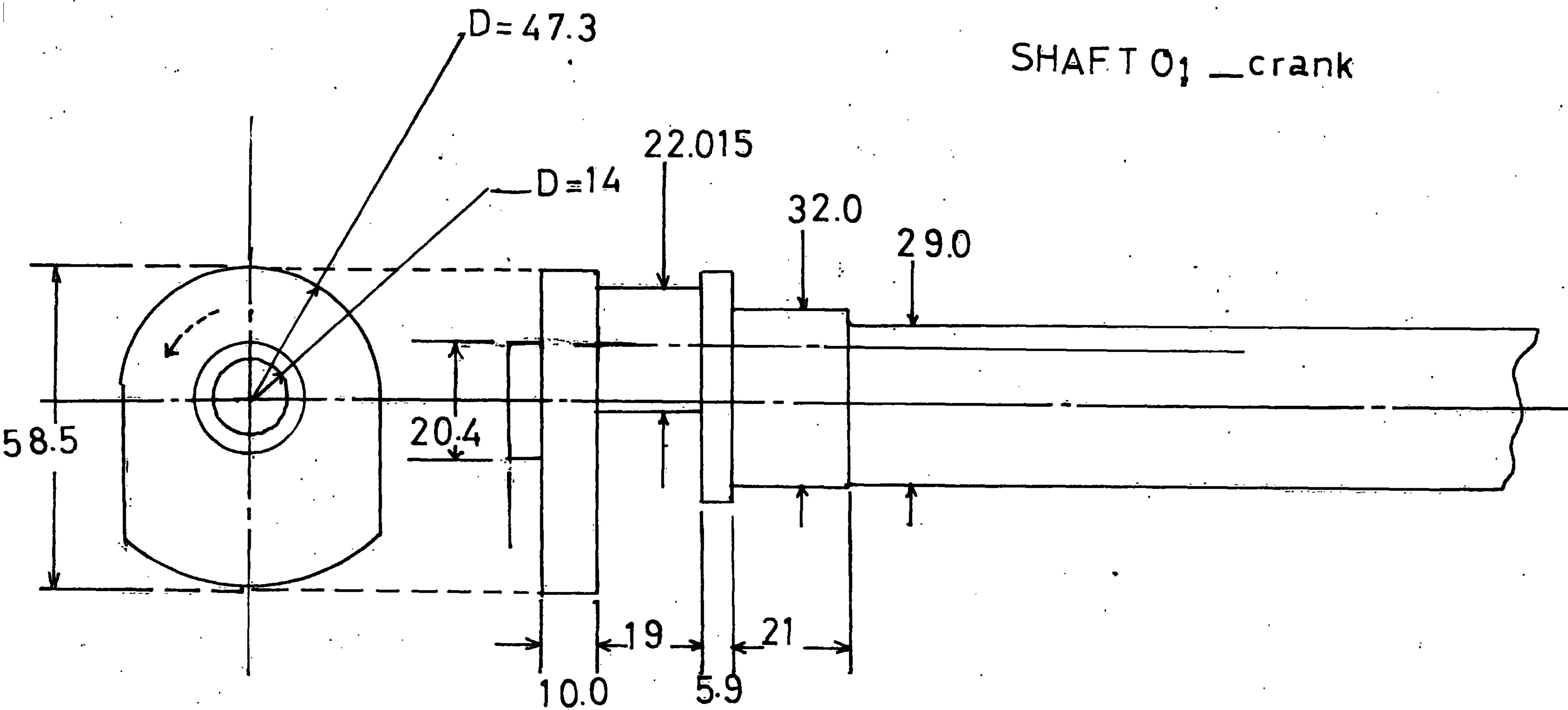

Fig. 1.4 Main drive shaft crank arm end detailed drawing

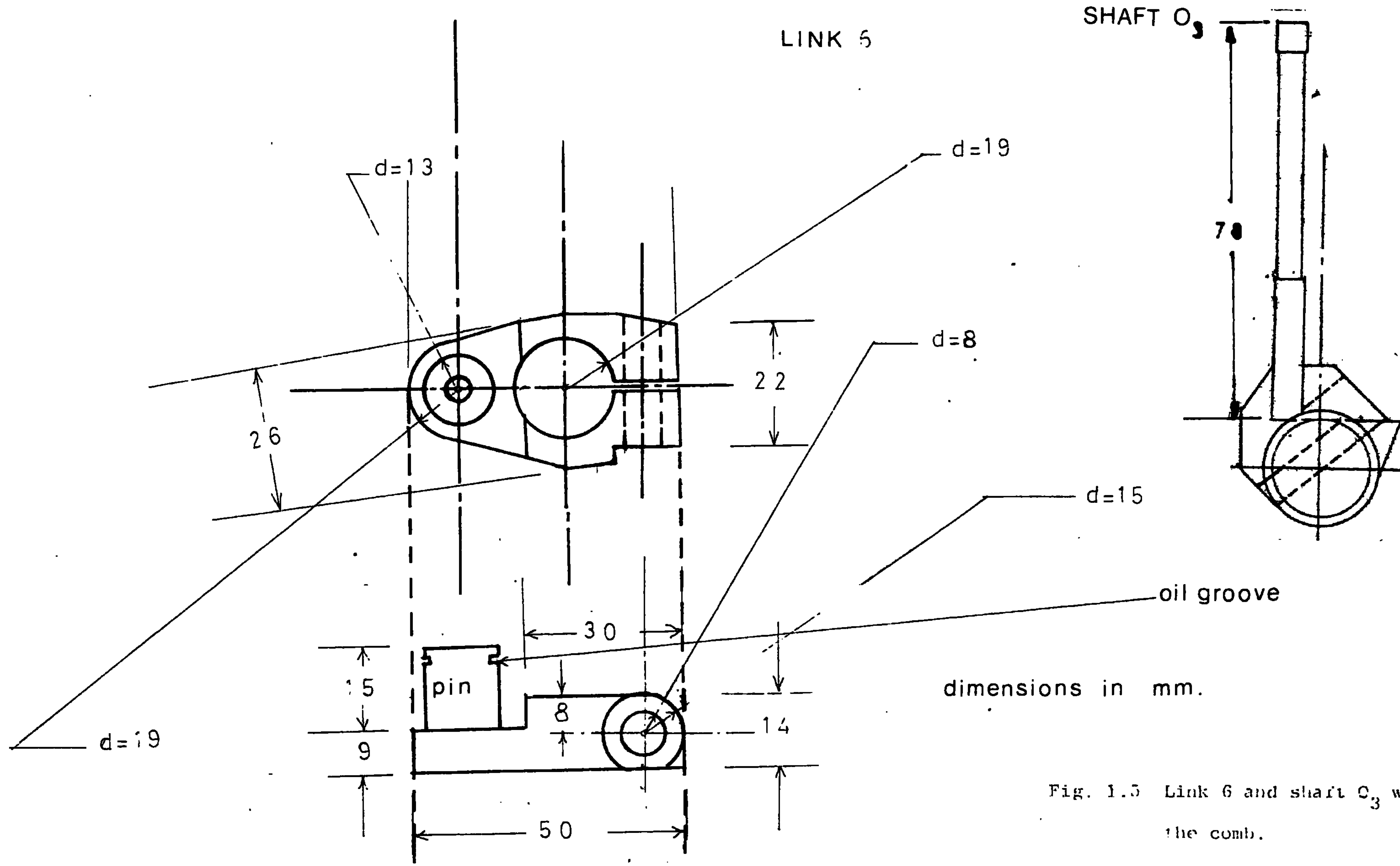

Fig. 1.5 Link 6 and shaft O_3 with the comb.

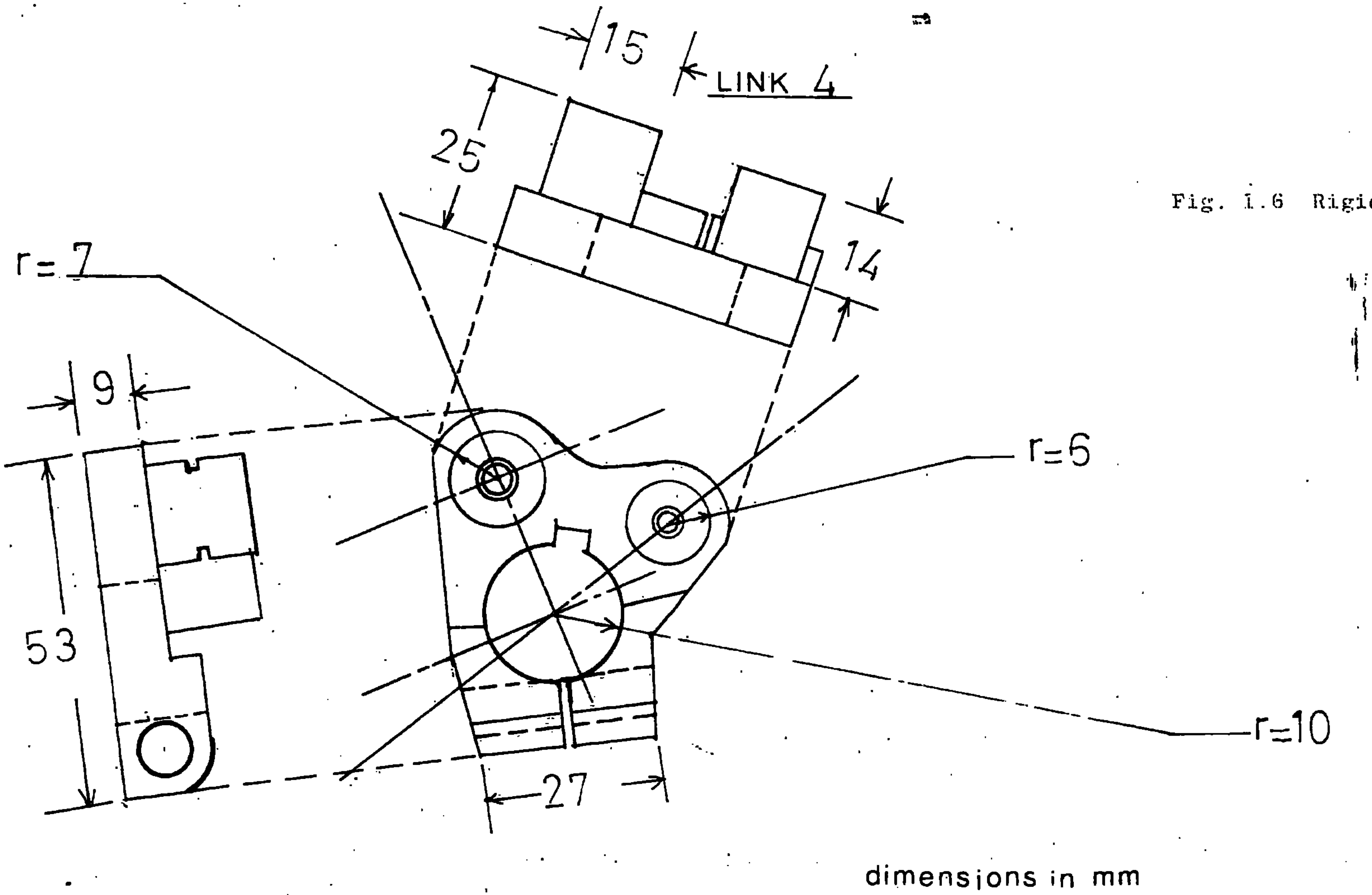

Fig. 1.6 Rigid triangular link 4

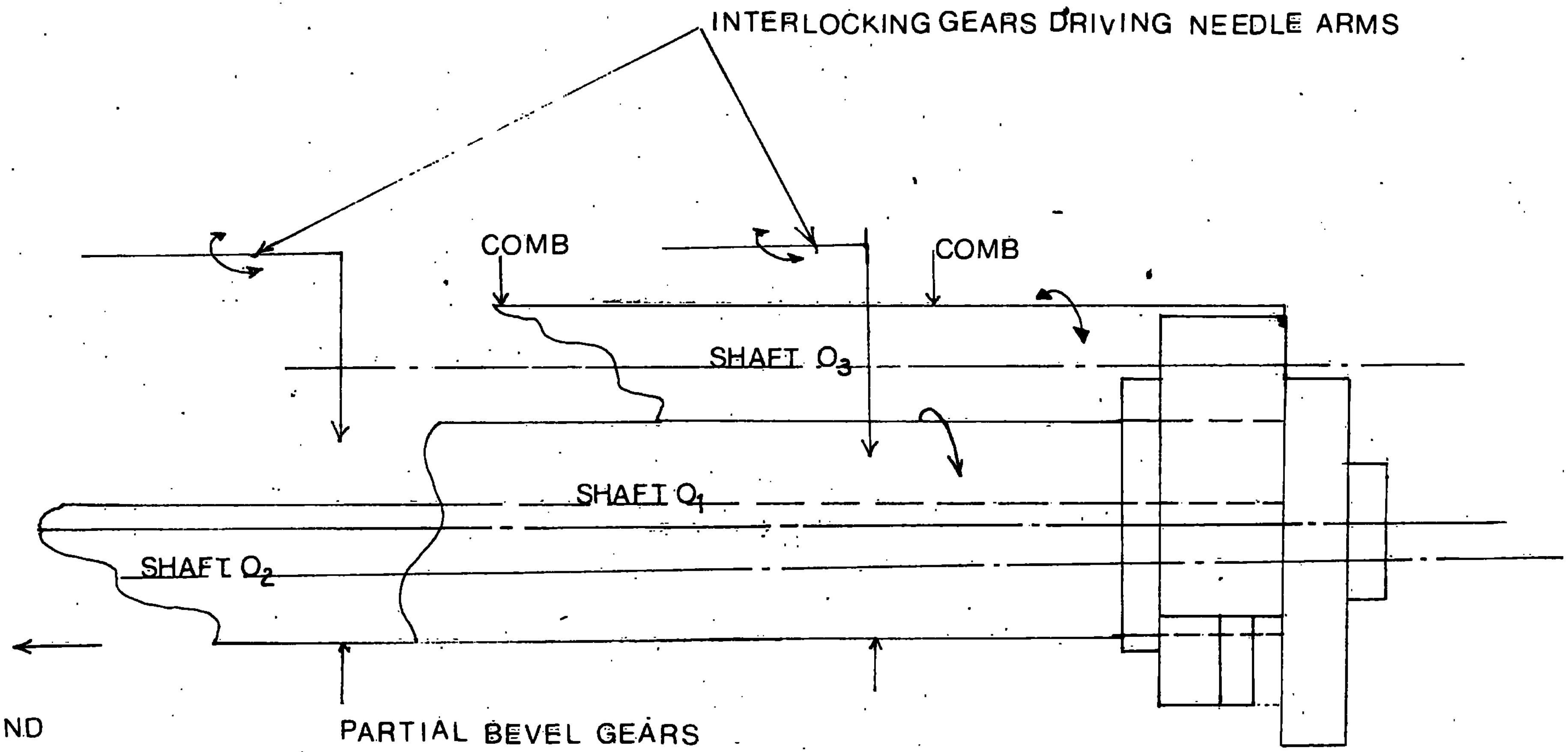

Fig. 1.7 Simplified weaving mechanism. Horizontal positioning of shafts O_1. O_2 and O_3

The experimental moment of inertia values presented in Tables 1.1 and 1.2 are determined by a trifilar suspension. The needle arms and shaft O_3 with the comb and bearings are shown in Plates 1.9 and 1.10. The masses of links 3, 4, 5 and 6 are: 0.116 kg, 0.116 kg, 0.0283 kg and 0.0749 kg respectively. The mass centres of the links are determined by using a knife edge. The top view of the mechanism unit box and shaft O_2 are shown in plates 1.7 and 1.8 respectively.

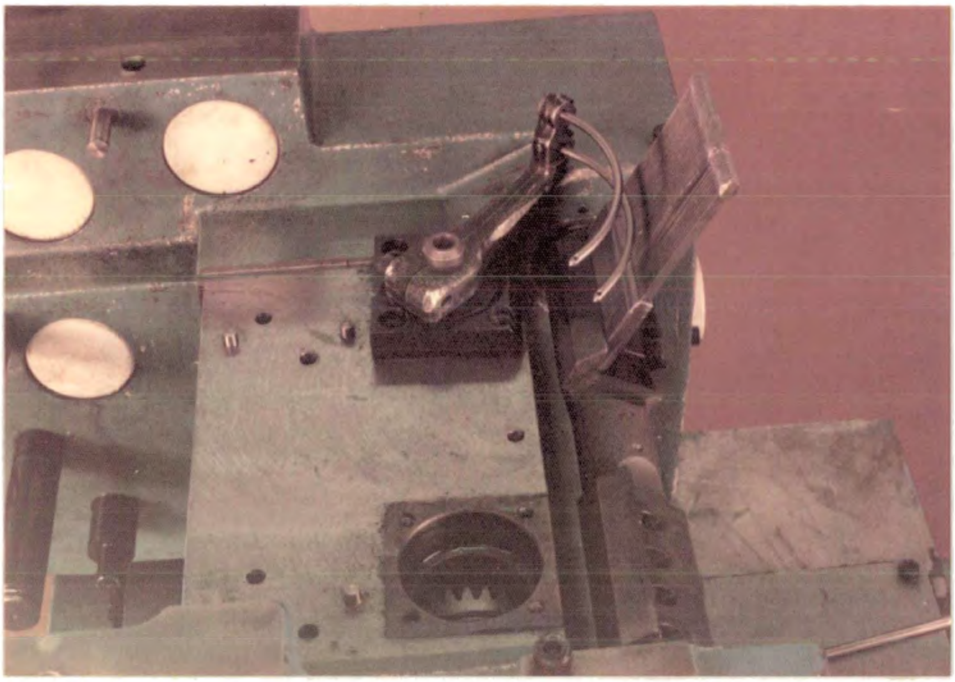

Plate 1.7 Top view - Mechanism unit box. Bevel gears carried by link O_2, weft needle arm, shaft O_3 and the reed.

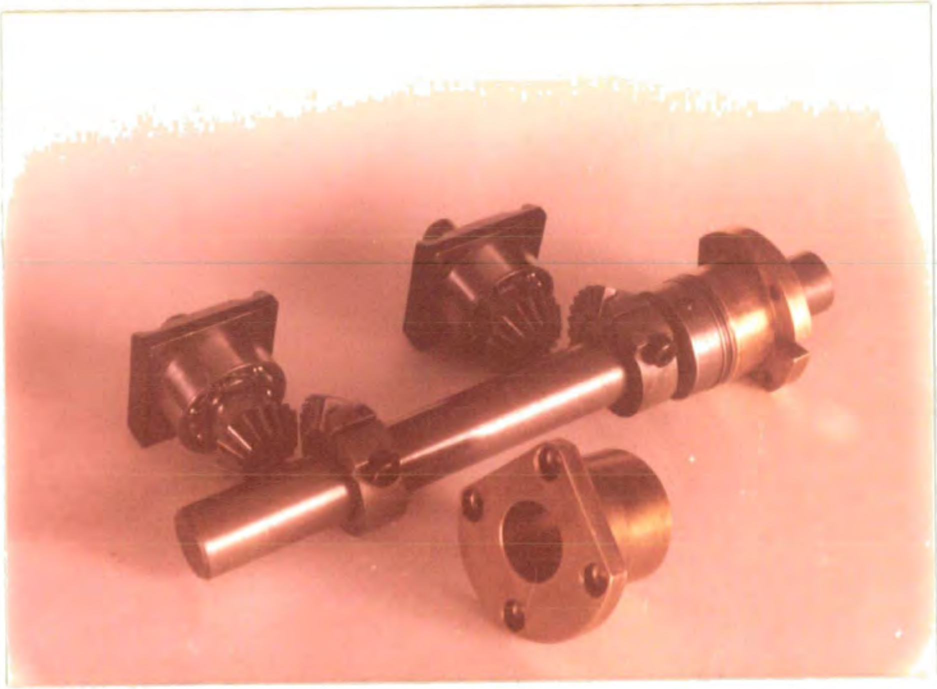

Plate 1.8 Shaft O_2, shaft bearings, and the bevel gears.

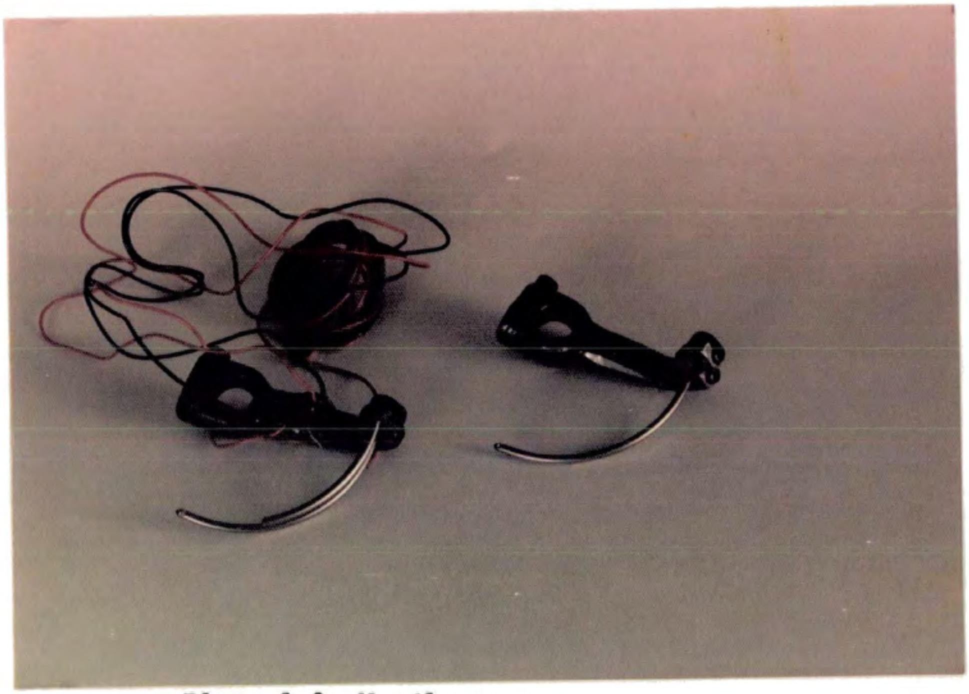

Plate 1.9 Needle arms

Plate 1.10 Shaft O_3, comb and bearings

Chapter 2

Kinematic Analysis of the Mechanism

2.1. Introduction to Kinematic Analysis of the Mechanism

Recently a variety of methods have been developed for dynamic and kinematic analysis of mechanisms such as methods based on kinematic constraints, motor algebra, matrix methods, quaternion and dual-number methods, relative motion and incremental equations utilizing numerical methods, in addition to the classical methods. Other basic methods are; Quinn's energy distribution method, Lagrangian method, solutions employing complex polar notation and complex numbers, kineto-elastodynamic analysis, Raven's analysis, velocity analysis by instantaneous centres, velocity analysis by components, velocity and acceleration image method, graphical and analytical velocity and acceleration analysis and various algebraic methods. In the following sections a complete kinematic analysis of the mechanism is presented to specify the motion of the mechanism and to determine the kinematic values. It is assumed that all the links of the mechanism move in the same plane and the crank speed is constant.

2.2 Geometry of the Mechanism

From Fig. (2.1); for ψ $0^{\circ} \longrightarrow 360^{\circ}$

$$O_1E = \cos(\psi)\,(0.011)$$

$$AE = \sin(\psi)\,(0.011)$$

$$AF = AE + 0.005$$

$$O_2F = 0.048 - O_1E$$

$$AO_2 = (AF)^2 + (O_2F)^2$$

$$\eta = \tan^{-1}\left(\frac{AF}{O_2F}\right)$$

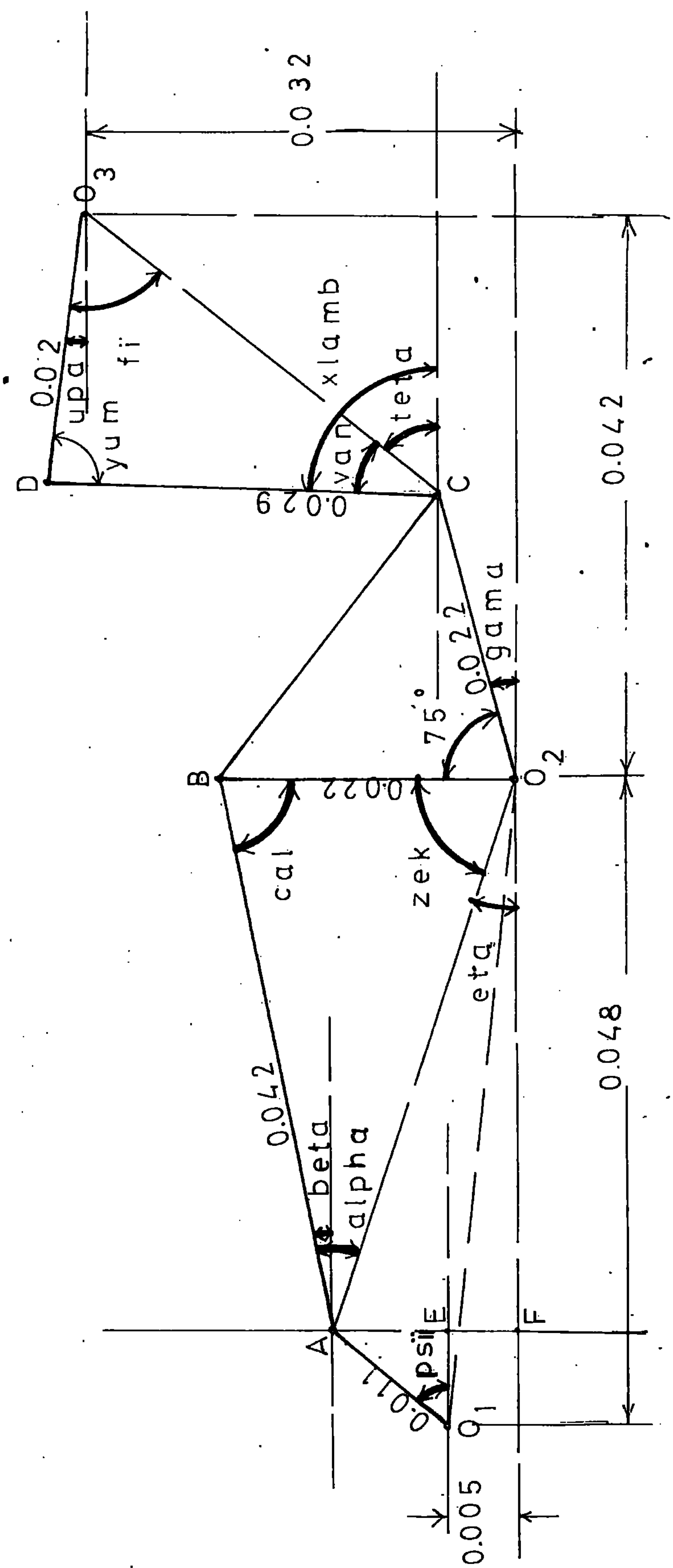

0.032
O3
D
0.02
upa
fi
yum
xlamb
teta
van
C
0.029
0.042
gama
0.022
75°
O2
B
0.022
cal
zek
eta
0.042
beta
alpha
0.048
A
E
F
psi
0.01
O1
0.005

Fig. 2.1

$$zek = \cos^{-1} \frac{0.00128 - (AO_2)^2}{(-0.044)\ (AO_2)^2}$$

$$cal = \cos^{-1} \frac{0.002248 - (AO_2)^2}{(0.001848}$$

$$\alpha = 180^\circ - (zek + cal)$$

$$\beta = \alpha - \eta$$

$$\gamma = 180^\circ - (\eta + zek + 75^\circ)$$

$$\theta = \tan^{-1} \frac{0.032 - \sin(\gamma)\ (0.022)}{0.042 - \cos(\gamma)\ (0.022)}$$

$$CO_3 = \frac{0.032 - \sin(\gamma)\ (0.022)}{\sin(\theta)}$$

$$van = \cos^{-1} \frac{(0.029)^2 + (CO_3)^2 - (0.02)^2}{(0.029)^2\ (CO_3)}$$

$$x\lambda = van + \theta$$

$$\omega = \cos^{-1} \frac{(0.02)^2 + (CO_3)^2 - (0.029)^2}{(0.04)\ (CO_3)}$$

$$upa = \omega - teta$$

$$yum = 180^\circ - (x\lambda + upa)$$

all the angles are in degrees. Relationships between ψ, γ, $x\lambda$ and upa depend upon the link lengths. Numerical variation of γ, β, $x\lambda$ and upa with ψ are given in (A 1) and are shown graphically in Figures (2.2), (2.3) (2.4) and (2.5). Variation of the transmission angles, cal and yum with ψ are shown in Fig. (2.6)

2 .3 Velocity and Acceleration Analysis - Analytic method

Angular positions of links 3,4,5 and 6 are determined relative to the x axis

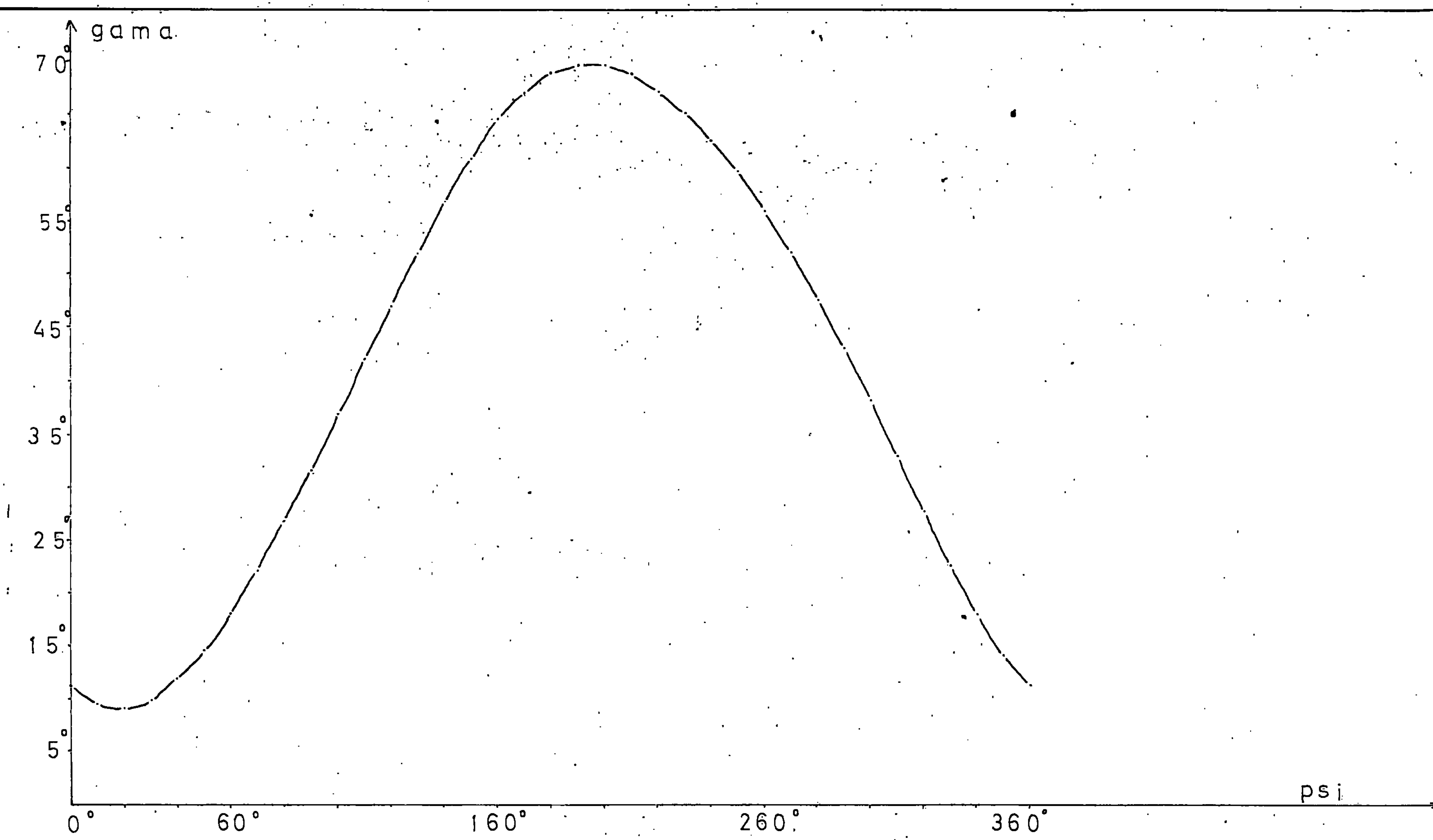

Fig. 2.2 Variation of angle gama by the crank angle psi (angles measured from horizontal in counter clockwise direction)

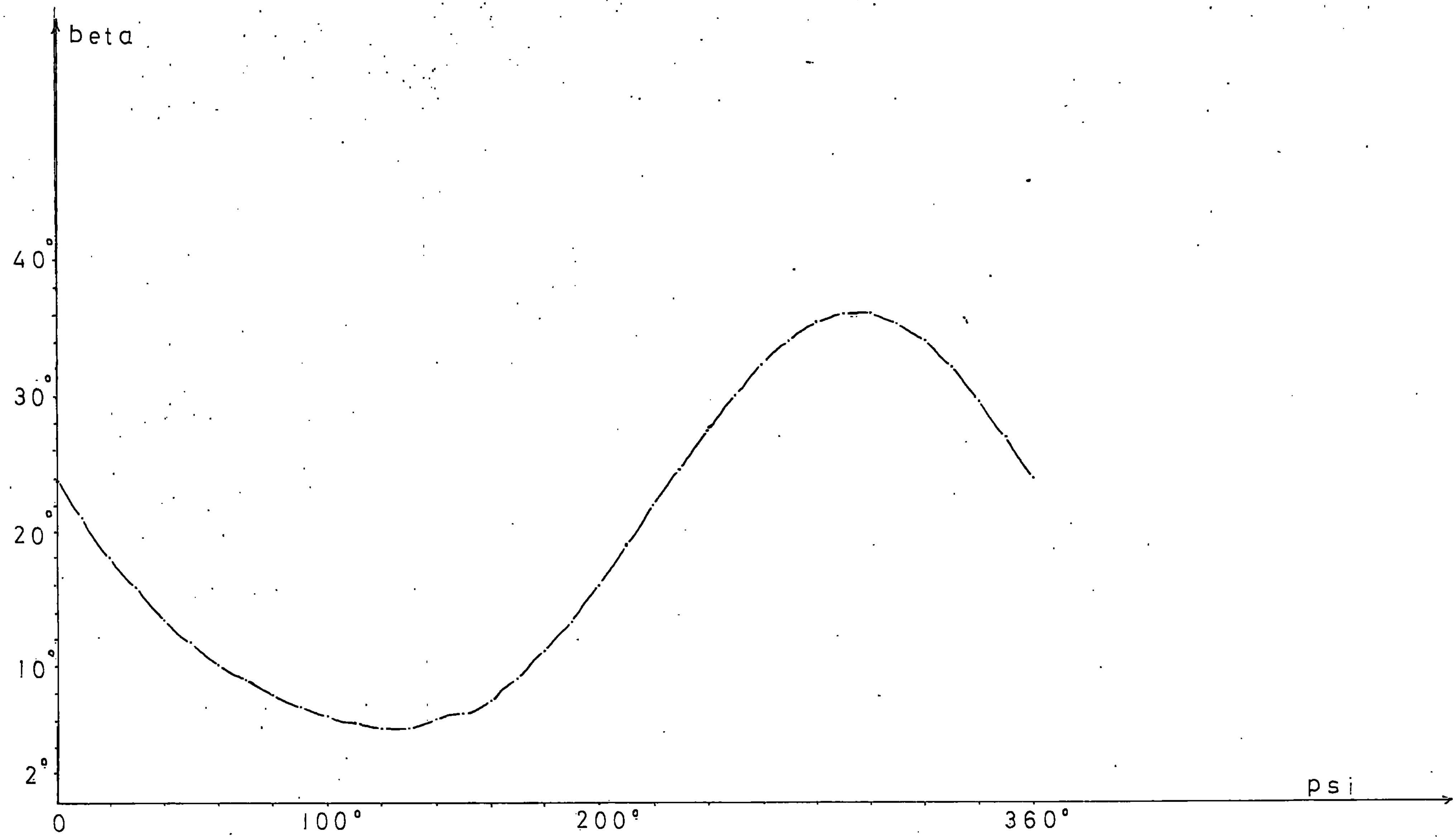

Fig. 2.3 Variation of angle beta by the crank angle psi (angles measured from horizontal in counter clockwise direction)

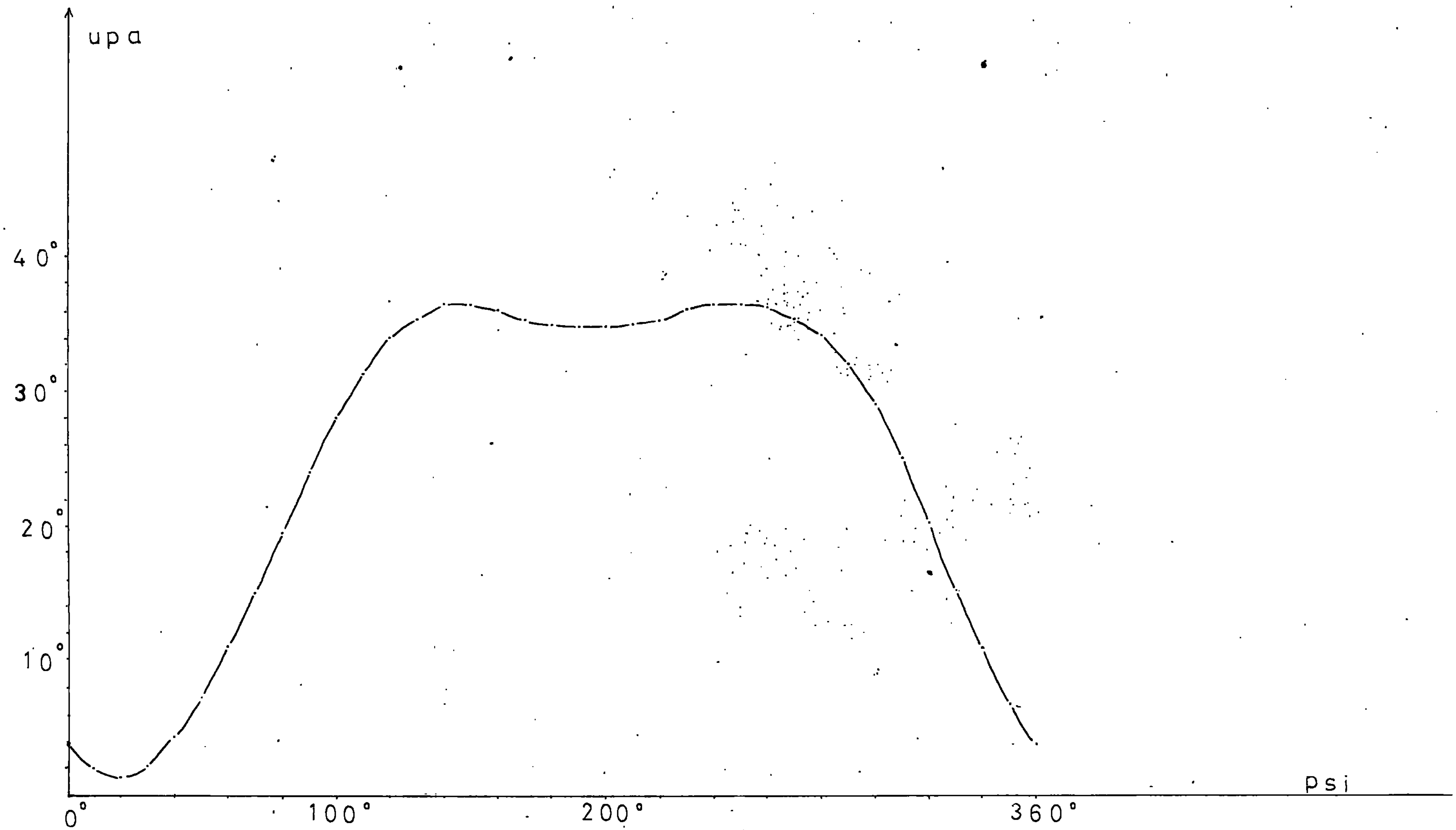

Fig. 2.4 Variation of angle upa with the crank angle psi (crank angle measured from horizontal in counter clockwise direction and upa measured from horizontal in clockwise direction)

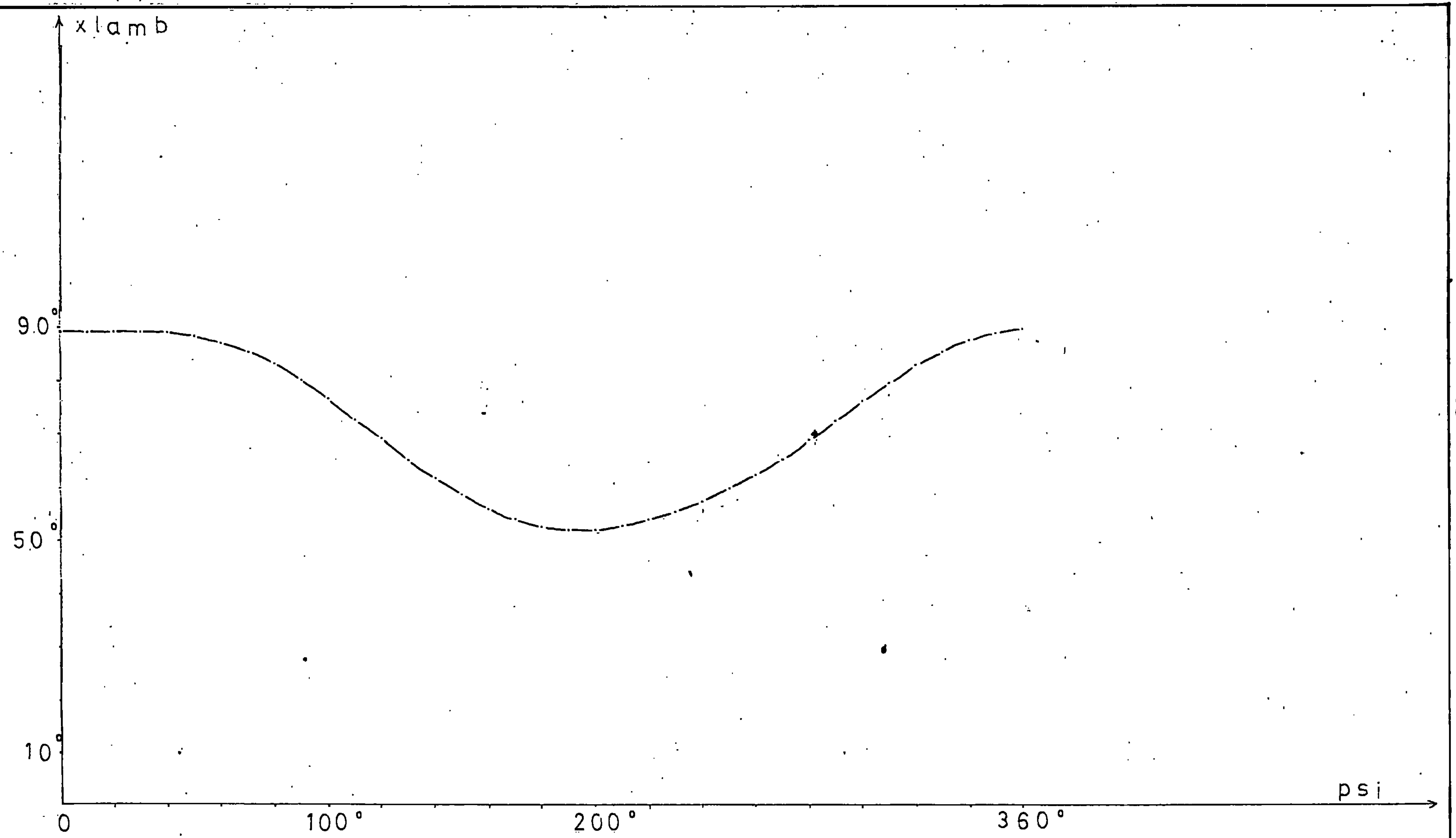

Fig. 2.5 Variation of angle xlamb with the crank angle psi (angles measured from horizontal in counter clockwise direction)

The velocity of A is;

$V_A = O_1A.\omega_2 \quad \theta$ (where θ shows angular position)

where $\theta = \psi + 90^o$

ω_2 = angular velocity of the crank arm in rad/s

The velocity of B is:

$V_B = \nu_B \angle \theta$

where $\theta = \gamma + 165^o$

The velocity of B with respect of A is

$V_{BA} = \nu_{BA} \angle \theta$

where $\theta = \beta + 90^o$

the directions are assumed for V_B and V_{BA} may be incorrect. Subsequent calculations will indicate whether this is true or not.

The relative velocity equation is;

$V_B = V_A + V_{BA}$

transforming V_B, V_A and V_{BA} into complex rectangular notation;

$$(\dot{x}_B + j\dot{y}_B) = (\dot{x}_A + j\dot{y}_A) + (\dot{x}_{BA} + j\dot{y}_{BA}) \qquad (2.1)$$

where $\dot{x}_A$ and $\dot{y}_A$ are known

Knowing the directions of V_B and V_{BA};

$$\frac{\dot{y}_B}{\dot{x}_B} = \tan(\gamma + 165^o) \qquad (2.2)$$

$$\frac{\dot{y}_{BA}}{\dot{x}_{BA}} = \tan(\beta + 90^o) \qquad (2.3)$$

solving equations (2.1),(2.2) and (2.3) simultaneously, $\dot{x}_{BA}$, $\dot{y}_{BA}$, $\dot{x}_B$ and $\dot{y}_B$ can be determined.

The angular velocity of links 3 and 4 may be calculated as;

$$\omega_3 = \frac{\nu_{BA}}{AB} \quad \text{and} \quad \omega_4 = \frac{\nu_B}{O_2B}$$

from the geometry of the mechanism;

$$\nu_B = \nu_C \text{ (in magnitude)}$$

$$V_C = \nu_C \angle \theta$$

where

$$\theta = \gamma + 90^\circ$$

the velocity of D is;

$$V_D = \nu_D \angle \theta$$

where

$$\theta = 90^\circ - \text{upa}$$

the velocity of D with respect of C is;

$$V_{DC} = \nu_{DC} \angle \theta$$

where

$$\theta = x\lambda + 90^\circ$$

the relative velocity equation is;

$$V_D = V_C + V_{DC}$$

transforming into complex rectangular notation;

$$(\dot{x}_D + j\dot{y}_D) = (\dot{x}_C + j\dot{y}_C) + (\dot{x}_{DC} + j\dot{y}_{DC}) \qquad (2.4)$$

knowing the directions of V_D and V_{DC}

$$\frac{\dot{y}_D}{\dot{x}_D} = \tan\,(90^\circ - \text{upa}) \qquad (2.5)$$

$$\frac{\dot{y}_{DC}}{\dot{x}_{DC}} = \tan\,(x\lambda + 90^\circ) \qquad (2.6)$$

solving equations (2.4),(2.5) and (2.6) simultaneously,

$\dot{x}_{DC}$, $\dot{y}_{DC}$, $\dot{x}_D$ and $\dot{y}_D$ can be determined

thus, the angular velocity of links 5 and 6 are;

$$\omega_5 = \frac{v_{DC}}{DC} \quad \text{and} \quad \omega_6 = \frac{v_D}{DO_3}$$

the components of acceleration can be obtained as follows;

$$A_A^{\ t} = O_1A \ \alpha_2 \angle \ \theta$$

where

$$\theta = \psi + 90^o$$

$$A_A^{\ t} = 0, \text{ since } \alpha_2 = 0$$

$$A_A^{\ r} = O_1A. \ \omega_2^{\ 2} \quad \theta$$

where

$$\theta = -(180^o - \psi)$$

$$A_{BA}^{\ r} = AB. \ \omega_3^{\ 2} \angle \ \theta$$

where

$$\theta = -(180^o - \beta)$$

$$A_B^{\ r} = O_2B. \ \omega_4^{\ 2} \angle \ \theta$$

where

$$\theta = -[180^o - (75^o + \gamma)]$$

from the geometry of the mechanism;

$A_B^{\ r} = A_C^{\ r}$ (in magnitude)

$A_B^{\ t} = A_C^{\ t}$ (in magnitude)

both $A_{BA}^{\ t}$ and $A_B^{\ t}$ are unknown and are to be determined

The relative acceleration equation is;

$$A_B^{\ t} + A_B^{\ r} = A_A^{\ t} + A_A^{\ r} + A_{BA}^{\ t} + A_{BA}^{\ r} \tag{2.7}$$

transforming the acceleration components into complex rectangular notation and substituting into equation (2.7) produces

$$(\ddot{x}_B{}^t + j\ddot{y}_B{}^t) + (\ddot{x}_B{}^r + j\ddot{y}_B{}^r) = (\ddot{x}_A{}^r + j\ddot{y}_A{}^r) + (\ddot{x}_{BA}{}^t + j\ddot{y}_{BA}{}^t) + (\ddot{x}_{BA}{}^r + j\ddot{y}_B{}^r) \quad (2.8)$$

the required slopes of these components are such that;

$$\frac{\ddot{y}_B{}^t}{\ddot{x}_B{}^r} = \tan(\gamma + 165^\circ) \quad (2.9)$$

$$\frac{\ddot{y}_{BA}{}^t}{\ddot{x}_{BA}{}^t} = \tan(90^\circ + \beta) \quad (2.10)$$

by equating the real and imaginary parts of equation (2.8) and solving simultaneously with equations (2.9) and (2.10) gives $\ddot{x}_B{}^t$, $\ddot{y}_B{}^t$, $\ddot{x}_{BA}{}^t$ and $\ddot{y}_{BA}{}^t$

The acceleration of B is;

$$A_B = A_B{}^t + A_B{}^r$$

where

$$A_B{}^t = \ddot{x}_B{}^t + j\ddot{y}_B{}^t$$

acceleration of link 3 is;

$$A_{BA} = A_{BA}{}^t + A_{BA}{}^r$$

where

$$A_{BA}{}^t = \ddot{x}_{BA}{}^t + j\ddot{y}_{BA}{}^t$$

the angular acceleration of links 3 and 4 are;

$$\alpha_3 = \frac{a_{BA}{}^t}{AB} \qquad \alpha_4 = \frac{a_B{}^t}{O_2B}$$

similarly, the relative acceleration equation for links 4, 5 and 6 can be written as

$$A_D{}^t + A_D{}^r = A_C{}^r + A_C{}^t + A_{DC}{}^t + A_{DC}{}^r \quad (2.11)$$

where

$$A_D^{\,r} = DO_3\,\omega_6^2 \angle \theta \quad ; \quad \theta = 360^\circ - upa$$

$$A_{DC}^{\,r} = DC\,\omega_5^2 \angle \theta \; ; \; \theta = 180^\circ + x\lambda$$

$$A_C^{\,r} = a_C^{\,r} \angle \theta \; ; \; \theta = 180^\circ + \gamma$$

$$A_C^{\,t} = a_C^{\,t} \angle \theta \; ; \; \theta = \gamma + 90^\circ$$

$\ddot{x}_C^{\,t}$ and $\ddot{y}_C^{\,t}$ are therefore known as well as $\ddot{x}_C^{\,r}$ and $\ddot{y}_C^{\,r}$. Again by transforming equation (2.11) into complex rectangular notation;

$$(\ddot{x}_D^{\,t} + j\ddot{y}_D^{\,t}) + (\ddot{x}_D^{\,r} + j\ddot{y}_D^{\,r}) = (\ddot{x}_C^{\,r} + j\ddot{y}_C^{\,r}) + (\ddot{x}_C^{\,t} + j\ddot{y}_C^{\,t}) + (\ddot{x}_{DC}^{\,t} + j\ddot{y}_{DC}^{\,t}) + (\ddot{x}_{DC}^{\,r} + j\ddot{y}_{DC}^{\,r}) \qquad (2.12)$$

the required slopes are;

$$\frac{\ddot{y}_D^{\,t}}{\ddot{x}_D^{\,t}} = \tan\,(90^\circ - upa) \qquad (2.13)$$

and

$$\frac{\ddot{y}_{DC}^{\,t}}{\ddot{x}_{DC}^{\,t}} = \tan\,(x\lambda + 90^\circ) \qquad (2.14)$$

from equations (2.12), (2.13) and (2.14), $\ddot{x}_D^{\,t}$, $\ddot{y}_D^{\,t}$, $\ddot{x}_{DC}^{\,t}$ and $\ddot{y}_{DC}^{\,t}$ can be obtained.

$$A_D^{\,t} = \ddot{x}_D^{\,t} + j\ddot{y}_D^{\,t}$$

the acceleration of D is;

$$A_D = A_D^{\,t} + A_D^{\,r}$$

angular acceleration of links 5 and 6 are;

$$\alpha_5 = \frac{a_{DC}^{\,t}}{DC}$$

$$\alpha_6 = \frac{a_D^{\,t}}{DO_3}$$

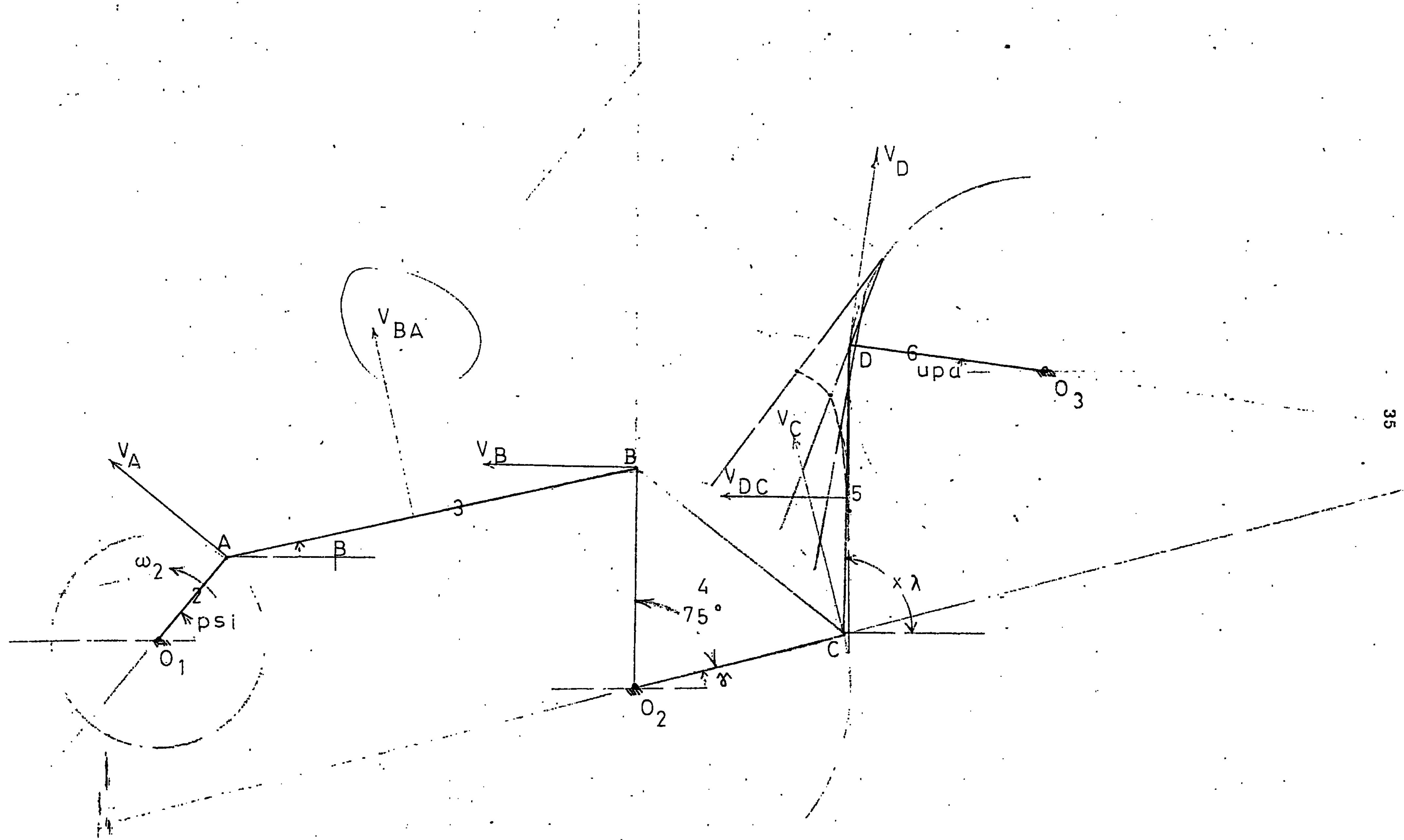

Fig 2.7 Analytical velocity and acceleration analysis

Variation of the angular acceleration of links 3,4,5 and 6 with crank angle ψ are shown in Fig. (2.8). Fig. (2.9), Fig. (2.10) and in Fig. (2.11). Variation of angular velocities of links 3,4,5 and 6 with the crank angle ψ are given in Fig. (2.12) for a crank speed of 2500 r.p.m. Ratio of angular velocity of the individual links to crank arm angular velocity is shown in Fig. (2.13), for a complete revolution of the crank arm. All the kinematic values calculated above, are presented in (A1) for a crank speed of 2500 r.p.m.

2.4 Algebraic Approach

The system is separated into two loops, Fig. (2.14, a and b) Fig. (2.15) The first loop represents a crank-rocker mechanism, also known as a crank-lever mechanism, which is a popular type of the well known four-bar linkage for converting continuous rotary motion to oscillation. The second loop is a four-bar chain attached to the rigid link 4 of the first loop at point C. The two extreme positions of the output lever (link 4) of the first loop are expected to occur when crank arm (link 2) is in line with the coupler. Proportions of the mechanism satisfy Grashoff's criterion as in the following:

Base link $<$ coupler + (output lever-driving crank)

$4.8 < 5.3$

Base link $>$ coupler - (output lever - driving crank)

$4.8 > 3.1$

Let A,B,C and D be lengths of input crank, coupler link, output lever, and base link of the first loop, Fig. (2.14a)

α_1, α_2 = angles showing dead-centre positions of output link

$\Delta\alpha = \alpha_2 - \alpha_1$

$\Delta\beta = \beta_2 - \beta_1 - \pi$

the unit of angles being in degrees.

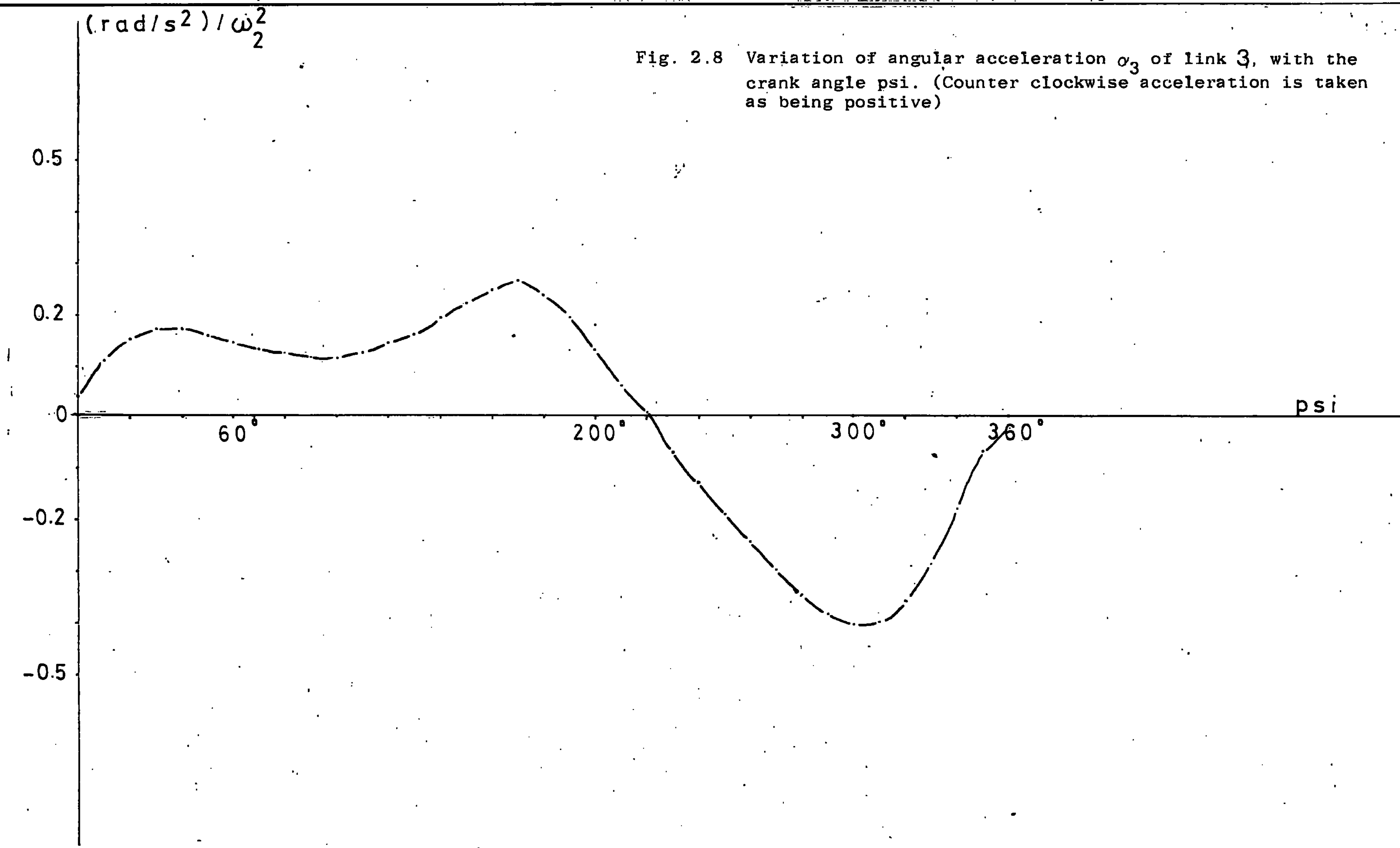

Fig. 2.8 Variation of angular acceleration α_3 of link 3, with the crank angle psi. (Counter clockwise acceleration is taken as being positive)

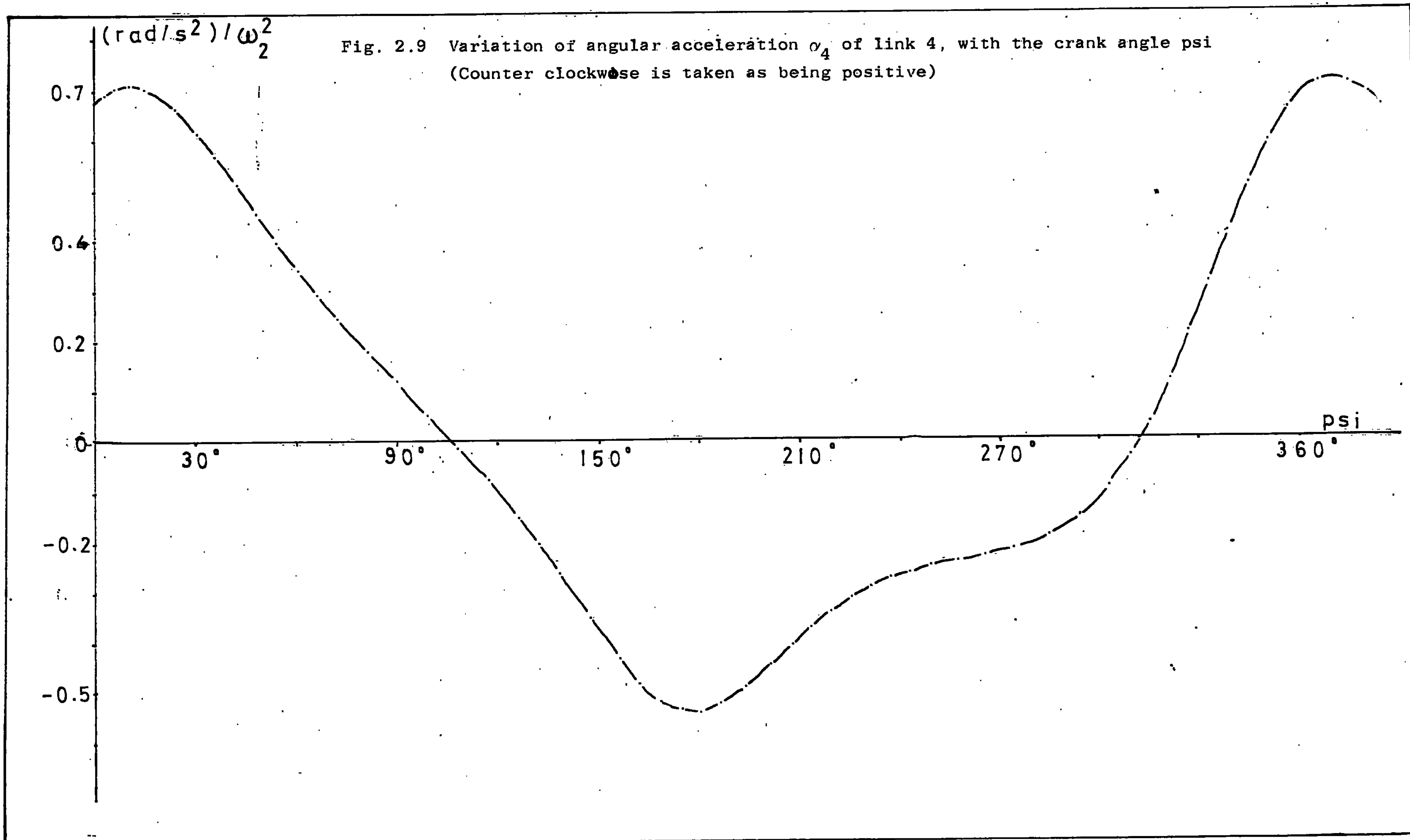

Fig. 2.9 Variation of angular acceleration α_4 of link 4, with the crank angle psi (Counter clockwise is taken as being positive)

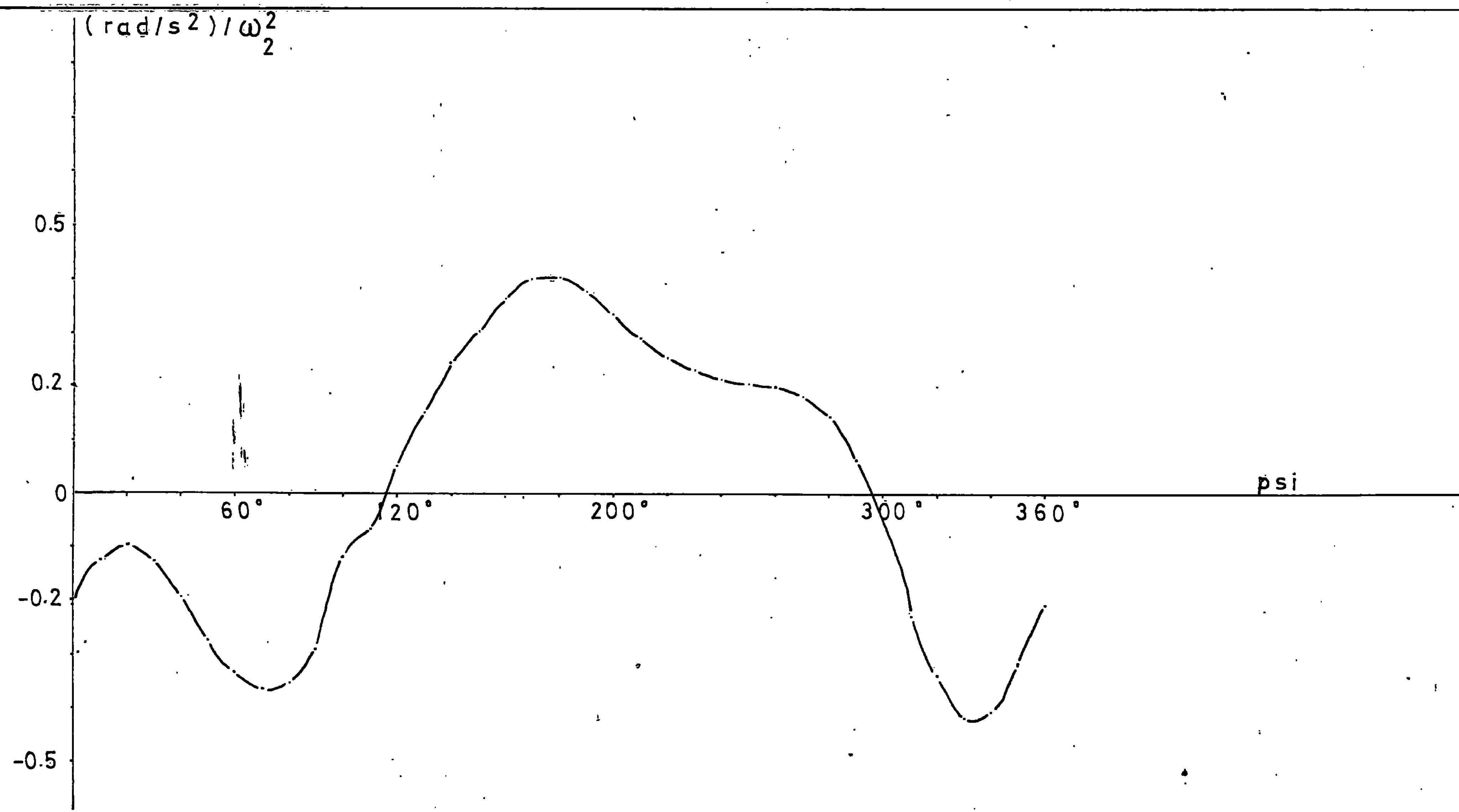

Fig. 2.10 Variation of angular acceleration α_5 of link 5 with the crank angle psi (counter clockwise acceleration is taken as being positive)

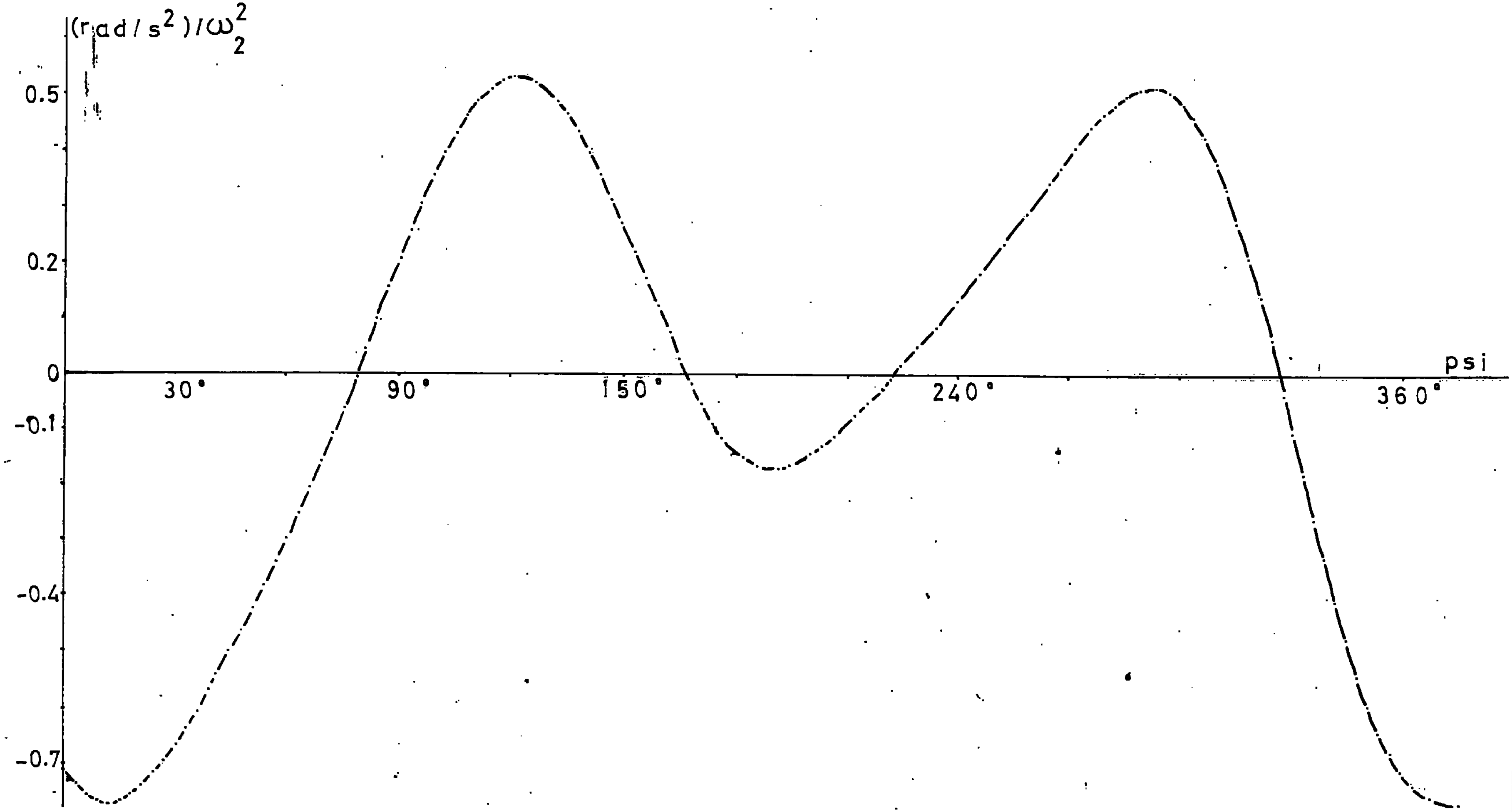

Fig. 2.11 Variation of angular acceleration α_6 of link 6 with the crank angle psi (counter clockwise acceleration is taken as being positive)

Fig. 2.12

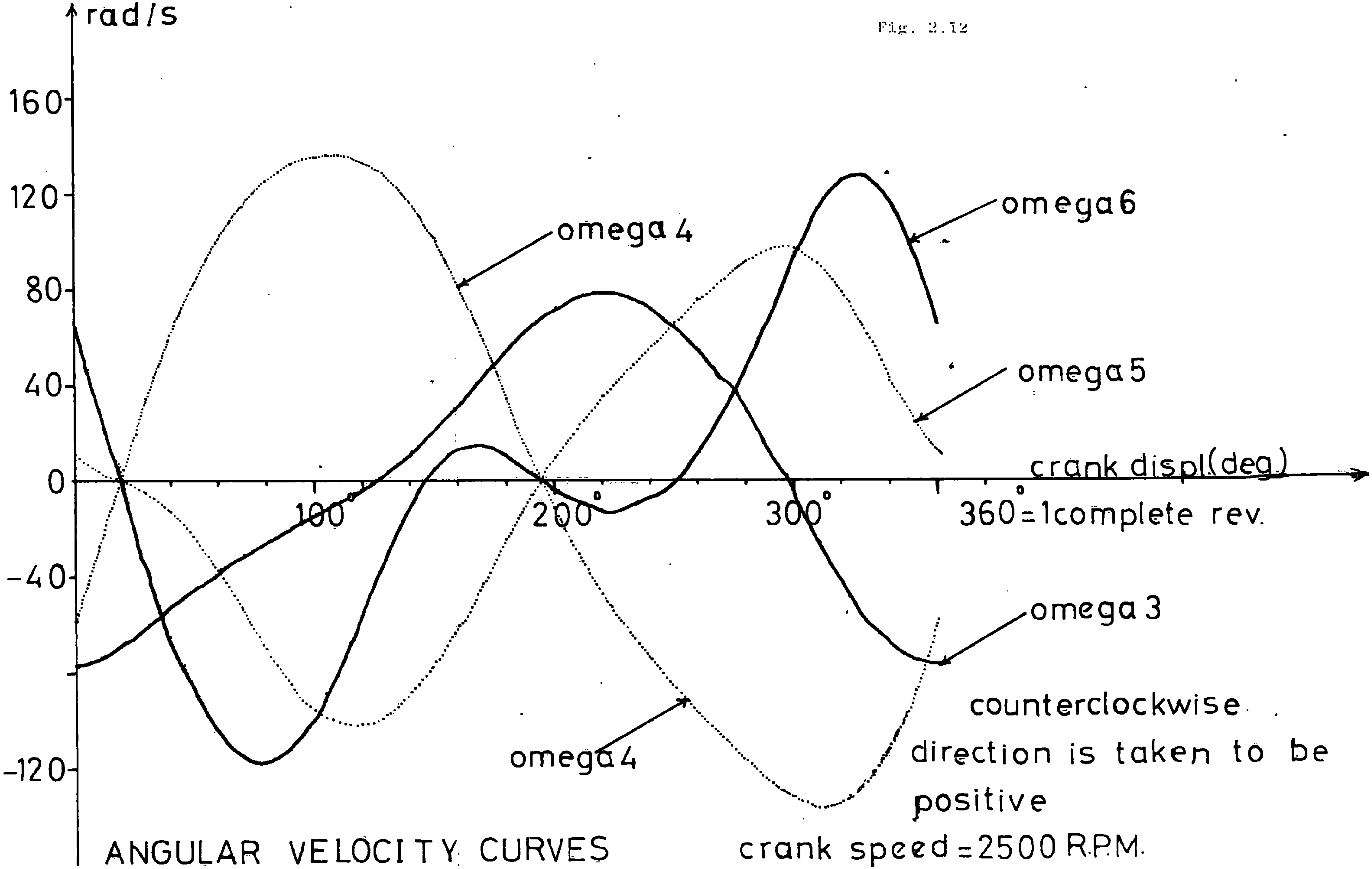

ANGULAR VELOCITY CURVES

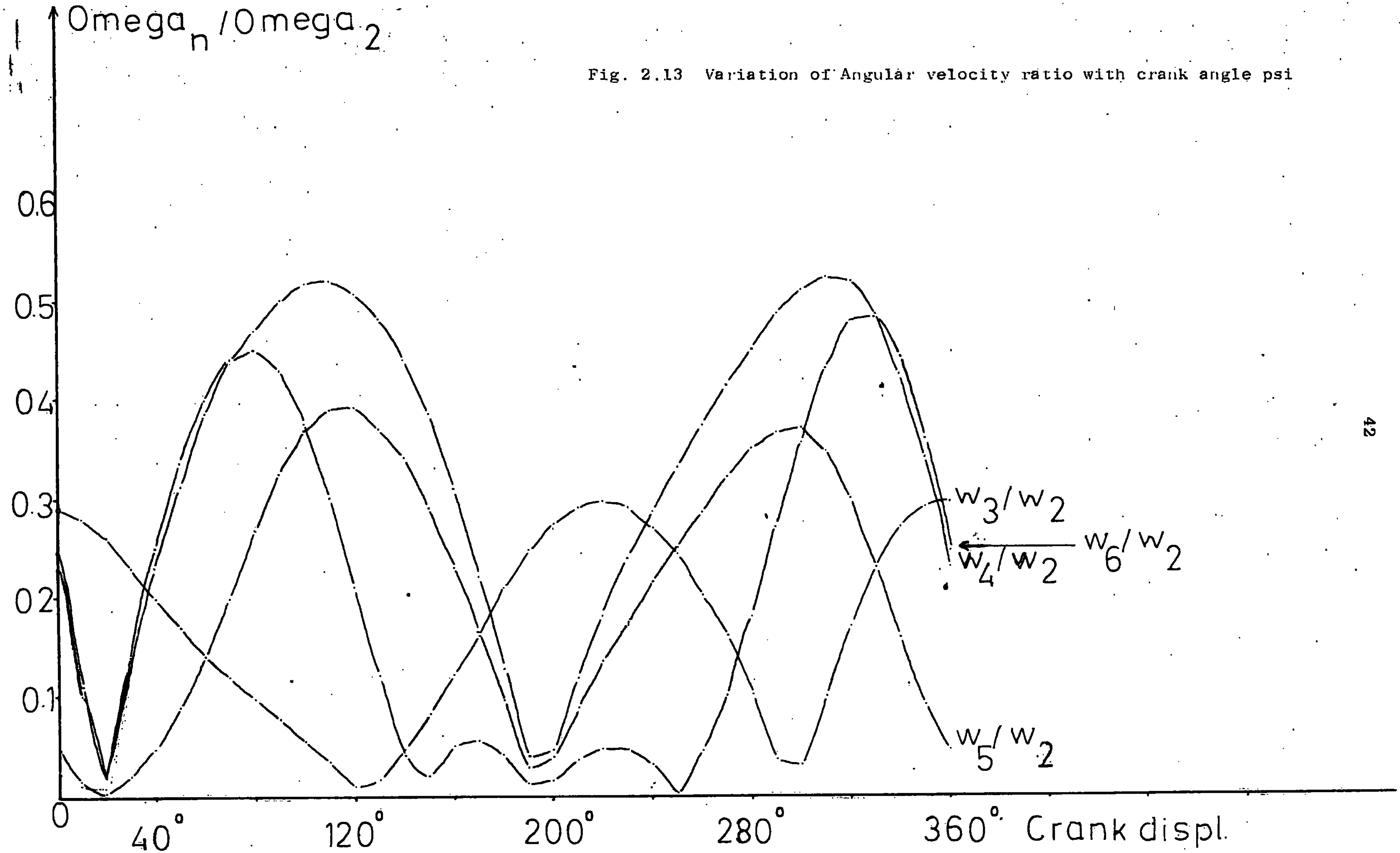

Fig. 2.13 Variation of Angular velocity ratio with crank angle psi

By using complex algebraic notation, the displacement equations can be expressed as;

$$(A + B)\, e^{i\beta_1} = D + C\, e^{i\alpha_1} \qquad (2.15)$$

$$Ae^{i\beta_2} + Be^{i(\beta_2 - \pi)} = D + Ce^{i\alpha_2} \qquad (2.16)$$

equating real and imaginary parts of equations (2.15) and (2.16) respectively;

$$(A + B) \cos\beta_1 - C \cos\alpha_1 = D \qquad (2.17)$$

$$(A + B) \sin\beta_1 - C \sin\alpha_1 = 0 \qquad (2.18)$$

$$(A - B) \cos\beta_2 - C \cos\alpha_2 = D \qquad (2.19)$$

$$(A - B) \sin\beta_2 - C \sin\alpha_2 = 0 \qquad (2.20)$$

from equations (2.17) and (2.18);

$$A + B = \frac{C \sin\alpha_1}{\sin\beta_1} = \frac{D + C \cos\alpha_1}{\cos\beta_1} \qquad (2.21)$$

from equations (2.19) and (2.20)

$$A - B = \frac{C \sin\alpha_2}{\sin\beta_2} = \frac{D + C \cos\alpha_2}{\cos\beta_2} \qquad (2.22)$$

from equation (2.21)

$$\frac{C}{D} = \frac{\sin\beta_1}{\sin(\alpha_1 - \beta_1)} \qquad (2.23)$$

from equation (2.22)

$$\frac{C}{D} = \frac{\sin\beta_2}{\sin(\alpha_2 - \beta_2)} \qquad (2.24)$$

equations (2.23) and (2.24) are combined to give;

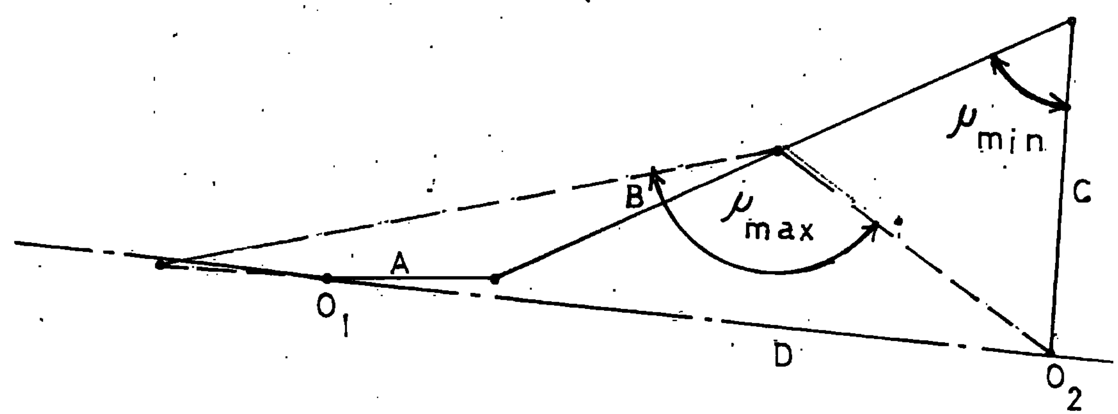

Fig. 2.14 a

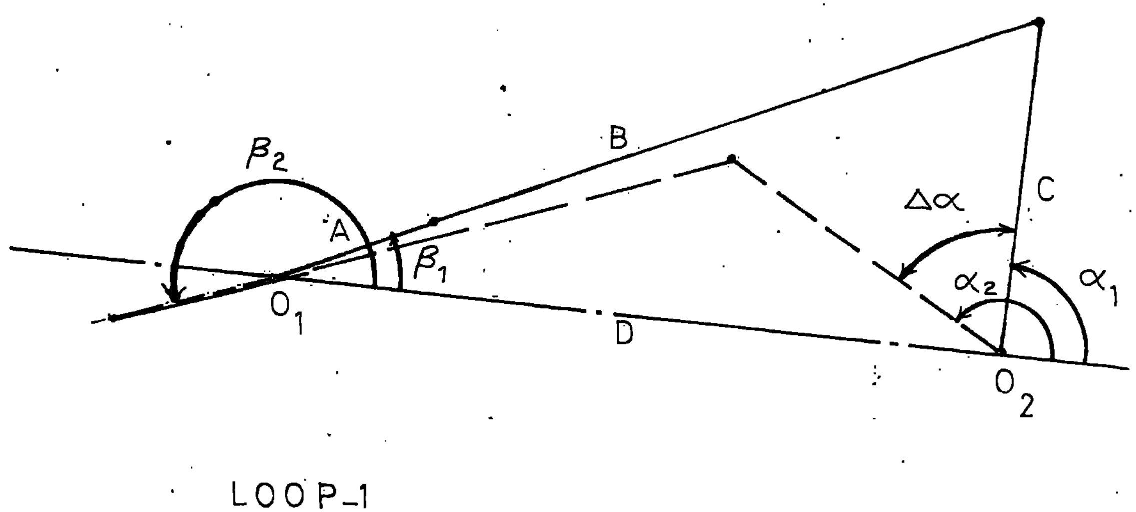

Fig. 2.14 b

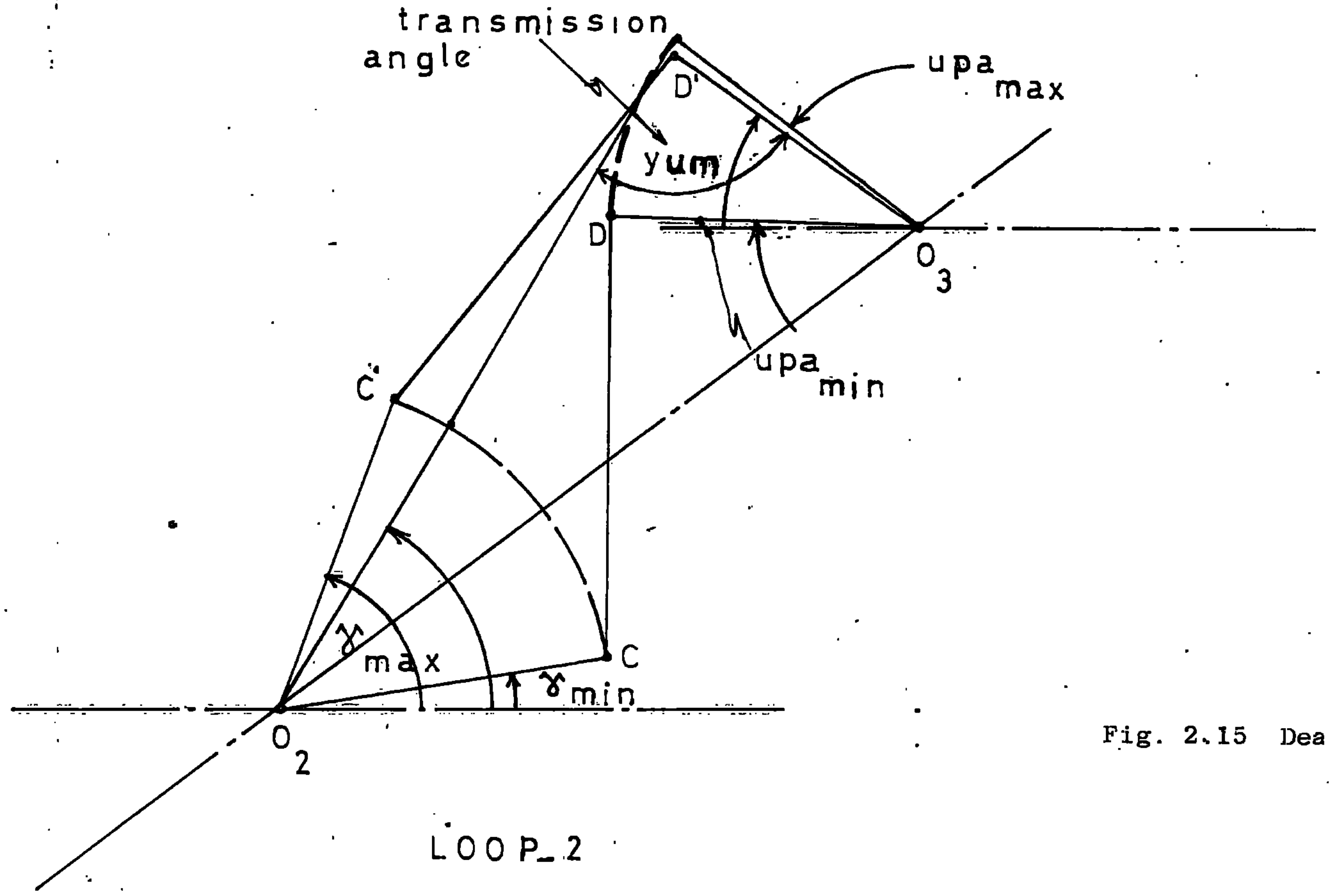

Fig. 2.15 Dead-centre positions for links 4 and 6

$$\frac{\sin \beta_1}{\sin (\beta_1 + \Delta\beta)} = \frac{\sin (\alpha_1 - \beta_1)}{\sin (\alpha_1 + \Delta\alpha - \beta_1 - \Delta\beta)} \qquad (2.25)$$

by expanding equation (2.25) and making the following substitutions;

$\gamma = \alpha_1 + \Delta\alpha - \Delta\beta$

$\delta = \alpha_1$

$\lambda = \Delta\beta$

$p = \cos \delta \cos \lambda - \cos \gamma$

$q = \sin \gamma + \cos \delta \sin \lambda - \sin \delta \cos \lambda$

$r = -\sin \delta \sin \lambda$

$$p \tan^2 \beta_1 + q \tan \beta_1 + r = 0 \qquad (2.26)$$

where $x = \tan \beta_1$

yield the quadratic equation;

$$p x^2 + qx + r = 0 \qquad (2.27)$$

where the initial angle of the input crank is;

$\beta_1 = \text{arc tan} (\pm x)$

($\pm x$) being the two roots.

There exists only one real root which gives the solution of β_1. The initial angle of the output lever arm can be calculated from;

$$\alpha_1 = \text{arc tan} \left[\frac{a (k + b)}{bf - ah} \right] \qquad (2.28)$$

where

$\xi = -\beta_1 + \Delta\alpha - \Delta\beta$

$a' = \sin \beta_1$

$b = \sin \beta_2$

$f = \cos \beta_1$

$h = \cos \xi$

$k = \sin \xi$

from equations (2.15) to (2.28), the following values have been calculated for loop 1;

$\beta_2 \cong 201^\circ$

$\beta_1 \cong 25^\circ$

$\alpha_1 \cong 90^\circ$

$\alpha_2 \cong 151^\circ$

It is desirable to have the transmission angle deviation as small as possible throughout the range of operation. The minimum permissible transmission angle depends on the magnitude of the transmitted forces, joint friction and manufacturing tolerances. The extreme values of the transmission angles are shown in Fig. (2.14 b). From the cosine law;

$$\mu_{min} = \arccos \left[\frac{B^2 + C^2 - (D - A)^2}{2\ BC} \right] \tag{2.29}$$

$$\mu_{max} = \arccos \left[\frac{B^2 + C^2 - (D + A)^2}{2\ BC} \right] \tag{2.30}$$

and

$$A^2 + D^2 = B^2 + C^2$$

while;

$$C = \frac{\sin\beta_1}{S_1} D \quad \text{or} \quad C = \frac{\sin\beta_2}{S_2} D$$

$$A = \left(\frac{r_1 + r_2}{2}\right) C \qquad B = \left(\frac{r_1 - r_2}{2}\right) C$$

where;

$$r_1 = \frac{\sin \alpha_1}{\sin \beta_1} \qquad r_2 = \frac{\sin \alpha_2}{\sin \beta_2}$$

$$s_1 = \sin (\alpha_1 - \beta_1)$$

$$s_2 = \sin (\alpha_2 - \beta_2)$$

substituting numerical values into equations (2.29) and (2.30)

$$\mu_{min} \cong 62^o$$

$$\mu min \cong 134^o$$

$$\Delta\mu \cong \mu_{max} - \mu_{min} = 72^o$$

In order to have a smooth motion throughout the whole range of operation, transmission angle is of the utmost importance. Freudenstein (1) has shown that a good choice of transmission angle also coincides with minimum overtones of the output lever, although a large transmission angle does not necessarily guarantee low fluctuation of torques. The force transmission from the coupler to the output lever is ideally effective when the transmission angle is nearly 90^o or deviates as little as possible from 90^o. A good discussion of the equations and procedure applied above are given in (1). Dead-centre positions of link 6 and link 4 are shown in Fig. (2.15). Variation of the transmission angle, yum, with crank angle psi has been presented in Fig. (2.6). Oscillating motion exercised by link 4 is transferred to link 6 via the intermediate link 5.

2.5 Application of Raven's Analysis

As shown in Fig. (2.16) each link is replaced by its position vector. Two seperate reference frames have been taken, x-y and x^1-y^1 corresponding to two seperate but dependent loops, loop 1 and loop 2 writing the summation law for the first loop, gives

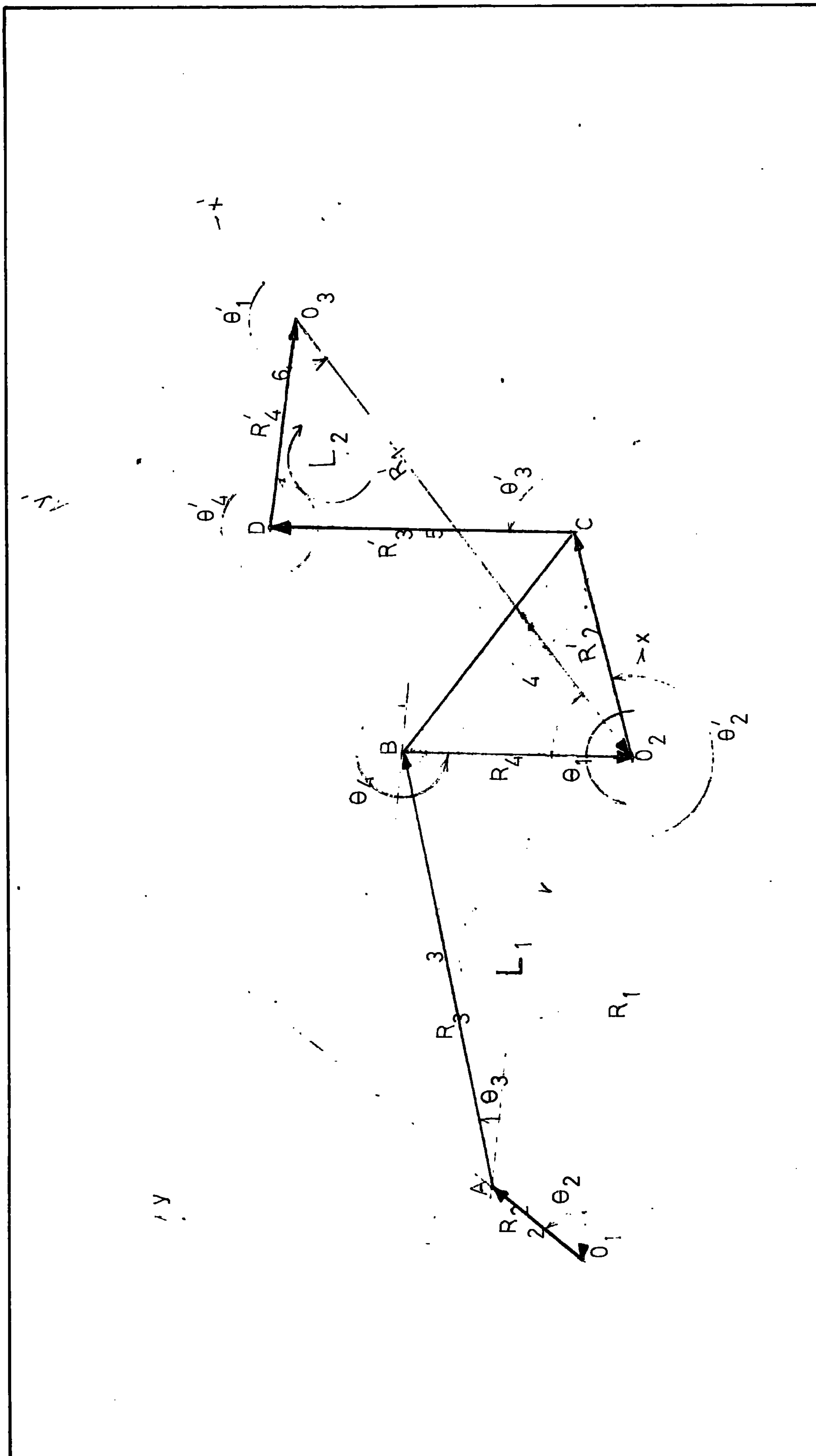

Fig. 2.16

$$R_1 + R_2 + R_3 + R_4 = 0 \qquad (2.31)$$

Transforming to complex notation,

$$r_1 e^{j\theta_1} + r_2 e^{j\theta_2} + r_3 e^{j\theta_3} + r_4 e^{j\theta_4} = 0 \qquad (2.31a)$$

In differentiating eq. (3.31a)

$$j r_2 \dot{\theta}_2 e^{j\theta_2} + j r_3 \dot{\theta}_3 e^{j\theta_3} + j r_4 \dot{\theta}_4 e^{j\theta_4} = 0 \qquad (2.32)$$

r_1, r_2, r_3, r_4 and θ_1 are constants.

Letting $\dot{\theta}_2 = \omega_2$, $\dot{\theta}_3 = \omega_3$ and $\dot{\theta}_4 = \omega_4$, gives

$$j r_2 \omega_2 e^{j\theta_2} + j r_3 \omega_3 e^{j\theta_3} + j r_4 \omega_4 e^{j\theta_4} = 0 \qquad (2.32a)$$

Equation (2.32a) contains the following quantities;

$$V_A = r_2\omega_2, \; V_{BA} = r_3\omega_3, \; V_B = r_4\omega_4,$$

and is the solution of the equation

$$V_B = V_A + V_{BA}$$

After a transformation to complex rectangular notation and a seperation of the real and imaginary terms eq. (2.32a) becomes;

$$r_2\omega_2 \cos\theta_2 + r_3\omega_3 \cos\theta_3 + r_4\omega_4 \cos\theta_4 = 0 \qquad (2.33a)$$

$$- r_2\omega_2 \sin\theta_2 - r_3\omega_3 \sin\theta_3 - r_4\omega_4 \sin\theta_4 = 0 \qquad (2.33b)$$

The unknown quantities in equations (2.33a) and 2.33b) are ω_3 and ω_4. Since there are two equations and two unknowns, ω_3 and ω_4 can be determined.

By differentiating equation (2.32a), using a uniform angular velocity of 2, gives

$$j^2 r_2\omega_2\dot{\theta}_2 e^{j\theta_2} + j r_3\dot{\omega}_3 e^{j\theta_3} + j^2 r_3\omega_3\dot{\theta}_3 e^{j\theta_3} + j r_4\dot{\omega}_4 e^{j\theta_4} + j^2 r_4\omega_4\dot{\theta}_4 e^{j\theta_4} = 0$$

(2.34)

where $j^2 = -1$ and $\dot{\omega}_n = \alpha_n$

$$- r_2\omega_2^2 e^{j\theta_2} + jr_3\alpha_3 e^{j\theta_3} - r_3\omega_3^2 e^{j\theta_3} + r_4\alpha_4 e^{j\theta_4} - r_4\omega_4^2 e^{j\theta_4} = 0 \qquad (2.34a)$$

the terms are identified as;

$$a_a^r = r_2\omega_2^2$$

$$a_{BA}^r = r_3\omega_3^2$$

$$a_B^r = r_4\omega_4^2$$

$$a_{BA}^t = r_3\alpha_3$$

$$a_B^t = r_4\alpha_4$$

$$a_a^t = 0$$

equation 2.34a corresponds to the vector equation,

$$A_B^t + A_B^r = A_A^t + A_A^r + A_{BA}^t + A_{BA}^r$$

corresponding to the acceleration polygon.

using the equation

$$e^{j\theta} = \cos\theta + j\sin\theta$$

equation (2.34a) can be transformed into complex rectangular notation.

Separating the real and imaginary terms gives;

$$- r_2\omega_2^2 \cos\theta_2 - r_3\alpha_3 \sin\theta_3 - r_3\omega_3^2 \cos\theta_3 - r_4\alpha_4 \sin\theta_4 - r_4\omega_4^2 \cos\theta_4 = 0 \qquad (2.35a)$$

$$- r_2\omega_2^2 \sin\theta_2 + r_3\alpha_3 \cos\theta_3 - r_3\omega_3^2 \sin\theta_3 + r_4\alpha_4 \cos\theta_4 - r_4\omega_4^2 \sin\theta_4 = 0 \qquad (2.35b)$$

the only unknowns in equations (2.35a) and (2.35b) are α_3 and α_4. The simultaneous solution of these equations utilising determinants yield values of α_3 and α_4.

Writing the summation law for the second loop gives,

$$R_1^1 + R_2^1 + R_3^1 + R_4^1 = 0$$

Transforming to complex notation

$$r_1^1 e^{j\theta_1^1} + r_2^1 e^{j\theta_2^1} + r_3^1 e^{j\theta_3^1} + r_4^1 e^{j\theta_4^1} = 0 \qquad (2.36)$$

where r_1^1, r_2^1, r_3^1, r_4^1 and θ_1^1 are constant

differentiating equation (2.36) gives

$$jr_2^1 \dot{\theta}_2^1 e^{j\theta_2^1} + jr_3^1 \dot{\theta}_3^1 e^{j\theta_3^1} + jr_4^1 \dot{\theta}_4^1 e^{j\theta_4^1} = 0 \qquad (2.37)$$

Letting $\dot{\theta}_2^1 = \omega_4$

$\dot{\theta}_3^1 = \omega_5$

$\dot{\theta}_4^1 = \omega_6$

$$jr_2^1 \omega_4 e^{j\theta_2^1} + jr_3^1 \omega_5 e^{j\theta_3^1} + jr_4^1 \omega_6 e^{j\theta_4^1} = 0 \qquad (2.37a)$$

equation (2.37a) contains the following quantities;

$V_c = r_2^1 \omega_4$

$V_{DC} = r_3^1 \omega_5$

$V_D = r_4^1 \omega_6$

and is the solution of the equation

$V_D = V_C + V_{DC}$

After a transformation to complex rectangular notation and a seperation of the real and imaginary terms eq. (2.37a) becomes;

$$r_2^1 \omega_4 \cos\theta_2^1 + r_3^1 \omega_5 \cos\theta_3^1 + r_4^1 \omega_6 \cos\theta_4^1 = 0 \qquad (2.38a)$$

$$- r_2^1 \omega_4 \sin\theta_2^1 - r_3^1 \omega_5 \sin\theta_3^1 - r_4^1 \omega_6 \sin\theta_4^1 = 0 \qquad (2.38b)$$

The unknown quantities in equations (2.38a) and (2.38b) are ω_5 and ω_6 . Solving them simultaneously gives ω_5 and ω_6. Differentiating equation (2.37) gives;

$$j r_2^1 \ddot{\theta}_2^1 e^{j\theta_2^1} - r_2^1 \dot{\theta}_2^{1\,2} e^{j\theta_2^1} + j r_3^1 \ddot{\theta}_3^1 e^{j\theta_3^1} - r_3^1 \dot{\theta}_3^{1\,2} e^{j\theta_3^1} + j r_4^1 \ddot{\theta}_4^1 e^{j\theta_4^1}$$
$$- r_4^1 \dot{\theta}_4^{1\,2} e^{j\theta_4^1} = 0 \qquad (2.39)$$

where

$$\ddot{\theta}_2^1 = \alpha_4 \qquad \dot{\theta}_2^{1\,2} = \omega_4^2$$

$$\ddot{\theta}_3^1 = \alpha_5 \qquad \dot{\theta}_3^{1\,2} = \omega_5^2$$

$$\ddot{\theta}_4^1 = \alpha_6 \qquad \dot{\theta}_4^{1\,2} = \omega_6^2$$

$$j r_2^1 \alpha_4 e^{j\theta_2^1} - r_2^1 \omega_4^2 e^{j\theta_2^1} + j r_3^1 \alpha_5 e^{j\theta_3^1} - r_3^1 \omega_5^2 e^{j\theta_3^1} + j r_4^1 \alpha_6 e^{j\theta_4^1}$$
$$- r_4^1 \omega_6^2 e^{j\theta_4^1} = 0 \qquad (2.40)$$

the terms are identified as;

$$a_c^r = r_2^1 \omega_4^2$$

$$a_c^t = r_2^1 \alpha_4$$

$$a_{Dc}^r = r_3^1 \omega_5^2$$

$$a_{Dc}^{t} = r_3^1 \alpha_5$$

$$a_D^{r} = r_4^1 \omega_6^2$$

$$a_D^{t} = r_4^1 \alpha_6$$

equation (2.40) corresponds to the vector equation,

$$A_D^t + A_D^r = A_C^t + A_C^r + A_{DC}^t + A_{DC}^r$$

corresponding to the acceleration polygon using the equation

$$e^{j\theta} = \cos\theta + j\sin\theta$$

equation (2.40) can be transformed into complex rectangular notation. Seperating the real and imaginary terms gives;

$$-r_2^1\alpha_4 \sin\theta_2^1 - r_2^1\omega_4^2\cos\theta_2^1 - r_3^1\alpha_5\sin\theta_3^1 - r_3^1\omega_5^2\cos\theta_3^1$$

$$- r_4^1\alpha_6\sin\theta_4^1 - r_4^1\omega_6^2\cos\theta_4^1 = 0 \qquad (2.41a)$$

$$r_2^1\alpha_4\cos\theta_2^1 - r_2^1\omega_4^2\sin\theta_2^1 + r_3^1\alpha_5\cos\theta_3^1 - r_3^1\omega_5^2\sin\theta_3^1$$

$$+ r_4^1\alpha_6\cos\theta_4^1 - r_4^1\omega_6^2\sin\theta_4^1 = 0 \qquad (2.41b)$$

The only unknowns in equations (2.41a) and (2.41b) are α_5 and α_6. A simultaneous solution of these equations yield values of α_5 and α_6.

2.6 Graphical Approach

The velocity and acceleration polygons have been solved graphically for a set of different crank positions and are presented in(A2).

2.7 Energy variation of the system

The total kinetic energy of the system at any instant is composed of the kinetic energy of translation about the mass centres of the links and the kinetic energy of rotation about the mass centres of the links and shafts. This can be expressed as in the following form;

$$\text{Total kinetic energy} = \tfrac{1}{2}\left[I_{01}\omega_2^2 + I_3\omega_3^2 + I_{02}\omega_4^2 + I_4\omega_4^2 + I_5\omega_5^2 + I_6\omega_6^2 + I_{03}\omega_6^2\right]$$

$$+ \tfrac{1}{2}\left[m_2V_{g2}^2 + m_3V_{g3}^2 + m_4V_{g4}^2 + m_5V_{g5}^2 + m_6V_{g6}^2\right] \qquad (2.42)$$

where $V_{g1\rightarrow6}$ = linear velocities of the mass centres of the corresponding links

in equation (2.42) $I_{01}\omega_2^2$ and $m_2V_{g2}^2$ are constants (since $\alpha_2 = 0$). The variation of the kinetic energies due to rotation of shafts O_2, O_3, link 4 and link 3 with the crank angle as shown in Fig. 2.17. The total kinetic energy due to translation is negligible in comparison with the kinetic energy due to rotation. Therefore equation 2.42 can be reduced to;

$$\text{Total kinetic energy} \cong \tfrac{1}{2}\left[I_3\omega_3^2 + I_{02}\omega_4^2 + I_4\omega_4^2 + I_5\omega_5^2 + I_6\omega_6^2 + I_{03}\omega_6^2\right] + C \qquad (2.43)$$

where $C = \tfrac{1}{2} I_{01}\omega_2^2$

variation of the total kinetic energy (excluding C) with the crank angle is shown in Fig. 2.18

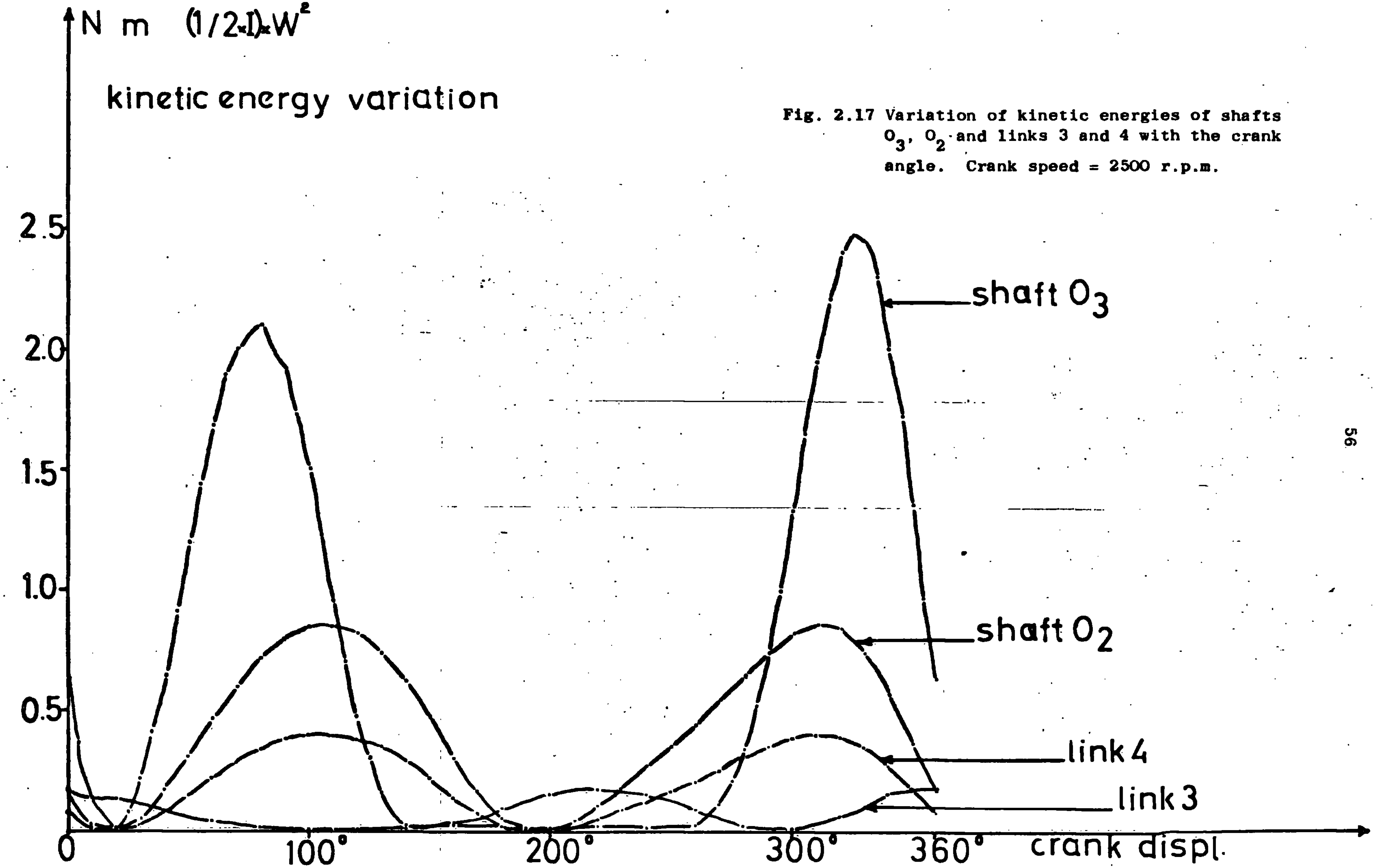

Fig. 2.17 Variation of kinetic energies of shafts O_3, O_2 and links 3 and 4 with the crank angle. Crank speed = 2500 r.p.m.

Fig. 2.18 Variation of the kinetic energy with the crank angle

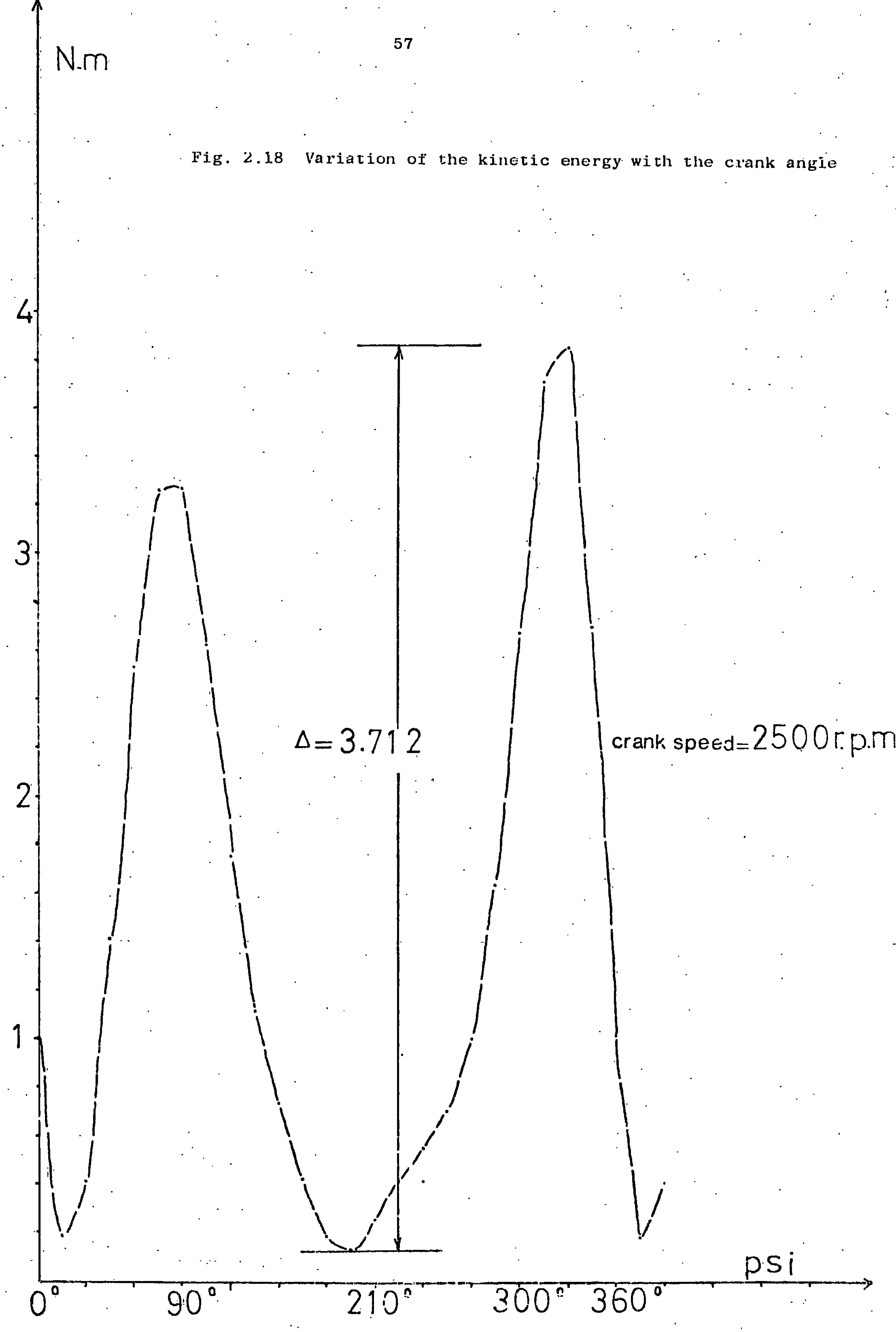

Chapter 3 Force and Stress Analysis

3.1 Kinetostatic Approach

The motion of the mechanism is completely specified and the purpose is to compute the bearing reactions, shaking forces, shaking moments as well as the forces and the torque required to produce the motion. The size, shape and material of each link are known. The inertia forces are taken as if they acted at a point on the links, although they are distributed along the links and are not concentrated at one point. In the following analysis the concern is only with the forces at points where the links are paired with other links. These forces are treated as external forces on the links. The shapes of the links are assumed to be rigid and the pin joints are considered to be frictionless. The inertia effects of the individual links, in comparison with the inertia effects of the shafts through O_2 and O_3 are reasonably negligible and this aspect of the dynamic analysis has been shown in further steps. However for a detailed dynamic analysis of the system, which is beyond the scope of the objective, the distribution of the inertia forces along the link can be important. In most advanced engineering cases the stresses due to inertia forces are determined by breaking the link into equal length sections. The inertia force for each section is determined from the mass of the section and the acceleration of the midpoint of the section which represents the distribution of the inertia forces along the link (21). In cases where the links are not of uniform cross section the accuracy of this approximation depends upon the number of sections that the link is broken into. By increasing the number of sections a greater accuracy can be achieved.

A solution to the dynamic force analysis of a four-bar planar mechanism has recently been presented (4), as a set of algebraic equations. The forces along the links 3 and 5 cause pure normal stresses, and the normal forces cause bending stresses. In the actual case the normal stresses vary along the links because of the inertia forces. The system has a single degree of freedom, the angular positions of links 3, 4, 5 and 6, given by $\phi_3 (t) = \beta$, $\phi_4 (t) = \gamma + 75^o$ $\phi_5 (t) = x\lambda$, and $\phi_6 (t) = 360^o$ - upa, are functions of the angular position $\phi_2 (t) = \psi$, and the length of the links. The link lengths are denoted by l_i , i = 2, 3, 4, 5 and 6, and each of the moving links has mass m_i , i = 2, 3, 4, 5, 6 and a moment of inertia I_i with respect to the centre of mass. The locations of the centres of mass of the members are defined by parameters l_i and θ_i. The bearing reaction F_{ij} is the force of member i on member j. The D'Alembert couple on link i is;

$$C_i = - I_i \ddot{\phi}_i$$

The x and y components of the D'Alembert force being;

$$D_{ix} = - m_i a_{ix}$$

and

$$D_{iy} = - m_i a_{iy}$$

where a_{ix} and a_{iy} are the corresponding acceleration components of the centre of mass of member i. The motion of the mechanism is known and the inertia loading on the system is defined. T_2 is the external torque on the input link 2, required to produce the prescribed motion. The dynamic equilibrium equations for the five moving links yield the following system of fifteen linear algebraic equations:

$$D_{2x} + F_{12x} - F_{23x} = 0 \quad \ldots\ldots\ldots\ldots\ldots \quad (3.1)$$

$$D_{2y} + F_{12y} - F_{23y} = 0 \quad \ldots\ldots\ldots\ldots\ldots \quad (3.2)$$

$$D_{3x} + F_{23x} - F_{34x} = 0 \quad \ldots\ldots\ldots\ldots\ldots \quad (3.3)$$

$$D_{3y} + F_{23y} - F_{34y} = 0 \quad \ldots\ldots\ldots\ldots\ldots \quad (3.4)$$

$$D_{4x} + F_{34x} + F_{14x} - F_{45x} = 0 \quad \ldots\ldots\ldots\ldots\ldots \quad (3.5)$$

$$D_{4y} + F_{34y} + F_{14y} - F_{45y} = 0 \quad \ldots\ldots\ldots\ldots\ldots \quad (3.6)$$

$$D_{5x} + F_{45x} - F_{56x} = 0 \quad \ldots\ldots\ldots\ldots\ldots \quad (3.7)$$

$$D_{5y} + F_{45y} - F_{56y} = 0 \quad \ldots\ldots\ldots\ldots\ldots \quad (3.8)$$

$$D_{6x} + F_{56x} - F_{67x} = 0 \quad \ldots\ldots\ldots\ldots\ldots \quad (3.9)$$

$$D_{6y} + F_{56y} - F_{67y} = 0 \quad \ldots\ldots\ldots\ldots\ldots \quad (3.10)$$

$$C_2 = - I_2 \ddot{\phi}_2$$

$$C_2' = - I_{01} \ddot{\phi}_2$$

$$C_2'' = - (I_2 + m_2 r_2^2 + I_{01}) \ddot{\phi}_2$$

where

I_{01} = Moment of inertia of the driving shaft through O_1

$$C_2'' - D_{2x} r_2 \sin \phi_2 + D_{2y} r_2 \cos \phi_2 + T_2 + F_{23x} l_2 \sin \phi_2 - F_{23y} l_2 \cos \phi_2 = 0 \ldots \quad (3.11)$$

$$C_3 = - I_3 \ddot{\phi}_3$$

$$C_3 - D_{3x} r_3 \sin\phi_3 + D_{3y} r_3 \cos\phi_3 + F_{34x} l_3 \sin\phi_3 - F_{34y} l_3 \cos\phi_3 = 0 \quad \ldots\ldots\ldots \quad (3.12)$$

$$C_4 = - I_4 \ddot{\phi}_4$$

$$C_4' = - I_{02} \ddot{\phi}_4$$

where

I_{02} = Moment of inertia of the shaft through O_2

$$C_4'' = - (I_4 + m_4 \, {}^{2}_{4} + I_{02}) \ddot{\phi}_4$$

$$C_4'' - D_{4x}r_4\sin(\phi_4 + \theta_4) + D_{4y}r_4\cos(\phi_4 + \theta_4)$$
$$- F_{34x}l_4\sin\phi_4 + F_{34y}l_4\cos\phi_4 - F_{45x}l_4\sin\phi_4^1$$
$$+ F_{45y}l_4\cos\phi_4' = 0 \quad \ldots\ldots \quad (3.13)$$

$$C_5 = -I_5\phi_5$$

$$C_5 - D_{5x}r_5\sin\phi_5 + D_{5y}r_5\cos\phi_5 + F_{56x}l_5\sin\phi_5$$
$$- F_{56y}l_5\cos\phi_5 = 0 \quad \ldots\ldots \quad (3.14)$$

$$C_6 = -I_6\ddot{\phi}_6$$

$$C_6' = -I_{03}\ddot{\phi}_6$$

where

I_{03} = Moment of inertia of the shaft through O_3

$$C_6'' = -(I_6 + m_6 r_6^2 + I_{03})\ddot{\phi}_6$$

$$C_6'' - D_{6x}r_6\sin\phi_6 - D_{6y}r_6\cos\phi_6 - F_{65x}l_6\sin\phi_6$$
$$+ F_{65y}l_6\cos\phi_6 = 0 \quad \ldots\ldots$$

(dot denotes differentiation with respect to time t)

The configuration of the mechanism and the free-body diagrams are shown in Fig.(3.1–3.2) for $\phi_2(t) = \psi = 50^o$. Relations of the form $F_{43x} = -F_{34x}$, etc., have been employed in the formulation of these equations. The shaking force F_s, is the resultant force on the frame. The x and y components of the shaking force are;

$$F_{sx} = F_{21x} + F_{41x} + F_{67x} = -F_{12x} - F_{14x} - F_{76x}$$
$$= D_{2x} + D_{3x} + D_{4x} + D_{5x} + D_{6x} \quad \ldots\ldots \quad (3.16)$$

and

$$F_{sy} = F_{21y} + F_{41y} + F_{67y} = -F_{12y} - F_{14y} - F_{76y} =$$
$$D_{2y} + D_{3y} + D_{4y} + D_{5y} + D_{6y} \quad \ldots\ldots \quad (3.17)$$

Fig. (3.1)

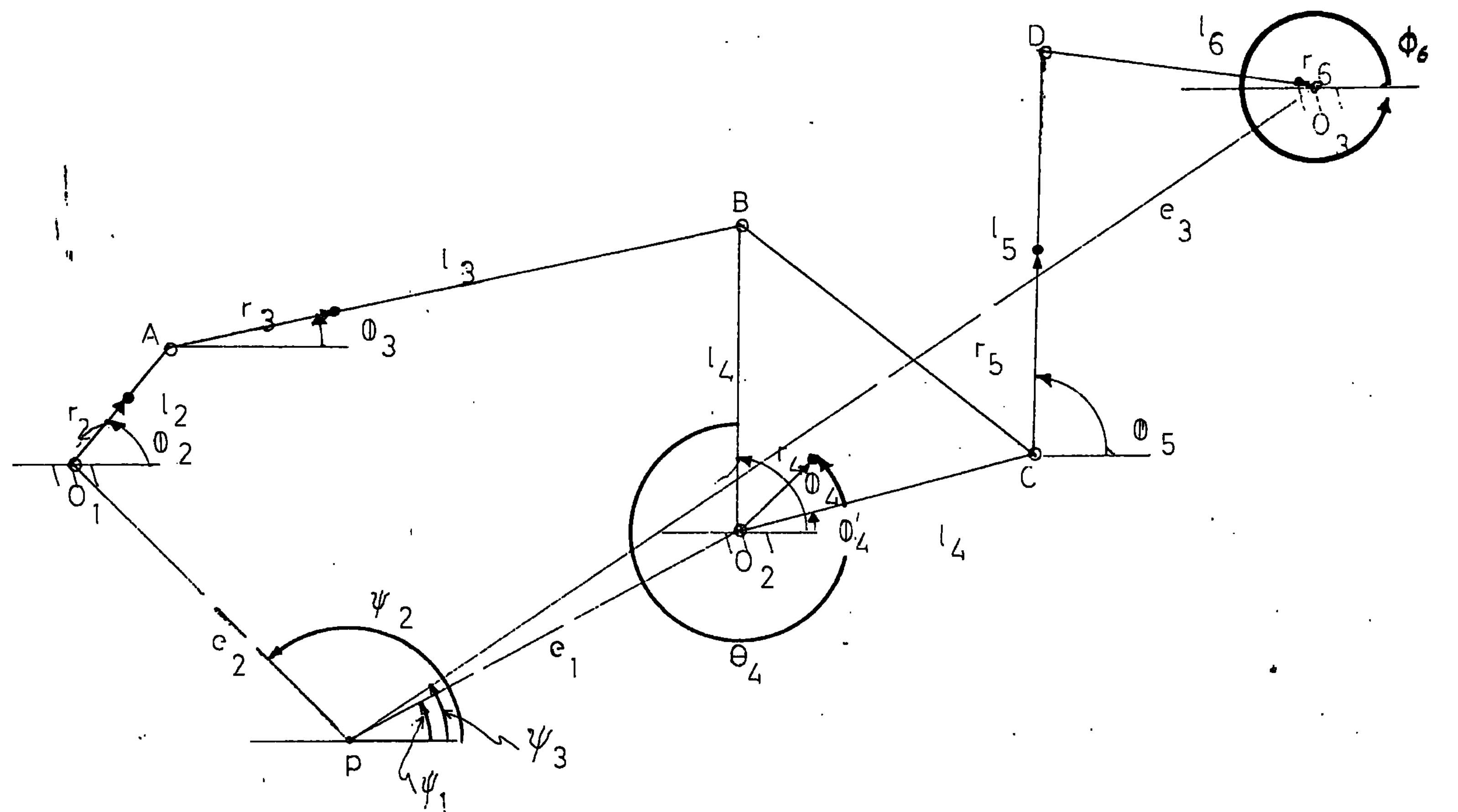
A
B
C
D
P
O1
O2
O3
l2
l3
l4
l5
l6
r2
r3
r4
r5
r6
e1
e2
e3
θ2
θ3
θ4
θ'4
θ5
Θ4
Φ6
ψ1
ψ2
ψ3

The shaking moment M_{sp} about an arbitrary point 'p' on the frame Fig. is

$$M_{sp} = -T_2 - F_{41x}e_1 \sin \psi_1 + F_{41y}e_1 \cos \psi_1$$

$$-F_{21x}e_2 \sin \psi_2 + F_{21y}e_2 \cos \psi_2 - F_{67x}e_3 \sin \psi_3$$

$$+F_{67y}e_3 \cos \psi_3 \quad \ldots\ldots\ldots\ldots\ldots\ldots\ldots \quad (3.18)$$

The effect of gravitational pull on the links has been neglected. The compressive and/or tensile forces acting on the links can be determined by resolving the forces acting on the links along themselves.

3.2 - Application of Virtual Work Method to the Mechanism

Energy methods can be used to short-cut the previous kinetostatic approach. The following solution, utilising the method of virtual work introduces greatest timesaving to the analysis. The main advantage of the method is that, it eliminates the link-to-link treatment, and permits an examination of the whole system at one time. A good discussion of this method is given in (8), and (9).

For any mechanism composed of n members, the method of virtual work is written:

$$T_n \cdot \Omega_n + F_n \cdot V_n + (-m_n A_{Gn} \cdot V_{Gn})$$

$$+ (-I_n \alpha_n \Omega_n) = 0 \quad \ldots \ldots \ldots \ldots \ldots \quad (3.19)$$

which can normally be solved for one quantity. Since the terms are vector quantities, the solution includes both the magnitude and direction of the unknown. Its major disadvantage is that since eq 3.19 contains only the applied forces and torques, it can not be used to solve for internal forces or the reactions between members of the mechanism. Formulation of eq. 3.19 utilizes an imaginary small displacement of the mechanism, being consistent with the constraints of the mechanism. The work done by the virtual displacements is referred to as virtual work and if the system is in static equilibrium under the action of the applied forces and torques then the work done with a virtual displacement is zero. Application of eq. 3.19 to the mechanism yields.

$$T_2 \Omega_2 + (-m_2 a_2 . v_2) + (-m_3 a_3 . v_3) + (-m_4 a_4 . v_4) + (-m_5 a_5 . v_5)$$
$$+ (-m_6 a_6 . v_6) + (-I_3 \alpha_3 \Omega_3) + (-I_5 \alpha_5 \Omega_5) + [-((I_4 + m_4 r_4^2) \alpha_4 \Omega_4]$$
$$+ [-((I_6 + m_6 r_6^2) + I_{03}) \alpha_6 \Omega_6] = 0 \quad \ldots\ldots\ldots\ldots\ldots\ldots \quad (3.20)$$

$$F_n V_n = 0$$

Substituting the appropriate values for 'ψ' equation (3.20) is used to calculate the external torque T_2. In the formulation of equation (3.19) the gravitational effects are neglected. A modified form of this equation taking account of gravitational effects is given in (8)

3.3 The Power equation

The power equation for the system can be written as;

$$T_2 \omega_2 - T_6 \omega_6 = T\omega \quad \ldots\ldots\ldots\ldots\ldots\ldots \quad (3.21)$$

where

T_2 = external torque applied on input link 2

T_6 = the torque transmitted by DO_3

$T\omega$ = power necessary to accelerate or to decelerate the system

ω = angular velocity of the shaft to which torque T is referred

Equation (3.21) corresponds to the dynamical relation:

Rate of work done by external forces = Rate of change of kinetic energy of the system

or alternatively:

Rate of work done by external forces = Rate of work done by effective forces

The variation of the torques transmitted by rigid link 4 and DO_3 are shown in Fig.(3.3) and in Fig.(3.4). The corresponding transmitted power is shown in Fig (3.5)

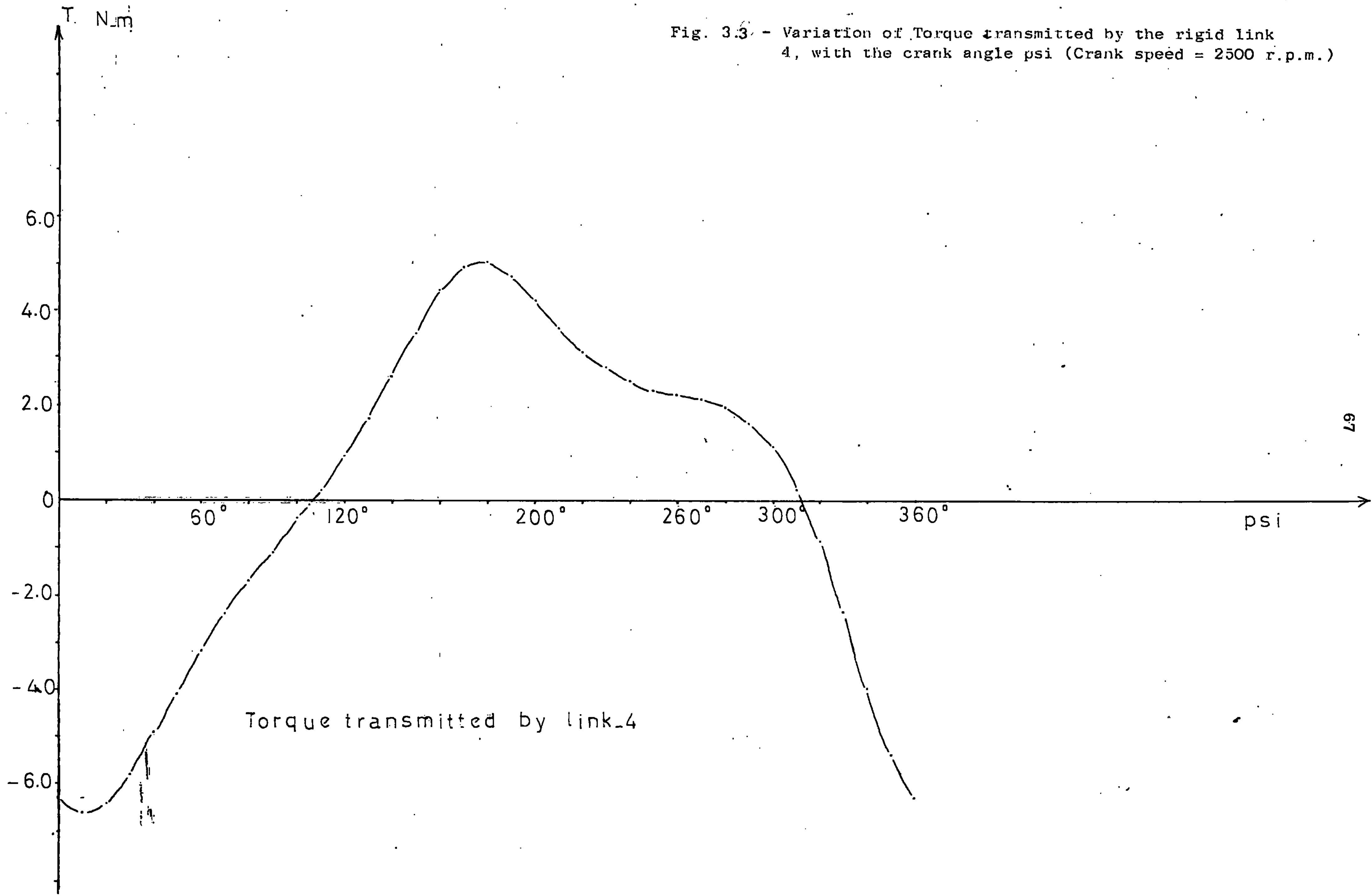

Fig. 3.3 - Variation of Torque transmitted by the rigid link 4, with the crank angle psi (Crank speed = 2500 r.p.m.)

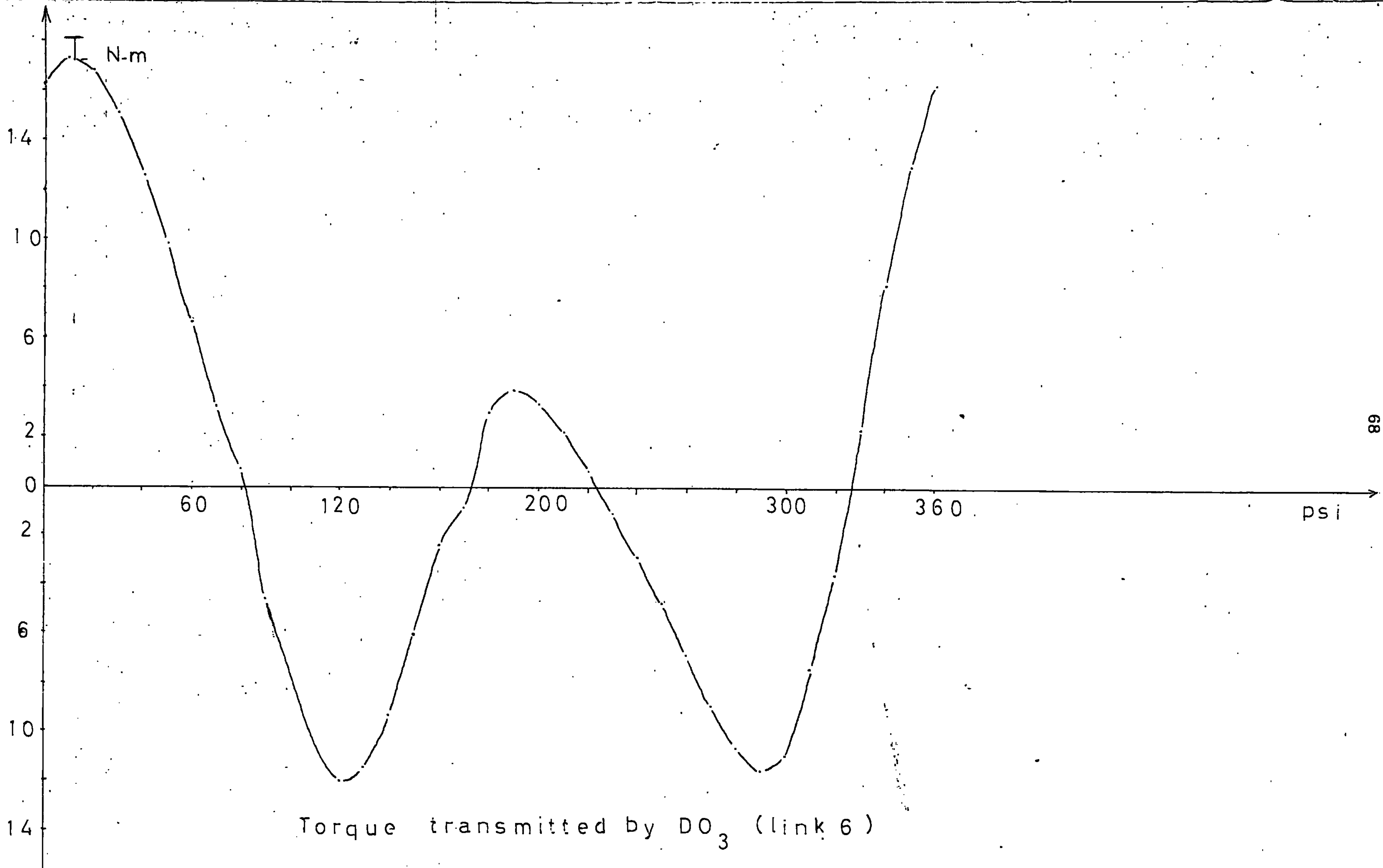

Fig. 3.4 - Variation of the Torque transmitted by link 6 (DO_3) with the crank angle psi (Crank speed = 2500 r.p.m.)

3.4 Graphical Approach

At any instant the motion of any induvidual link is equivalent to the rotation of the link as a whole about a fixed point in space. By determining instantaneous centres of rotation, (as shown in Figure (3.6) graphical force analysis), it is possible to determine the dynamic forces acting on the mechanism. A detailed analysis of this procedure is presented in (21), (14), (12), (13) and (3).

Referring to Fig.(3.6), $O_1ab\ O_2$ and $O_2\ cd\ O_3$ can be treated as two separate but dependent four-bar chains, I_1 and I_2 are the locations of the instantaneous centres of rotation. Both the linear velocity of the mass centres and the angular velocity of rotation vary from instant to instant. The line of action of the force applied to the links does not pass through their mass centres. The individual links are constrained to move in a definite way by the adjacent links to which they are connected, and the resultant of all the forces applied through those connections is equal to the force required to accelerate the link, the effective force R_i. The magnitudes of the effective force is replaced by another force equal to $-m_i\ a_{cgi}$, displaced from the mass centre a distance h_i. This fictitious force replaces the combined effects of the inertia torque and the inertia force. ab is a link with pins at A and B, constrained to move along the paths shown. Since the weight of the links is small in comparison to the other forces which act on the link, the effect of gravity is ignored as previously. The magnitude and lines of action of R_3 is determined. A similar procedure is applied to link cd. The force F_A which is applied to the link AB at pin A, by the crank arm O_1A will have a component F_a^{1}, tangential to the path of A and also a component F_a^{11}, perpendicular to the path of A. F_a^{1} does the useful work on the link, F_a^{11} constrains the pin A to follow the given path. This assumption is similarly valid for the forces acting at b,c and d. By calculating the

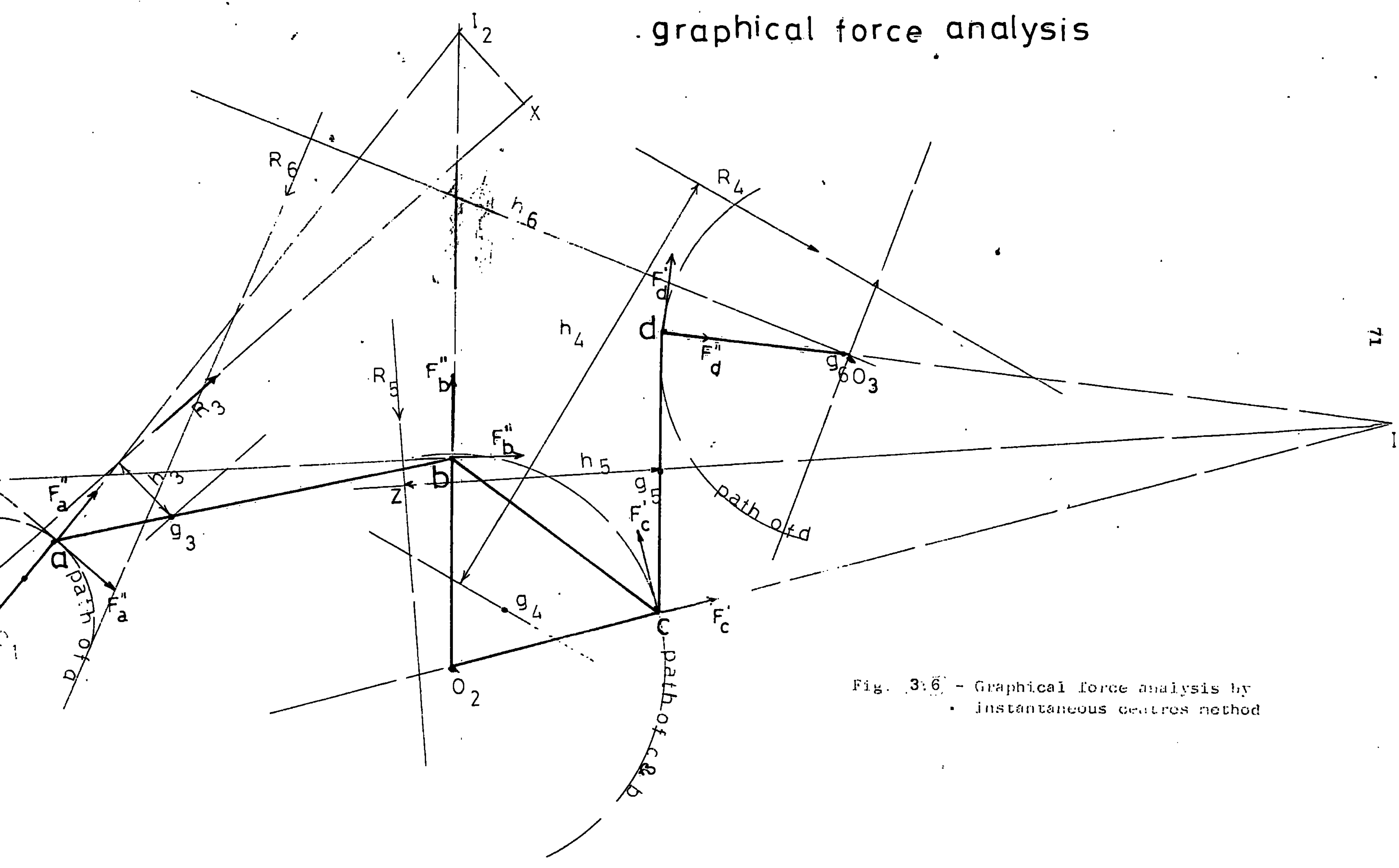

Fig. 3.6 - Graphical force analysis by instantaneous centres method

component in the tangential direction, the component in the normal direction and the two other components acting on the next pin are found from the equilibrium conditions of the link, namely, the vector sum of all the forces which act on the link being zero, and the algebraic sum of the moments of the forces about any point in their plane being zero. Components of F_a, F_b, F_c and F_d, normal to the paths of a, b, c and d are known. For link ab, the moments are taken about I_2, the point of intersection of the lines of action of F_b^{11} and F_a^{11}, and for link cd, about I_1, the intersection of the lines of action of F_c^{11} and F_d^{11}. The equations for F_b^1 and F_d^1 are then

$$F_b^1 = \frac{-F_a^1(ax) - R_3(I_2x)}{(bI_2)} \quad \ldots\ldots\ldots\ldots\ldots \quad (3.22)$$

$$F_d^1 = \frac{R_5(zI) - F_c^1(cI_1)}{(dI_1)} \quad \ldots\ldots\ldots\ldots\ldots \quad (3.23)$$

where

$R_3 = m_3 a_{g3}$ $\qquad h_3 = \dfrac{I_3\alpha_3}{-R_3}$

$R_4 = -m_4 a_{g4}$ $\qquad h_4 = \dfrac{I_4\alpha_4}{-R_4}$

$R_5 = -m_5 a_{g5}$ $\qquad h_5 = \dfrac{I_5\alpha_5}{-R_5}$

$R_6 = -m_6 a_{g6}$ $\qquad h_6 = \dfrac{I_6\alpha_6}{-R_6}$

The moment of inertia values for the shafts are included in the above expressions as appropriately. After the magnitudes of F_a^{11}, F_b^{11}, F_c^{11} and F_d^{11} are obtained by drawing the force polygon. The torque which must be applied by the crank arm O_1a, to the whole system, in order to overcome the combined effects of inertia is given by the product $F_a^1 . O_1a$.

As in the earlier sections, the crank is assumed to rotate at constant angular velocity ω_2.

3.5 Simplified Force Analysis

As mentioned in section 3.1 neglecting the inertia effects of links 3,4,5 and 6, which are relatively small in comparison with the inertia effects of shafts through O_2 and O_3, the force analysis can be simplified to a large extent. From Fig.(3.7), the force applied to link 5 by link 6, F_5, is determined by taking moment about O_3

$$T_6 = -I_{03}\alpha_6 = F_5 k_1 \quad \ldots\ldots\ldots \qquad (3.24)$$

where k_1 = Moment arm

from equation (3.24)

$$F_5 = \frac{-I_{03}\alpha_6}{k_1}$$

Repeating the same procedure for O_2

$$-I_{02}\,\alpha_4 + F_5 k_2 + F_3 k_3 = 0 \quad \ldots\ldots\ldots \qquad (3.25)$$

$$F_5^{1} = -F_5$$

$$F_3^{1} = -F_3$$

from equation (3.25)

$$F_3 = \frac{I_{02}\alpha_4 - F_5 k_2}{k_3}$$

Torque required to drive the mechanism is then,

$$T_2 = F_3 k_4$$

Although the analysis presented above does not give very accurate results, it offers a quick and reasonable method to determine the axial loading range on links 3 and 5.

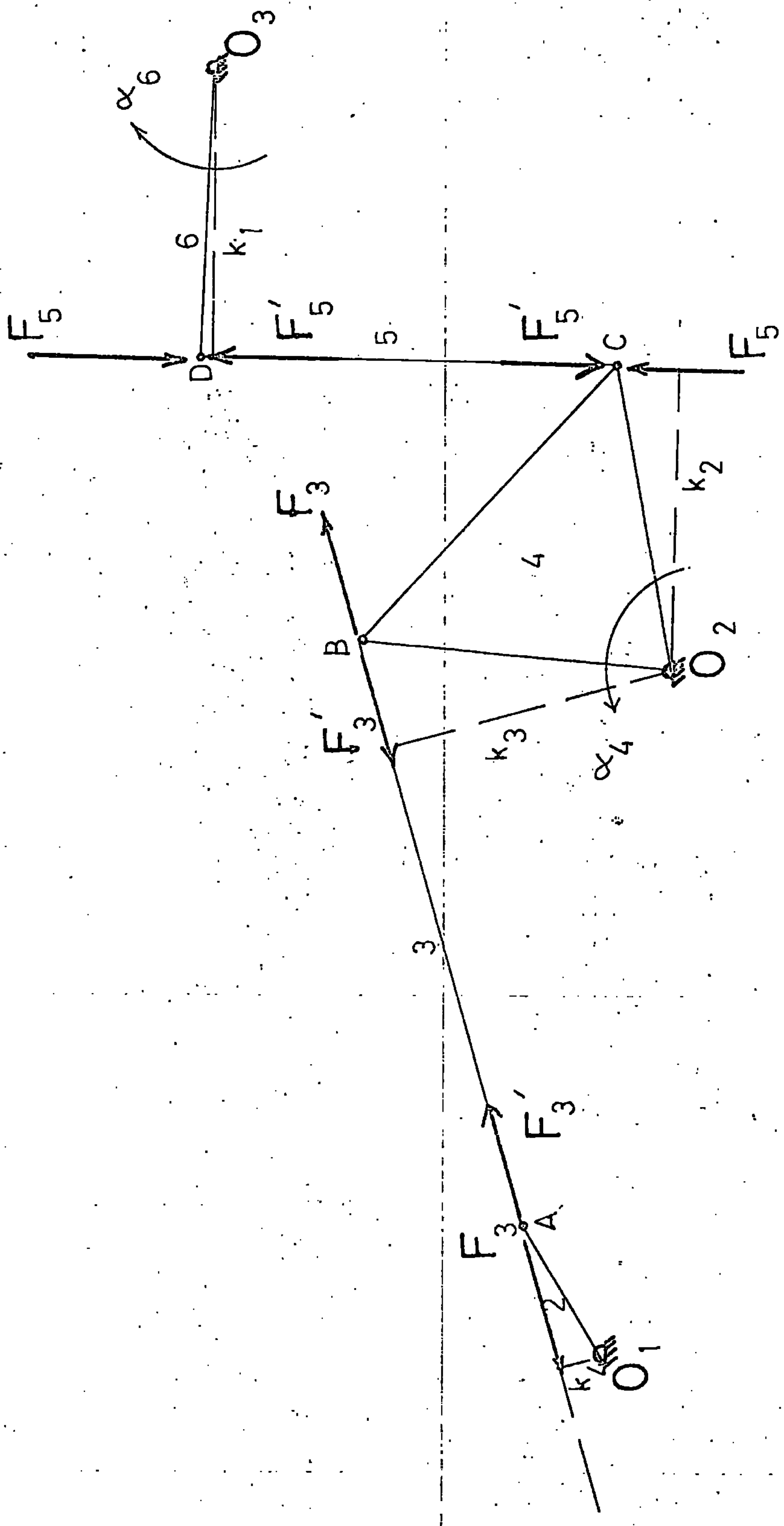

F_5
F'_5
F'_5
F_5
D
C
B
A
O_1
O_2
O_3
F_3
F'_3
F'_3
F_3
k_1
k_2
k_3
k
α_6
α_4
6
5
4
3
2

Fig. 3.7

3.6 Stress Analysis

The axial stress variation for links 3 and 5 are determined from;

$$\sigma_{5AX} = \frac{F_{5AX}}{A_1} \text{ and } \sigma_{3AX} = \frac{F_{3AX}}{A_2}$$

From Fig. (3.9) and (3.10)

A_1 = cross sectional area - link 3 - BB = $10^{-5} \times 14.95\ m^2$

A_2 = cross sectional area - link 5 - CC = $10^{-5} \times 6.32\ m^2$

The links do not have a uniform cross-sectional area thus axial stress varies accordingly. Stresses are proportional with the square of the crank speed. Variation of axial stresses for A_1 and A_2 are shown in Fig. (3.7) for a complete cycle, at a crank speed of 2500 r.p.m.

The peak to peak (maximum to minimum) stress values are referred to as stress range, and the variation of this range with respect to the square of the crank-arm angular velocity is given in Fig. (3. 8). Plane bending stress values for the same cross-sections of links 3 and 5 can be calculated from

$$\sigma_{5b} = \frac{M_5 y_{c5}}{I_{c5}} = \frac{F_{5b}(l_5/2)\ y_{c5}}{I_{c5}} \qquad \text{.................. (3.26)}$$

where y_{c5} = distance from the neutral axial-cross-section CC

I_{c5} = Moment of inertia of the cross-section CC

and

$$\sigma_{3b} = \frac{M_3 y_{b3}}{I_{B3}} = \frac{F_{3b}(l_3/2)\ y_{b3}}{I_{B3}} \qquad \text{.................. (3.27)}$$

where y_{b3} = distance from the neutral axis-cross-section BB

I_{B3} = Moment of inertia of the cross-section BB

and F_{5b} = force component acting normal to link 5

F_{3b} = force component acting normal to link 3

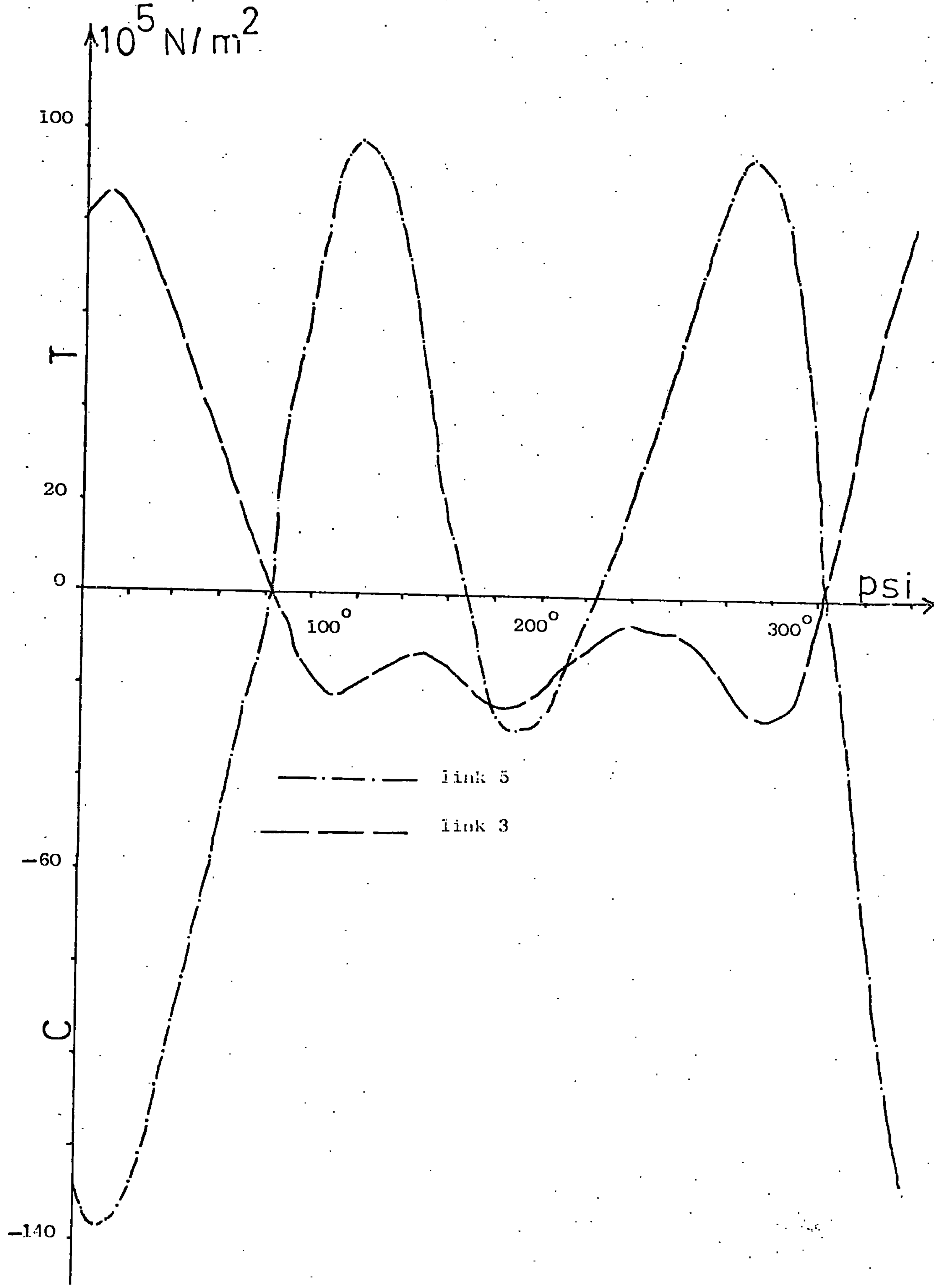

Fig. 3.7 Variation of axial stresses in links 3 and 5 with the crank angle (crank speed = 2500 r.p.m.)

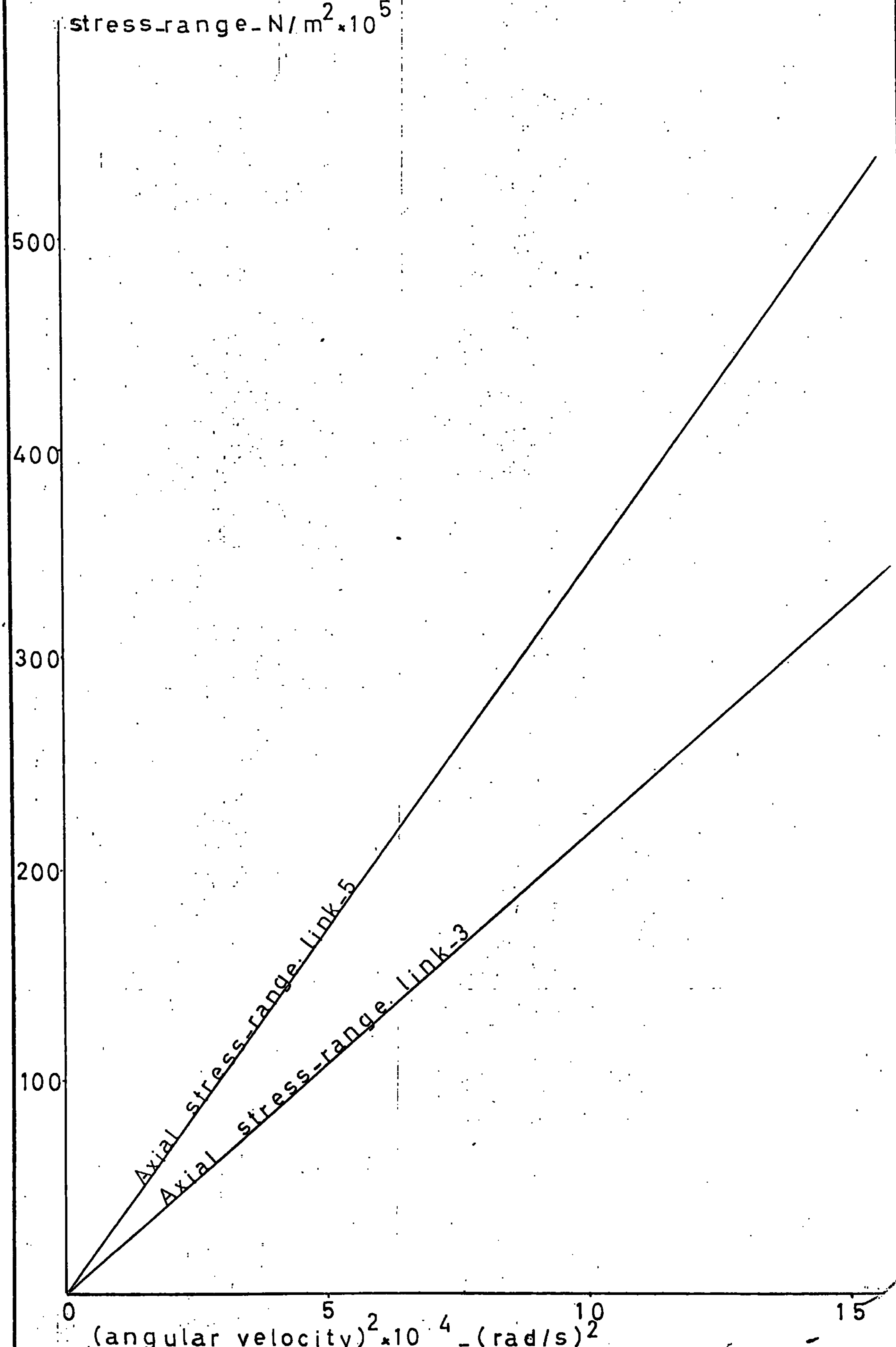

Fig. 3.8 - Theoretical variation of axial stress - range by the square of crank-speed

The links are treated to be beams of non-uniform cross-section, and magnitude of stress and deflection is assumed to be directly proportional to the load.

Resultant stress over a cross-section is then given by:

$$\sigma = \frac{F_{nax}}{A_n} \pm \frac{My_{cn}}{I_{cn}} \qquad \ldots\ldots\ldots\ldots\ldots\ldots \quad (3.28)$$

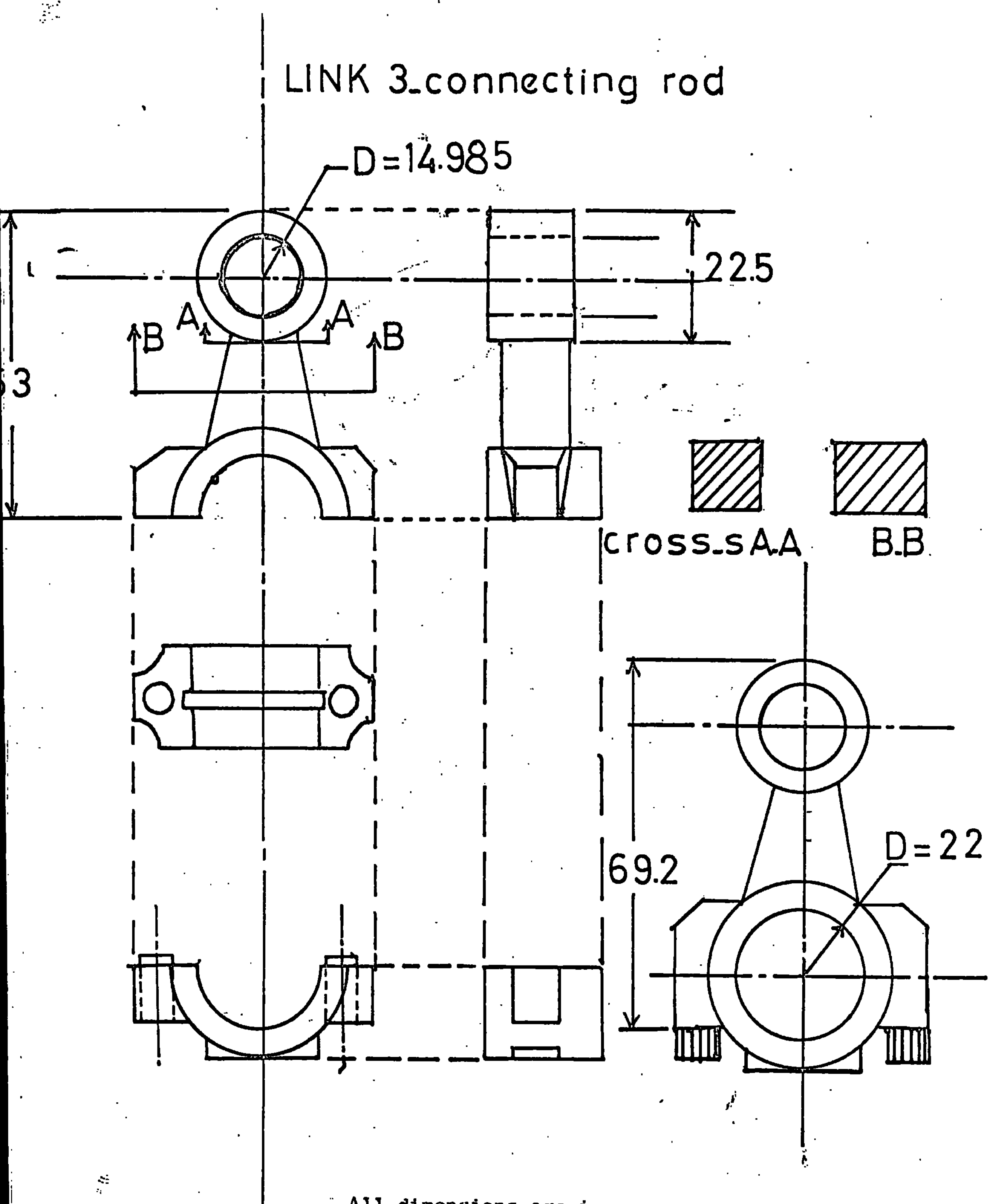

All dimensions are in mm

Fig. 3.9 Link 3

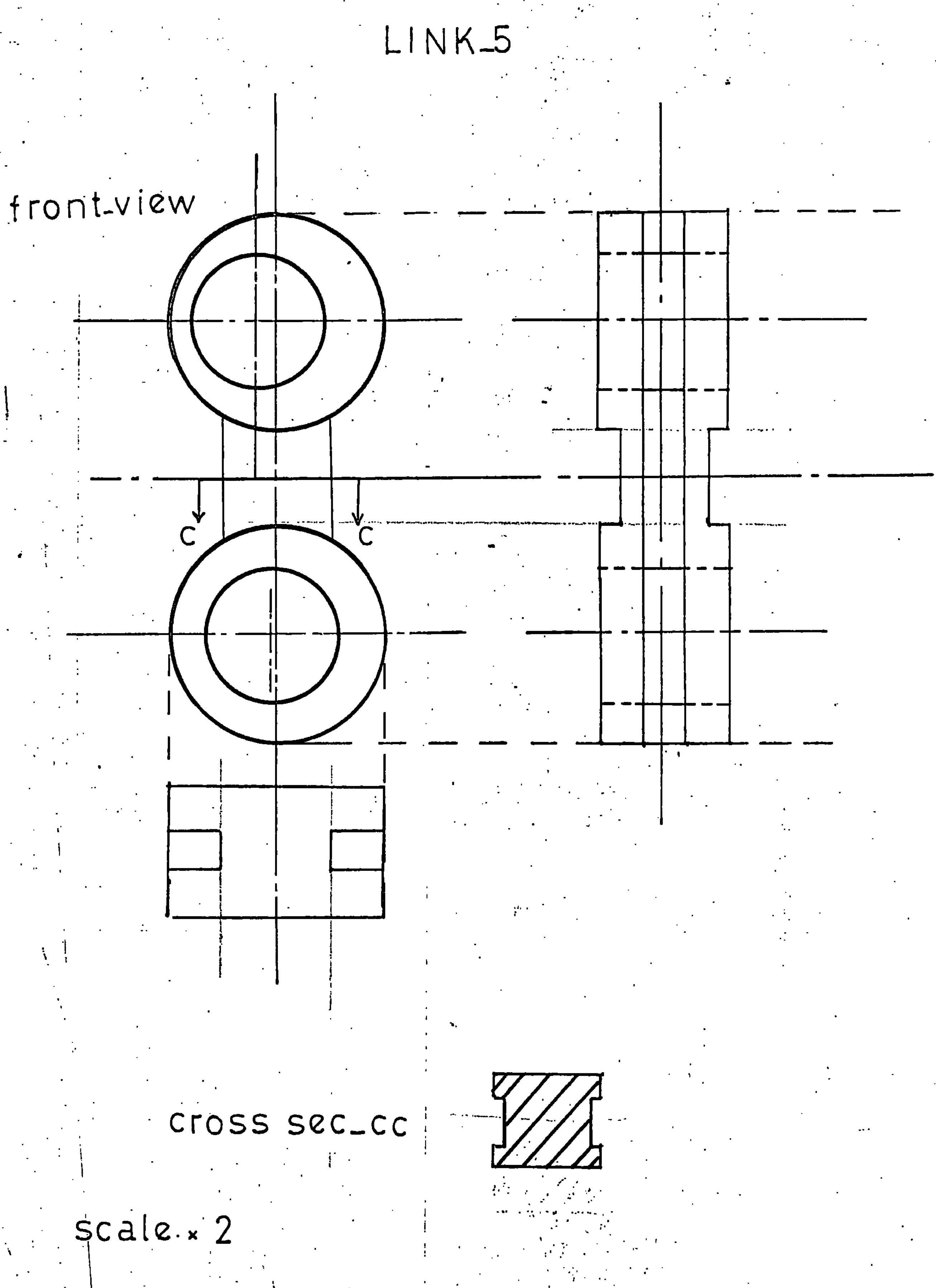

Fig. 3.10

Fig.3 11 - Variation of the external Torque T_2 required to drive the mechanism, with the crank angle psi

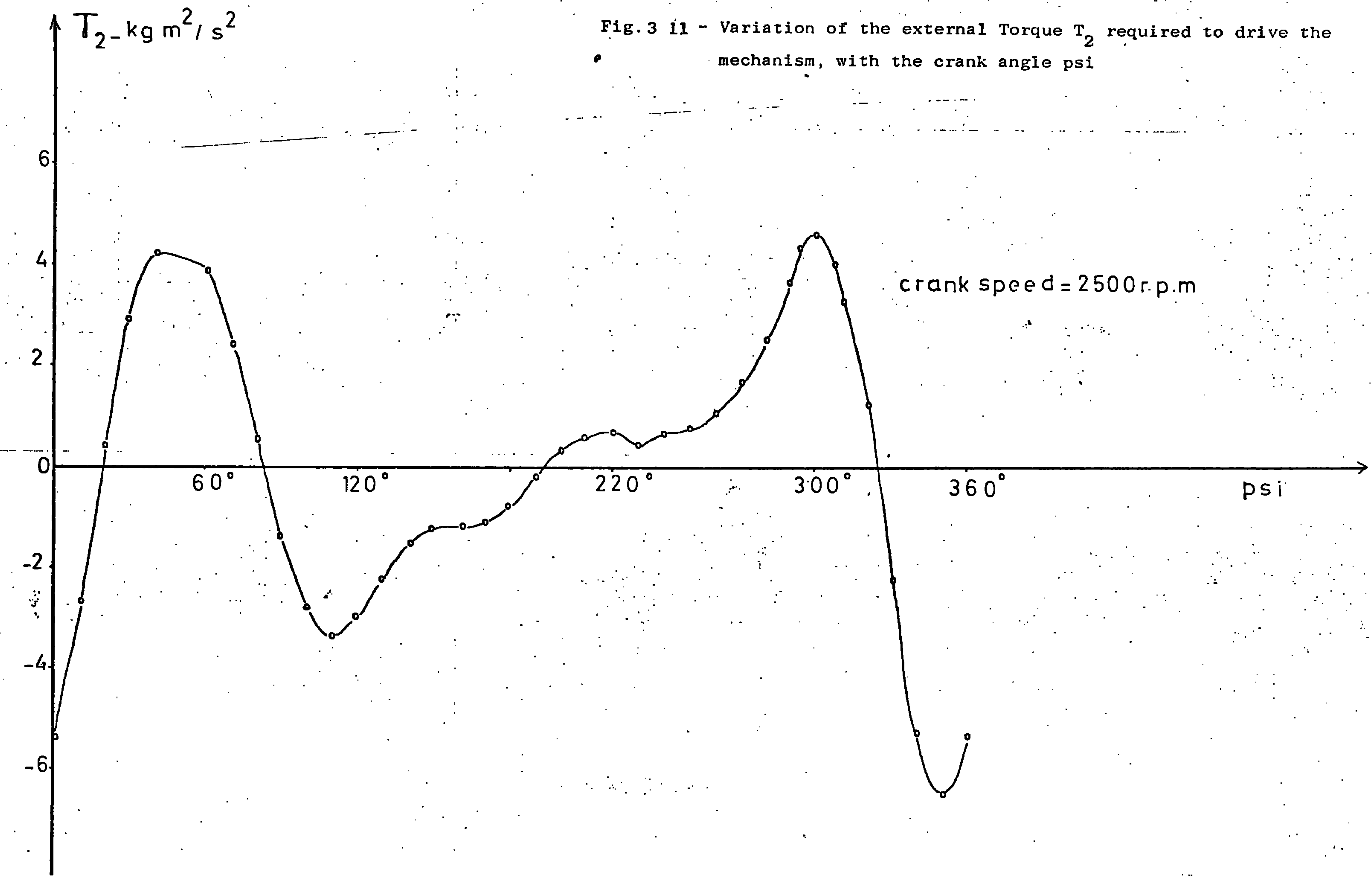

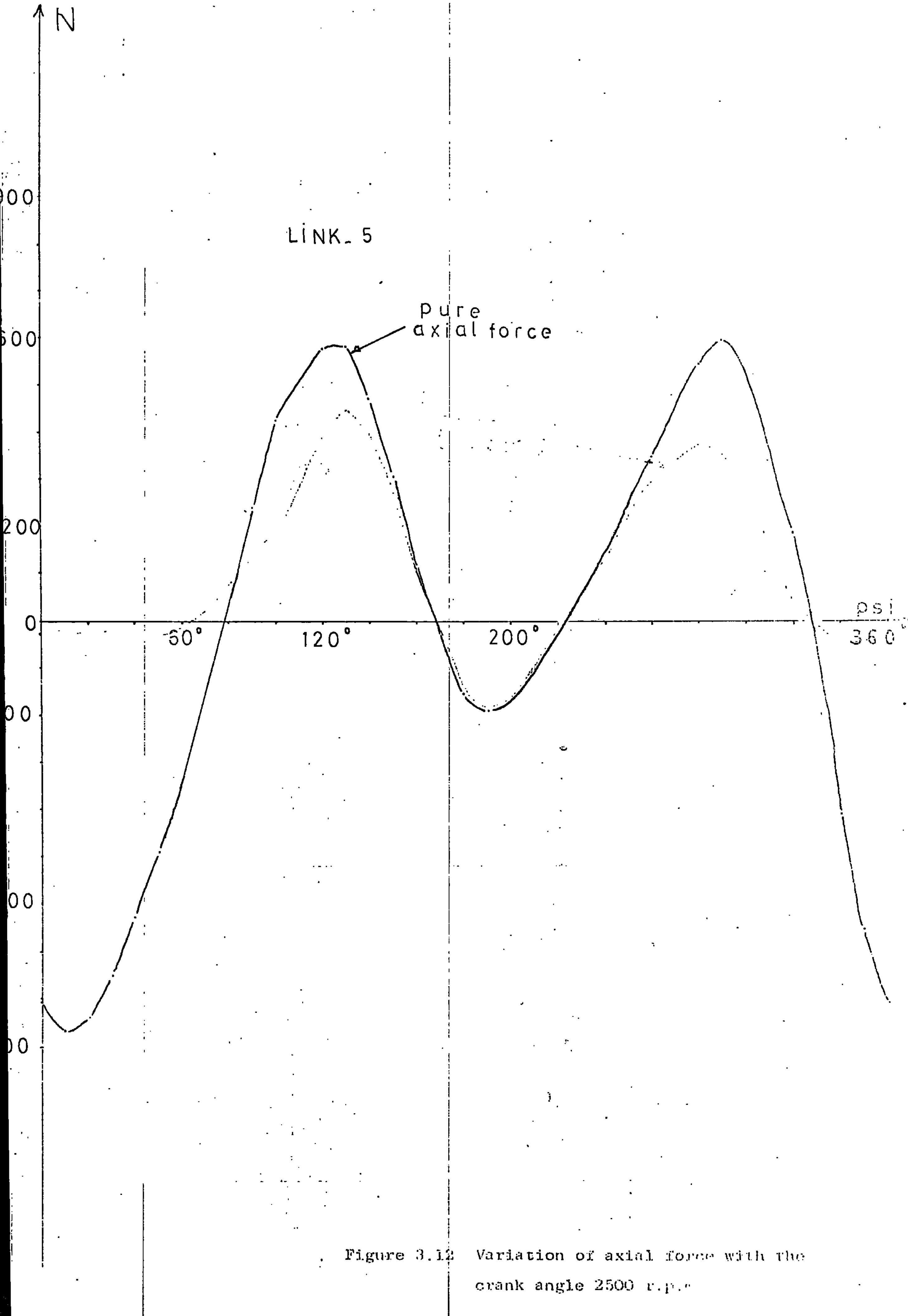

Figure 3.12 Variation of axial force with the crank angle 2500 r.p.m

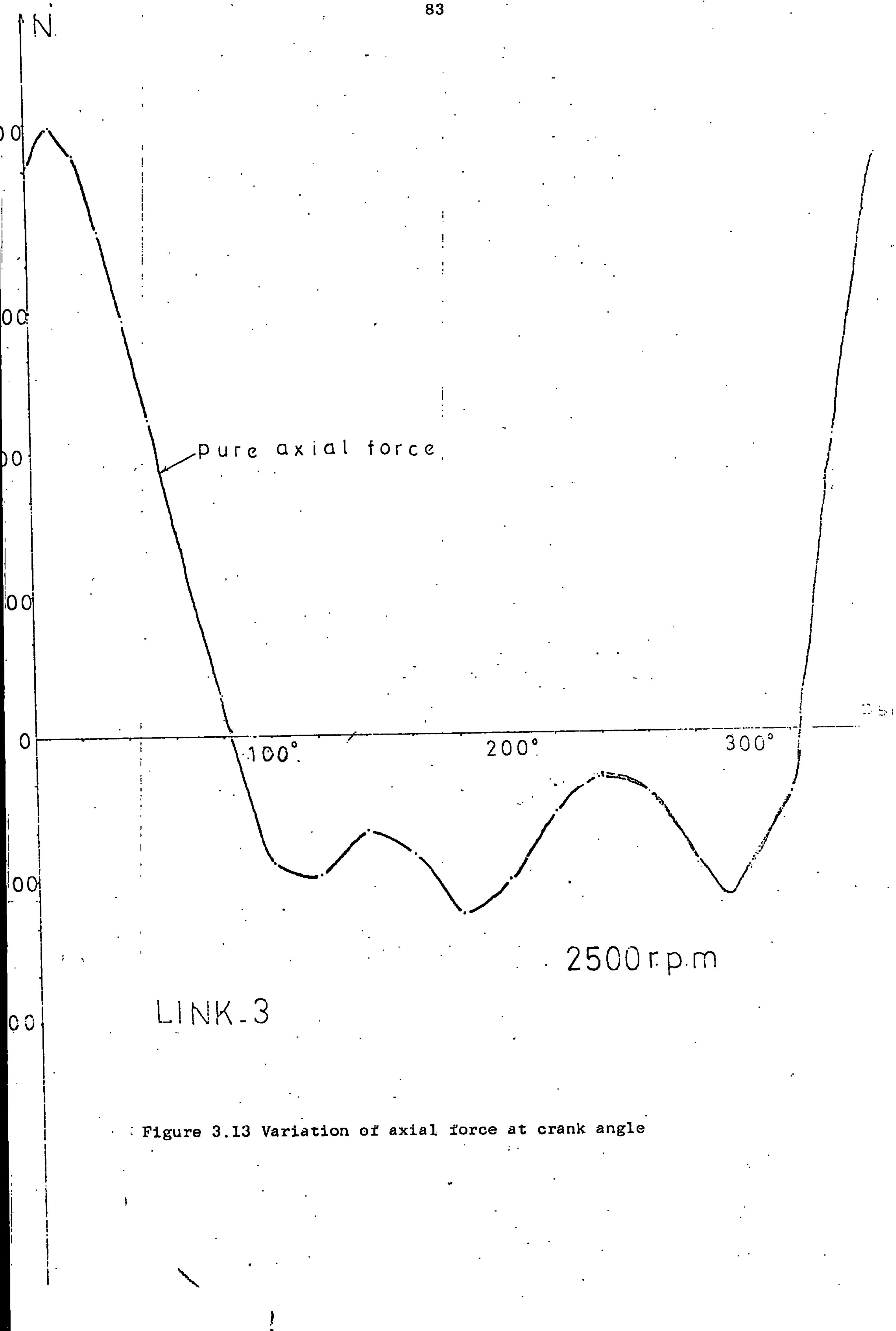

Figure 3.13 Variation of axial force at crank angle

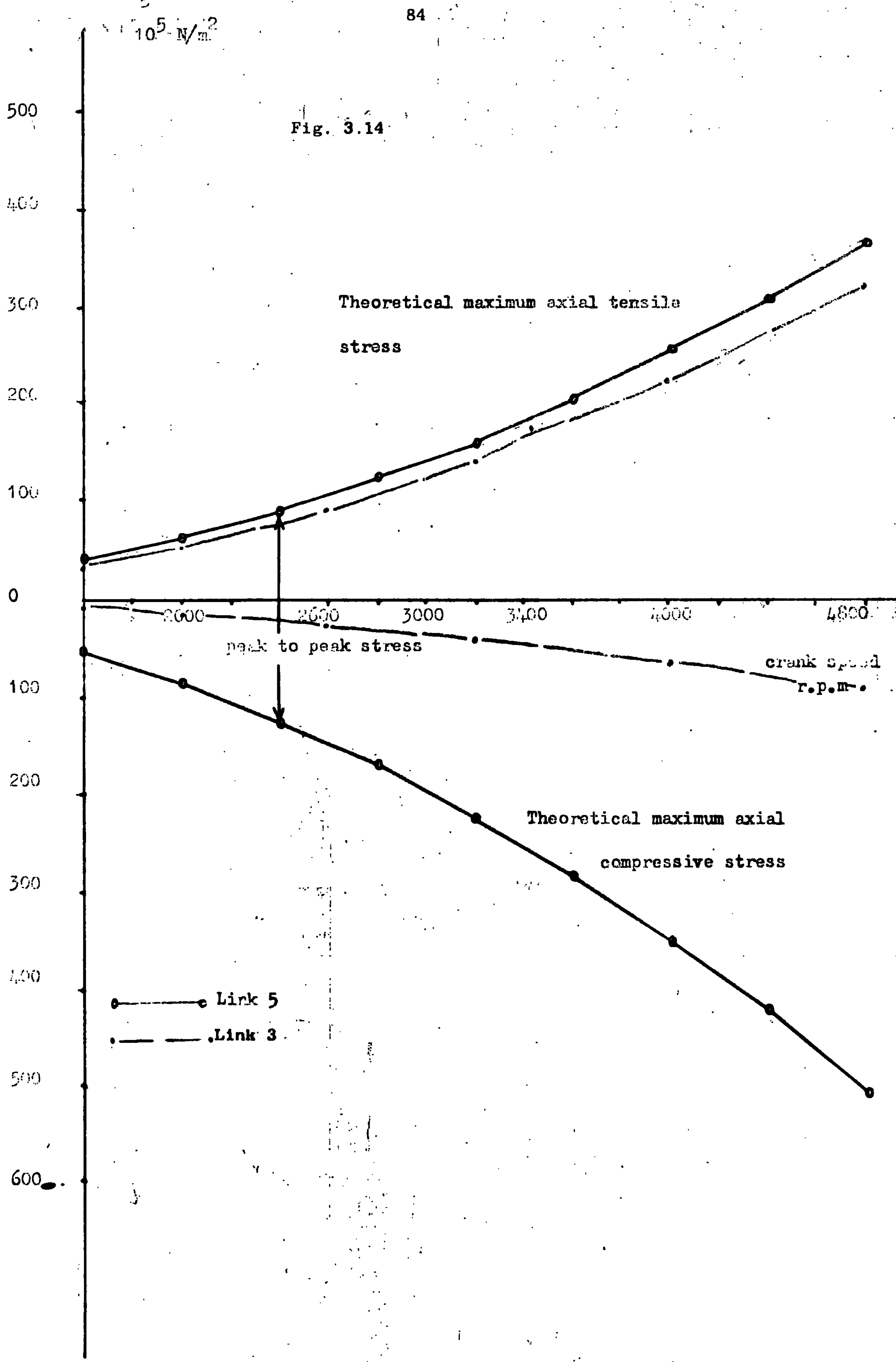

10^5 N/m^2
Fig. 3.14
500
400
300
200
100
0
100
200
300
400
500
600
Theoretical maximum axial tensile stress
2000
2600
3000
3400
4000
4800
peak to peak stress
crank speed r.p.m.
Theoretical maximum axial compressive stress
Link 5
Link 3

Chapter 4

Instrumentation, Experiments and Experimental Results

4.1 Instrumentation

The strain gauge installation and ancillary equipment is shown in Figs. (4.1),(4.2), Plate (4.1) and Plate (4.2). Each pair of gauges is wired in various configurations on the extension box to measure only axial and only bending (z direction) strains. The output from the extension box is fed into the carrier-amplifier where a metre is used in conjunction with the balance knobs on the extension box to balance the bridge circuit. The output from the amplifier is fed through a lead to an ultra-violet recorder where dynamic records are produced on photo-sensitive paper. To prevent failure due to overloading resistors and a fuse are connected in the leads to the u.v. recorder. If a record was not requir ed it was convenient to display the response of the strain gauges on the oscilloscope to examine the strain pattern.A slotted metal disc is attached to the drive shaft and an electro-magnetic pick-up unit is placed close to the disc to produce a variable voltage. This variable voltage showed one blip for each revolution of the shaft which is recorded by the u.v. recorder at the same time as the trace from the strain gauges was recorded, which enabled the speed of the shaft to be determined for each recording. A variable-speed 2HP electric motor is used to drive the loom Plate (4.2). The wires leading from the tag strips on the specimens to the extension box were partially protected by plastic tubes against fatigue failure. In order to prevent damage due to fracture at high operating speeds, a sheet steel cover is used over the combs. The basic principle applied in the design of the dynamic measuring system is that the whole set-up will faithfully measure the strain no matter how it varies with time. Since the signal from the strain-guage circuits is small a carrier amplifier is engaged, which is capable of recieving signals in the millivolt range and

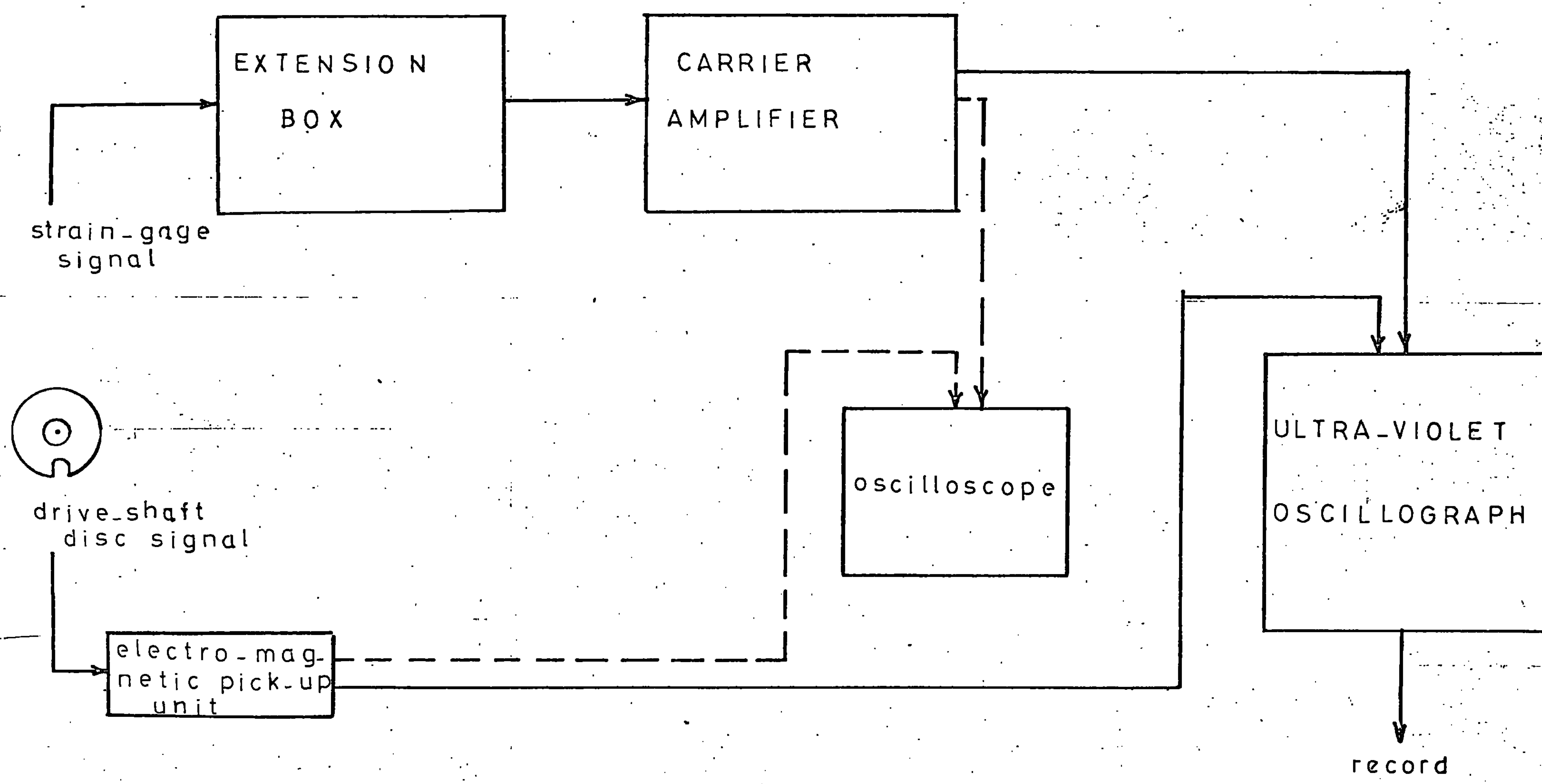

Fig. 4.1 Experimental set-up. Block diagram

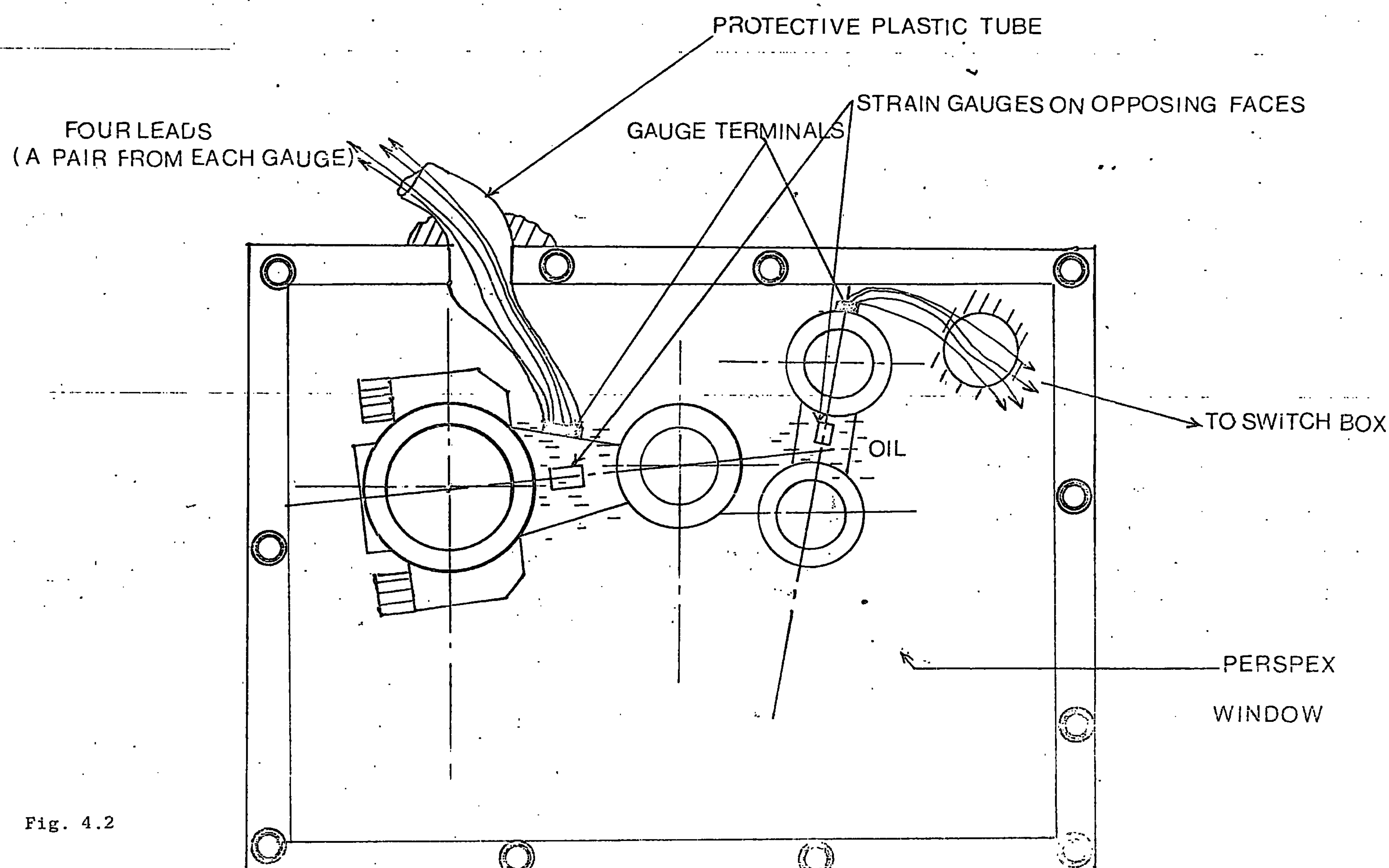
PROTECTIVE PLASTIC TUBE
STRAIN GAUGES ON OPPOSING FACES
FOUR LEADS
(A PAIR FROM EACH GAUGE)
GAUGE TERMINALS
TO SWITCH BOX
OIL
PERSPEX
WINDOW

Fig. 4.2

Plate 4.1 Oscilloscope, amplifier, switch box, u.v. recorder (with speed pick-up connection)

Plate 4.2 Featuring the viewing window modified to accept the strain gauge leads

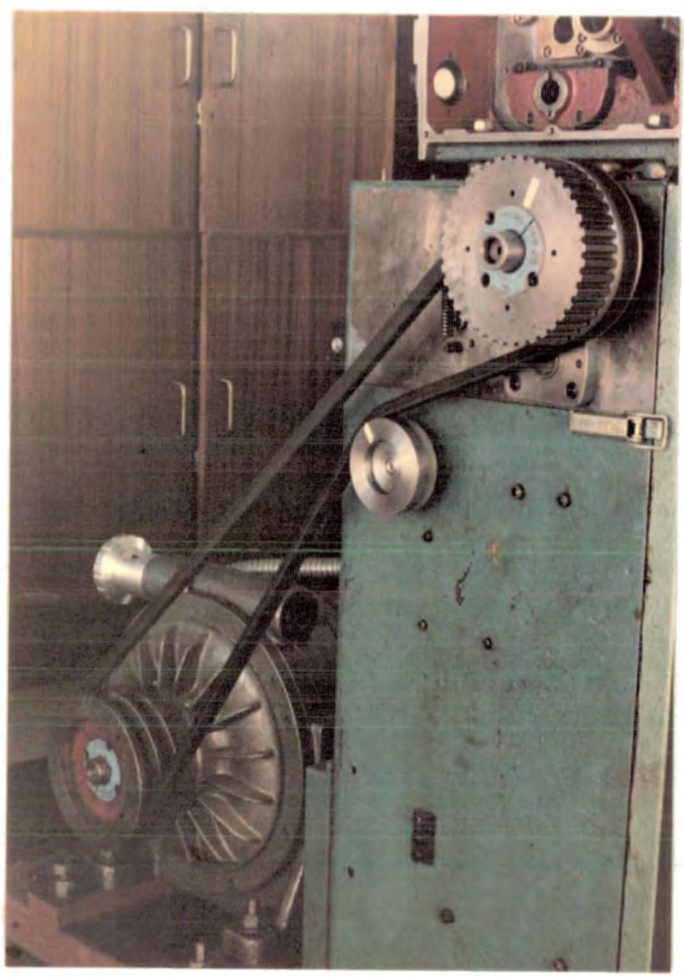

Plate 4.3 2 HP Electric motor and speed variator unit

of supplying a signal in the volt range. The record is on sensitized paper which requires no developing. A polaroid land-type camera is fitted to the oscilloscope to photograph the experiemntal strain pattern. The results are all taken from records produced by the u.v. recorder. It is assumed that the only resistive elements in the strain-gauge circuit are the gauges themselves (the presence of leads which affect sensitivity and calibration are negligable).

4.2 Elements of the Experimental Set-up.

1. Carrier-Amplifier; A Universal carrier-amplifier, type 581 DNH-Peekel, is used. Eleven gauge factors were available, ranging from 1.75 to 2.25, with an accuracy of 0.5%. Half and quarter-bridge (120 Ω) circuits are employed. There are six internal calibration values, 30, 100, 300, 1000, 3000 and 10000 microstrain. Bridge voltage is 5 volts, on the most sensitive range (3 μs, full-scale deflection) for one active strain-guage. The output gives 1 volt for full scale of the metre and remains linear for dynamic measurements even up to 10 volts. The specified accuracy of the equipment for dynamic measurements is ± 0.75% for all ranges. Time delay is 0.5 ms for 5000 Hz. Linearity of the recorder output is ± 0.05% for 2 volts peak-to-peak output and ± 0.1% for 20 volts peak-to-peak output, provided that the input is balanced for capacity. Drift is approximately 1 μ strain/day

2. Ultra-Violet Recorder; A "Southern Instruments" ultraviolet oscillograph 10-100 series is used for continuous direct recording of input signals. Signal is fed to a minature tubular galvanometer which reflects a spot of intense ultraviolet light onto the photosensitive record paper. The deflection of the galvanometer is a function of the amplitude of the input-signal current. A choice of eight paper speeds is available. Two of the input sockets are used. First one for the carrier-amplifier output-signal and the second one for the electromagnetic pick-up unit output-signal. A

paper speed of 37 mm/s is used for calibration while paper speeds of 111 and 333 m/s are alternatively used dueing actual measurements. Four fixed time intervals are available, 0.01, 0.1, 1 and 10 seconds, and the specified accuracy of the printed lines is within ± 2%. Paper speed stability is ± 3%. Since, instead of pen-aim, an ultraviolet light beam of zero mass is introduced, direct recording of frequencies up to 10 KHz can be performed. SMI, Type SMI/N, Ser. No. 1480-2 galvanometer is employed for recording.

3. Extension Box: A "Peekel 4-channel 4 UD" type switch box is used. There are four input channels, for full-bridge, half-bridge or quarter-bridge, 120 Ω configurations. Each channel has four balancing controls, three for resistive balancing and one for capacitive balancing of the bridge circuit. The specified typical error of switch contacts is 1 - 2 microstrain. Ranges of resistive and capacitive balancing are ± 6000 μs and ± 1000 pf respectively.

4. Oscilloscope: A cathode ray oscilloscope is employed to display the rapidly varying strain waveform. Since the output of the strain gauge circuit is connected to vertical amplifiers, vertical deflection is related to strain. The internal sweep circuit allows the trace to be driven horizontally at a preselected rate.

4.3 Strain gauges and gauge installations

Since strain gauges are used to measure varying and repeated strains, special care is exercised in gauge selection, in gauge bonding and in lead attachment. "Timsley, Telcon" elements type 7/120/EC, of different batch numbers, gauge factor = 2.18 Range = 120 Ω ± 1%, electrical strain gauges are employed. The resistive element is fixed to a transparent plastic base, and is bonded to the point at which strain is measured. The gauges are placed on the specimens as shown in Fig. (4.2). Although it was felt that helically wound wire gauges and "Isoelastic" wire gauges offer a superior fatigue life, recent research has shown that other standard gauges have as great or even greater fatigue life (6). Flat-grid, wire and foil metal gauges on paper back and bonded with cellulose nitrate cement have been strain cycled ($\pm$ 1000 μs / in for 1,250,000 cycles without failure (6)). Epoxy-backed foil metal gauges bonded with epoxy cements are capable of more than 300,000 cycles at $\pm$ 1500 μs. However it is generally agreed that as the magnitude of cyclic strain increases from 1500 μs, the fatigue life is reduced very rapidly (6). A well established fact is that the connection of the lead wires is one of the most critical steps in the installation of a gauge for cyclic strain service. Cyanoacrylate (Locktite, IS - 12 adhesive) is used to bond the base to the specimen. However since it is a poor gap filler the surface of the specimen is filed to obtain a smooth area and is cleaned with carbon tetracholoride and/or acetone. Dove and Adams (6) have used cyano-acrylate to measure dynamic strains (rise time 1 millisecond) as high as 2000 μs. Cyanoacrylate cement bonds under the action of modest contact pressure, and works satisfactorily up to temperatures of 120°C. Cement cures by chemical polymerization, and obtains its optimum adhesive strength after about 48 hours. In vibration environments the weak point of the gauge is the point at which the filament is connected to the gauge lead. The gauges are checked for correct bonding, gauge resistance and guage-to-specimen resistance by using a low-voltage type of mega ohm metre. The transverse sensitivity of the gauge is negligible, and it is assumed that, since the specimens have a relatively high modulus of elasticity, the strain is uniform, through the cross-sections at which the gauges are applied. The minor effect of localised stiffening on the surface, producing distortion of the strain pattern is neglected. The gauge factor is taken to be constant. since practically it is unchanged even in the plastic region. Unless, thermal or mechanical shock is expected, cyanoacrylate cement is regarded as superior to other gauge bonding materials for dynamic strain measurements. The oil temperature does not vary in short term operations and is assumed to stay constant.

The bonded gauges were firstprotected with Araldite against oil. However ordinary Araldite coating is attacked by the oil (Mobil Vactra oil) and failed to hold the installation. This major installation problem is solved by using "Micro Measurement Inc. M-Coat G Compound". In order to be able to measure the strains accurately, gauge instability and mechanical damage are minimized. Basic mechanical damages were due to vibration, high operating speed and limited available space. During measurements strain-gauge installations have been replaced several times because of mechanical damage and instability. Oil act to reduce the gauge-to-surface resistance or partially to short-circuit sections of the gauge itself. The effect of oil is to place a resistance path in parallel with the strain gauge, producing a change in resistance equivalent to strain. This effect is very important since the change associated with strain is very small. The coating material employed is a two-part 100% solids polysulphide modified epoxy compound, which provides a tough flexible layer, offering good protection against commercial oils, greases, gasoline, most acids, alkalis and most solvents. It cures to a firm, tack free condition in six hours at 24°C. Full cure in 24 hours again at 24°C. It can be safely used up to an oil temperature of 82°C. An incomplete protection around leadwires was very frequent and a common cause of oil penetration into the gauge installations. By introducing practical solutions, and getting familiar with the vital problems created by hostile environment, the number of installation failures are reduced, and longer terms of stability and accuracy in readings are achieved. Coatings are applied to cleaned surfaces, since coatings extending into unclean areas will loosen with time. Generally a thick coating offers a more difficult path for oil penetration than a thin one. M-Coat G forms a flexible rubbery coating, and its chemical resistance may be further improved by a one hour bake at 93^{o} C. The solder joints and wiring terminals are covered with a thin layer of M-Coat D (an air-drying solvent thinned acrylic coating) before applying M-Coat G in order to prevent any electrical leakage under adverse conditions. The prime coat dries in 15 minutes under normal ambient conditions. In applying M-Coat G care is taken to avoid air pockets and the coating is extended out as far as possible on all sides beyond the edges of the M-Coat D layer. Oil, most often, enters coated strain-gauge installations along insulated lead wires producing signals which are unrelated to, but hardly distinguishable from strain. For this reason wires are completely coated as far back from the installation as practical, which is usually not more than one cm, due to space limitations. However, most of the time insulated wire does not bond well to the coating.

4.4. Experiments

1. Dynamic Strain Measurements

As shown in Plate (4.3), a variable speed (480-4320 output r.p.m.), 2 HP, 3 phase 50 cycles electric motor is used to run the loom, replaced by the original 1.1 Kw, 1410 r.p.m., 1.5 HP, 3 phase 50 cycles motor. A tachometer is used to check drive shaft speed in addition to the u.v. recorder. The motor is calibrated against the drive shaft speed by using the variac speed selector unit. The bending strains measured are in the z direction, perpendicular to the x-y plane of the mechanism. The strains due to plane bending are not measured, (as explained in the introduction, see Section 1).

The results of the dynamic strain measurements are given in Table (4.2). Measurement periods,usually did not exceed 15 minutes. The drive shaft speed is gradually increased from approximately 1050 r.p.m to 2550 r.p.m. The circuit is rebalanced for resistance and capacitance before each run, and a calibration trace has been recorded. The basic problems encountered during dynamic-measurements are:

a - Gauge installation failures

b - Excess noise and vibration due to improper contact of bevel gears at high operating speeds

c - Mechanical failure due to slip between link 6 and shaft O_3

d - stretching and bending of the lead wires

2 Static Bending-strain measurement

To examine the nature of bending strains, a static bending strain test is performed on the mechanism. Fig. (4. 3) shows the simple set up. A 0.3 m lever arm is attached to the drive shaft to apply torques of known magnitude to the system. The test results are given in table (4. 3). The shaft O_3 is locked by a clamp mechanism to allow the forces to be transmitted throughout the links. Both axial and bending strains (z direction) are measured under the same loading conditions.

The variation of axial and bending (z direction) stresses with the applied torque in each link are shown in Figs. (4.4) and (4.5). Applied torque is increased up to 74 N.m. Half-bridge (120 Ω) circuits are employed during measurements. The crank angle 'psi' is kept 90° (from the horizontal in counter-clockwise direction).

3 Stress distribution in links 3 and 5

Using the same experimental set-up, strain variation within the links themselves are measured. Strain-gauges on opposing faces of link 5 are identified as gauges m and k. Quarter-bridge (120 Ω) circuit is employed to measure the combined axial and bending strain on each face separately by feeding the two lead-wires directly into the carrier amplifier. The procedure is repeated for both gauges by reversing the link. During the measurements crank angle 'psi' is kept at 90°. A maximum torque of 35.3 N.m is applied to the main drive shaft via the lever-arm. The pure axial compressive strain is then

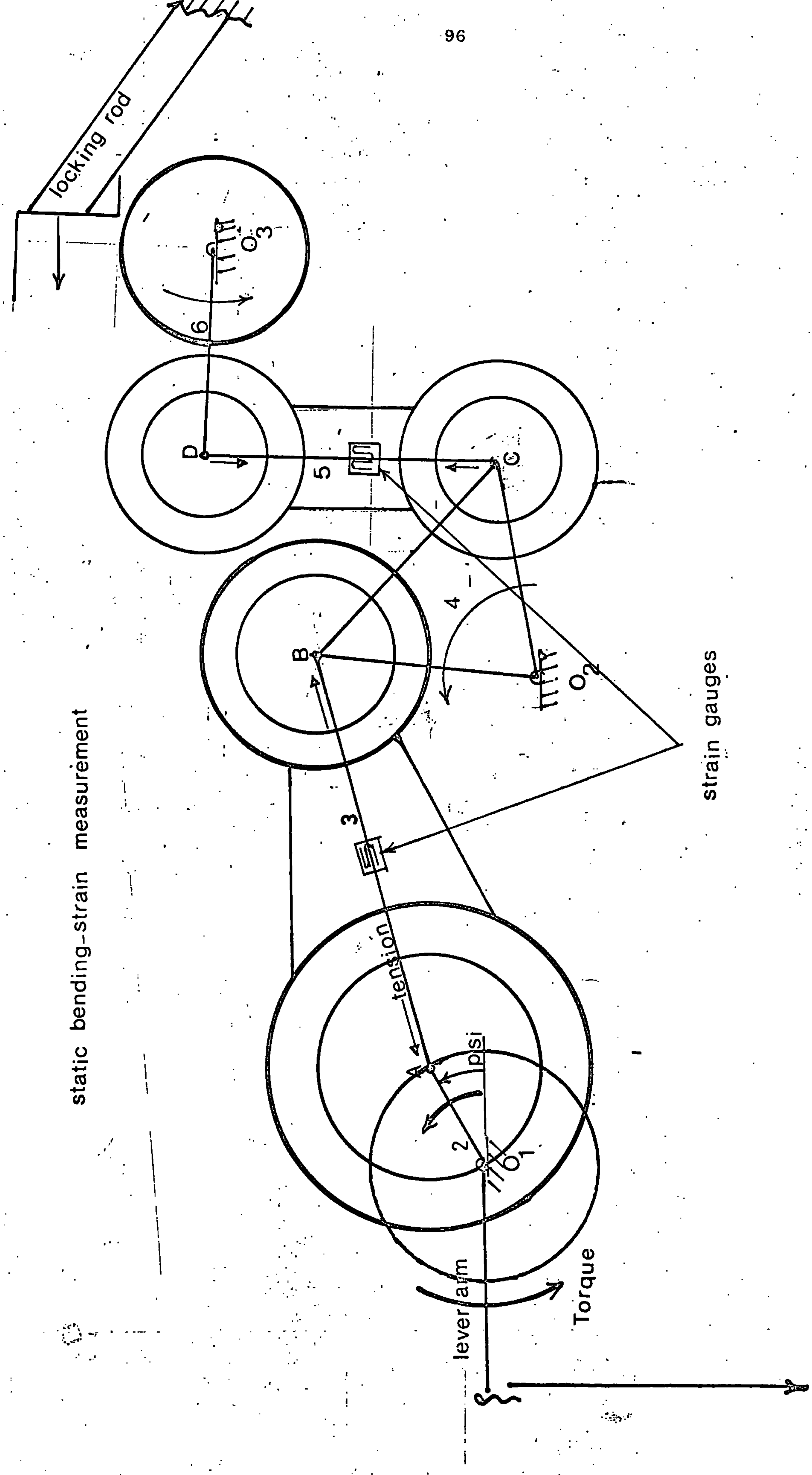
static bending-strain measurement
locking rod
O_3
6
D
C
5
B
4
O_2
strain gauges
3
tension
psi
A
2
O_1
lever arm
Torque
W

Fig. 4.3

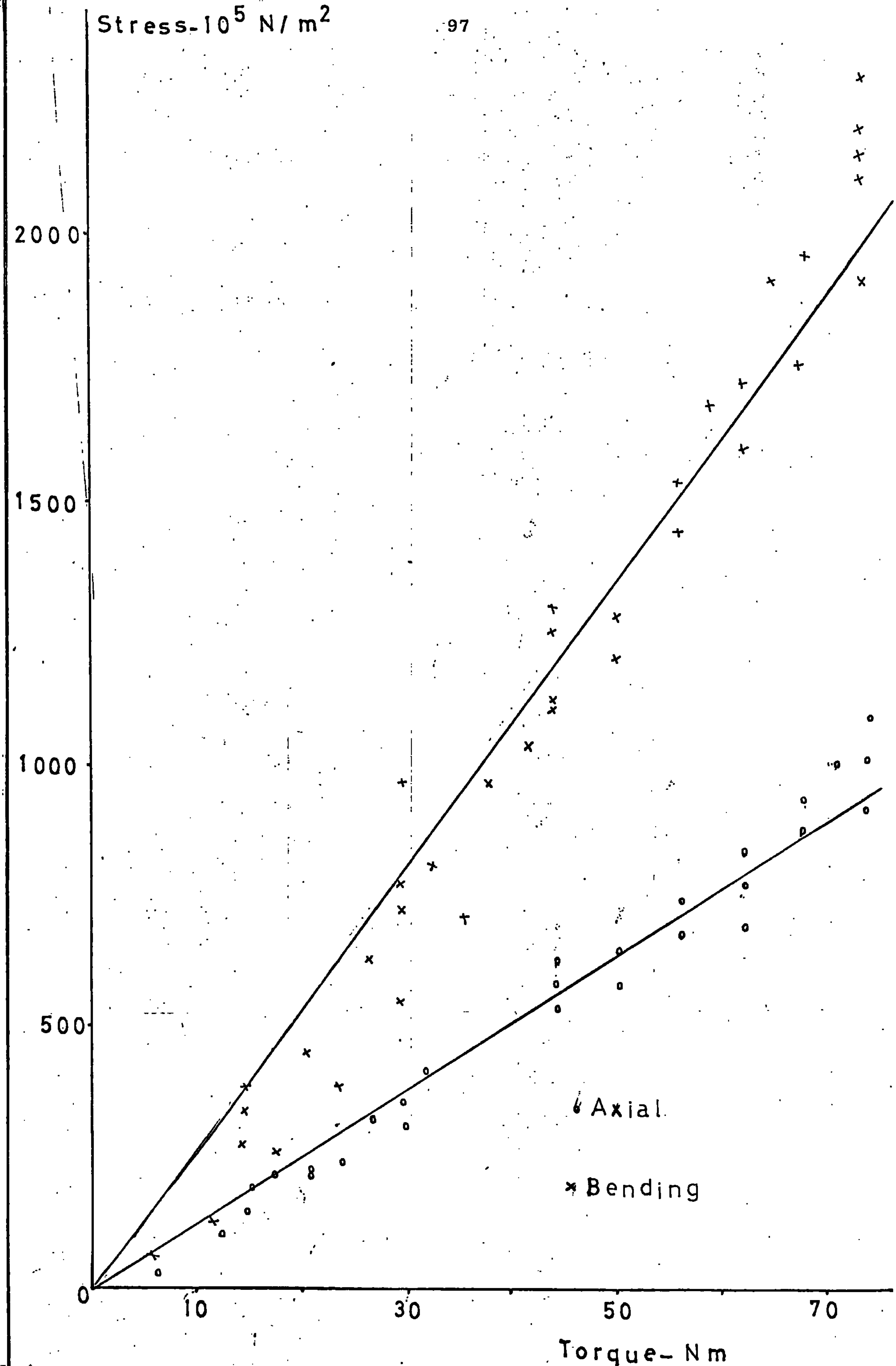

Fig. 4.4 Static Bending - strain test for link 5. Variation of axial and bending (z-direction) stresses with the applied torque.

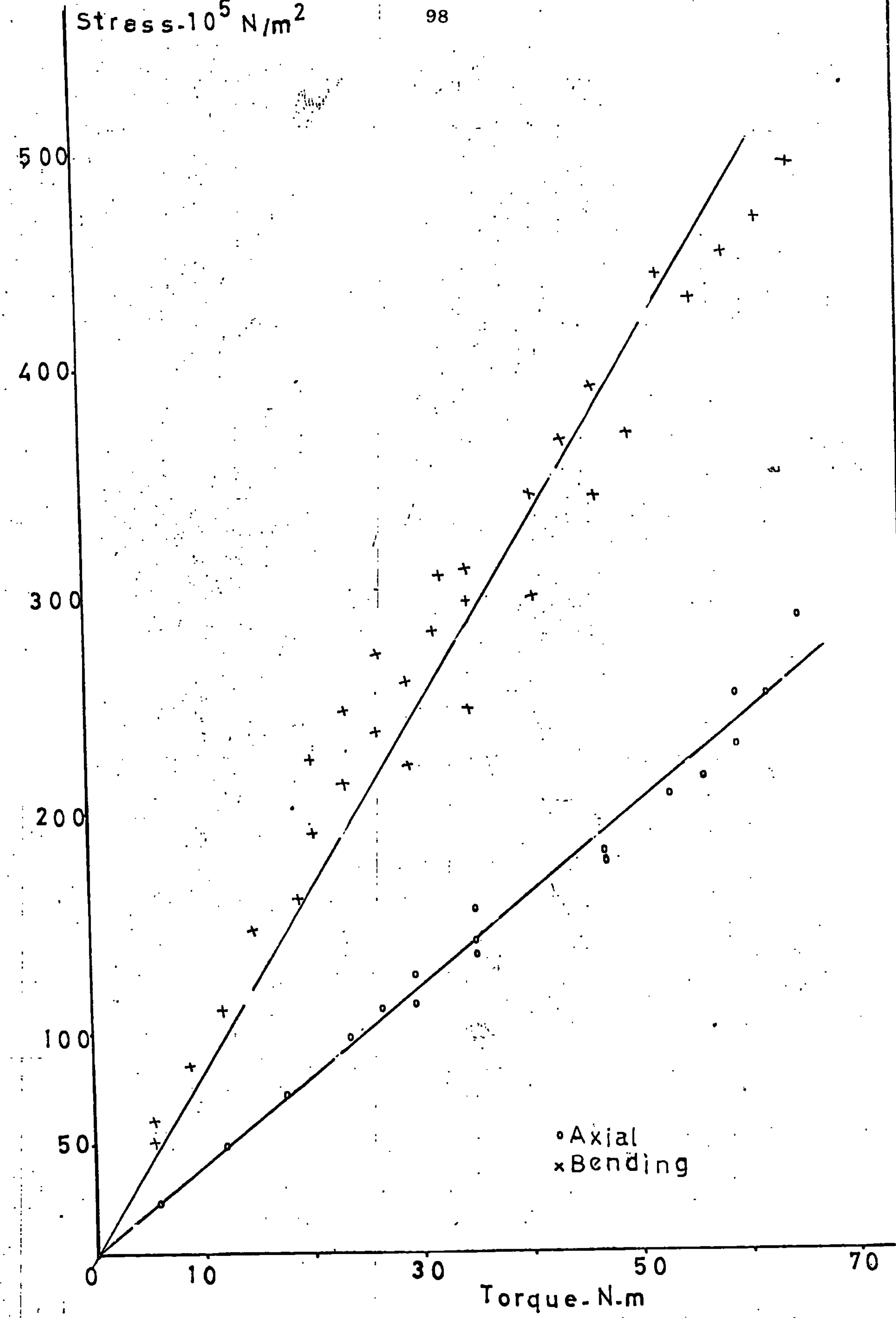

Fig. 4.5 Static bending strain test for link 3 - Variation of axial and bending (z-direction) stresses with the applied torque.

measured by using a half-bridge circuit. Strain gauges on opposing faces of link 3 are identified as gauges c and d, and the above procedure is similarly applied to determine the strain variation. Results are shown in Figures (4.6) and (4.7).

4. Tensile Test

Separate tensile tests are performed on links 3 and 5. A "Servomex Controls Ltd., tensometer, metric type-E" is used in combination with a "Peekel 4-channel 4 UD" extension box and a "Peekel type 581 DNH" Universal carrier-amplifier. The test machine is provided with a unit which automatically draws a tensile test diagram representing the relation between the load and the extension. Two strain gagues are fixed on opposing faces of the links, connected to the extension box. A half-bridge 120 Ω circuit is used to measure the tensile strain. A 2500 N capacity load cell is employed. Motor speed was 600 r.p.m. and the cross-head speed was 9 mm/min. A pair of specially manufactured chucks are used for each link to grip them between the moving cross head and the base. The chucks were fitted with heat treated steel pins, having diameters as close as practical to the inner end bore diameters of the links. The chucks were designed to ensure a central application of the load. The direction of the paper movement was the same as that of the crosshead. The event marker switch is used from time to time to record the actual applied load at certain strain values registered on the carrier amplifier. The moduli of elasticity and yield point strengths are determined from the experimental data shown in Fig. 4.8 for cross-sections BB and AA of the links 3 and 5 respectively.

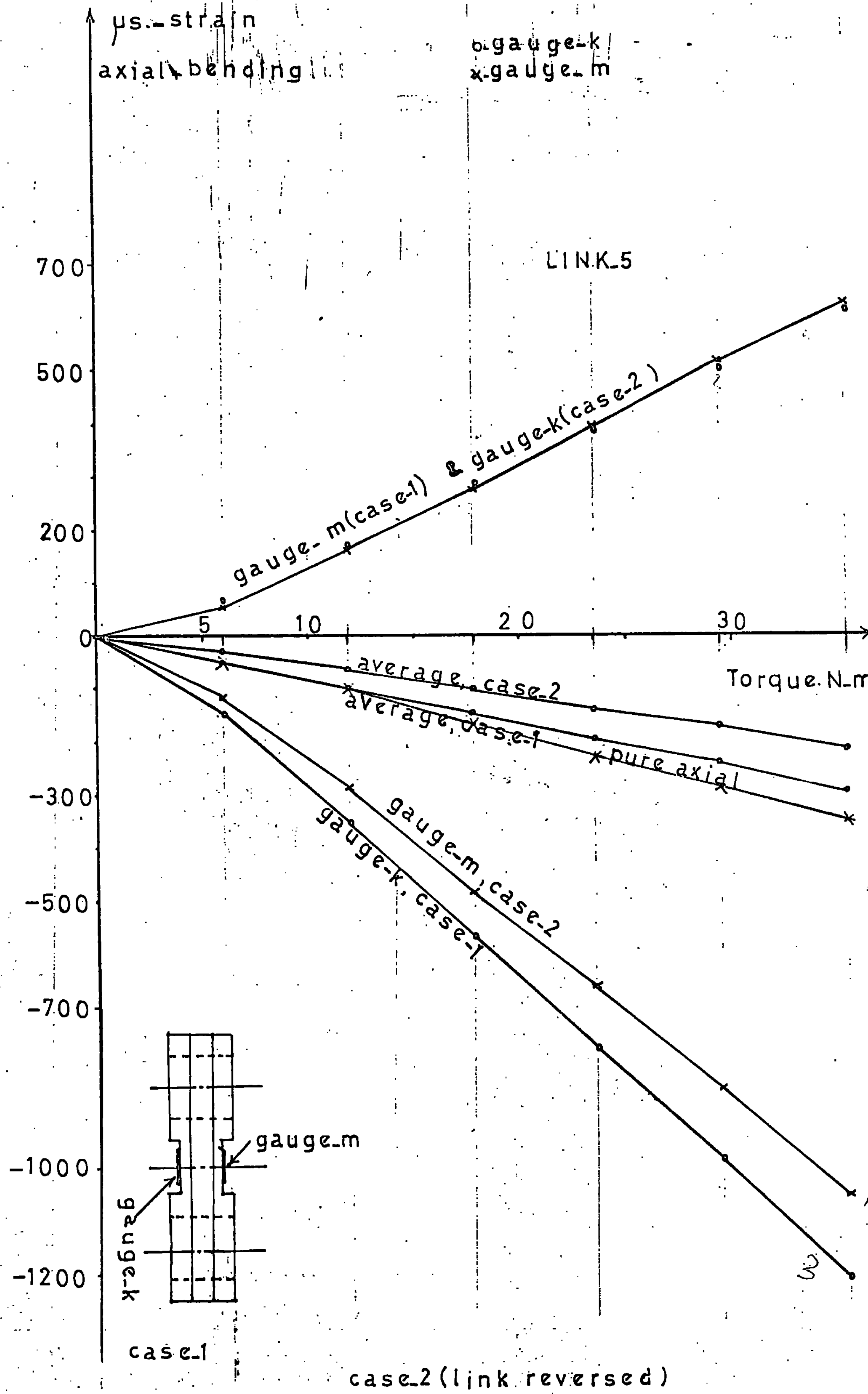
μs._strain
axial+bending
o gauge_k
x gauge_m
LINK_5
700
500
200
0
-300
-500
-700
-1000
-1200
5
10
20
30
Torque. N_m
gauge_m(case-1) & gauge-k(case-2)
average, case_2
average, case-1
pure axial
gauge-m, case-2
gauge-k, case-1
gauge_m
gauge-k
case_1
case_2 (link reversed)

Fig. 4.67

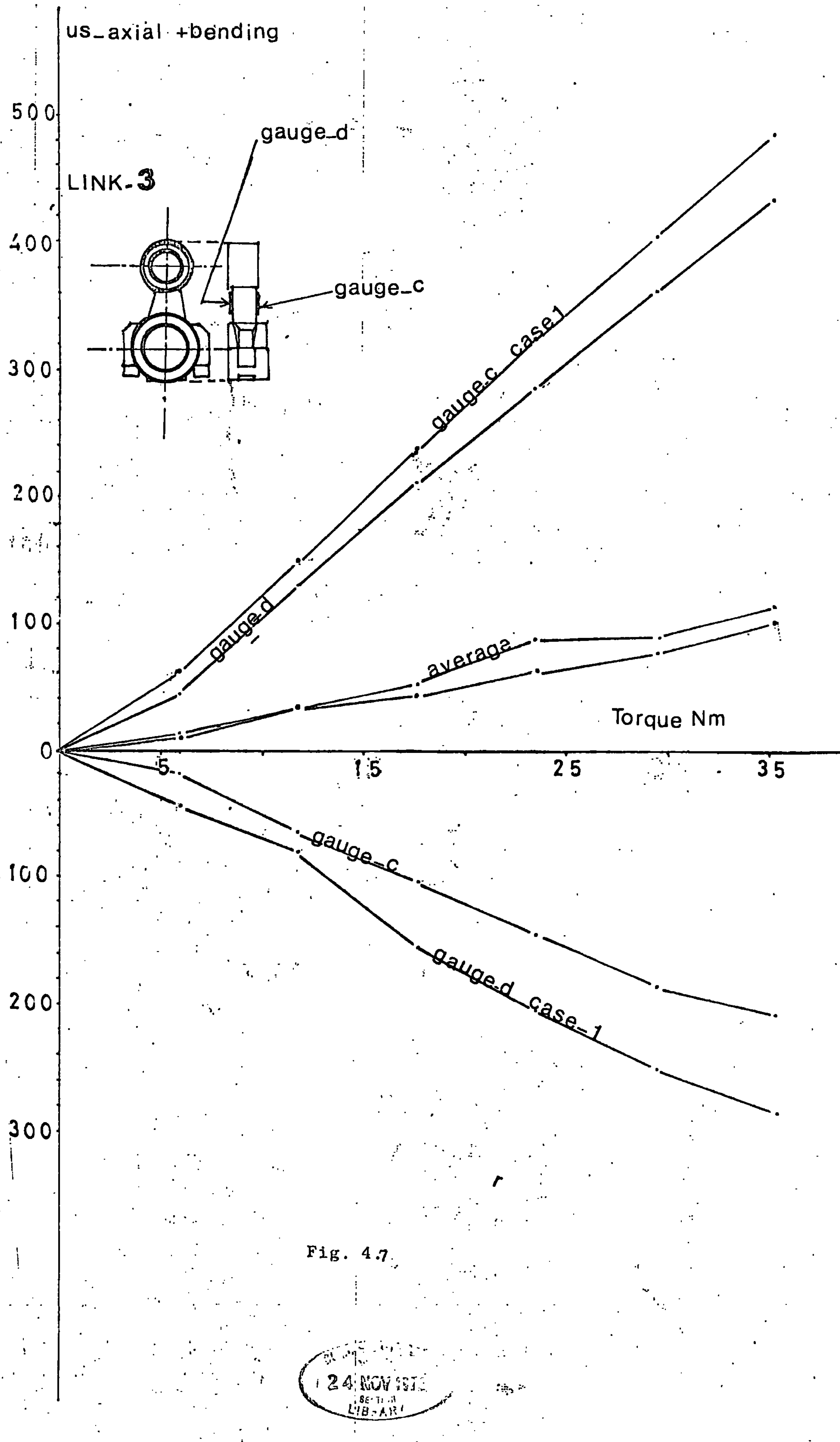

us_axial +bending
500
400
300
200
100
0
100
200
300
LINK-3
gauge_d
gauge_c
gauge_c case1
gauge_d
average
Torque Nm
5
15
25
35
gauge_c
gauge_d case_1

Fig. 4.7

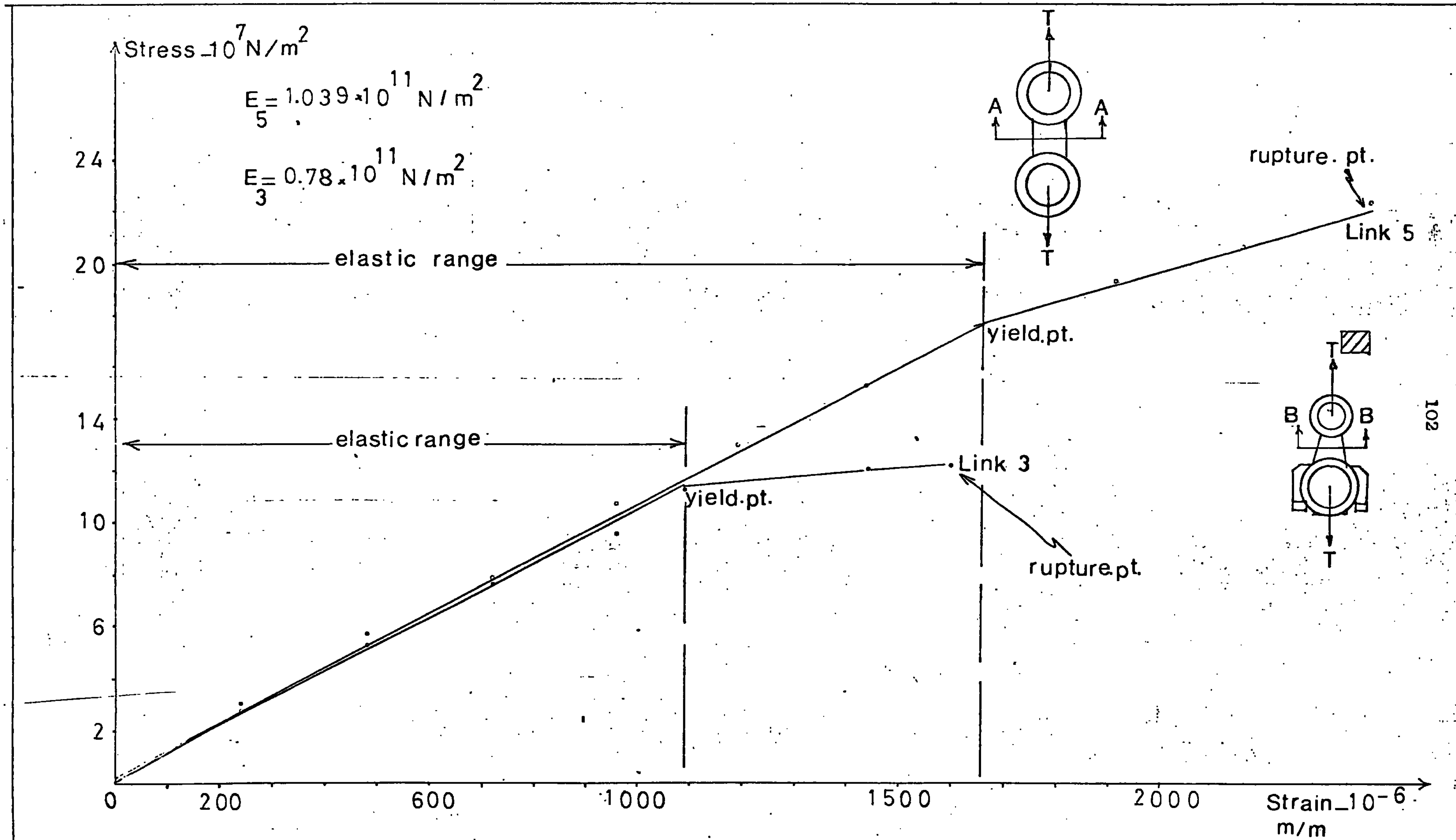

Fig. 4.8 Tensile Test for links 3 and 5

4.5 Dynamic Strain Measurement Results

Since two active gauges are connected in a half-bridge circuit for each set of results, the reading from the bridge is twice that which would be expected if only one active gauge were used. The results are therefore divided by two to obtain the real strain and stress values shown in Table (4.2) The variation of the peak to peak stresses (both axial and bending) with the crank speed for links 3 and 5 are shown in Figures 4.9 to 4.13 Experimental sample strain patterns obtained are shown in Fig. 4.14, a - f for various crank speeds. Experimental variation of the cyclic axial stresses in both links with the crank angle ψ are presented in Figures 4.15 and 4.16.

4.6 Speed Fluctuation

Crank arm speed is assumed to remain constant during a measurement. However the following simplified theoretical calculation based on total kinetic energy of the system is made to predict an estimation;

Let

I_1 = Moment of inertia of the main drive shaft with the flywheel

I_2 = Moment of inertia of shaft O_2

I_3 = Moment of inertia of shaft O_3

From Fig. 3.6 (Torque diagram, for the crank speed = 2500 r.p.m.), Let Ω_2 be the angular velocity of the crank arm at the crank angle $\psi = 50^o$. Also let Ω_4 and Ω_6 be the angular velocities of shafts O_2 and O_3 at the same crank angle. Then 2 (Total Kinetic energy) $I_1\Omega_2^2 + I_2\Omega_4^2 + I_3\Omega_6^2$ = constant

or

$$\frac{2\ (K.E)}{\Omega_2^2} \quad I_1 + I_2\left(\frac{\Omega_4}{\Omega_2}\right)^2 + I_3\left(\frac{\Omega_6}{\Omega_2}\right)^2 = \text{constant} \qquad (4.1)$$

The variation of Ω_2 are shown in Table 4.1 for various crank angles, $0^o \rightarrow 360^o$ by 10^o intervals at an average crank speed of 2500 r.p.m. = 261.798 rad/s.

From table 4.1, coefficient of speed fluctuation is;

$$C_s = \frac{\Omega_{max} - \Omega_{min}}{\Omega_{av}} = \frac{267.43 - 253.95}{261.798} \quad 0.0515$$

speed fluctuation is also measured experimentally by using the u.v recorder and the speed pick-up unit in combination as explained in 4.1. The experimental average value of coefficient of speed fluctuation obtained was 0.082

Table 4.1

crank angle psi (degrees)	Ω_2 rad/s	crank angle psi (degrees)	Ω_2 rad/s
0	263.95	190	267.43
10	266.68	200	267.41
20	267.43	210	267.19
30	266.26	220	266.88
40	263.82	230	266.56
50	260.93	240	266.25
60	258.29	250	265.91
70	256.39	260	265.39
80	255.58	270	264.53
90	255.99	280	263.10
100	257.50	290	260.96
110	259.64	300	258.26
120	261.81	310	255.61
130	263.52	320	253.95
140	264.63	330	254.12
150	265.35	340	256.35
160	265.97	350	260.05
170	266.60	360	263.95
180	267.14		

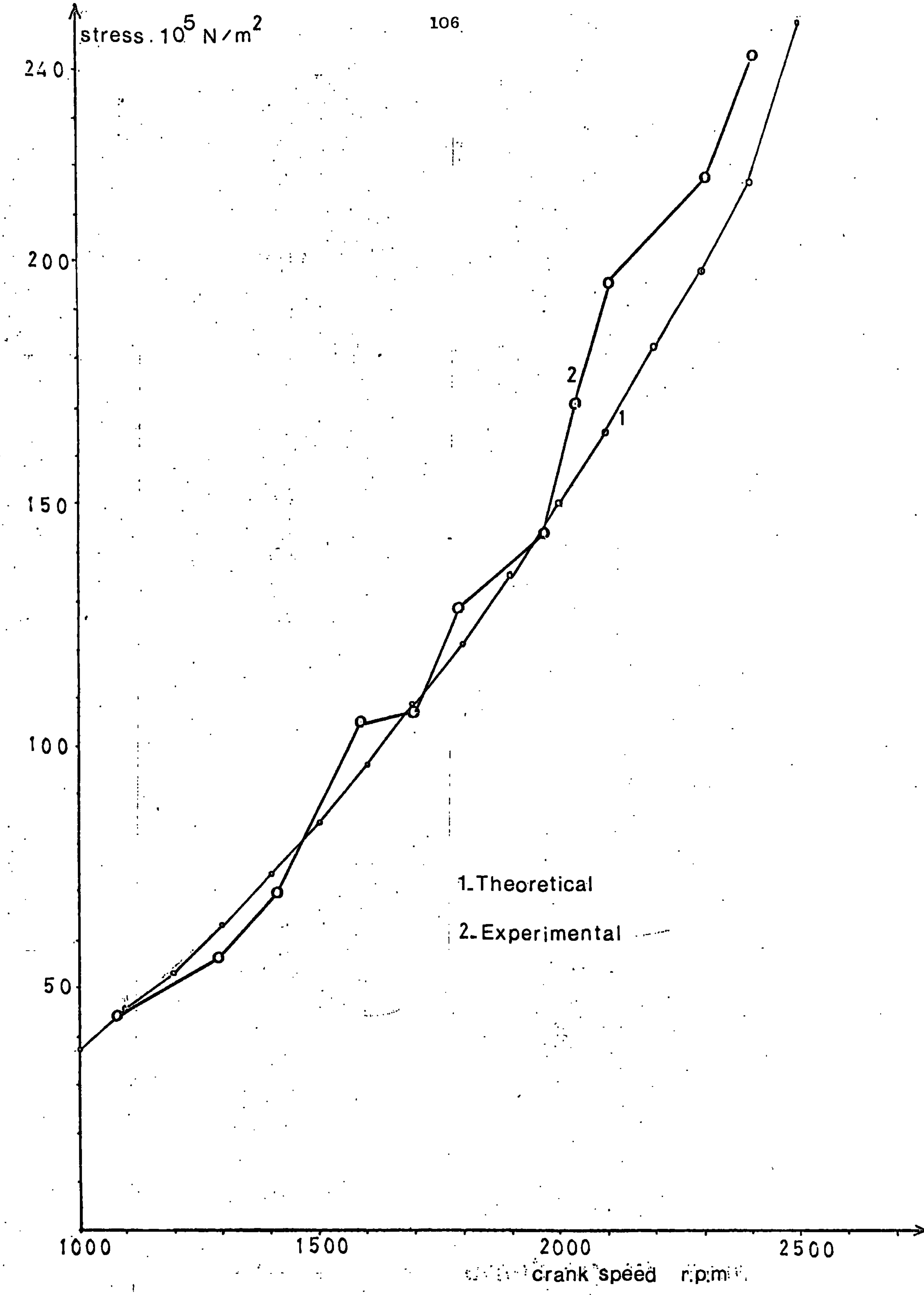

Fig. 4.9 Theoretical and experimental variation of axial stress range (peak to peak stress) in link 5 with the crank speed.

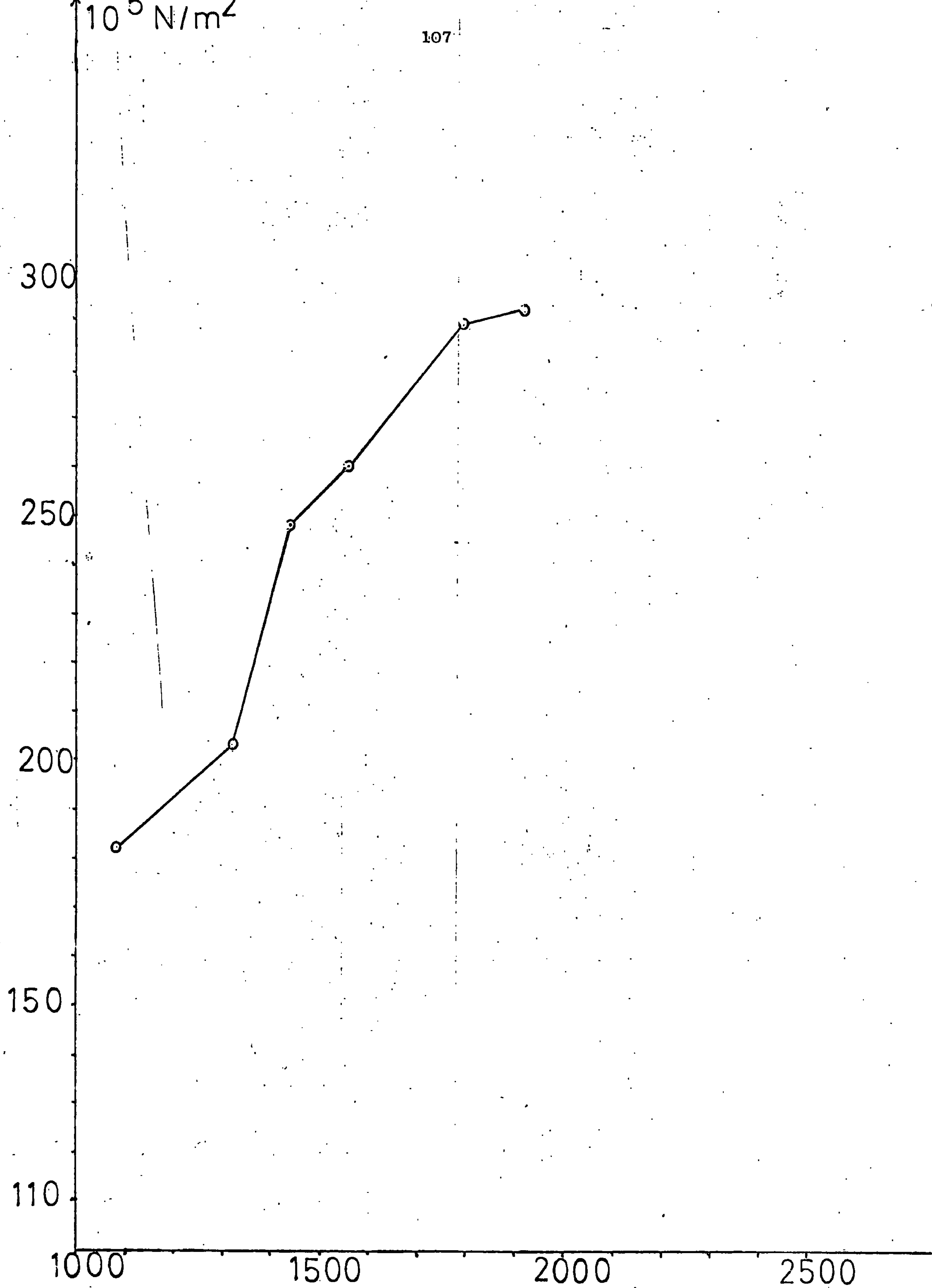

Fig. 4.10 Experimental variation of bending (z-direction) peak to peak stress (stress range) in link 3 with the crank speed.

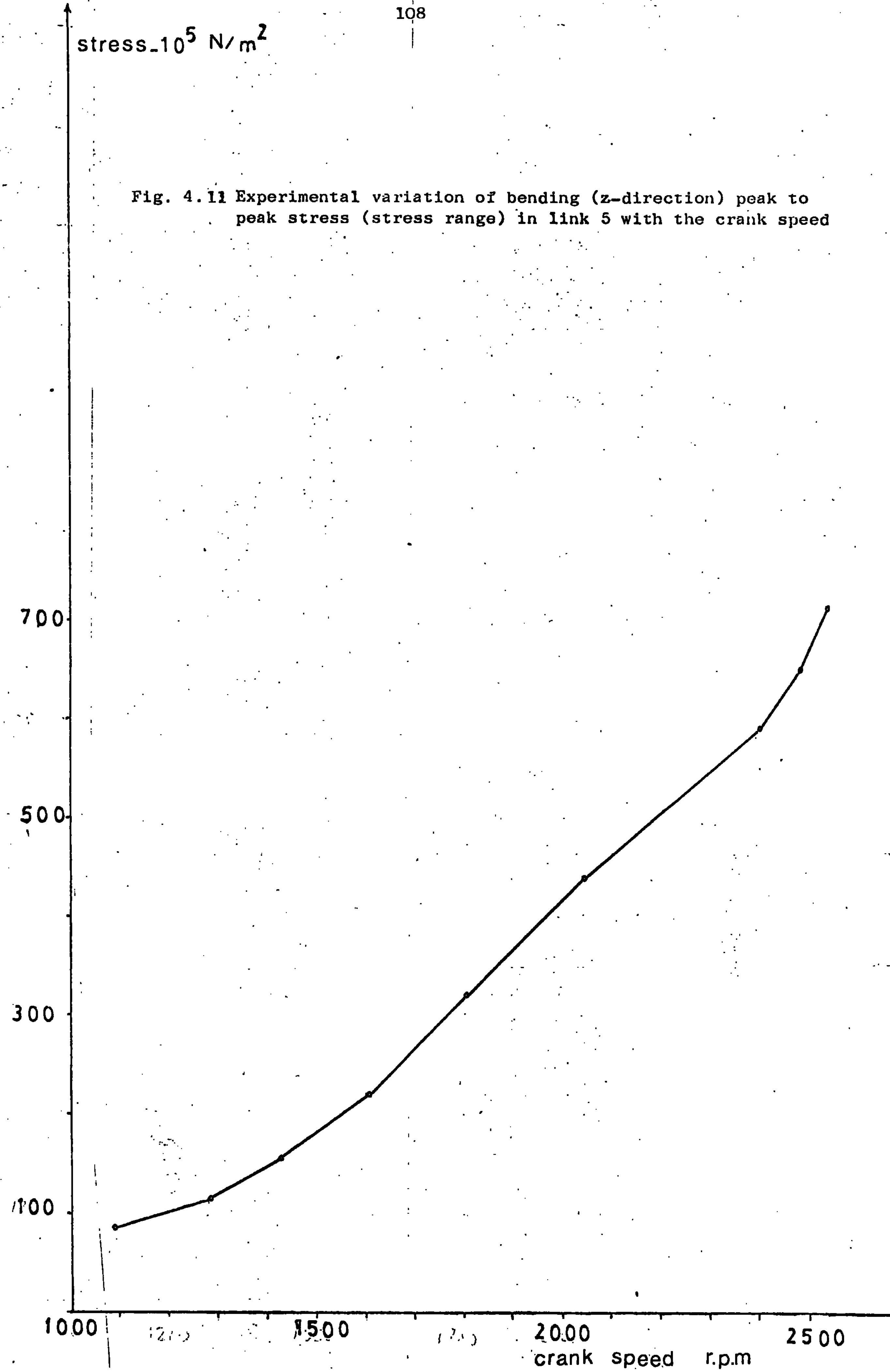

Fig. 4.11 Experimental variation of bending (z-direction) peak to peak stress (stress range) in link 5 with the crank speed

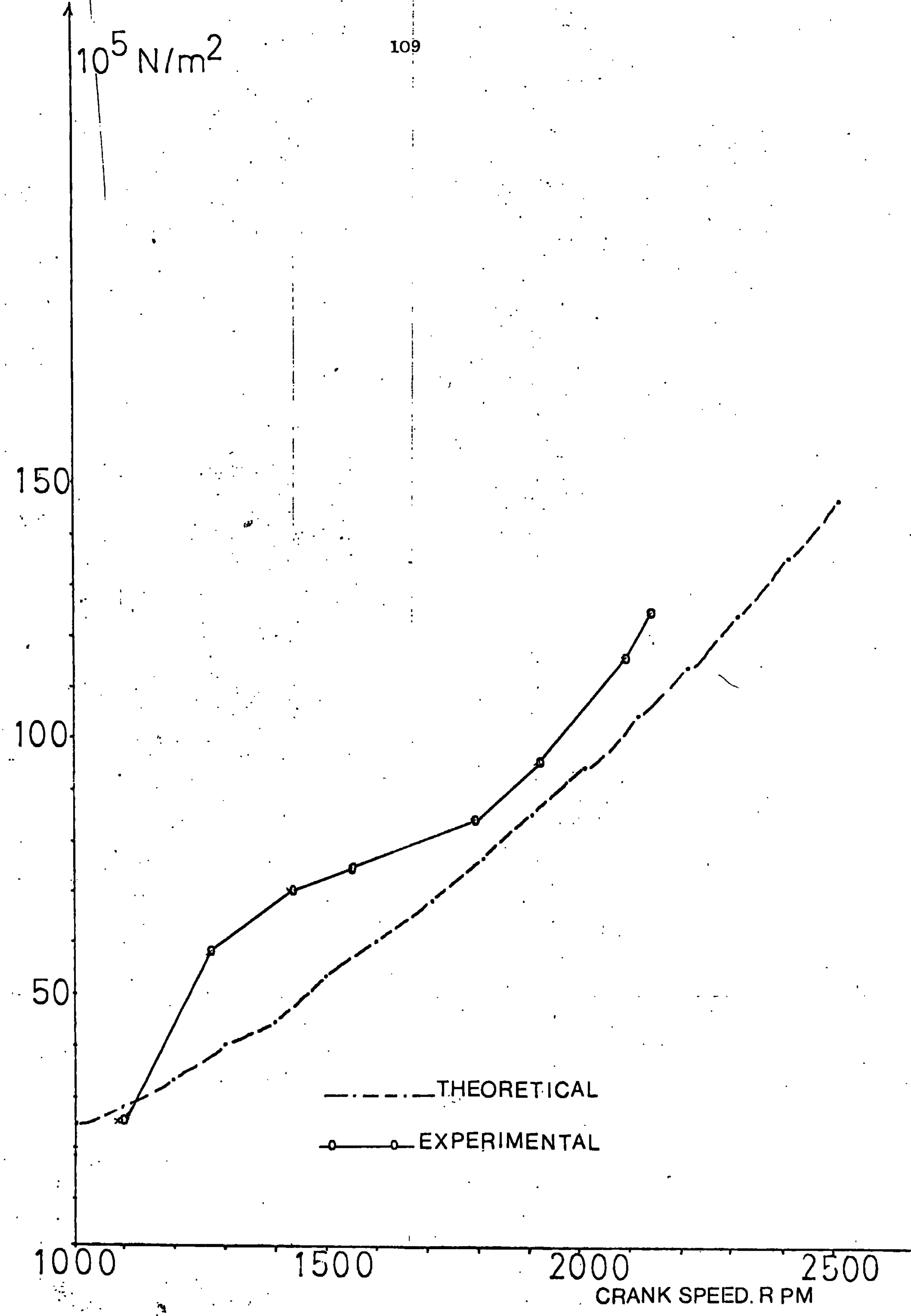

Fig. 4.12 Theoretical and experimental variation of axial peak to peak stress (Stress range) in link 3 with the crank speed

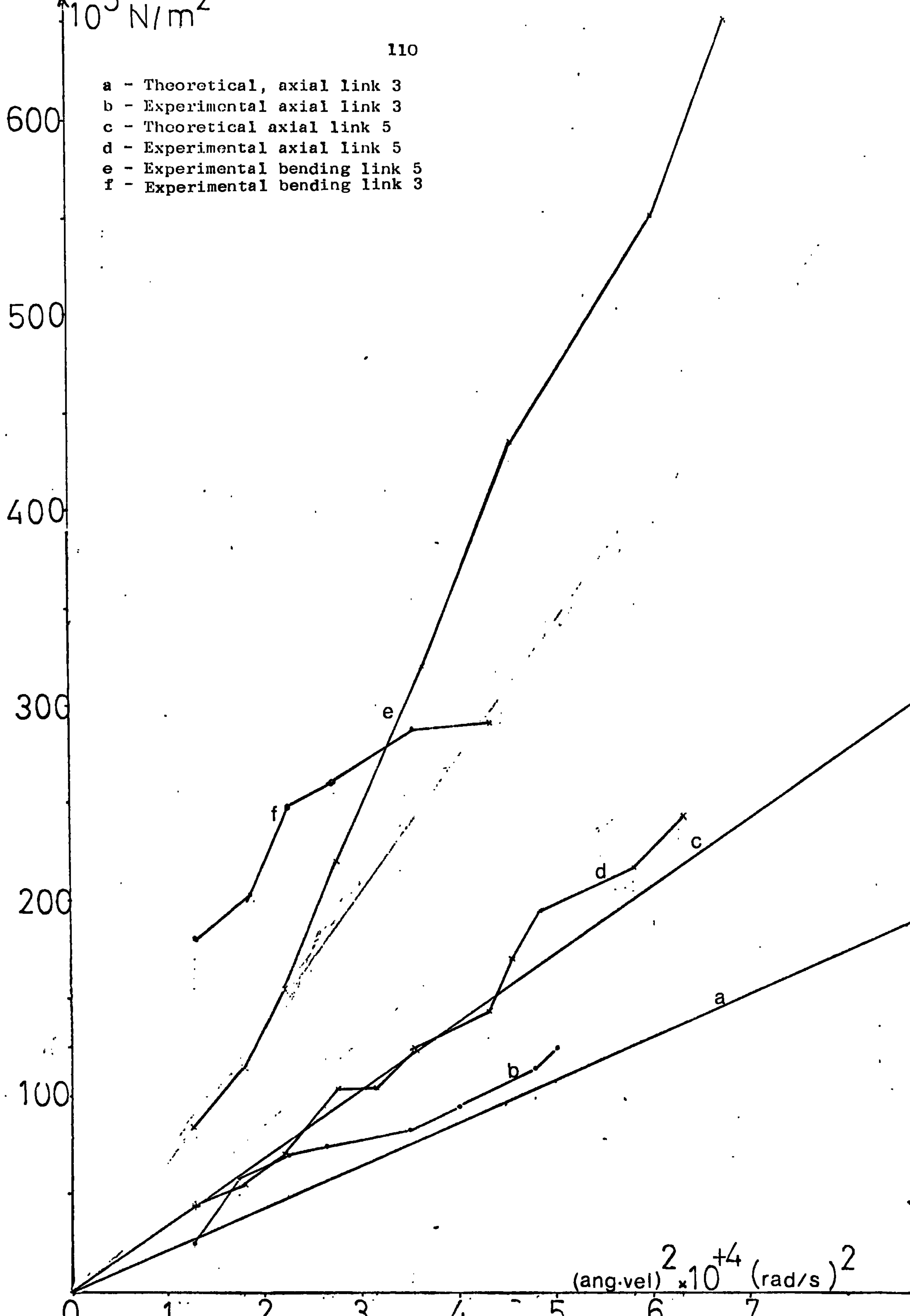

Fig. 4.13 Variation of peak to peak stresses in links 3 and 5 with the square of the crank speed

Fig. 4.14 Experimental strain patterns

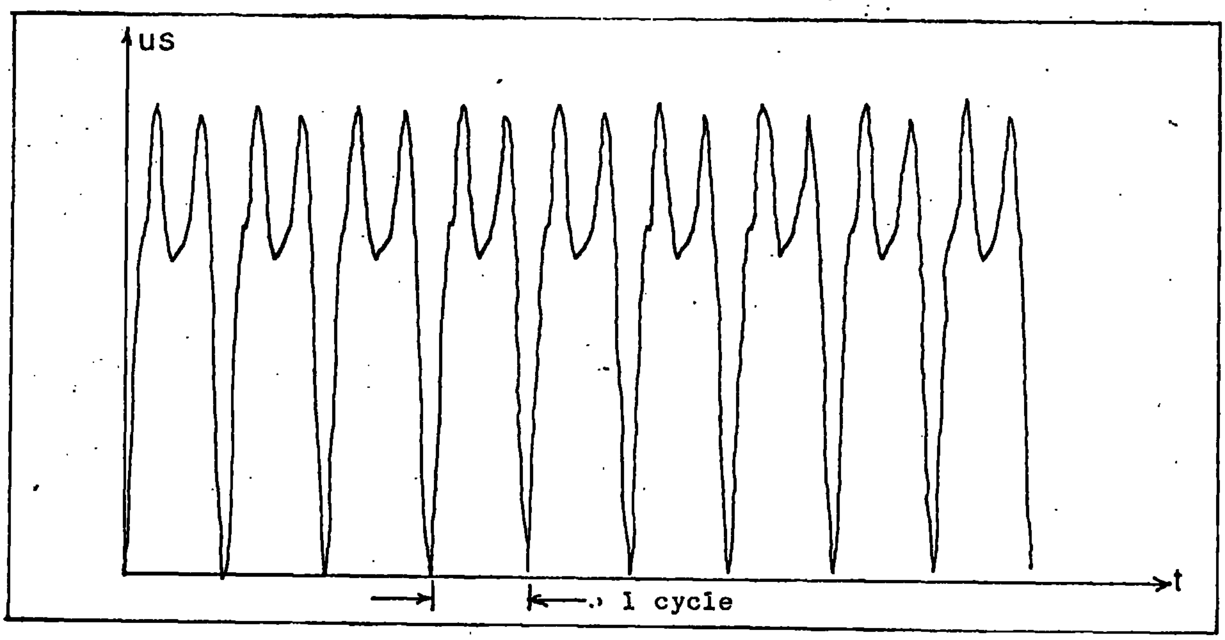

a Record 80. Link 5. Experimental bending (z-direction) strain pattern. Crank speed = 1573 r.p.m. ½ Bridge (120Ω) circuit. Peak to peak strain = 197.4 μs, Peak to peak stress = 205 x 10^5 N/m^2

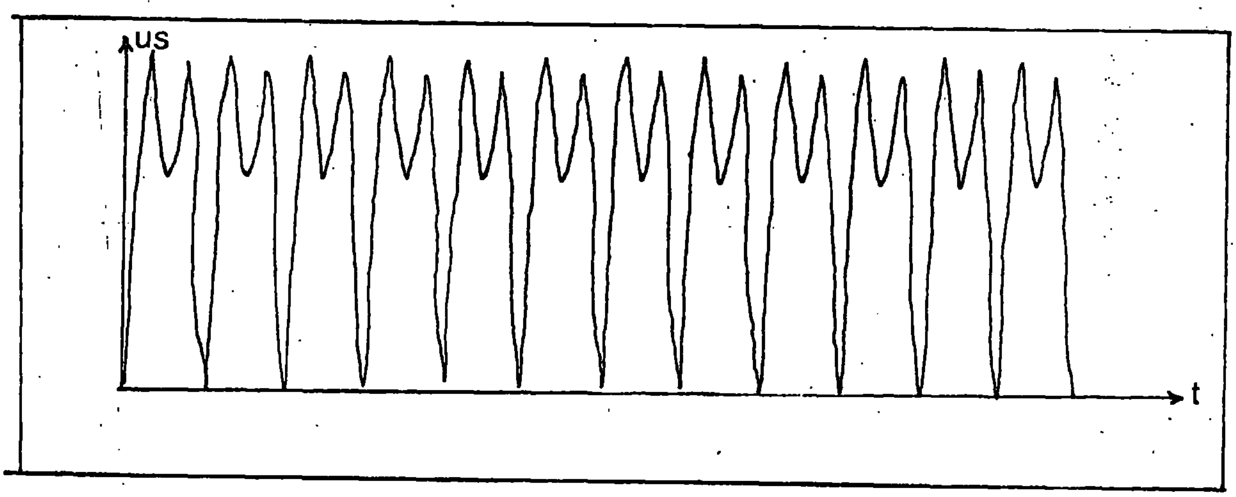

b Record 99. Link 5. Experimental bending (z-direction) strain pattern. Crank speed = 2023 r.p.m. ½ Bridge (120Ω) circuit. Peak to peak strain = 417.5 μs Peak to peak stress = 433.8 x 10^5 N/m^2

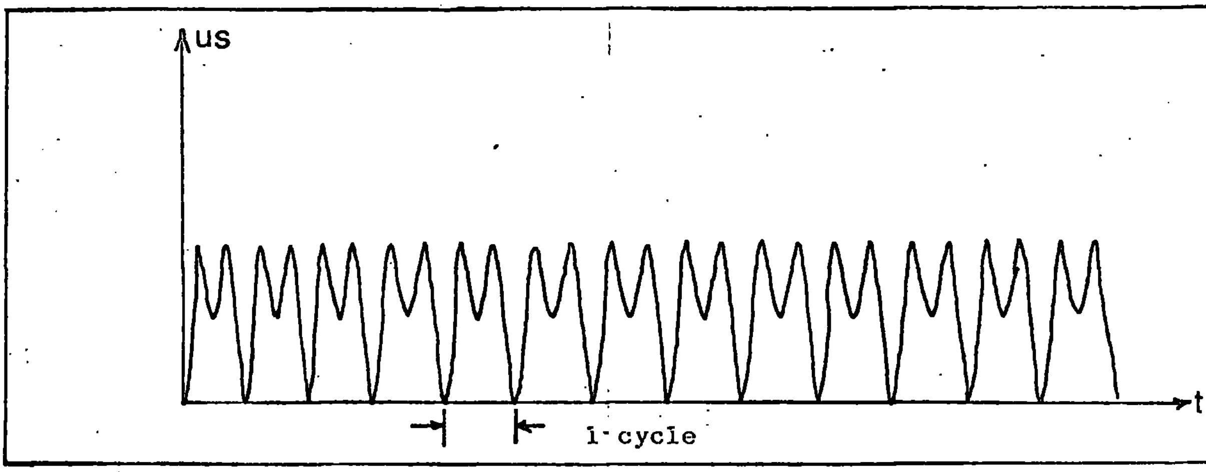

c Record 131 Link 5 Experimental axial strain pattern. Crank speed = 2130 ½ Bridge (120Ω) circuit. Peak to peak strain = 203.9 μs. Peak to peak stress = 211.8 x 10^5 N/m^2

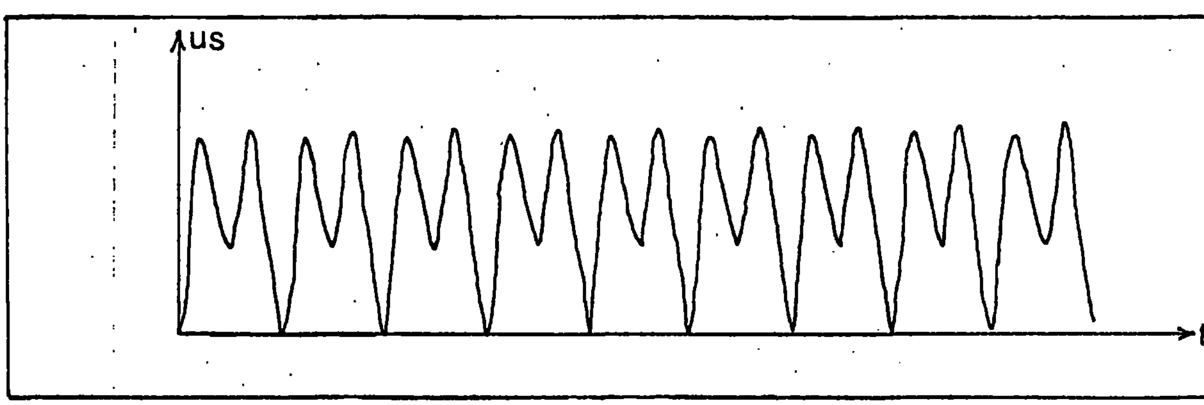

d Record 16. Link 5. Experimental axial strain pattern. Crank speed = 1634 r.p.m. ½ Bridge (120Ω) circuit. Peak to peak strain = 86.7 μs, Peak to peak stress = 90 x 10^5 N/m^2

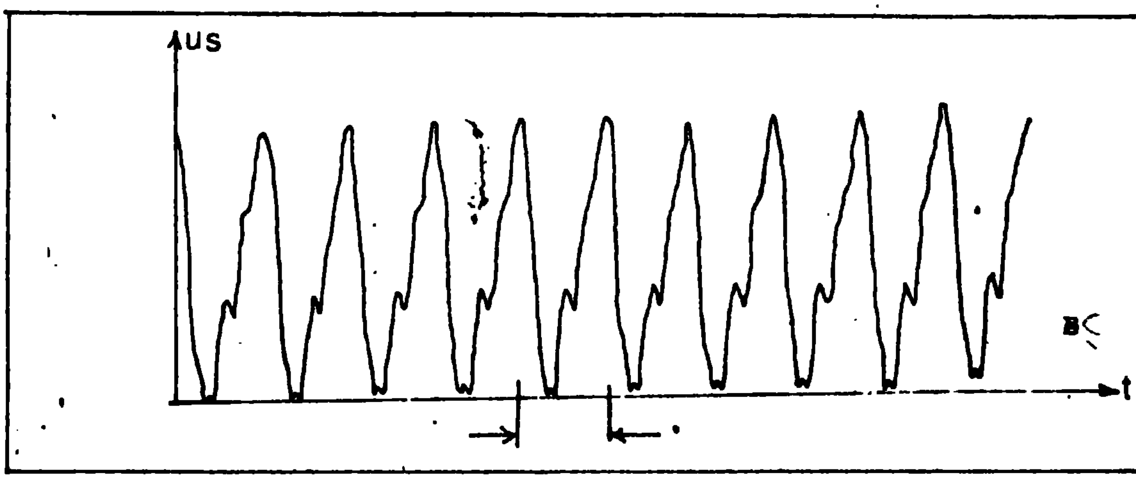

Record 49. Link 3. Experimental bending (z direction) strain pattern. Crank speed = 1770 r.p.m. ½ Bridge (120) circuit. Peak to peak stress 291.2 x 10^5 N/m^2

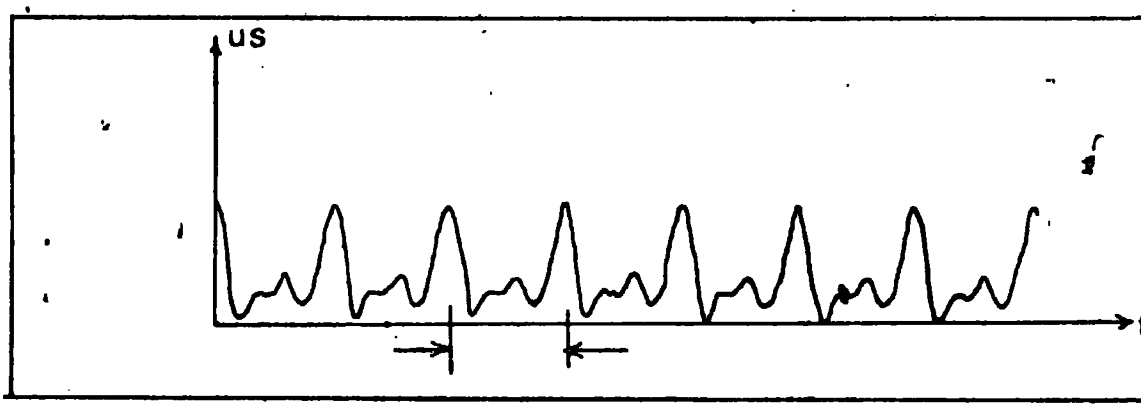

Record 13. Link 3. Experimental axial strain pattern. Crank speed = 1424 r.p.m. ½ Bridge (120) circuit. Peak to peak strain = 48.5 µs, peak to peak stress = 38.8 x 10^5 N/m^2

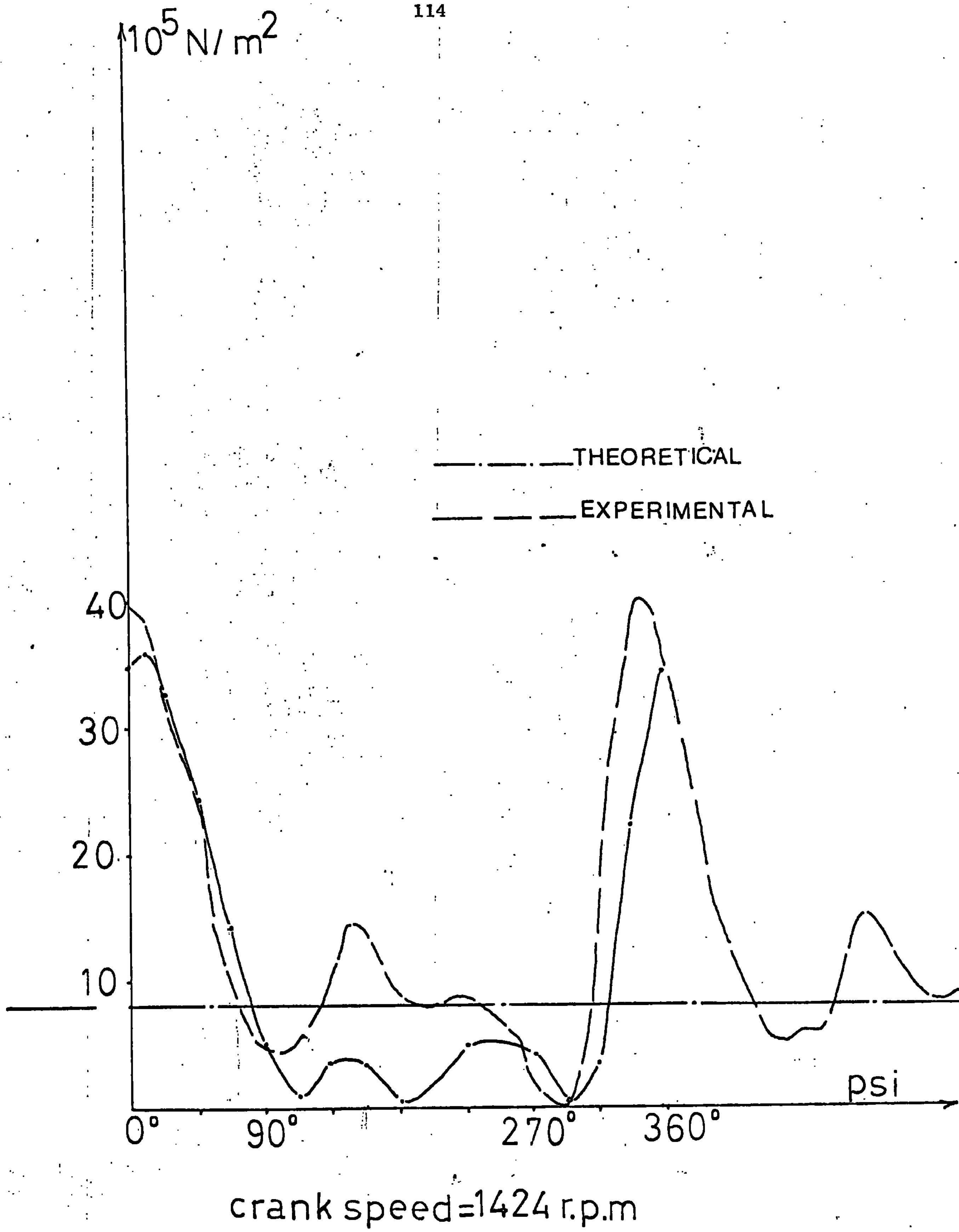

Fig. 4.15 Experimental and theoretical variation of axial stress in link 3 with the crank angle psi at a crank speed of 1424 r.p.m. (cross sectional area subject to stress = 14.95×10^{-5} m^2)

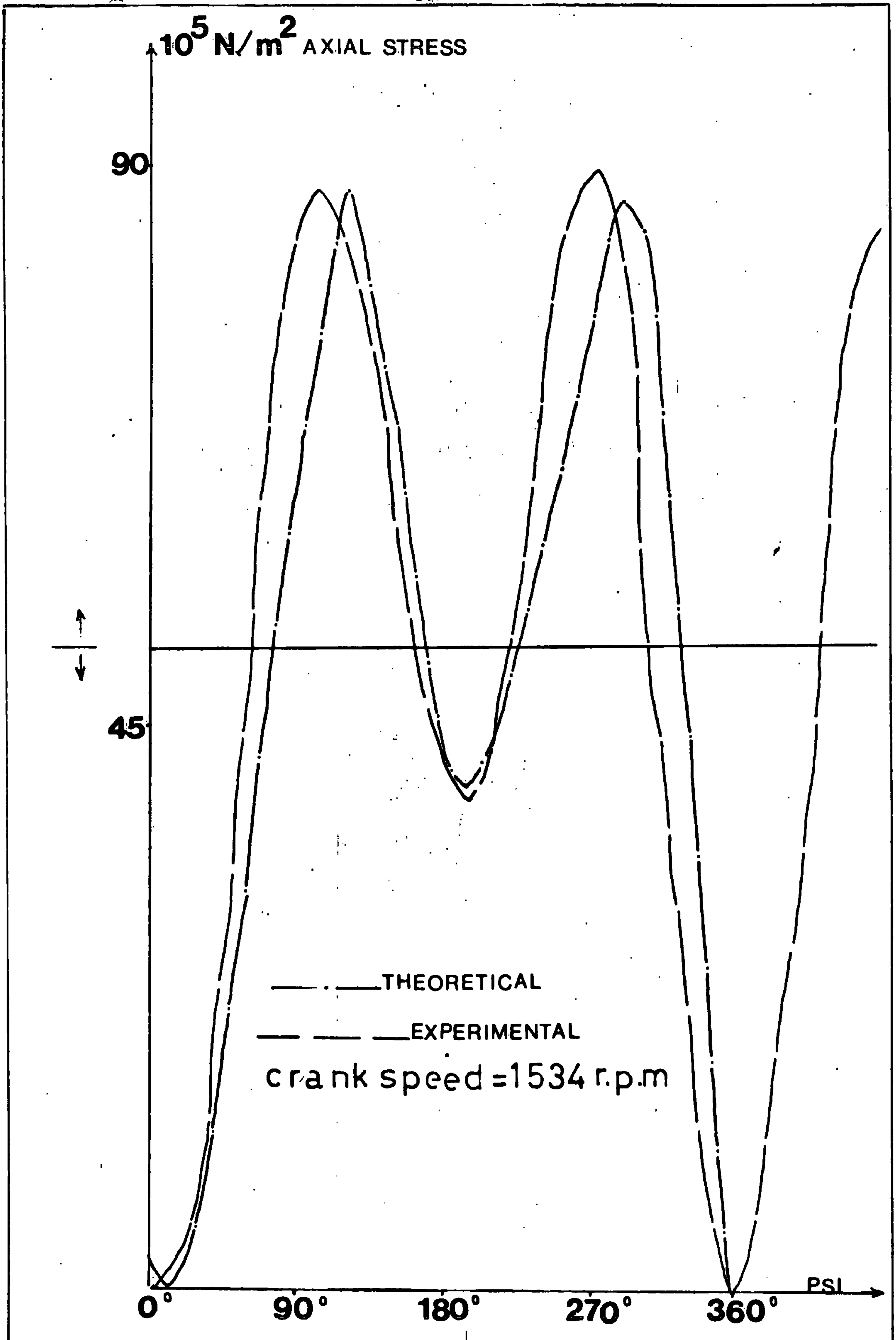

Fig. 4.16 Theoretical and experimental variation of axial stress in link 5 with the crank angle psi, at a crank speed of 1534 r.p.m.

Table 4.2

Record number	Link number	Motor scale	Nominal paper speed.mm/s.	uv. recorder speed pick-up signal. r.p.m.	Tachometer r.p.m.	From timer line 1 sec = mm.	1 cycle covers mm.	Type of strain measured	Bridge configuration	initial range us.	range shifted to. us.	Calibration us.	Calibration signal.mm.	full scale deflection mm.	Record range mm.	Strain range us.	Stress range $x10^5$ N/m^2.
1-	5	220	111	1089	1080	118	6.5	Axial	½, Two Active arms	300	300	100	50.5	151.5	30.5	30.2	31.4
2-	"	"	"	"	"	"	"	Bending	"	"	1000	"	"	"	26	85.8	89.1
3-	3	"	"	"	"	119	"	Axial	"	"	3000	"	50	150	31	30.9	24.7
4-	"	"	"	1037	"	121	7	"	"	3000	3000	1000	50.5	"	3.5	35	28
5-	"	"	"	1089	"	118	6.5	"	"	300	300	100	"	151.5	29.5	29.2	23.3
6-	"	"	"	"	"	"	"	Bending	"	"	3000	"	"	"	26	257.4	205.9
7-	5	200	333	1424	1440	356	15	"	"	3000	"	1000	50	150	46	153.3	159.3
8-	"	"	"	"	"	"	"	Axial	"	300	300	100	"	"	56	56	58.2
9-	"	"	111	1416	"	354	"	Bending	"	"	3000	"	"	"	15.5	155	161
10-	"	"	333	1424	"	356	"	"	"	"	1000	"	"	"	42.5	141.6	147.1
11-	3	"	"	1473	"	"	14.5	"	"	1000	"	300	46.0	153.3	95	309.8	247.8
12-	3	"	"	1424	"	"	15	"	"	"	3000	"	"	"	32	313.1	250.5
13-	3	"	"	"	"	"	"	Axial	"	300	1000	100	51.5	154.5	15	248.5	38.8

Record number	Link number	Motor scale	Nominal paper speed.mm/s.	uv. recorder speed pick-up signal. r.p.m.	Tachometer r.p.m.	From timer line 1 sec = mm.	1 cycle covers mm.	Type of strain measured	Bridge configuration	initial range us.	range shifted to. us.	Calibration us.	Calibration signal.mm.	full scale deflection mm.	Record range mm.	Strain range us.	Stress range x10^5 N/m^2.
14-	5	200	333	1416	1440	354	15	Axial	½ Two Active arms	300	3000	100	51.5	154.5	7	67.9	70.6
15-	"	190	"	1517	1560	"	14	"	"	"	"	"	"	"	9.2	89.3	92.8
16-	"	"	"	1634	"	"	13	"	"	"	1000	"	"	"	26.8	86.7	90
17-	"	180	"	1709	1800	356	12.5	"	"	"	3000	"	"	"	12	116.5	121
18-	"	"	"	1780	"	"	12	"	"	"	"	"	"	"	"	"	"
19-	"	185	"	1770	1680	354	"	"	"	"	"	"	"	"	10	97	100.8
20-	"	175	"	2023	1980	"	10.5	"	"	"	"	"	"	"	14	136	141.3
21-	"	210	"	1256	1320	356	17	"	"	"	1000	"	"	"	14.5	46.9	48.7
22-	"	185	"	1709	1680	"	12.5	"	"	"	"	"	"	"	29.5	95.5	99.2
23-	"	220	111	1089	1080	118	6.5	"	"	"	"	"	"	"	11.5	37.2	38.6
24-	"	"	"	1108	"	120	"	"	"	"	"	"	"	"	"	"	"
25-	"	180	333	1770	1800	354	12	"	"	"	3000	"	"	"	12	116.5	121
26-	"	175	"	1942	1980	356	11	"	"	"	"	"	"	"	14	135.9	141.2

Record number	Link number	Motor scale	Nominal paper speed.mm/s.	uv. recorder speed pick-up signal. r.p.m.	Tachometer r.p.m.	From timer line 1 sec = mm.	1 cycle covers mm.	Type of strain measured	Bridge configuration	initial range us.	range shifted to. us.	Calibration us.	Calibration signal.mm.	full scale deflection mm.	Record range mm.	Strain range us.	Stress range $x10^5$ N/m^2.
27-	5	170	333	2034	2040	356	10.5	Axial	½ Two Active arms	300	3000	100	51.5	154.5	15.5	150.5	156.4
28-	"	165	"	2023	2160	354	"	"	"	3000	"	1000	"	"	18.5	179.6	186.6
29-	"	"	"	1931	"	"	11	"	"	300	"	100	"	"	18	174.7	181.5
30-	3	190	"	1517	1560	"	14	"	"	"	"	"	"	"	10	97	77.6
31-	"	180	111	1785	1800	119	"	"	"	3000	"	1000	"	"	11.5	116.6	89.3
32-	"	175	333	1942	1920	356	11	"	"	300	1000	100	"	"	36	116.5	"
33-	"	170	"	2136	2040	"	10	"	"	"	3000	"	"	"	14.8	143.7	115
34-	"	165	"	2124	2160	354	"	"	"	3000	"	"	"	"	16	155.3	124.24
35-	5	170	"	1942	2040	356	11	"	"	300	"	"	"	"	16.2	157.3	163.4
36-	3	220	"	1062	1080	354	20	"	"	"	1000	"	"	"	15	48.5	38.8
37-	"	"	"	1089	"	"	19.5	"	"	"	"	"	"	"	6.5	21	16.8
38-	"	210	"	1214	1320	"	17.5	"	"	3000	3000	1000	"	"	7.5	72.8	58.2
39-	"	200	"	1416	1440	"	15	"	"	"	"	"	"	"	9.5	92.2	73.7

Record number	Link number	Motor scale	Nominal paper speed.mm/s.	uv. recorder speed pick-up signal. r.p.m.	Tachometer r.p.m.	From timer line 1 sec = mm.	1 cycle covers mm.	Type of strain measured	Bridge configuration	initial range us.	range shifted to. us.	Calibration us.	Calibration signal.mm.	full scale deflection mm.	Record range mm.	Strain range us.	Stress range $x10^5$ N/m^2.
40-	3	190	333	1564	1560	352	13.5	Axial	½ Two Active arms	300	3000	100	51.5	154.5	9	87.4	69.9
41-	"	180	"	1780	1800	356	12	"	"	3000	"	1000	"	"	10	97	77.6
42-	"	175	"	1847	1980	354	11.5	"	"	"	"	"	"	"	13	126.2	101
43-	"	220	"	1062	1080	"	20	Bending	"	300	1000	100	"	"	73	236.2	188.9
44-	"	210	"	1249	1320	"	17	"	"	"	3000	"	"	"	27	262.1	209.7
45-	"	200	"	1355	1440	350	15.5	"	"	"	"	"	"	"	30.5	296.1	236.9
46-	"	190	"	1573	1560	354	13.5	"	"	"	"	"	"	"	31.5	305.8	244.6
47-	"	185	"	1709	1680	356	12.5	"	"	"	"	"	"	"	32.3	313.5	250.8
48-	"	180	"	1765	1800	353	12	"	"	"	"	"	"	"	37	359.2	287.3
49-	"	175	"	1770	1980	354	"	"	"	"	"	"	"	"	37.5	364	291.2
50-	"	190	"	1625	1560	352	13	"	"	"	"	"	"	"	35	339.8	271.8
51-	"	180	"	1770	1800	354	12	"	"	"	"	"	"	"	37.5	364	291.2
52-	"	220	"	1095	1080	356	19.5	"	"	"	1000	"	"	"	24	77.7	80.7

Record number	Link number	Motor scale	Nominal paper speed.mm/s.	uv. recorder speed pick-up signal. r.p.m.	Tachometer r.p.m.	From timer line 1 sec = mm.	1 cycle covers mm.	Type of strain measured	Bridge configuration	initial range us.	range shifted to. us.	Calibration us.	Calibration signal.mm.	full scale deflection mm.	Record range mm.	Strain range us.	Stress range $x10^5$ N/m^2.
53-	5	210	333	1256	1320	356	17	Bending	½ Two Active arms	300	3000	100	51.5	154.5	12.5	121.3	126
54-	"	200	"	1424	1440	"	15	"	"	"	"	"	"	"	16	155.3	161.3
55-	"	195	"	1517	1500	354	14	"	"	"	"	"	"	"	18	174.7	181.5
56-	"	190	"	1582	1560	356	13.5	"	"	"	"	"	"	"	21.5	203.9	211.8
57-	"	185	"	1709	1680	356	12.5	"	"	"	"	"	"	"	26.5	257.3	267.3
58-	"	180	"	1837	1800	352	11.5	"	"	"	"	"	"	"	31	301	312.7
59-	"	190	"	1508	1560	"	14	"	"	"	"	"	"	"	22	213.6	221.9
60-	"	210	"	1214	1320	354	17.5	"	"	"	"	"	"	"	11	106.8	111
61-	"	220	"	1089	1080	"	19.5	"	"	"	1000	"	"	"	31	100.3	104.2
62-	"	"	"	1062	"	"	20	"	"	"	3000	"	"	"	8	77.6	80.6
63-	"	210	"	1287	1320	"	16.5	"	"	"	"	"	"	"	11	106.8	111
64-	"	200	"	1420	1440	355	15	"	"	"	"	"	"	"	15.5	150.5	156.3
65-	"	195	"	1465	1500	354	14.5	"	"	"	"	"	"	"	18.5	179.6	186.6

Record number	Link number	Motor scale	Nominal paper speed.mm/s.	uv. recorder speed pick-up signal. r.p.m.	Tachometer r.p.m.	From timer line 1 sec = mm.	1 cycle covers mm.	Type of strain measured	Bridge configuration	initial range us.	range shifted to. us.	Calibration us.	Calibration signal.mm.	full scale deflection mm.	Record range mm.	Strain range us.	Stress range $x10^5$ N/m^2.
66-	5	190	333	1517	1560	354	14	Bending	½ Two Active arms	300	3000	100	51.5	154.5	22	213.6	221.9
67-	"	185	"	1770	1680	"	12	"	"	"	"	"	"	"	26.5	257.3	267.3
68-	"	180	"	1780	1800	356	"	"	"	"	"	"	"	"	31	301	312.7
69-	3	220	"	1077	1080	359	20	"	"	"	"	"	"	"	22.5	218.4	174.7
70-	"	210	"	1256	1320	356	17	"	"	"	"	"	"	"	25.2	244.6	195.7
71-	"	200	"	1424	1440	"	15	"	"	"	"	"	"	"	29.5	286.4	229
72-	"	195	"	1526	1500	"	14	"	"	"	"	"	"	"	32	310.7	248.5
73-	"	190	"	1643	1560	"	13	"	"	"	"	"	"	"	34	330	264
74-	"	185	"	1699	1680	354	12.5	"	"	"	"	"	"	"	"	"	"
75-	"	180	"	1780	1800	356	12	"	"	"	"	"	"	"	36	349.5	279.6
76-	5	220	"	1068	1080	"	20	"	"	"	1000	"	"	"	22.5	72.8	75.6
77-	"	210	"	1221	1320	"	17.5	"	"	"	"	"	"	"	30.5	98.7	102.5
78-	"	200	"	1416	1440	354	15	"	"	"	"	"	"	"	43	139.1	144.5

Record number	Link number	Motor scale	Nominal paper speed.mm/s.	uv. recorder speed pick-up signal. r.p.m.	Tachometer r.p.m.	From timer line 1 sec = mm.	1 cycle covers mm.	Type of strain measured	Bridge configuration	initial range us.	range shifted to. us.	Calibration us.	Calibration signal.mm.	full scale deflection mm.	Record range mm.	Strain range us.	Stress range $x10^5$ N/m^2.
79-	5	195	333	1473	1500	356	14.5	Bending	½ Two Active arms	300	1000	100	51.5	154.5	49	158.6	164.8
80-	"	190	"	1573	1560	354	13.5	"	"	"	"	"	"	"	61	197.4	205
81-	"	"	"	1634	"	"	13	"	"	"	"	"	"	"	20.5	199	206.7
82-	"	185	"	1770	1680	"	12	"	"	"	"	"	"	"	25	242.7	252.1
83-	"	180	"	1847	1800	"	11.5	"	"	"	"	"	"	"	31	301	312.7
84-	"	175	"	1931	1980	"	11	"	"	"	"	"	"	"	36.5	354.3	368.1
85-	"	220	"	1068	1080	356	20	"	"	"	"	"	"	"	8	77.6	80.7
86-	"	190	"	1573	1560	354	13.5	"	"	"	"	"	"	"	22.5	213.6	221.9
87-	"	175	"	1826	1980	350	11.5	"	"	"	"	"	"	"	37.5	364	378
88-	"	220	"	1062	1080	354	20	Axial	"	"	"	"	"	"	5	48.5	50.4
89-	"	210	"	1256	1320	356	17	"	"	"	"	"	"	"	6	58.2	60.5
90-	"	200	"	1384	1440	346	15	"	"	"	"	"	"	"	8	77.7	80.7
91-	"	190	"	1634	1560	354	13	"	"	"	"	"	"	"	11	106.8	111

Record number	Link number	Motor scale	Nominal paper speed.mm/s.	uv. recorder speed pick-up signal. r.p.m.	Tachometer r.p.m.	From timer line 1 sec = mm.	1 cycle covers mm.	Type of strain measured	Bridge configuration	initial range us.	range shifted to. us.	Calibration us.	Calibration signal.mm.	full scale deflection mm.	Record range mm.	Strain range us.	Stress range $x10^5$ N/m^2.
92-	5	185	333	1699	1680	354	12.5	Axial	½ Two Active arms	300	3000	100	51.5	154.5	12	116.5	121
93-	"	180	"	1770	1800	"	12	"	"	"	"	"	"	"	13	126.2	131.1
94-	"	220	"	1062	1080	"	20	Bending	"	"	"	"	"	"	7	67.9	70.5
95-	"	200	"	1370	1440	"	15.5	"	"	"	"	"	"	"	16	155.3	161.3
96-	"	190	"	1517	1560	"	14	"	"	"	"	"	"	"	21	203.9	211.8
97-	"	180	"	1699	1800	"	12.5	"	"	"	"	"	"	"	31	301	312.7
98-	"	175	"	1847	1980	"	11.5	"	"	"	"	"	"	"	37	359.2	373.2
99-	"	170	"	2023	2040	"	10.5	"	"	"	"	"	"	"	43	417.5	433.8
100-	"	220	"	1062	1080	"	20	"	"	"	"	"	"	"	9	87.4	90.8
101-	"	200	"	1416	1440	"	15	"	"	"	"	"	"	"	18.5	179.6	186.6
102-	"	190	"	1770	1560	"	13.5	"	"	"	"	"	"	"	27.5	267	277.4
103-	"	180	"	"	1800	"	12	"	"	"	"	"	"	"	36	349.5	363.1
104-	"	175	"	1847	1920	"	11.5	"	"	"	"	"	"	"	41.5	403	418.7

Record number	Link number	Motor scale	Nominal paper speed.mm/s.	uv. recorder speed pick-up signal. r.p.m.	Tachometer r.p.m.	From timer line 1 sec = mm.	1 cycle covers mm.	Type of strain measured	Bridge configuration	initial range us.	range shifted to. us.	Calibration us.	Calibration signal.mm.	full scale deflection mm.	Record range mm.	Strain range us.	Stress range x10^5 N/m^2.
105-	5	170	333	2023	2040	354	10.5	Bending	½ Two Active arms	300	3000	100	51.5	154.5	48	466	484.2
106-	"	165	"	2236	2160	"	9.5	"	"	"	"	"	"	"	55	534	554.8
107-	"	"	"	2124	"	"	10	"	"	"	"	"	"	"	56	543.7	564.9
108-	"	170	"	2023	2040	"	10.5	"	"	"	"	"	"	"	48.5	470.9	489.3
109-	"	175	"	1847	1980	"	11.5	"	"	"	"	"	"	"	40	388.3	403.4
110-	"	160	"	2236	2375	"	9.5	"	"	"	"	"	"	"	63	611.6	635.4
111-	"	220	"	1089	1080	"	19.5	Axial	"	"	"	"	"	"	5	48.5	50.4
112-	"	210	"	1287	1320	"	16.5	"	"	"	"	"	"	"	6	58.2	60.5
113-	"	200	"	1416	1440	"	15	"	"	"	"	"	"	"	8	77.7	80.7
114-	"	190	"	1634	1560	"	13	"	"	"	"	"	"	"	11	106.8	111
115-	"	180	"	1847	1800	"	11.5	"	"	"	"	"	"	"	13.5	131	136.1
116-	"	175	"	1931	1980	"	11	"	"	"	"	"	"	"	15	145.6	151.3
117-	"	170	"	2023	2040	"	10.5	"	"	"	"	"	"	"	17.5	170	176.6

Record number	Link number	Motor scale	Nominal paper speed.mm/s.	uv. recorder speed pick-up signal. r.p.m.	Tachometer r.p.m.	From timer line 1 sec = mm.	1 cycle covers mm.	Type of strain measured	Bridge configuration	initial range us.	range shifted to. us.	Calibration us.	Calibration signal.mm.	full scale deflection mm.	Record range mm.	Strain range us.	Stress range $x10^5$ N/m^2.
118-	5	165	333	2124	2160	354	10	Axial	½ Two Active arms	300	3000	100	51.5	154.5	19	184.5	191.7
119-	"	160	"	2236	2375	"	9.5	"	"	"	"	"	"	"	21.5	208.7	216.8
120-	"	155	"	2360	2450	"	9	"	"	"	"	"	"	"	24	233	242
121-	"	153	"	"	2500	"	"	"	"	"	"	"	"	"	23	223.3	232
122-	"	190	111	1785	1600	119	4	Bending	"	"	"	"	52	156	21.2	203.8	211.7
123-	"	150	333	2499	2550	354	8.5	"	"	"	1000	"	51.5	154.5	19.5	631	655.7
124-	"	220	"	1068	1075	356	20	Axial	"	"	"	"	"	"	15.5	50.1	52.1
125-	"	180	"	1775	1810	355	12	"	"	"	3000	"	"	"	14.5	140.8	146.2
126-	"	"	"	1847	"	354	11.5	"	"	"	"	"	"	"	12.1	117.5	122
127-	"	190	"	1639	1600	355	13	"	"	"	"	"	"	"	11.1	107.7	112
128-	"	200	"	1370	1355	354	15.5	"	"	"	"	"	"	"	9	87.4	90.8
129-	"	190	"	1643	1600	356	13	Bending	"	"	"	"	"	"	21	203.9	211.8
130-	"	170	"	2094	2050	"	10.2	Axial	"	"	"	"	"	"	18.5	179.6	186.6

Record number	Link number	Motor scale	Nominal paper speed.mm/s.	uv. recorder speed pick-up signal. r.p.m.	Tachometer r.p.m.	From timer line 1 sec = mm.	1 cycle covers mm.	Type of strain measured	Bridge configuration	initial range us.	range shifted to. us.	Calibration us.	Calibration signal.mm.	full scale deflection mm.	Record range mm.	Strain range us.	Stress range $x10^5$ N/m^2.
131-	5	165	333	2130	2124	355	10	Axial	½ Two Active arms	300	3000	100	51.5	154.5	21	203.9	211.8
132-	"	220	"	1068	1075	356	20	"	"	"	1000	"	"	"	15	48.5	50.4
133-	"	170	"	2124	2050	354	10	Bending	"	"	10000	"	"	"	12	388.3	403.5
134-	"	160	"	2373	2375	356	9	"	"	"	"	"	"	"	15.2	491.9	511
135-	"	155	"	2421	2375	355	8.8	"	"	"	"	"	"	"	17	550.1	571.6
136-	"	190	"	1643	1600	356	13	"	"	"	3000	"	"	"	21	203.9	211.8
137-	"	220	111	1190	1075	119	6	"	"	"	"	"	"	"	9.5	92.2	95.8
138-	"	210	"	1298	1230	"	5.5	"	"	"	"	"	"	"	12	116.5	121
139-	"	200	"	1440	1355	120	5	"	"	"	"	"	"	"	16	155.3	161.4
140-	"	170	333	1942	2050	356	11	"	"	"	10000	"	"	"	11.2	362.5	376.6
141-	"	180	"	1780	1810	"	12	"	"	"	"	"	"	"	9	291.3	302.6
142-	"	155	"	2373	2450	"	9	"	"	"	30000	"	"	"	6.3	611.6	635.5
143-	"	145	"	2499	-	354	8.5	"	"	"	10000	"	"	"	21.5	695.8	722.9

Record number	Link number	Motor scale	Nominal paper speed.mm/s.	uv. recorder speed pick-up signal. r.p.m.	Tachometer r.p.m.	From timer line 1 sec = mm.	1 cycle covers mm.	Type of strain measured	Bridge configuration	initial range us.	range shifted to. us.	Calibration us.	Calibration signal.mm.	full scale deflection mm.	Record range mm.	Strain range us.	Stress range $x10^5$ N/m^2.
144	5	155	111	2373	-	356	9	Bending	½ Two active arms	300	10000	100	51.5	154.5	17	550.2	571.6
145	5	160	333	"	2375	"	"	"	"	"	"	"	"	"	15	485.4	504.4
146	5	135	111	2832	-	118	2.5	Axial + Bending	¼ one active arm	"	30000	"	"	"	6.3	1223.3	1271
147	5	140	"	2723	-	"	2.6	"	"	"	10000	"	"	"	16	1035.6	1076

Record number	Link number	Strain gauges	Bridge configuration	Type of strain measured	Calibration us.	Initial range us.	Range shifted to us.	Calibration signal mm.	Full scale deflection mm.
1	3	AB	½ 2 Active arms	Axial	100	300	3000	54.5	163.5
2	3	XY	"	Bending	"	"	"	"	"
3	3	XY	"	"	"	"	10000	"	"
4	5	CC	"	"	"	"	30000	"	"
5	5	CC	"	"	"	"	"	"	"
6	5	CC	"	"	"	"	"	"	"
7	5	CC	"	"	"	"	"	"	"
8	5	CC	"	"	"	"	100000	"	"
9	5	CC	"	"	"	"	10000	"	"
10	5	CC	"	"	"	"	3000	"	"
11	3	XY	"	"	"	"	10000	"	"
12	3	AB	"	"	"	"	1000	"	"

Table 4.3

Record number	Link number	Strain gauges	Bridge configuration	Type of strain measured	Calibration us.	Initial range us.	Range shifted to us.	Calibration signal mm.	Full scale deflection mm.
13	5	CC	½ 2 Active arms	Bending	100	300	10000	54.5	163.5
14	3	XY	"	Axial	30	100	1000	49	163.3
15	3	"	"	"	100	300	"	54.5	163.5
16	3	AB	"	"	"	"	"	"	"
17	3	"	"	"	"	"	"	"	"
18	5	CC	"	"	"	"	3000	"	"
19	5	"	"	"	"	"	30000	"	"
20	5	"	"	"	"	"	"	"	"
21	5	"	"	"	"	"	10000	"	"
22	5	"	"	"	"	"	"	"	"
23	3	XY	"	"	"	"	3000	"	"
24	3	AB	"	"	"	"	300	"	"

Record number	Link number	Strain gauges	Bridge configuration	Type of strain measured	Calibration us.	Initial range us.	Range shifted to us.	Calibration signal mm.	Full scale deflection mm.
25	5	CC	½ 2 Active arms	Bending	100	300	30000	54.5	163.5
26	3	XY	"	"	"	"	10000	"	"
27	3	XY	"	"	"	"	"	"	"
28	3	XY	"	Axial	"	"	3000	"	"

Record No. - 1				
Applied Force N	Torque Nm	Record trace deflection mm	Strain us.	Stress x10^5 N/m^2
98	29.4	10	91.7	73.4
196	58.8	20	183.5	146.8
215.6	64.7	21	192.7	154.2
235.2	70.6	22.5	206.4	165.1
254.8	76.4	24	220.2	176.2
274.4	82.3	26	238.5	190.8

Record No. - 2				
Applied Force N	Torque Nm.	Record trace deflection mm	Strain us.	Stress x10^5 N/m^2
19.6	5.9	7	64.2	51.4
39.2	11.8	15	137.6	110
58.8	17.7	22	201.8	161.5
68.6	20.6	26	238.5	190.8
78.4	23.5	29	266	212.8
88.2	26.5	32	293.6	234.9
107.8	32.3	38	348.6	278.9
117.6	35.3	42	385.3	308.2

Record No. - 3

Applied Force N	Torque Nm	Record trace deflection mm	Strain us.	Stress x10^5 N/m^2
98	29.4	9	275.2	220.2
117.6	35.3	10	305.8	244.6
137.2	41.2	12	367	293.6
156.8	47	14	428.1	342.5
166.6	50	15	458.7	367
176.4	52.9	18	550.5	440.4
196	58.8	18.5	565.7	452.6
205.8	61.7	19	581	464.8
215.6	64.7	20	611.6	489.3

Record No. - 4

Applied Force N	Torque Nm.	Record trace deflection mm	Strain us.	Stress x10^5 N/m^2
49	14.7	3.5	321.1	333.6
147	44.1	13.5	1238.5	1286.8
245	73.5	23	2110	2192.4
264.6	79.4	25	2293.6	2383
284.2	85.3	27	2477	2573.6
303.8	91.1	29	2660.5	2764.3

Record No. - 5

Applied Force N	Torque Nm	Record trace deflection mm	Strain us.	Stress $x10^5$ N/m^2
98	29.4	7.5	688	714.9
147	44.1	11.5	1055	1096.2
166.6	50	12.5	1146.8	1191.5
186.2	55.9	16	1467.9	1525.1
205.8	61.7	18	1651.4	1715.8

Record No. - 6

Applied Force N	Torque Nm.	Record trace deflection mm	Strain us.	Stress $x10^5$ N/m^2
49	14.7	3.5	321.1	333.6
147	44.1	13	1192.6	1239.2
245	73.5	22.5	2064.2	2144.7
264.6	79.4	24.5	2247.7	2335.4
284.2	85.2	27	2477	2573.6
303.8	91.1	29	2660.5	2764.3

Record No. - 7

Applied Force N	Torque Nm	Record trace deflection mm	Strain us.	Stress x10^5 N/m^2
49	14.7	4	366.9	381.3
147	44.1	13	1192.7	1239.2
245	73.5	22	2018.3	2097
264.6	79.4	24	2201.8	2287.7
284.2	85.2	25.5	2339.4	2430.7
303.8	91.1	26.5	2431.2	2526

Record No. - 8

Applied Force N	Torque Nm.	Record trace deflection mm	Strain us.	Stress x10^5 N/m^2
98	29.4	3	917.4	953.2
147	44.1	3.5	1070.3	1112
166.6	50	4	1223.2	1271
186.2	55.9	4.5	1376.1	1429.8
205.8	61.7	5	1529	1588.7
225.4	67.6	5.5	1682	1747.5
245	73.5	6	1834.8	1906.4

Record No. - 9				
Applied Force N	Torque Nm	Record trace deflection mm	Strain us.	Stress x10^5 N/m^2
19.6	5.9	2	61.1	63.5
39.2	11.7	4	122.3	127
58.8	17.6	8	244.6	254.2
78.4	23.5	12	367	381.3
98	29.4	17	520	540.1
117.6	35.3	22	672.8	699

Record No. - 10				
Applied Force N	Torque Nm.	Record trace deflection mm	Strain us.	Stress x10^5 N/m^2
19.6	5.9	6.5	59.6	62
39.2	11.7	22	201.8	209.7
49	14.7	30.5	279.8	290.7
58.8	17.6	41	376.1	390.8

Record No. - 11

Applied Force N	Torque Nm	Record trace deflection mm	Strain us.	Stress x10^5 N/m^2
19.6	5.9	2.5	76.5	61.1
29.4	8.8	3.5	107	85.6
49	14.7	6	183.5	146.8
68.6	20.6	9	275.2	220.2
78.4	23.5	10	305.8	244.6
88.2	26.5	11	336.4	269.1
107.8	32.3	12.5	382.2	305.8

Record No. - 12

Applied Force N	Torque Nm.	Record trace deflection mm	Strain us.	Stress x10^5 N/m^2
19.6	5.9	3	9.17	7.3
39.2	11.7	6.5	19.9	15.9
49	14.7	8.5	26	20.8
58.8	17.6	10	30.6	24.5
78.4	23.5	13.5	41.3	33

Record No. - 13

Applied Force N	Torque Nm	Record trace deflection mm	Strain us.	Stress $x10^5$ N/m^2
49	14.7	8.5	259.9	270
68.6	20.6	14	428.1	444.8
88.2	26.5	19.5	596.3	619.6
107.8	32.3	25	764.5	794.3
127.4	38.2	30	917.4	953.1

Record No. - 14

Applied Force N	Torque Nm.	Record trace deflection mm	Strain us.	Stress $x10^5$ N/m^2
98	29.4	46	140.8	112.7
117.6	35.3	55	168.4	134.7
137.2	41.1	64	195.9	156.7
156.8	47	72.5	222	177.6

Record No. - 15				
Applied Force N	Torque Nm	Record trace deflection mm	Strain us.	Stress x10^5 N/m^2
19.6	5.9	9.5	29	23.2
39.2	11.7	20	61.1	48.9
58.8	17.6	29.5	90.2	72.1
78.4	23.5	40	122.3	97.9
88.2	26.5	45.5	139.1	111.3
98	29.4	51	155.9	124.8
117.6	35.3	64	195.7	156.6

Record No. - 16				
Applied Force N	Torque Nm.	Record trace deflection mm	Strain us.	Stress x10^5 N/m^2
98	29.4	24	73.4	58.7
117.6	35.3	31	94.8	75.8
137.2	41.2	38	116.2	93
156.8	47	46	140.6	112.5

Record No. - 17

Applied Force N	Torque Nm	Record trace deflection mm	Strain us.	Stress x10^5 N/m^2
19.6	5.9	2	6.1	4.9
39.2	11.7	6	18.3	14.7
58.8	17.6	13.5	41.3	33
78.4	23.5	21.5	65.8	52.6
98	29.4	30	91.7	73.4
117.6	35.3	40	122.3	97.9

Record No. - 18

Applied Force N	Torque Nm.	Record trace deflection mm	Strain us.	Stress x10^5 N/m^2
19.6	5.9	2.5	22.9	23.8
39.2	11.7	10.5	96.3	100
58.8	17.6	22	201.8	209.7
68.6	20.6	22	201.8	209.7
78.4	23.5	24.5	224.8	233.5
98	29.4	31.5	289	300.3

Record No. - 19

Applied Force N	Torque Nm	Record trace deflection mm	Strain us.	Stress x10^5 N/m^2
98	29.4	3	275.2	286
147	44.1	5.5	504.6	524.3
166.6	50	6	550.5	571.9
186.2	55.8	7	642.2	667.2
205.8	61.7	8	733.9	762.6
225.4	67.6	9	825.7	857.9
245	73.5	9.5	871.5	905.5

Record No. - 20

Applied Force N	Torque Nm.	Record trace deflection mm	Strain us.	Stress x10^5 N/m^2
49	14.7	2	183.5	190.6
147	44.1	6.5	596.3	619.6
245	73.5	10.5	963.3	1000.9
264.6	79.4	-	-	-

Record No. - 21

Applied Force N	Torque Nm	Record trace deflection mm	Strain us.	Stress x10^5 N/m^2
98	29.4	11	336.4	349.5
147	44.1	18	550.5	571.9
166.6	50	20	611.6	635.5
186.2	55.9	23	703.3	730.8
205.8	61.7	26	795.1	826.1
225.4	62.6	29	886.8	921.4
235.2	70.5	31	948	985
245	73.5	34	1039.7	1080.3

Record No. - 22

Applied Force N	Torque Nm.	Record trace deflection mm	Strain us.	Stress x10^5 N/m^2
49	14.7	4.5	137.6	143
68.6	20.6	7	214	222.4
88.2	26.5	10	305.8	317.7
107.8	32.3	13	397.5	413
205.8	61.7	21.5	657.5	683.1

Record No. - 23

Applied Force N	Torque Nm	Record trace deflection mm	Strain us.	Stress $x10^5$ N/m^2
98	29.4	10.5	96.3	77
117.6	35.3	19	174.3	139.4
137.2	41.2	21.5	197.2	157.8
156.8	47	24.5	224.8	179.8
176.4	52.9	28	256.9	205.5
186.2	55.9	29	266	212.8
196	58.8	31	284.4	227.5
205.8	61.7	34	311.9	249.5

Record No. - 24

Applied Force N	Torque Nm.	Record trace deflection mm	Strain us.	Stress $x10^5$ N/m^2
19.6	5.9	6	5.5	4.4
39.2	11.7	25	22.9	18.3
58.8	17.6	50	45.9	36.7
78.4	23.5	77	70.6	56.5
98	29.4	115	105.5	84.4

Record No. - 25

Applied Force N	Torque Nm	Record trace deflection mm	Strain us.	Stress $x10^5$ N/m^2
98	29.4	8	733.9	762
196	58.8	17.5	1605.5	1668.1
215.6	64.7	20	1834.9	1906.4
264.6	79.4	24.5	2247.7	2335.4

Record No. - 26

Applied Force N	Torque Nm.	Record trace deflection mm	Strain us.	Stress $x10^5$ N/m^2
98	29.4	10.5	321.1	256.9
117.6	35.3	12	367	293.6
137.2	41.1	14	428.1	342.5
147	44.1	15	458.7	367
156.8	47	16	489.3	391.4
176.4	52.9	16	489.3	391.4
186.2	55.9	17.5	535.1	428.1

Record No. - 27				
Applied Force N	Torque Nm	Record trace deflection mm	Strain us.	Stress $x10^5$ N/m^2
98	29.4	9.5	290.5	232.4
117.6	35.3	11	336.4	269.1
127.4	38.2	11.5	351.7	281.3
137.2	41.1	12	367	293.6
156.8	47	13.5	412.8	330.3

Record No. - 28				
Applied Force N	Torque Nm.	Record trace deflection mm	Strain us.	Stress $x10^5$ N/m^2
98	29.4	17.5	160.5	128.4
196	58.8	34	311.9	249.5
215.6	64.7	39	357.8	286.2

Chapter 5 - Discussion of Results

5.1 Determination of Axial working stress for link 5 - A theoretical approach

Load and stress variation in link 5 have been theoretically determined in chapter 3. Before comparing the experimental and theoretical stress variation in detail, the following analytical analysis is performed on the link to determine the safe working axial stress line assuming that the machine is designed for a crank speed of 4000 r.p.m. and the links are perfectly elastic, homogeneous and isotropic. The surface roughness and eccentricity in the bore axes have been neglected. The joints are taken to be ideal without any play (play in the joints introduces a mechanical error of an appreciable amount - because of hydrodynamic action of the lubricant the pin axis will not touch the end bore circle when the mechanism is in motion). From Fig. (5.1)-b, the minimum cross sectional area for link 5 is approximately 4×10^{-5} m^2 (cross-section XX) while the maximum cross sectional area is approximately 6.32×10^{-5} m^2 (cross-section ZZ). The ratio of maximum cross-sectional area to minimum cross-sectional area being 1.58. The actual axial laoding diagram for the link is shown in Fig. (5.2a) for a crank speed of 4000 r.p.m. The stress variation for cross-section XX at the same crank speed is shown in Fig. (5.2b). The stress waveform is complex and an idealized model for the stress variation is necessary to determine the fatigue strength and the safe working stress line. Assuming a sinusoidal model, the stress variation can be expressed by the following equation:

$$\sigma = \sigma_m + \sigma_r \sin \frac{2\pi t}{T} \quad \ldots\ldots\ldots\ldots \quad (5.1)$$

where σ_m = mean stress

σ_r = variable stress

T = time for one complete cycle = 0.015 s (4000 r.p.m.)

$2\sigma_r$ = stress variation

Fig 5.1

Link 3 and Link 5 (clearances are extremely exaggerated)

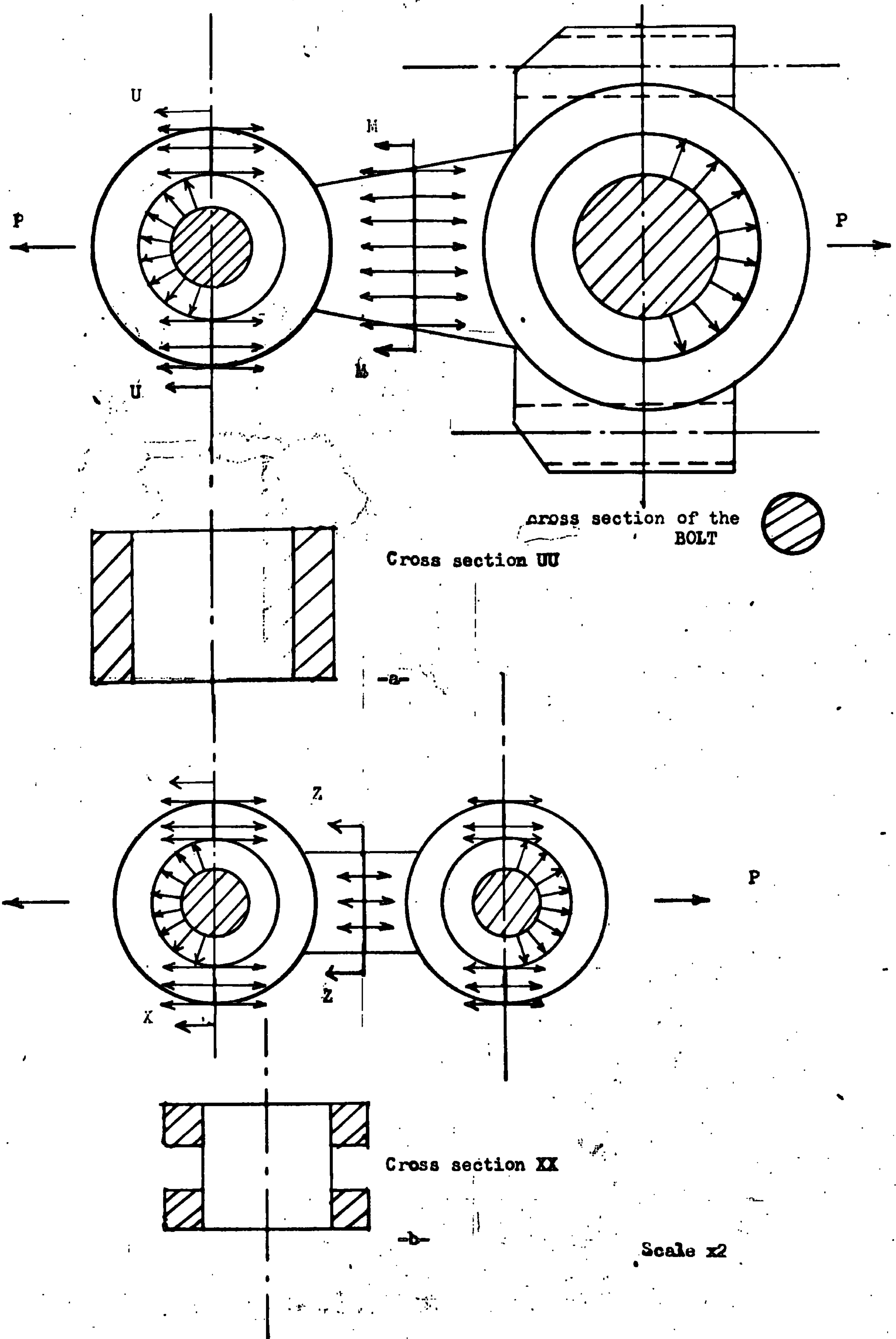

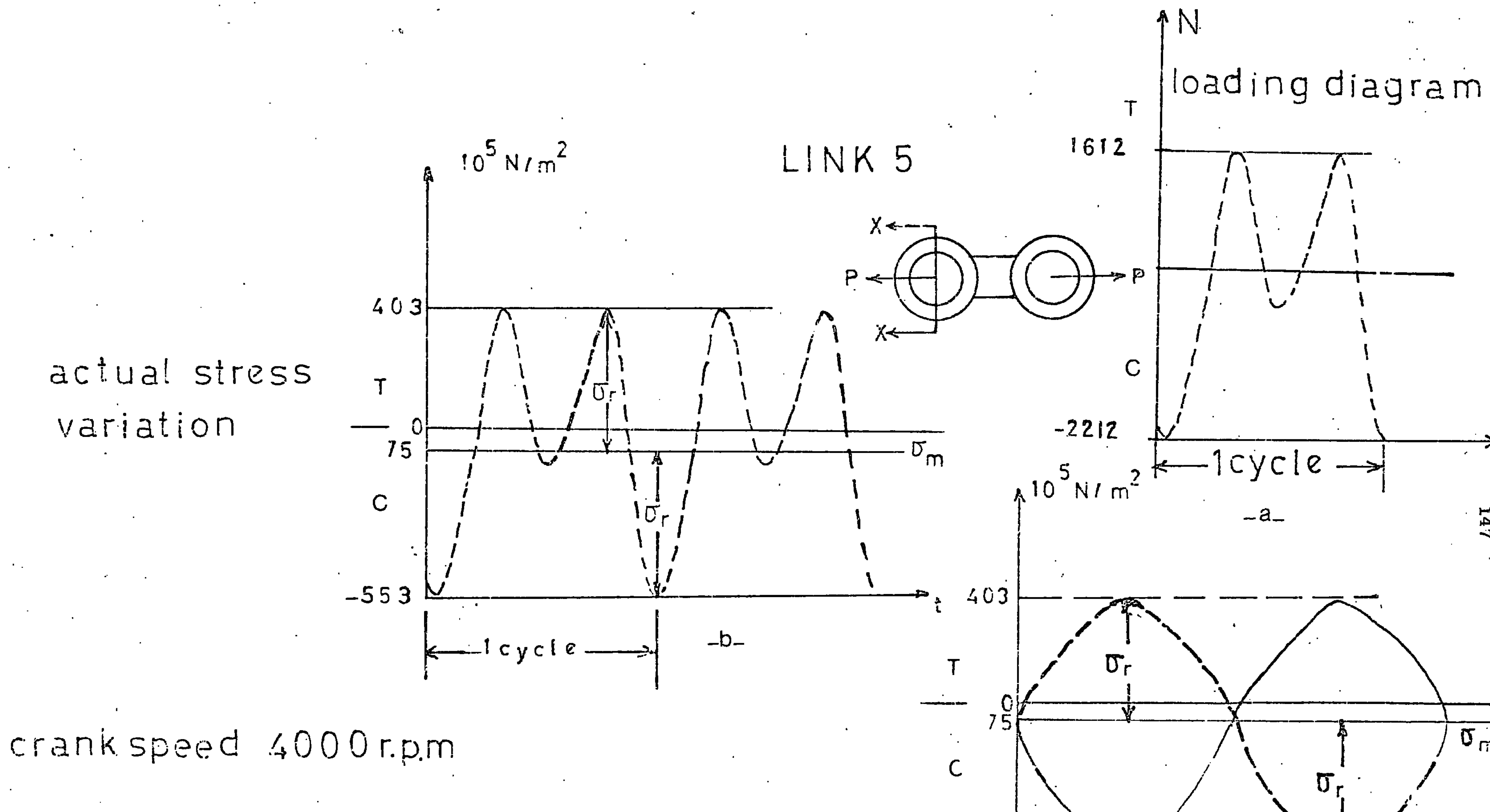
LINK 5
loading diagram
N
T
1612
P
C
-2212
1cycle
t
-a-
actual stress variation
10^5 N/m^2
403
T
0
75
C
-553
σ_r
σ_m
1 cycle
-b-
crank speed 4000 r.p.m
idealized sinusoidal model
-c-
X
P

Fig. 5.2

Substituting the numerical values eq. (5.1) yields:

$$\sigma \cong -75 \times 10^5 \pm 478 \times 10^5 \sin \frac{2\pi t}{0.015} \quad (4000 \text{ r.p.m.})$$

which is shown in Fig. (5.3)

Stress ratio is determined as:

$$R = \frac{\sigma_{min}}{\sigma_{max}} = -\frac{553 \times 10^5}{103 \times 10^5} = -1.37$$

The factor of safety F.S can now be calculated as:

$$\left|\sigma_{max}\right| = \frac{\sigma_{y.p}}{F.S}$$

$$F.S. = \frac{17.6 \times 10^7}{553 \times 10^5} \cong 3.18$$

where the yield point strength $\sigma_{y.p} = 17.6 \times 10^7$ is taken from Fig. (4.8)

There are a number of different empirical failure equations defining the relation between the variable and mean stresses. Three of the most commonly used relations are employed to calculate the endurance strength σ_e as in the following:

a - Gerber parabolic relation;

$$\left(\frac{\sigma_r}{\sigma_e}\right) + \left(\frac{\sigma_m}{\sigma_{ult}}\right)^2 = 1$$

where σ_{ult} = ultimate tensile strength $\cong 22.4 \times 10^7 \text{ N/m}^2$ (From Fig. (4.8))

$$\sigma_e = \pm 4.78 \times 10^7 \text{ N/m}^2$$

b - Modified Goodman Relation;

$$\left(\frac{\sigma_r}{\sigma_e}\right) + \left(\frac{\sigma_m}{\sigma_{ult}}\right) = 1$$

$$\sigma_e = \pm 4.62 \times 10^7 \ N/m^2$$

c - Soderberg relation

$$\left(\frac{\sigma_r}{\sigma_e}\right) + \left(\frac{\sigma_m}{\sigma_{yp}}\right) = 1$$

$$\sigma_e = \pm 4.58 \times 10^7 \ N/m^2$$

The safe working axial stress line, employing Soderberg's criteria is shown in Fig. (5.3). The axial stress at a crank speed of 4000 r.p.m. can hardly be approximated by Gerber's criteria and is above the approximate lines of failure by Soderberg and modified Goodman methods, while the axial stress at a crank speed of 25000 r.p.m. is slightly under the conservative safe stress line approximated by Soderberg criteria. A good discussion of the above procedure can be found in (20) (26) and (5). It should be noted that the values calculated are only rough estimates. No standard basis for obtaining working fatigue stress relations has been universally accepted. The fatigue strength is also affected by the clearance between the pin and hole, the distribution of shear stress around the hole boundary, lubrication, pin material and pin bending effects, surface conditions, prior overloads, environmental effects, material and manufacturing effects. The calculated endurance limit stress, σ_e, is the maximum completely reversing stress that the link can sustain for an unlimited number of cycles without fatigue failure. If the completely reversed stress is higher than σ_e, the

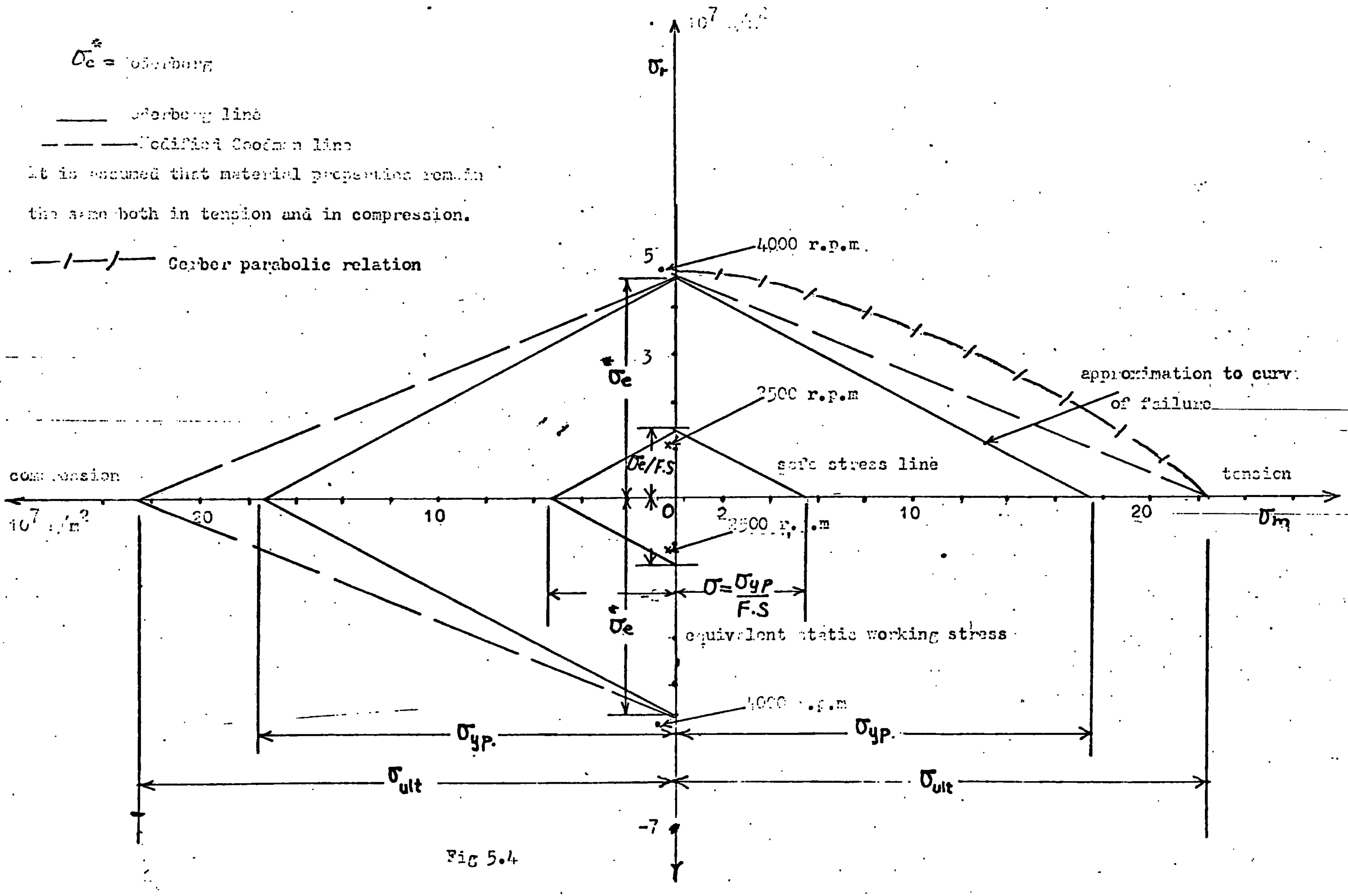
σ_c^* =
line
line
it is assumed that material properties remain
the same both in tension and in compression.
Gerber parabolic relation
σ_r
10^7
5
3
-7
4000 r.p.m.
2500 r.p.m
2500 r.p.m
4000 r.p.m
σ_e
$\sigma_e/F.S$
$\sigma = \frac{\sigma_{yp}}{F.S}$
safe stress line
equivalent static working stress
approximation to curv
of failure
compression
tension
σ_m
20
10
0
2
10
20
$\sigma_{yp.}$
$\sigma_{yp.}$
σ_{ult}
σ_{ult}

Fig 5.4

failure can be expected to take place after some finite number of cycles. The higher the stress the fewer will be the cycles before failure can be expected.

5.2 Theoretical and experimental axial stress range variation with the crank speed in link 5

The variation of the experimental axial stress range for link 5 with the crank speed and with the square of the crank speed are presented in Figures 4.9 and 4.13 respectively. Due to gauge installation and structural failures (due to slip), causing severe mechanical damage; the maximum crank arm speed could not be increased beyond about 25000 r.p.m. although various unseccesful attempts have been made to reach 3000 r.p.m. or more. The speed fluctuation effect has been neglected (as explained in chapter 4, $\pm$ 0.08 experimental speed fluctuation coefficient has been regarded as being of no importance). The basic factors introducing error are identified as follows;

1 - Sensitivity and accuracy of the measuring devices employed in the experimental set-up.

2 - Effect of the hostile enivronment

3 - Effect of the additional moment of inertia introduced by the strain-gauges and their leads on the links

4 - Error in experimental determination of the cross-sectional areas and values of Young's moduli.

5 - Personal error in interpreting the data (u.v. Traces).

In general the experimental results are in good agreement with the calculated axial stress range values for link 5. By applying method of least squares the experimental axial stress range curve is approximated by the following straight line

$$y = 38.6\,x - 7.7$$

where y = experimental axial-stress range -10^5 N/m^2

x = square of the crank speed -10^4 (rad/s)^2

The theoretical variation is in the form;

$$y = 34.6x$$

a detailed examination of Fig. 4.9 is presented in the following table:

Table 5.1

approximate crank speed r.p.m.	A approximate Theoretical axial stress range x 10^5 N/m^2	B approximate Experimental axial stress range x 10^5 N/m^2	$\left\|\frac{B-A}{A}\right\|$ x100
1100	45	45	0
1300	63	55	12.7
1410	73	69	5.5
1600	95	104	9.5
1700	108	106	1.9
1800	120	128	6.7
1970	143	143	0
2030	154	171	11
2110	164	194	18.3
2310	197	216	9.6
2410	216	242	12

Average value of $\left|\frac{B-A}{A}\right|$ x100 = 7.9

The maximum deviation occurs at a crank speed of 2110 r.p.m. (18.3%, corresponding to a difference of 30 x 10^5 N/m^2 between theoretical and experimental stress range). The experimental values consistently tend to be higher than calculated values after 1970 r.p.m. A comparison of theoretical and experimental variation of stress in a complete cycle (1 rev = 360^o) for a crank speed of 1534 r.p.m. is shown in Fig. 4.16. The close resemblance between the waveforms is significant. An approximate shift of 20^{o} is observed at the two peak tensile stress values, between the two waveforms. The sample of the recorded axial stress waveform over one cycle shown in Fig. 4.16 is in better agreement with the calculated waveform than the experimental waveform presented and compared with the calculated waveform by Alexander and Lawrence(15), for bending strain variation in the coupler of a model four-bar planar mechanism.

5.3 Calculation of eccentricity from experimental data, for links 5 and 3

a - Link 5

From Fig. 4.4 - static bending strain test for link 5, the equation of the line approximating axial stress variation with the applied torque is:

$$\frac{\sigma_{ax}}{T} = 12.7$$

where σ_{ax} = axial stress on the cross section = $\frac{\text{Axial force}}{\text{cross-sectional area}}$

T = Torque applied to the crank arm via the lever

and the equation of the straight line approximating the bending stress variation with the applied torque is:

$$\frac{\sigma_b}{T} = 26.6$$

where σ_b = bending stress = $\frac{M_C}{I}$

where I = Moment of inertia of the cross section

c = Maximum distance from the neutral axia

M = $F_{ax}.d$

where d = eccentricity

The ratio of the bending stress to axial stress is

$$K = \frac{\sigma_b}{\sigma_{ax}} = 2$$

The eccentricity d can now be calculated as:

$$K = \frac{\sigma_b}{\sigma_{ax}} = 2 = \frac{d.c.A.}{I} \quad \text{................} \quad (5.2)$$

where A = cross sectional area

eq. (5.2) can be written as

$$d = \frac{KI}{cA} \quad \ldots\ldots\ldots\ldots\ldots\ldots\ldots \quad (5.3)$$

assuming the cross sectional area to be a perfect rectangle;

$$I = \frac{bh^3}{12}$$

where b = base length of the rectangle

h = height of the rectangle

c = h/2

eq. (5.3) becomes

$$d = \frac{Kh}{6} \quad \ldots\ldots\ldots\ldots\ldots\ldots\ldots \quad (5.4)$$

substituting the appropriate values:

$$d = \frac{H}{3} \cong 2.8 \text{ mm}$$

b - Link 3

Similarly from Fig 4.5 static bending strain test for link 3:

$$\frac{\sigma_{ax}}{T} = 4 \quad \text{and} \quad \frac{\sigma_b}{T} = 8.75$$

$$k = \frac{\sigma_b}{\sigma_{ax}} = 2.2$$

$$d = \frac{Kh}{6} = 0.36h = 4.3 \text{ mm}$$

In the above calculations it is assumed that the material follows Hooke's law and the magnitude of the stress is proportional to the distance from the neutral axis.

5.4 Eccentricity - dynamic case

The variation of axial and bending stresses in links 5 and 3 with the crank speed were shown in Figures 4.9, 4.11, 4.12 and 4.10 respectively. The ratio K_d of the experimental bending stress ranges to experimental axial strain ranges for both links are given in the following table, Table 5.2 a and b.

Table 5.2-a

crank speed r.p.m.	K dynamic link 5
1080	1.9
1280	2
1420	2.2
1610	2
1800	2.5
2050	2.4
2400	2.4

K dynamic average = 2.2

Table 5.2-b

crank speed r.p.m.	k dynamic link 3
1082	7.3
1320	3.3
1440	3.5
1560	3.4
1800	3.4
2040	2.6

K dynamic average = 3.9

Average value of K dynamic for link 5 is in good agreement with the K value for the static case while the average value of K dynamic for link 3 is about 1.77 times of the K value obtained for the static case

5.5 Determination of Axial working stress for link 3 - A theoretical approach

Applying the same assumptions and method shown in section 5.1., the working stress is determined for the minimum cross sectional area (cross section UU, Fig. 5.1) as in the following;

The loading diagram and axial cyclic stress variation are shown in Fig. 5.4 for the cross section at a crank speed of 4000 r.p.m.

A = cross sectional area $11 \times 10^{-5}\ m^2$

$\sigma_{max} = 302 \times 10^5\ N/m^2$

$\sigma_{min} = -88 \times 10^5\ N/m^2$

$\sigma_m = 107 \times 10^5\ N/m^2$

$\sigma_r = 195 \times 10^5\ N/m^2$

$2\sigma_r = 390 \times 10^5\ N/m^2$

$T = 0.015\ s$

using eq. (5.1) the actual stress pattern is approximated by the following sinusoidal model:

$$\sigma = 107 \times 10^5 + 195 \times 10^5 \sin \frac{2\pi t}{0.015}$$

which is shown in Fig. (5.4)

The stress ratio is:

$$R = \frac{\sigma_{min}}{\sigma_{max}} = -0.3$$

From Fig (4.8)

$\sigma_{yp} = 11.4 \times 10^7 \ N/m^2$

$\sigma_{ult} = 12.4 \times 10^7 \ N/m^2$

The factor of safety can be calculated as

$$|\sigma_{max}| = \frac{\sigma_{yp}}{F.S}$$

$F.S \cong 3.77$

Soderberg relation gives an endurance strength of $2.15 \times 10^7 \ N/m^2$. σ_e calculated by modified Goodman relation is $2.13 \times 10^7 \ N/m^2$. The working stress diagram is shown in Fig. (5.5). Axial stress acting on the cross section is above the Soderberg line. Cross section MM (Fig. 5.1) is also represented on the same diagram.

5.6 Theoretical and experimental axial stress range variation with the crank speed in link 3.

The variation of the experimental axial stress range for link 3 with the crank speed and with the square of the crank speed are presented in Figures 4.12 and 4.13 respectively. Crank speed could not be increased beyond about 2100 r.p.m. (due to gauge installation failures, and drift in the u.v. traces). By applying the method of least squares the experimental axial stress range curve is approximated by the straight line

$$y = 21.8x + 11.4$$

where y = experimental axial stress range $-10^5 \ N/m^2$

x = square of the crank speed $-10^4 \ (rad/s)^2$

the 'theoretical variation is in the form:

$$y = 21.4x$$

a detailed examination of Fig. 4.12 is presented in the following table:

Table 5.3

approximate crank speed r.p.m.	A Approximate theoretical axial stress range 10^5 N/m^2	B Approximate experimental axial stress range 10^5 N/m^2	$\left\lvert\frac{B-A}{A}\right\rvert x100$
1100	27	24	11.1
1260	36	57	58.3
1430	47	70	49
1550	57	74	30
1790	75	83	10.6
1910	85	94	10.6
2080	100	114	14
2130	105	123	17.1

average value of $\left\lvert\frac{B-A}{A}\right\rvert$ x100 = 25

which is about 3 times higher than that of link 5. The experiment values are generally higher than the calculated values. The maximum deviation occurs at a crank speed of 1260 r.p.m. (58.3%). A comparison of theoretical and experimental cyclic axial stress variation is shown in Fig. 4.15

5.7 Bending stresses in a direction normal to plane of the mechanism

The variation of peak to peak bending stresses with the crank speed for links 3 and 5 are shown in Figures 4.10 and 4.11 respectively.

The bending stress range curves can be approximated by the straight lines:

$y = 37x + 150$ .... (link 3)

$y = 104x - 58$ .... (link 5)

where again:

y = bending axial stress range - 10^5 N/m^2

x = square of crank speed -10 (rad/s)^2

At a crank speed of 4000 r.p.m. the expected bending stress range values for the links 3 and 5 can be calculated as 800 x 10^5 N/m^2 and 1767 x 10^5 N/m^2 respectively. The expected axial stress ranges at the same crank speed for the links are 395 x 10^5 N/m^2 (link 3) and 670 x 10^5 N/m^2 (link 5)(values based on experimental data). The variable stress values are well above the endurance strength of the links. The combined effect of bending and axial stresses (method of superposition) at a crank speed of 4000 r.p.m. would indicate a state of failure.

5.8 Stress distribution in the links

The main objective of the test explained in section 4.4.3 was to determine whether the bending stresses are due to an initial permanent link deformation, an offset,or due to the pins, tolerance and/or clearance effects or other misalignments which are factors external to the links themselves. A detailed examination of Figures 4.6 and 4.7 are presented in Tables (5.4 - 7). Results of the tests for both links show that the bending stress (z-direction) are due to effects which are external to the links. The basic factors introducing error to the results are identified as follows:

1 - Effects of deviation in the crank angle ($90^\circ \pm 5^\circ$)

2 - Friction in the bearings

3 - Effects of elasticity of the shafts and links

The possible bending mechanisms are shown in Figures (5.6) and (5.7)

Applied Torque = T N.m.	$\sigma ax = P/A$ (compressive) 10^5 N/m^2	Gauge m (Tension) axial and bending stress = σ comp 1 10^5 N/m^2	Gauge k (compression) axial + bending stress = $\sigma comp\ 2$ 10^5 N/m^2	Net bending stress (tensile) $\sigma comp\ 1 + \sigma ax = \sigma bm$ 10^5 N/m^2	Net bending stress (compressive) $\sigma comp\ 2 - \sigma ax = \sigma bk$ 10^5 N/m^2	eccentricity 1 $e_1 = \frac{\sigma_{bm}\ h}{6\ \sigma_{ax}}$ mm	eccentricity 2 $e_2 = \frac{\sigma_{bk}\ h}{6\ \sigma_{ax}}$ mm	Av. eccentricity $\frac{e_1 + e_2}{2}$ mm	Bending moment 1 $e_1.P$ N.m.	Bending moment 2 $e_2.P$ N.m
6	52	52	156	104	104	2.8	2.8	2.8	0.9	0.9
12	104	166	364	270	260	3.6	3.5	3.5	2.3	2.3
17.8	176	280	582	456	406	3.6	3.2	3.4	4	3.5
23.5	239	405	800	644	561	3.8	3.3	3.5	5.7	5
30	301	540	1018	841	717	3.9	3.3	3.6	7.4	6.3
35.5	364	655	1246	1019	882	3.9	3.4	3.6	9	7.8

From Fig. 4.6 - Static bending test for link 5 - Stress distribution profile
Case 1 - based on experimental data

Table 5.4

Applied Torque = T N.m.	$\sigma_{ax} = P/A$ (compressive) 10^5 N/m^2	Gauge k (Tension) axial and bending stress = $\sigma_{comp\,1}$ 10^5 N/m^2	Gauge m (compression) axial + bending stress = $\sigma_{comp\,2}$ 10^5 N/m^2	Net bending stress (tensile) $\sigma_{comp\,1} + \sigma_{ax} = \sigma_{bk}$ 10^5 N/m^2	Net bending stress (compressive) $\sigma_{comp\,2} - \sigma_{ax} = \sigma_{bm}$ 10^5 N/m^2	eccentricity 1 $e_1 = \frac{\sigma_{bk}\,h}{6\,\sigma_{ax}}$ mm	eccentricity 2 $e_2 = \frac{\sigma_{bm}\,h}{6\,\sigma_{ax}}$ mm	Av. eccentricity $\frac{e_1 + e_2}{2}$ mm	Bending moment 1 $e_1 . P$ N.m.	Bending moment 2 $e_2 . P$ N.m
6	31	62	119	93	88	4.2	4	4.1	0.8	0.8
12	62	176	291	238	229	5.4	5.2	5.3	2.1	2
17.8	104	301	499	405	395	5.5	5.4	5.45	3.6	3.5
23.5	145	395	686	540	541	5.2	5.2	5.2	4.8	4.8
30	176	519	883	695	707	5.6	5.7	5.65	6.2	6.3
35.5	223	623	1091	846	868	5.3	5.5	5.4	7.4	7.7

From Fig. 4.6 - Static bending test for link 5 - Stress distribution profile
Case 2 - based on experimental data

Table 5.5

Applied Torque = T N.m.	σax = P/A (Tensile) 10^5 N/m^2	Gauge c (Tension) axial and bending stress = σ comp 1 10^5 N/m^2	Gauge d (compression) axial + bending stress = σcomp 2 10^5 N/m^2	Net bending stress (tensile) σcomp 1 − σax = σ_{bc} 10^5 N/m^2	Net bending stress (compressive) σcomp 2 + σax = σ_{bd} 10^5 N/m^2	eccentricity 1 $e_1 = \frac{\sigma_{bc}\, h}{6\, \sigma_{ax}}$ mm	eccentricity 2 $e_2 = \frac{\sigma_{bd}\, h}{6\, \sigma_{ax}}$ mm	Av. eccentricity $\frac{e_1 + e_2}{2}$ mm	Bending moment 1 $e_1.P$ N.m.	Bending moment 2 $e_2.P$ N.m
6	7	48	35	41	42	13.6	14	13.8	1.4	1.5
12	30	120	64	90	94	7	7.3	7.15	3.1	3.3
17.8	35	192	123	157	158	10.4	10.5	10.45	5.4	5.5
23.5	48	258	163	210	211	10.2	10.2	10.2	7.3	7.3
30	62	323	198	261	260	9.8	9.8	9.8	9	9
35.5	80	387	227	307	307	8.9	8.9	8.9	10.6	10.6

From Fig. 4.7 - static bending test for link 3 - stress distribution profile
Case 1 - based on experimental data

Table 5.6

Applied Torque = T N.m.	$\sigma ax = P/A$ (Tensile) 10^5 N/m^2	Gauge d (Tension) axial and bending stress = σ comp 1 10^5 N/m^2	Gauge c (compression) axial + bending stress = $\sigma comp\ 2$ 10^5 N/m^2	Net bending stress (tensile) $\sigma comp\ 1 - \sigma ax = \sigma_{b,d}$ 10^5 N/m^2	Net bending stress (compressive) $\sigma comp\ 2 + \sigma ax = \sigma_{bc}$ 10^5 N/m^2	eccentricity 1 $e_1 = \frac{\sigma_{bd}\ h}{6\ \sigma_{ax}}$ mm	eccentricity 2 $e_2 = \frac{\sigma_{bc}\ h}{6\ \sigma_{ax}}$ mm	Av. eccentricity $\frac{e_1 + e_2}{2}$ mm	Bending moment 1 $e_1.P$ N.m.	Bending moment 2 $e_2.P$ N.m
6	11	35	13	24	24	5	5	5	0.8	0.8
12	32	102	51	70	83	5.1	6	5.5	2.4	2.8
17.8	43	170	83	127	126	6.9	6.8	6.8	4.4	4.3
23.5	64	230	115	166	179	6	6.5	6.2	5.7	6.2
30	76	288	147	212	223	6.5	6.8	6.6	7.3	7.7
35.5	104	344	166	240	270	5.4	6	5.7	8.4	9.3

From Fig. 4.7 Static bending test for link 3 - Stress distribution profile
Case 2 - based on experimental data

Table 5.7

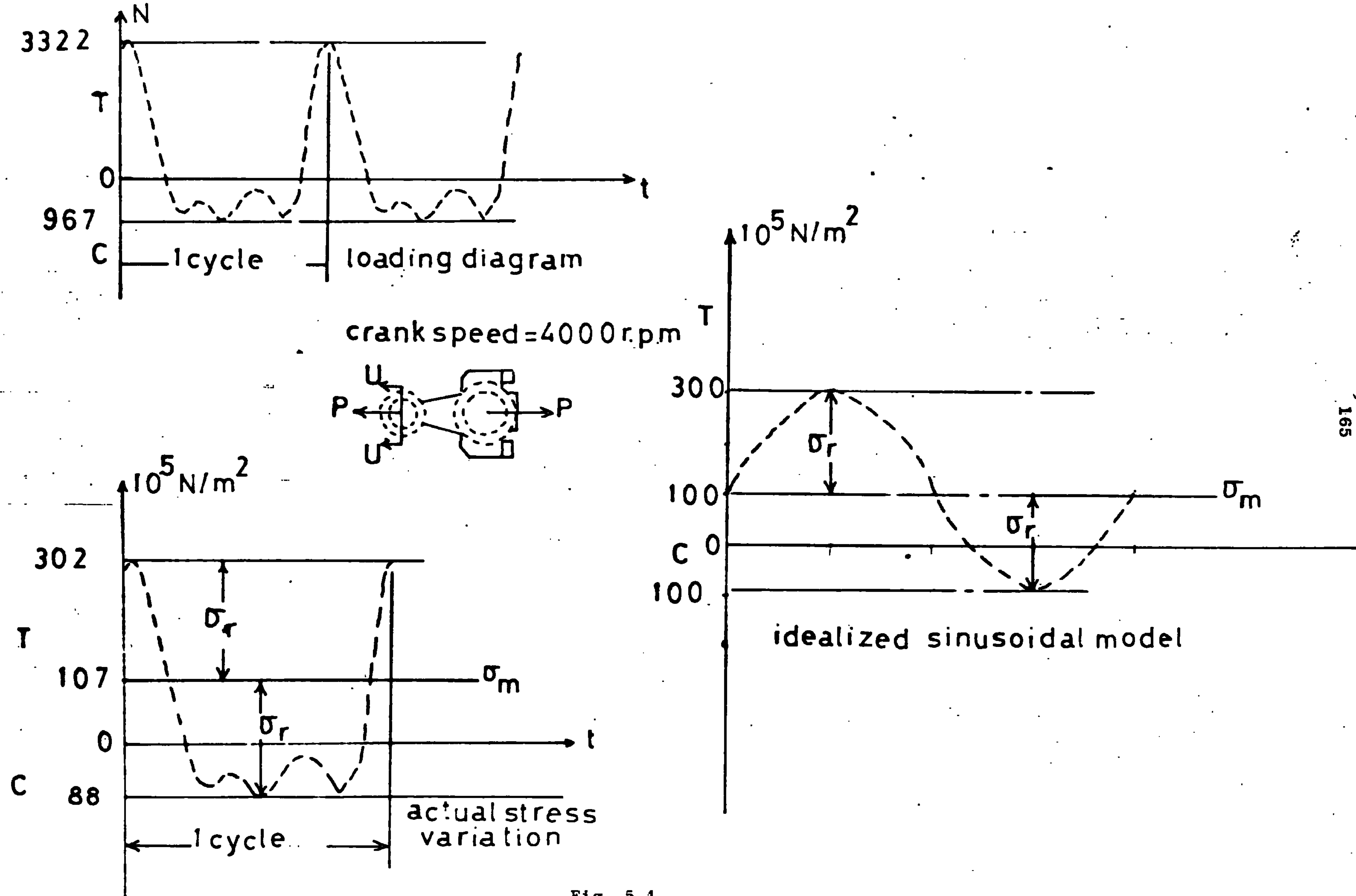
N
3322
T
0
t
967
C
1cycle
loading diagram
crank speed=4000 r.p.m
U
P
U
P
$10^5 N/m^2$
302
T
σ_r
107
σ_m
σ_r
0
t
C
88
1 cycle
actual stress variation
$10^5 N/m^2$
T
300
σ_r
100
σ_m
σ_r
C
0
100
idealized sinusoidal model

Fig. 5.4

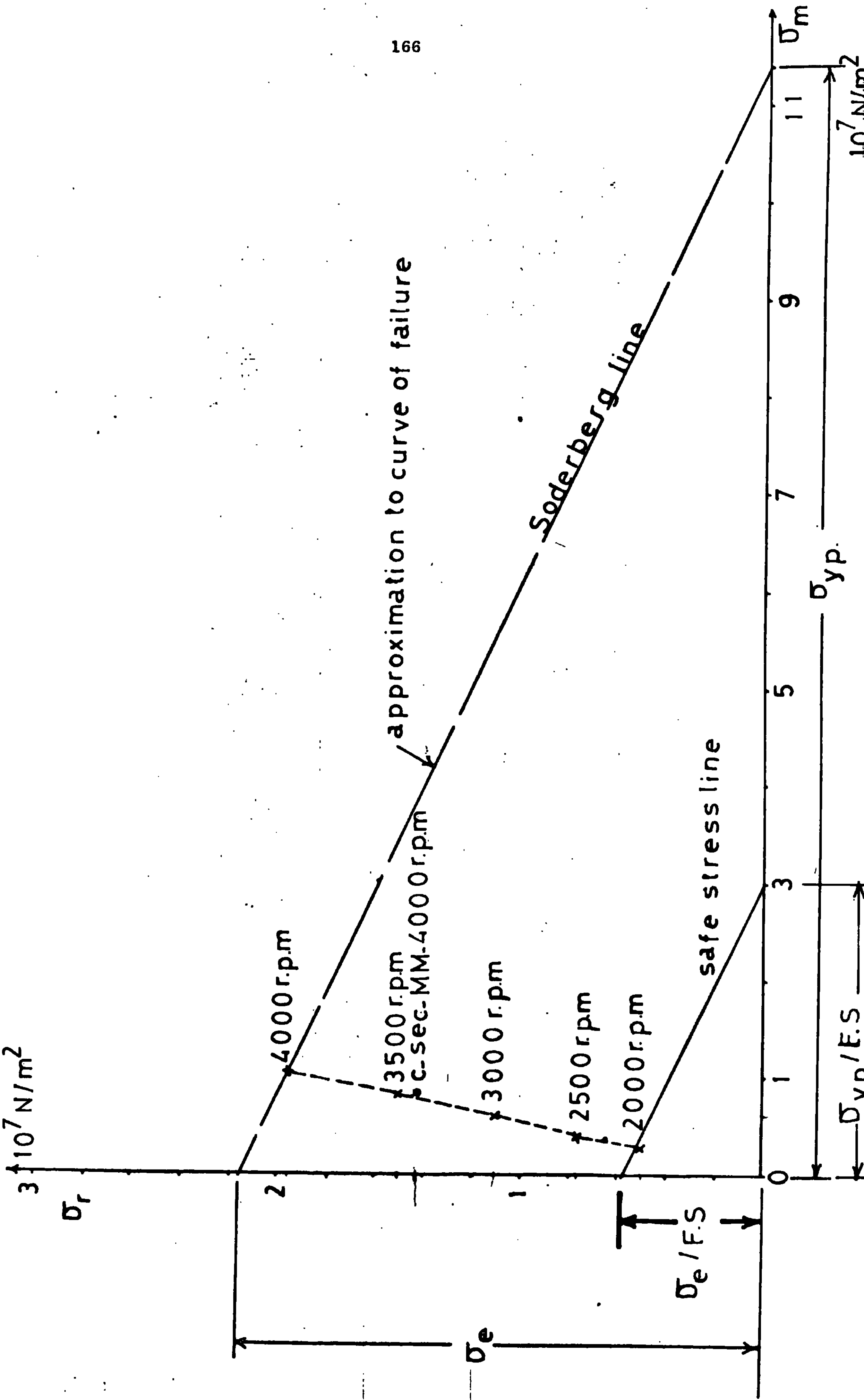
approximation to curve of failure
Soderberg line
safe stress line
4000 r.p.m
3500 r.p.m
c-sec-MM-4000 r.p.m
3000 r.p.m
2500 r.p.m
2000 r.p.m
$10^7 N/m^2$
σ_r
σ_m
σ_e
σ_e / F.S
$\sigma_{y.p.}$
$\sigma_{y.p}$ / F.S
0
1
2
3
5
7
9
11

Fig. 5.5

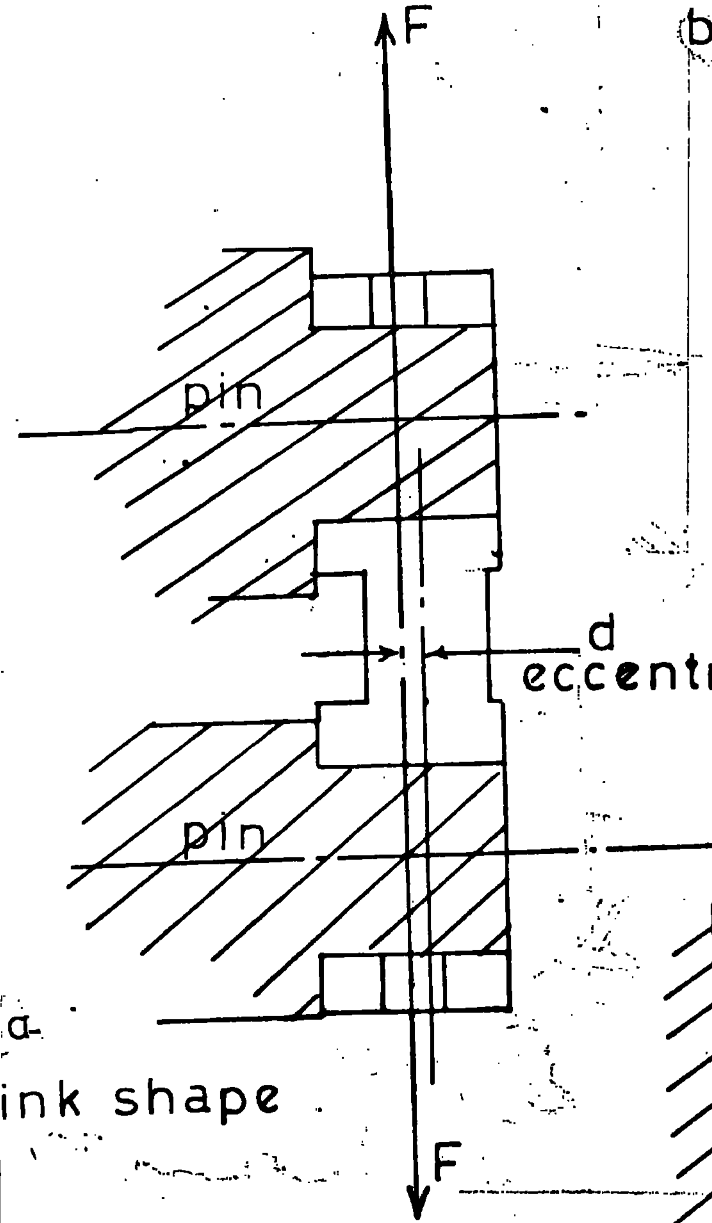
F
pin
d
eccentricity
pin
a-
ink shape
F

Fig. 5.6

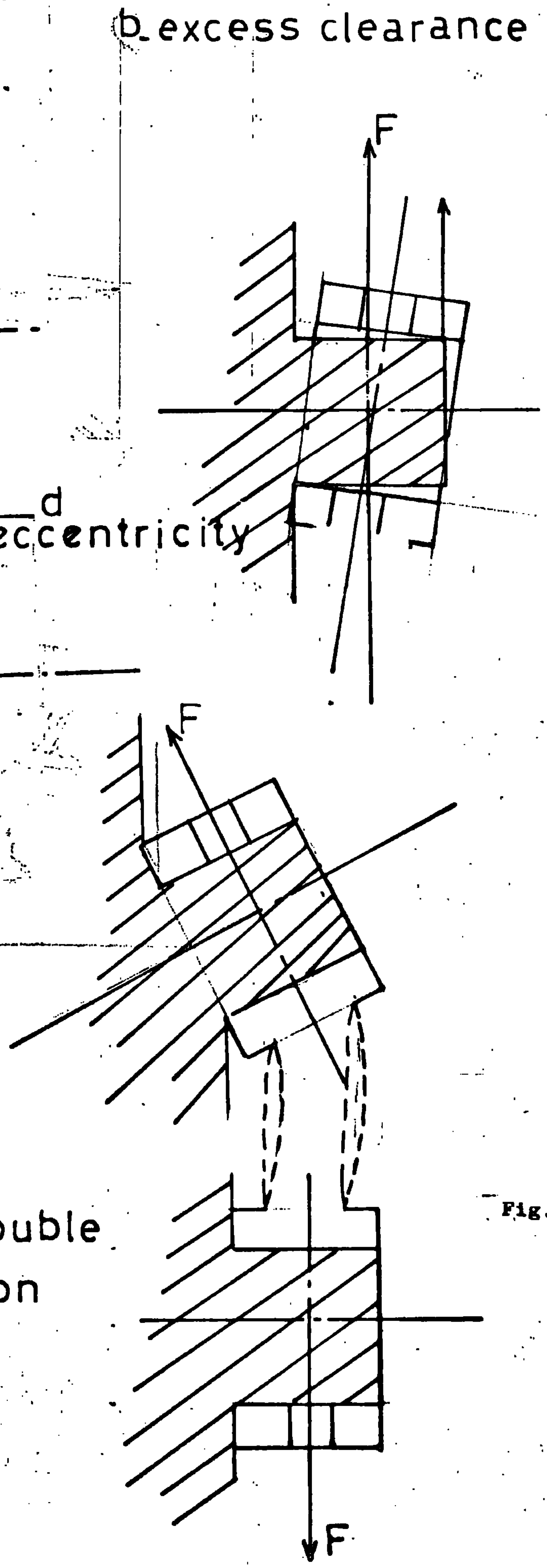
b-excess clearance
F
F
c-single or double
pin deformation
F

Fig. 5.7

5.9 General Considerations

During the actual weaving operation the stresses would increase due to the external resistance introduced by the threads on the combs and needle arms. The value of this expected increase is unknown. The hardness and tensile tests performed on the connecting rods showed that there is a difference between material properties of the two links although they were expected to be the same (phosphor bronze alloy). Mechanical damage (scratches inside the link bores and flange sides) is detected on both links. The effect of friction has completely been neglected in the analytical calculations. Stress waveform pattern is complex in structure for both links and is very destructive in nature from a fatigue point of view.

Chapter 6 - Conclusion

Bending stresses in a direction normal to the plane of the mechanism are present in both of the links investigated and have a dominating effect. The axial cyclic and peak to peak stress variation in both links is generally in good agreement with the calculated values. The bending stresses normal to the plane of the mechanism are due to misalignment effects which are external to the connecting rods themselves. The dominating characteristic of the dynamic bending stresses has been confirmed with static tests carried out on the mechanism. Even by neglecting the bending stress effects on the links the present design is found to be unsatisfactory at a crank speed of 4000 r.p.m. since the axial stress values are above the working axial stress line approximated by the Soderberg criteria. In the presence of bending stresses fatigue failure can be expected to occur at approximately 2000 r.p.m. However if bending stresses are negligible the present design can be used up to a crank speed of 2500 r.p.m. (See Appendix A3)

To increase the speed of the mechanism the following general basic major points are suggested:

1. A detailed deflection tolerance and clearance analysis to reduce the bending stresses due to misalignments theoretically to zero which would automatically increase the crank speed range up to 2500 r.p.m.
2. Fatigue tests on the links to determine the experimental endurance strength.
3. The stress constraints are determined. Any increase in the critical cross sections of the connecting rods will decrease the stresses, and therefore would yield a higher operating speed.
4. It was found that extreme axial stresses in a complete cyle of input crank roatation occurs at different angles of input crank

rotation for the two connecting rods. Any slight changes in link lengths and geometry to decrease the extreme angular acceleration values for links 4 and 6 will accordingly decrease the axial stresses on the two connecting rods and change the cyclic axial stress pattern.

5 Without changing the configuration of the mechanism, any suitable material change with a higher endurance and yield point limit will accordingly permit an increase in the crank speed.

Appendix A-1

```
C  COMPLETE KINEMATIC,FORCE & STRESS ANALYSIS OF THE MECHANISM
C  SERDAR GULEN
C  UNIVERSITY OF DURHAM, DEPT. OF ENGINEERING SCIENCE
C
      PI=3.14159265
      DO1 I=0,360,15
      PSI=I
      PSI=PSI/180.0*PI
      OMEGA2=(2.0*PI*2500.0)/(60.0)
      VA=OMEGA2*0.011
      O1E=COS(PSI)*0.011
      AE=SIN(PSI)*0.011
      AF=AE+0.005
      O2F=0.043-O1E
      AO2=SQRT(AF**2+O2F**2)
      ETA=ATAN(AF/O2F)
      ZEK=ARCOS((0.00128-AO2**2)/(-0.044*AO2))
      CAL=ARCOS((0.002248-AO2**2)/(0.001848))
      ALPHA=PI-(ZEK+CAL)
      BETA=ALPHA-ETA
      YI=PSI-BETA
      Z=SIN(YI)*0.011
      GAMA=PI-(ETA+ZEK+75.0/180.0*PI)
      DO=SIN(GAMA+75.0/180.0*PI-BETA)*0.022
      XDBA=VA*(((SIN(PSI)*TAN(GAMA+165.0/180.0*PI))+COS(PSI)
     9)/(TAN(GAMA+165.0/180.0*PI)-TAN(BETA+0.5*PI)))
      YDBA=XDBA*TAN(BETA+0.5*PI)
      VBA=SQRT(XDBA**2+YDBA**2)
      XDB=(VA*(-SIN(PSI)))+XDBA
      YDB=(VA*COS(PSI))+YDBA
      VB=SQRT(XDB**2+YDB**2)
      OMEGA3=VBA/0.042
```

```
> 29    OMEGA3=VBA/0.042
> 29.1  EN4=(0.5*0.0000584)*(OMEGA3**2)
> 300   OMEGA4=VB/0.022
> 30.05 EN1=(0.5*0.000092265)*(OMEGA4**2)
> 30.06 EN3=(0.5*0.000043502)*(OMEGA4**2)
> 310   ADR=0.022*(OMEGA4**2)
> 32    ABAR=0.042*(OMEGA3**2)
> 330   TETA=ATAN((0.032-SIN(GAMA)*0.022)/(0.042-COS(GAMA)*0.022))
> 340   CO3=((0.032-SIN(GAMA)*0.022)/(SIN(TETA)))
> 350   VAN=ARCOS((0.029**2+CO3**2-0.02**2)/(0.029*2*CO3))
> 36    XLAMB=VAN+TETA
> 36.1  RE=SIN(XLAMB-GAMA)*0.022
> 37    FI=ARCOS((0.02**2+CO3**2-0.029**2)/(0.04*CO3))
> 38    UPA=FI-TETA
> 38.1  YUM=PI-(UPA+XLAMB)
> 38.2  D=COS(XI)*0.02
> 390   XDDC=VB*((COS(GAMA)+SIN(GAMA)*TAN(0.5*PI-UPA)))/
> 400   6(TAN(0.5*PI-UPA)-TAN(0.5*PI+XLAMB))
> 41    XDD=(VB*(-SIN(GAMA)))+XDDC
> 42    YDDC=XDDC*(TAN(0.5*PI+XLAMB))
> 430   YDD=XDD*(TAN(0.5*PI-UPA))
> 44    VD=SQRT(XDD**2+YDD**2)
> 45    VDC=SQRT(XDDC**2+YDDC**2)
> 460   OMEGA6=VD/0.02
> 46.01 EN2=(0.5*0.000306872)*(OMEGA6**2)
> 46.02 EN6=(0.5*0.000022674)*(OMEGA6**2)
> 47    OMEGA5=VDC/0.029
> 47.1  EN5=(0.5*0.0000075)*(OMEGA5**2)
> 48    ADR=0.02*(OMEGA6**2)
> 49    ADCR=0.029*(OMEGA5**2)
> 49.2  AAR=(OMEGA2**2)*0.011
> 50    V1=ABR*COS(255.0/180.0*PI+GAMA)
> 51    V2=ABR*SIN(255.0/180.0*PI+GAMA)
```

```
> 520 V3=AAR*COS(PI+PSI)
> 153 V4=AAR*SIN(PI+PSI)
> 54 V5=ABAR*COS(PI+BETA)
> 55 V6=ABAR*SIN(PI+BETA)
> 56 V7=TAN(165.0/180.0*PI+GAMA)
> 57 V8=TAN(BETA+0.5*PI)
> 58 XDDBAT=(-V7*(V3+V5-V1)+V6+V4-V2)/(V7-V8)
> 58.1 YDDBAT=XDDBAT*V8
> 58.2 XDDBT=XDDBAT+V3+V5-V1
> 58.3 YDDBT=XDDBT*V7
> 590 ABT=SQRT(XDDBT**2+YDDBT**2)
> 60. ABAT=SQRT(XDDBAT**2+YDDBAT**2)
> 60.10 ANGC3=ABAT/0.042
> 60.11 B1=ANGC3*0.0000584
> 60.12 BI=(ANGC3)/(OMEGA2**2)
> 60.2 ANGC4=ABT/0.022
> 60.22 B2=ANGC4*0.000043502
> 60.23 B5=ANGC4*0.000092265
> 610 P1=-ADR*COS(UPA)+ABR*COS(PI+GAMA)+ABT*COS(1.5*PI+GAMA)
> 61.01 "+ADCR*COS(PI+XLAMB)
> 61.10 P2=-ADR*SIN(-UPA)+ABR*SIN(PI+GAMA)+ABT*SIN(1.5*PI+GAMA)
> 61.2 "+ADCR*SIN(PI+XLAMB)
> 61.30 P3=TAN(1.5*PI-UPA)
> 61.4 P4=TAN(XLAMB-0.5*PI)
> 61.50 XDDCT=(-P1*P3+P2)/(P3-P4)
> 61.51 YDDCT=P4*XDDCT
> 61.52 ADCT=SQRT(XDDCT**2+YDDCT**2)
> 61.53 XDDDT=P1+XDDCT
> 61.54 YDDDT=P2+YDDCT
> 61.55 ADT=SQRT(XDDDT**2+YDDDT**2)
> 62.8 ANGC5=ADCT/0.029
> 62.8010 TIM=(ANGC5)/(OMEGA2**2)
> 62.802 ANGC6=ADT/0.02
> 62.810 B3=ANGC5*0.0000075
```

```
> 62.810   B3=ANGC5*0.0000075
> 62.820   B4=ANGC6*0.000022674
> 62.830   B6=ANGC6*0.000306872
> 630      AB=SQRT(ABR**2+ABT**2)
> 63.50    PIK1=ANGC3*OMEGA3*0.0000584
> 63.51    PIK2=0.0000075*ANGC5*OMEGA5
> 63.70    PIK3=0.5*0.0000584*(OMEGA3**2)
> 63.8     PIK4=0.5*0.0000075*(OMEGA5**2)
> 63.81    RT1=OMEGA3/OMEGA2
> 63.91    RT2=OMEGA4/OMEGA2
> 63.92    RT3=OMEGA5/OMEGA2
> 63.93    RT4=OMEGA6/OMEGA2
> 640      PSI=PSI*57.2957795
> 650      XLAMB=XLAMB*57.2957795
> 65.10    YUM=YUM*57.2957795
> 66       BETA=BETA*57.2957795
> 67       UPA=UPA*57.2957795
> 67.10    CAL=CAL*57.2957795
> 680      GAMA=GAMA*57.2957795
> 68.10    ZEK=ZEK*57.2957795
> 68.20    ETA=ETA*57.2957795
> 68.3500  A1=0.000092265*OMEGA4*ANGC4
> 68.3510  A2=0.000043502*OMEGA4*ANGC4
> 68.3520  A3=0.000306872*OMEGA6*ANGC6
> 68.3530  A4=0.000022674*OMEGA6*ANGC6
> 68.3540  WER=B4+B6
> 68.3550  POW=WER*OMEGA6
> 68.951   TR=(B4+B6)/(D)
> 68.952   STR=(TR)/(6.32)
> 68.953   HOM1=(0.689655*B3*COS(2.0*PI-UPA))/(COS(XLAMB))
> 68.954   HOM2=-0.02*SIN(2.0*PI-UPA)+0.02*TAN(XLAMB)
> 68.955   F56X=(-WER-HOM1)/(HOM2)
> 68.956   HOM3=B3+F56X*(0.029)*SIN(XLAMB)
> 68.957   F56Y=(HOM3)/(0.029*COS(XLAMB))
```

```
> )) 68.957     F56Y=(HOM3)/(0.029*COS(XLAMB))
> )) 68.97      QER=B2+B5
>  ) 68.98      POW1=QER*OMEGA4
> )) 68.99      STRESS=(0.000329546*ANGC6)/(D*6.32)
> ) )68.992     STRS3=((STRESS*6.32*RE)+QER)/(DO*14.95)
> )))68.993     TORQUE=STRS3*14.95*Z
> )) 68.99400   F5=STRESS*6.32
> )))68.9950    F3=STRS3*14.95
>  ) 68.996     ENTOT=EN1+EN3+EN4+EN2+EN6+EN5
> )) 69         WRITE(6,2)PSI,VBA,VB,VDC,VD
>  ))70       2 FORMAT(2X,'PSI=',F6.2,2X,'VBA=',F12.5,2X,'VB=',F12.5,2X,
> )) 71         &'VDC=',F12.5,2X,'VD=',F12.5)
> )) 72       1 CONTINUE
>  ) 73         STOP
> .) 74         END
#END OF FILE
#
```

```
$r -load#
#EXECUTION BEGINS
 PSI=  0.0    VBA=   3.24050  VB=   1.31081  VDC=   0.33994  VD=   1.28271
 PSI= 15.00   VBA=   2.97831  VB=   0.25167  VDC=   0.04699  VD=   0.24801
 PSI= 30.00   VBA=   2.52188  VB=   0.75752  VDC=   0.16003  VD=   0.74486
 PSI= 45.00   VBA=   2.03102  VB=   1.59194  VDC=   0.51007  VD=   1.54669
 PSI= 60.00   VBA=   1.58230  VB=   2.21668  VDC=   1.08243  VD=   2.09160
 PSI= 75.00   VBA=   1.19012  VB=   2.64496  VDC=   1.79655  VD=   2.33648
 PSI= 90.00   VBA=   0.83772  VB=   2.90031  VDC=   2.46652  VD=   2.23615
 PSI=105.00   VBA=   0.49422  VB=   2.99685  VDC=   2.89305  VD=   1.79150
 PSI=120.00   VBA=   0.11970  VB=   2.93125  VDC=   2.97052  VD=   1.11426
 PSI=135.00   VBA=   0.33292  VB=   2.68153  VDC=   2.71753  VD=   0.41261
 PSI=150.00   VBA=   0.90632  VB=   2.21863  VDC=   2.20783  VD=   0.10094
 PSI=165.00   VBA=   1.59992  VB=   1.54521  VDC=   1.51304  VD=   0.30120
 PSI=180.00   VBA=   2.31904  VB=   0.74672  VDC=   0.72547  VD=   0.21170
 PSI=195.00   VBA=   2.89952  VB=   0.03069  VDC=   0.02976  VD=   0.00952
 PSI=210.00   VBA=   3.21894  VB=   0.68693  VDC=   0.66745  VD=   0.19371
 PSI=225.00   VBA=   3.24541  VB=   1.21350  VDC=   1.18668  VD=   0.25263
 PSI=240.00   VBA=   2.99431  VB=   1.64895  VDC=   1.63186  VD=   0.15779
 PSI=255.00   VBA=   2.48572  VB=   2.03290  VDC=   2.04348  VD=   0.10567
 PSI=270.00   VBA=   1.73501  VB=   2.38646  VDC=   2.42695  VD=   0.55220
 PSI=285.00   VBA=   0.76613  VB=   2.70337  VDC=   2.72390  VD=   1.16978
 PSI=300.00   VBA=   0.36142  VB=   2.94059  VDC=   2.79316  VD=   1.86095
 PSI=315.00   VBA=   1.52082  VB=   3.01082  VDC=   2.46961  VD=   2.40263
 PSI=330.00   VBA=   2.51002  VB=   2.79739  VDC=   1.75345  VD=   2.52979
 PSI=345.00   VBA=   3.11517  VB=   2.21750  VDC=   0.92981  VD=   2.12218
 PSI=360.00   VBA=   3.24050  VB=   1.31082  VDC=   0.33994  VD=   1.28272

 STOP   0
#EXECUTION TERMINATED
#
```

```
$r -load#
#EXECUTION BEGINS
 PSI=  0.0   ABR=   78.10159  ABT= 1019.03882  ANGC4=  46319.9453
 PSI= 15.00  ABR=    2.87890  ABT= 1063.48584  ANGC4=  48340.2656
 PSI= 30.00  ABR=   26.08369  ABT=  934.05835  ANGC4=  42457.1953
 PSI= 45.00  ABR=  115.19414  ABT=  729.81055  ANGC4=  33173.2031
 PSI= 60.00  ABR=  223.34811  ABT=  522.51392  ANGC4=  23750.6289
 PSI= 75.00  ABR=  317.99194  ABT=  338.27515  ANGC4=  15376.1406
 PSI= 90.00  ABR=  382.35449  ABT=  174.89513  ANGC4=   7949.7773
 PSI=105.00  ABR=  408.23291  ABT=   17.66414  ANGC4=    802.9153
 PSI=120.00  ABR=  390.55591  ABT=  152.67662  ANGC4=   6939.8438
 PSI=135.00  ABR=  326.84521  ABT=  352.25195  ANGC4=  16011.4492
 PSI=150.00  ABR=  223.74129  ABT=  574.22046  ANGC4=  26100.9297
 PSI=165.00  ABR=  108.53107  ABT=  758.14087  ANGC4=  34460.9453
 PSI=180.00  ABR=   25.34523  ABT=  812.11890  ANGC4=  36914.4922
 PSI=195.00  ABR=   10.04282  ABT=  725.25635  ANGC4=  32966.1953
 PSI=210.00  ABR=   21.44885  ABT=  586.86938  ANGC4=  26675.8789
 PSI=225.00  ABR=   66.93509  ABT=  473.47852  ANGC4=  21521.7500
 PSI=240.00  ABR=  123.59282  ABT=  404.30542  ANGC4=  18377.5156
 PSI=255.00  ABR=  187.85001  ABT=  367.24121  ANGC4=  16692.7812
 PSI=270.00  ABR=  258.87158  ABT=  338.98071  ANGC4=  15408.2109
 PSI=285.00  ABR=  332.19189  ABT=  287.84937  ANGC4=  13084.0586
 PSI=300.00  ABR=  393.04907  ABT=  171.88420  ANGC4=   7812.9180
 PSI=315.00  ABR=  412.04688  ABT=   51.94815  ANGC4=   2361.2795
 PSI=330.00  ABR=  355.70020  ABT=  390.49927  ANGC4=  17749.9648
 PSI=345.00  ABR=  223.51381  ABT=  763.05737  ANGC4=  34684.4258
 PSI=360.00  ABR=   78.10228  ABT= 1019.03760  ANGC4=  46319.8906

 STOP 0
#EXECUTION TERMINATED
#
```

```
$r -load#
#EXECUTION BEGINS
PSI=  0.0   OMEGA3=   77.15477  OMEGA4=   59.58249  OMEGA5=   11.72194  OMEGA6=   64.13559
PSI= 15.00  OMEGA3=   70.91211  OMEGA4=   11.43937  OMEGA5=    1.62034  OMEGA6=   12.40072
PSI= 30.00  OMEGA3=   60.04488  OMEGA4=   34.43288  OMEGA5=    5.51820  OMEGA6=   37.24315
PSI= 45.00  OMEGA3=   48.35762  OMEGA4=   72.36090  OMEGA5=   17.58873  OMEGA6=   77.33464
PSI= 60.00  OMEGA3=   37.67369  OMEGA4=  100.75807  OMEGA5=   37.32526  OMEGA6=  104.57988
PSI= 75.00  OMEGA3=   28.33611  OMEGA4=  120.22556  OMEGA5=   61.94992  OMEGA6=  116.82414
PSI= 90.00  OMEGA3=   19.94580  OMEGA4=  131.83229  OMEGA5=   85.05232  OMEGA6=  111.80748
PSI=105.00  OMEGA3=   11.76708  OMEGA4=  136.22058  OMEGA5=   99.76045  OMEGA6=   89.57524
PSI=120.00  OMEGA3=    2.85010  OMEGA4=  133.23869  OMEGA5=  102.43175  OMEGA6=   55.71294
PSI=135.00  OMEGA3=    7.92662  OMEGA4=  121.88768  OMEGA5=   93.70793  OMEGA6=   20.63028
PSI=150.00  OMEGA3=   21.57910  OMEGA4=  100.84671  OMEGA5=   75.13214  OMEGA6=    5.04721
PSI=165.00  OMEGA3=   38.09331  OMEGA4=   70.23698  OMEGA5=   52.17387  OMEGA6=   15.06009
PSI=180.00  OMEGA3=   55.21526  OMEGA4=   33.94196  OMEGA5=   25.01616  OMEGA6=   10.58485
PSI=195.00  OMEGA3=   69.03607  OMEGA4=    1.39512  OMEGA5=    1.02636  OMEGA6=    0.47609
PSI=210.00  OMEGA3=   76.64148  OMEGA4=   31.22417  OMEGA5=   23.01567  OMEGA6=    9.68526
PSI=225.00  OMEGA3=   77.27158  OMEGA4=   55.15891  OMEGA5=   40.91989  OMEGA6=   12.63142
PSI=240.00  OMEGA3=   71.29318  OMEGA4=   74.95238  OMEGA5=   56.27098  OMEGA6=    7.88945
PSI=255.00  OMEGA3=   59.18387  OMEGA4=   92.40475  OMEGA5=   70.46492  OMEGA6=    5.28341
PSI=270.00  OMEGA3=   41.30975  OMEGA4=  108.47533  OMEGA5=   83.68791  OMEGA6=   27.60994
PSI=285.00  OMEGA3=   18.24112  OMEGA4=  122.88058  OMEGA5=   93.92773  OMEGA6=   58.48907
PSI=300.00  OMEGA3=    8.60522  OMEGA4=  133.66330  OMEGA5=   96.31590  OMEGA6=   93.04771
PSI=315.00  OMEGA3=   36.20999  OMEGA4=  136.85542  OMEGA5=   85.15897  OMEGA6=  120.13173
PSI=330.00  OMEGA3=   59.75231  OMEGA4=  127.15422  OMEGA5=   60.46390  OMEGA6=  126.48959
PSI=345.00  OMEGA3=   74.17067  OMEGA4=  100.79544  OMEGA5=   32.06226  OMEGA6=  106.10875
PSI=360.00  OMEGA3=   77.15477  OMEGA4=   59.58275  OMEGA5=   11.72212  OMEGA6=   64.13588

STOP   0
#EXECUTION TERMINATED
#
```

```
$r -load#
#EXECUTION BEGINS
 PSI=  0.0    BETA=   23.80717  GAMA=   11.28314  XLAMB=   89.07616  UPA=    3.72884
 PSI= 15.00   BETA=   19.53186  GAMA=    9.23906  XLAMB=   89.42213  UPA=    1.52058
 PSI= 30.00   BETA=   15.76888  GAMA=    9.92623  XLAMB=   89.31837  UPA=    2.26468
 PSI= 45.00   BETA=   12.66548  GAMA=   13.03031  XLAMB=   88.69186  UPA=    5.60297
 PSI= 60.00   BETA=   10.20738  GAMA=   18.03487  XLAMB=   87.15282  UPA=   10.88072
 PSI= 75.00   BETA=    8.32220  GAMA=   24.40552  XLAMB=   84.31889  UPA=   17.30084
 PSI= 90.00   BETA=    6.94199  GAMA=   31.66185  XLAMB=   80.08264  UPA=   23.93680
 PSI=105.00   BETA=    6.03242  GAMA=   39.37505  XLAMB=   74.73526  UPA=   29.78036
 PSI=120.00   BETA=    5.60757  GAMA=   47.13141  XLAMB=   68.88387  UPA=   33.97580
 PSI=135.00   BETA=    5.74137  GAMA=   54.48360  XLAMB=   63.21619  UPA=   36.14128
 PSI=150.00   BETA=    6.57141  GAMA=   60.91283  XLAMB=   58.31439  UPA=   36.52240
 PSI=165.00   BETA=    8.27036  GAMA=   65.85439  XLAMB=   54.61446  UPA=   35.86711
 PSI=180.00   BETA=   10.94947  GAMA=   68.85065  XLAMB=   52.39787  UPA=   35.07826
 PSI=195.00   BETA=   14.53367  GAMA=   69.76382  XLAMB=   51.72549  UPA=   34.78006
 PSI=210.00   BETA=   18.74011  GAMA=   68.79901  XLAMB=   52.43596  UPA=   35.09433
 PSI=225.00   BETA=   23.18230  GAMA=   66.29965  XLAMB=   54.28391  UPA=   35.76837
 PSI=240.00   BETA=   27.46861  GAMA=   62.55725  XLAMB=   57.07643  UPA=   36.39465
 PSI=255.00   BETA=   31.23491  GAMA=   57.75487  XLAMB=   60.71075  UPA=   36.51152
 PSI=270.00   BETA=   34.14043  GAMA=   51.99402  XLAMB=   65.13399  UPA=   35.61368
 PSI=285.00   BETA=   35.86896  GAMA=   45.35529  XLAMB=   70.24570  UPA=   33.18156
 PSI=300.00   BETA=   36.15749  GAMA=   37.98087  XLAMB=   75.74832  UPA=   28.83652
 PSI=315.00   BETA=   34.86707  GAMA=   30.18243  XLAMB=   81.02036  UPA=   22.65979
 PSI=330.00   BETA=   32.08517  GAMA=   22.54541  XLAMB=   85.24081  UPA=   15.47143
 PSI=345.00   BETA=   28.19534  GAMA=   15.93368  XLAMB=   87.87656  UPA=    8.68377
 PSI=360.00   BETA=   23.80721  GAMA=   11.28320  XLAMB=   89.07616  UPA=    3.72891

 STOP    0
#EXECUTION TERMINATED
#
```

```
$r -load#
#EXECUTION BEGINS
  PSI=  0.0   ABAR=   250.01991  ABAT=    97.32770  ANGC3=  2317.32593
  PSI= 15.00  ABAR=   211.19797  ABAT=   392.19482  ANGC3=  9337.96875
  PSI= 30.00  ABAR=   151.42624  ABAT=   493.30322  ANGC3= 11745.31250
  PSI= 45.00  ABAR=    98.21529  ABAT=   476.18530  ANGC3= 11337.74219
  PSI= 50.00  ABAR=    59.61089  ABAT=   419.42163  ANGC3=  9986.22656
  PSI= 75.00  ABAR=    33.72325  ABAT=   367.99414  ANGC3=  8761.76172
  PSI= 90.00  ABAR=    16.70906  ABAT=   342.00513  ANGC3=  8142.97656
  PSI=105.00  ABAR=     5.81549  ABAT=   351.65967  ANGC3=  8372.84766
  PSI=120.00  ABAR=     0.34117  ABAT=   405.36035  ANGC3=  9651.43359
  PSI=135.00  ABAR=     2.63892  ABAT=   507.63647  ANGC3= 12086.58203
  PSI=150.00  ABAR=    19.55760  ABAT=   640.19067  ANGC3= 15242.63281
  PSI=165.00  ABAR=    60.94618  ABAT=   730.95532  ANGC3= 17403.69531
  PSI=180.00  ABAR=   128.04642  ABAT=   677.47510  ANGC3= 16130.35937
  PSI=195.00  ABAR=   200.17101  ABAT=   462.24561  ANGC3= 11005.84766
  PSI=210.00  ABAR=   246.70438  ABAT=   172.34203  ANGC3=  4103.37891
  PSI=225.00  ABAR=   250.77756  ABAT=   116.09473  ANGC3=  2764.16016
  PSI=240.00  ABAR=   213.47401  ABAT=   382.63623  ANGC3=  9110.38281
  PSI=255.00  ABAR=   147.11465  ABAT=   632.21533  ANGC3= 15052.74609
  PSI=270.00  ABAR=    71.67281  ABAT=   865.67188  ANGC3= 20611.23437
  PSI=285.00  ABAR=    13.97501  ABAT=  1062.77808  ANGC3= 25304.23828
  PSI=300.00  ABAR=     3.11009  ABAT=  1171.45801  ANGC3= 27891.85547
  PSI=315.00  ABAR=    55.06885  ABAT=  1112.63428  ANGC3= 26491.28906
  PSI=330.00  ABAR=   150.00441  ABAT=   827.58911  ANGC3= 19704.50000
  PSI=345.00  ABAR=   231.05397  ABAT=   365.21899  ANGC3=  8695.68750
  PSI=360.00  ABAR=   250.01991  ABAT=    97.32504  ANGC3=  2317.26294

  STOP    0
#EXECUTION TERMINATED
#
```

```
$r -load#
#EXECUTION BEGINS
PSI=  0.0   RT1=  0.29471 RT2=  0.22759 RT3=  0.04477 RT4=  0.24498
PSI= 15.00  RT1=  0.27086 RT2=  0.04370 RT3=  0.00619 RT4=  0.04737
PSI= 30.00  RT1=  0.22935 RT2=  0.13152 RT3=  0.02108 RT4=  0.14226
PSI= 45.00  RT1=  0.18471 RT2=  0.27640 RT3=  0.06718 RT4=  0.29540
PSI= 60.00  RT1=  0.14390 RT2=  0.38487 RT3=  0.14257 RT4=  0.39947
PSI= 75.00  RT1=  0.10824 RT2=  0.45923 RT3=  0.23663 RT4=  0.44624
PSI= 90.00  RT1=  0.07619 RT2=  0.50356 RT3=  0.32488 RT4=  0.42707
PSI=105.00  RT1=  0.04495 RT2=  0.52032 RT3=  0.38106 RT4=  0.34215
PSI=120.00  RT1=  0.01089 RT2=  0.50893 RT3=  0.39126 RT4=  0.21281
PSI=135.00  RT1=  0.03028 RT2=  0.46558 RT3=  0.35794 RT4=  0.07880
PSI=150.00  RT1=  0.08243 RT2=  0.38521 RT3=  0.29080 RT4=  0.01928
PSI=165.00  RT1=  0.14551 RT2=  0.26829 RT3=  0.19929 RT4=  0.05753
PSI=180.00  RT1=  0.21091 RT2=  0.12965 RT3=  0.09555 RT4=  0.04043
PSI=195.00  RT1=  0.26370 RT2=  0.00533 RT3=  0.00392 RT4=  0.00182
PSI=210.00  RT1=  0.29275 RT2=  0.11927 RT3=  0.08791 RT4=  0.03700
PSI=225.00  RT1=  0.29516 RT2=  0.21069 RT3=  0.15630 RT4=  0.04825
PSI=240.00  RT1=  0.27232 RT2=  0.28630 RT3=  0.21494 RT4=  0.03014
PSI=255.00  RT1=  0.22607 RT2=  0.35296 RT3=  0.26916 RT4=  0.02018
PSI=270.00  RT1=  0.15779 RT2=  0.41435 RT3=  0.31966 RT4=  0.10546
PSI=285.00  RT1=  0.06968 RT2=  0.46037 RT3=  0.35878 RT4=  0.22341
PSI=300.00  RT1=  0.03287 RT2=  0.51056 RT3=  0.36790 RT4=  0.35542
PSI=315.00  RT1=  0.13831 RT2=  0.52275 RT3=  0.32528 RT4=  0.45887
PSI=330.00  RT1=  0.22828 RT2=  0.48569 RT3=  0.23096 RT4=  0.48316
PSI=345.00  RT1=  0.28331 RT2=  0.38501 RT3=  0.12247 RT4=  0.40531
PSI=360.00  RT1=  0.29471 RT2=  0.22759 RT3=  0.04478 RT4=  0.24498

 STOP  0
#EXECUTION TERMINATED
#
```

```
$r -load#
#EXECUTION BEGINS
 PSI=  0.0   CAL=  62.47589  YUM=  87.19501
 PSI= 15.00  CAL=  64.70712  YUM=  89.05725
 PSI= 30.00  CAL=  69.15730  YUM=  88.41690
 PSI= 45.00  CAL=  75.36473  YUM=  85.70515
 PSI= 60.00  CAL=  82.82741  YUM=  81.96642
 PSI= 75.00  CAL=  91.08324  YUM=  78.38023
 PSI= 90.00  CAL=  99.71982  YUM=  75.98050
 PSI=105.00  CAL= 108.34259  YUM=  75.48434
 PSI=120.00  CAL= 116.52379  YUM=  77.14032
 PSI=135.00  CAL= 123.74220  YUM=  80.64250
 PSI=150.00  CAL= 129.34137  YUM=  85.16316
 PSI=165.00  CAL= 132.58397  YUM=  89.51842
 PSI=180.00  CAL= 132.90115  YUM=  92.52380
 PSI=195.00  CAL= 130.23012  YUM=  93.49442
 PSI=210.00  CAL= 125.05884  YUM=  92.46967
 PSI=225.00  CAL= 118.11729  YUM=  89.94768
 PSI=240.00  CAL= 110.08859  YUM=  86.52887
 PSI=255.00  CAL= 101.51993  YUM=  82.77768
 PSI=270.00  CAL=  92.85352  YUM=  79.25232
 PSI=285.00  CAL=  84.48627  YUM=  76.57269
 PSI=300.00  CAL=  76.82329  YUM=  75.41512
 PSI=315.00  CAL=  70.31531  YUM=  76.31981
 PSI=330.00  CAL=  65.46014  YUM=  79.28772
 PSI=345.00  CAL=  62.73824  YUM=  83.43967
 PSI=360.00  CAL=  62.47589  YUM=  87.19490

  STOP   0
#EXECUTION TERMINATED
#
```

```
$r -load#
#EXECUTION BEGINS
 PSI=  0.0    EN2=  0.63114  EN3=  0.07722  EN4=  0.17382  EN5=  0.00052  EN6=  0.04663
 PSI= 15.00   EN2=  0.02369  EN3=  0.00285  EN4=  0.14683  EN5=  0.00001  EN6=  0.00174
 PSI= 30.00   EN2=  0.21282  EN3=  0.02579  EN4=  0.10528  EN5=  0.00011  EN6=  0.01573
 PSI= 45.00   EN2=  0.01765  EN3=  0.11389  EN4=  0.06828  EN5=  0.00116  EN6=  0.06780
 PSI= 60.00   EN2=  1.67812  EN3=  0.22082  EN4=  0.04144  EN5=  0.00522  EN6=  0.12399
 PSI= 75.00   EN2=  2.09408  EN3=  0.31439  EN4=  0.02345  EN5=  0.01439  EN6=  0.15473
 PSI= 90.00   EN2=  1.91809  EN3=  0.37803  EN4=  0.01162  EN5=  0.02713  EN6=  0.14172
 PSI=105.00   EN2=  1.23113  EN3=  0.40361  EN4=  0.00404  EN5=  0.03732  EN6=  0.09096
 PSI=120.00   EN2=  0.47625  EN3=  0.38614  EN4=  0.00024  EN5=  0.03935  EN6=  0.03519
 PSI=135.00   EN2=  0.06530  EN3=  0.32315  EN4=  0.00183  EN5=  0.03293  EN6=  0.00483
 PSI=150.00   EN2=  0.00391  EN3=  0.22121  EN4=  0.01360  EN5=  0.02174  EN6=  0.00029
 PSI=165.00   EN2=  0.03480  EN3=  0.10730  EN4=  0.04237  EN5=  0.01021  EN6=  0.00257
 PSI=180.00   EN2=  0.01719  EN3=  0.02506  EN4=  0.08902  EN5=  0.00235  EN6=  0.00127
 PSI=195.00   EN2=  0.00003  EN3=  0.00004  EN4=  0.13917  EN5=  0.00000  EN6=  0.00000
 PSI=210.00   EN2=  0.01439  EN3=  0.02121  EN4=  0.17152  EN5=  0.00199  EN6=  0.00106
 PSI=225.00   EN2=  0.02448  EN3=  0.06618  EN4=  0.17435  EN5=  0.00628  EN6=  0.00181
 PSI=240.00   EN2=  0.00955  EN3=  0.12219  EN4=  0.14842  EN5=  0.01187  EN6=  0.00071
 PSI=255.00   EN2=  0.00428  EN3=  0.18572  EN4=  0.10228  EN5=  0.01862  EN6=  0.00032
 PSI=270.00   EN2=  0.11697  EN3=  0.25594  EN4=  0.04983  EN5=  0.02626  EN6=  0.00864
 PSI=285.00   EN2=  0.52490  EN3=  0.32843  EN4=  0.00972  EN5=  0.03308  EN6=  0.03878
 PSI=300.00   EN2=  1.32843  EN3=  0.38860  EN4=  0.00216  EN5=  0.03479  EN6=  0.09815
 PSI=315.00   EN2=  2.21433  EN3=  0.40738  EN4=  0.03829  EN5=  0.02720  EN6=  0.16361
 PSI=330.00   EN2=  2.45492  EN3=  0.35167  EN4=  0.10429  EN5=  0.01371  EN6=  0.18139
 PSI=345.00   EN2=  1.72755  EN3=  0.22098  EN4=  0.16064  EN5=  0.00385  EN6=  0.12764
 PSI=360.00   EN2=  0.63115  EN3=  0.07722  EN4=  0.17382  EN5=  0.00052  EN6=  0.04663

 STOP   0
#EXECUTION TERMINATED
#
```

PSI=100.00	ANGC5= 8404.0859	ANGC6= 29679.0898
PSI=105.00	ANGC5= 7725.5664	ANGC6= 30552.1367
PSI=110.00	ANGC5= 4716.9102	ANGC6= 32998.2891
PSI=115.00	ANGC5= 570.8191	ANGC6= 35337.5703
PSI=120.00	ANGC5= 3399.4050	ANGC6= 36402.3164
PSI=125.00	ANGC5= 7103.8398	ANGC6= 36154.7969
PSI=130.00	ANGC5= 10499.7617	ANGC6= 34627.6484
PSI=135.00	ANGC5= 13583.8047	ANGC6= 31914.9766
PSI=140.00	ANGC5= 16376.4375	ANGC6= 28162.4375
PSI=145.00	ANGC5= 18903.6211	ANGC6= 23560.4102
PSI=150.00	ANGC5= 21179.1641	ANGC6= 18341.4648
PSI=155.00	ANGC5= 23190.9766	ANGC6= 12778.9258
PSI=160.00	ANGC5= 24895.7266	ANGC6= 7181.9648
PSI=165.00	ANGC5= 26225.2812	ANGC6= 1878.9473
PSI=170.00	ANGC5= 27103.6836	ANGC6= 2812.0103
PSI=175.00	ANGC5= 27472.2773	ANGC6= 6624.3242
PSI=180.00	ANGC5= 27312.6680	ANGC6= 9381.9844
PSI=185.00	ANGC5= 26659.8672	ANGC6= 11023.2734
PSI=190.00	ANGC5= 25599.7187	ANGC6= 11598.8555
PSI=195.00	ANGC5= 24252.6758	ANGC6= 11246.2266
PSI=200.00	ANGC5= 22750.9687	ANGC6= 10149.5859
PSI=205.00	ANGC5= 21217.8398	ANGC6= 8501.1797
PSI=210.00	ANGC5= 19753.2148	ANGC6= 6471.5508
PSI=215.00	ANGC5= 18427.9344	ANGC6= 4194.1914
PSI=220.00	ANGC5= 17284.4297	ANGC6= 1761.2251
PSI=225.00	ANGC5= 16340.0703	ANGC6= 772.7747
PSI=230.00	ANGC5= 15592.9727	ANGC6= 3382.5974
PSI=235.00	ANGC5= 15026.1367	ANGC6= 6063.8789
PSI=240.00	ANGC5= 14610.4844	ANGC6= 8824.2969
PSI=245.00	ANGC5= 14306.7070	ANGC6= 11674.8555
PSI=250.00	ANGC5= 14065.1602	ANGC6= 14622.7773
PSI=255.00	ANGC5= 13824.9648	ANGC6= 17663.1836
PSI=260.00	ANGC5= 13512.2383	ANGC6= 20771.6406
PSI=265.00	ANGC5= 13038.9766	ANGC6= 23895.0312
PSI=270.00	ANGC5= 12302.3437	ANGC6= 26943.4922
PSI=275.00	ANGC5= 11187.1211	ANGC6= 29782.2852
PSI=280.00	ANGC5= 9571.8594	ANGC6= 32228.7227
PSI=285.00	ANGC5= 7341.4023	ANGC6= 34053.2695
PSI=290.00	ANGC5= 4406.6641	ANGC6= 34991.8437
PSI=295.00	ANGC5= 731.1526	ANGC6= 34769.5898
PSI=300.00	ANGC5= 3639.1833	ANGC6= 33137.8516

ECUTION BEGINS

PSI= 0.0	ANGC5= 14550.5508	ANGC6= 49035.0078
PSI= 5.00	ANGC5= 11149.7656	ANGC6= 51542.2617
PSI= 10.00	ANGC5= 8582.5352	ANGC6= 52615.8672
PSI= 15.00	ANGC5= 7050.7656	ANGC6= 52376.9297
PSI= 20.00	ANGC5= 6610.4141	ANGC6= 51001.2930
PSI= 25.00	ANGC5= 7193.0391	ANGC6= 48696.9492
PSI= 30.00	ANGC5= 8639.7617	ANGC6= 45676.2812
PSI= 35.00	ANGC5= 10738.0430	ANGC6= 42130.8086
PSI= 40.00	ANGC5= 13253.2461	ANGC6= 38212.3164
PSI= 45.00	ANGC5= 15950.9414	ANGC6= 34022.2773
PSI= 50.00	ANGC5= 18609.9141	ANGC6= 29611.8633
PSI= 55.00	ANGC5= 21028.6055	ANGC6= 24989.5000
PSI= 60.00	ANGC5= 23027.4336	ANGC6= 20135.0430
PSI= 65.00	ANGC5= 24451.2617	ANGC6= 15017.2344
PSI= 70.00	ANGC5= 25173.1367	ANGC6= 9613.4531
PSI= 75.00	ANGC5= 25100.6758	ANGC6= 3928.9604
PSI= 80.00	ANGC5= 24184.6523	ANGC6= 1985.9404
PSI= 85.00	ANGC5= 22427.2539	ANGC6= 8025.3125
PSI= 90.00	ANGC5= 19886.4141	ANGC6= 14024.6562
PSI= 95.00	ANGC5= 16675.1250	ANGC6= 19768.5547

PSI=305.00	ANGC5= 15547.9492	ANGC6= 22230.7344
PSI=310.00	ANGC5= 15916.3242	ANGC6= 22324.8750
PSI=315.00	ANGC5= 18780.2305	ANGC6= 18627.5742
PSI=320.00	ANGC5= 23264.2109	ANGC6= 10882.9844
PSI=325.00	ANGC5= 26729.4219	ANGC6= 2192.7832
PSI=330.00	ANGC5= 28813.2148	ANGC6= 6985.7969
PSI=335.00	ANGC5= 29313.0391	ANGC6= 16171.3867
PSI=340.00	ANGC5= 28231.9844	ANGC6= 24911.3008
PSI=345.00	ANGC5= 25783.6562	ANGC6= 32820.3242
PSI=350.00	ANGC5= 22355.2500	ANGC6= 39600.0234
PSI=355.00	ANGC5= 18439.1484	ANGC6= 45043.8945
PSI=360.00	ANGC5= 14550.6797	ANGC6= 49034.9375

Appendix A3

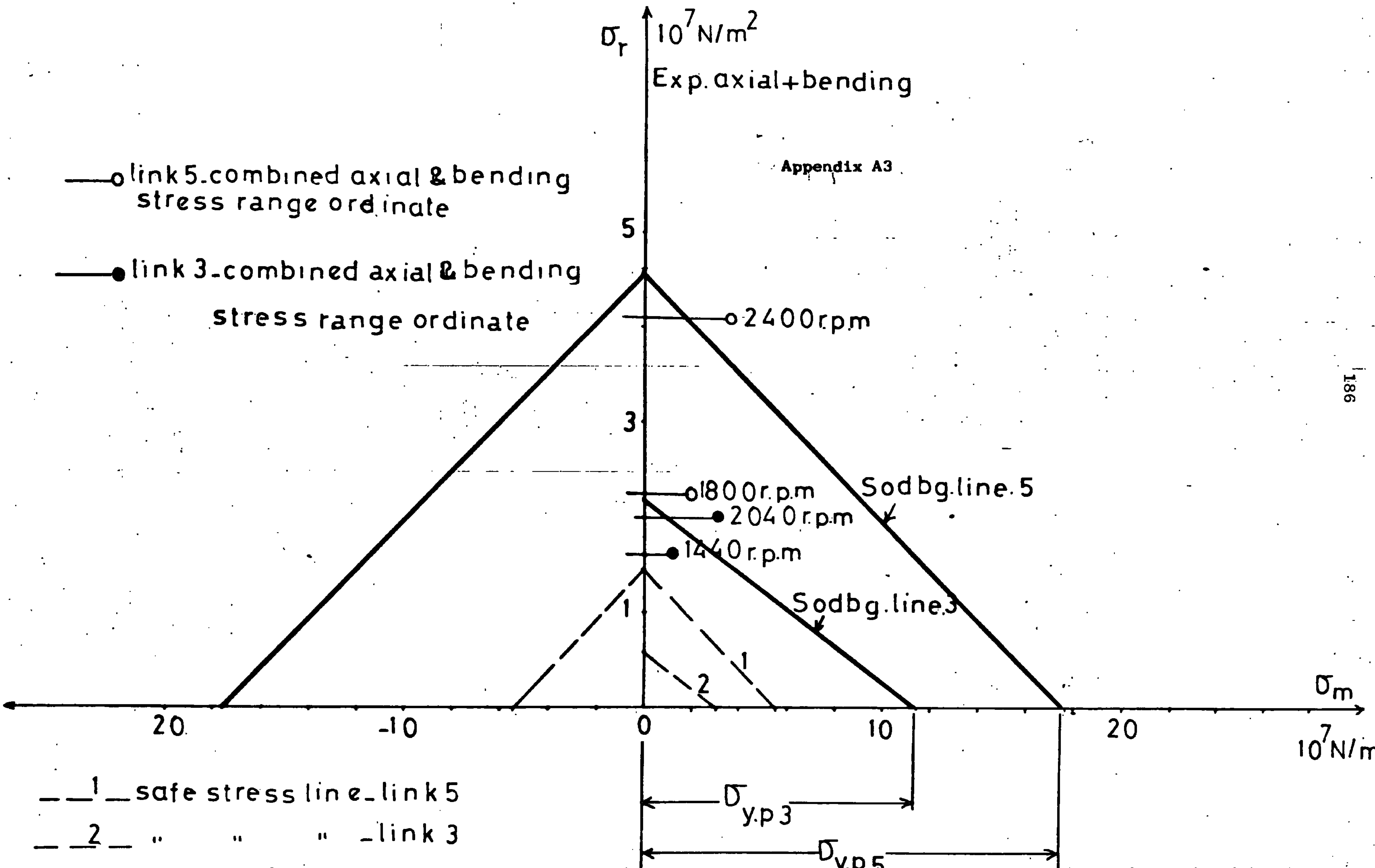
σr 10^7 N/m^2
Exp. axial+bending
link 5-combined axial & bending stress range ordinate
link 3-combined axial & bending stress range ordinate
5
3
1
2400 r.p.m
1800 r.p.m
2040 r.p.m
1440 r.p.m
Sodbg.line.5
Sodbg.line.3
1
2
σm
10^7 N/m
20
-10
0
10
20
σy.p 3
σy.p 5
1 safe stress line-link 5
2 " " " -link 3

REFERENCES

(1) Chen, F.Y. An analytical method for synthesizing the four-bar crank-rocker mechanism. Journal of Engineering for Industry, Trans. ASME February 1969. p. 45-54

(2) Lord, P.R. and Mohamed, M.H. An analysis of the picking mechanism of a textile loom. Journal of Engineering for Industry, Trans. ASME. May 1975. p. 385-390

(3) Bevan, T. The Theory of Machines. Longmans, Green & Co. Ltd., 1964

(4) Conte, F.L., George, G.R., Mayne, R.W., and Sadler, J.P. Optimum Mechanism Design combining Kinematic and Dynamic-Force considerations. Journal of Engineering for Industry, Trans. ASME. May 1975, p. 662-670

(5) Spotts, M.F. Design of Machine Elements (4th Edition). Prentice-Hall Inc. Englewood Cliffs, N.J., U.S.A. 1971

(6) Dove, R.C. and Adams, P.H. Experimental Stress Analysis and Motion Measurement. Charles E. Merill Books. Inc., Ohio, U.S.A. 1964

(7) Marin, J. Mechanical Behaviour of Engineering Materials. Prentice-Hall Inc., Englewood Cliffs, N.J., U.S.A. 1962

(8) Green, W.G. Theory of Machines (2nd Edition) Blackie & Son Ltd., 1962

(9) Shigley, J.E. Theory of Machines (International Student Ed.) McGraw-Hill Book Co. Inc. 1961

(10) Tepper, F.R. and Lowen, G.G. Shaking Force Optimisation of Four-bar Linkage with Adjustable Constraints on Ground Bearing Forces. Journal of Engineering for Industry, Trans. ASME. May 1975, p 643-651

(11.) Wojcik, C.K. Synthesis of Four-bar Linkage Function generators by means of Equations of Motion. Journal of Engineering for Industry. Trans. ASME. May 1965. p. 170-176

(12) Maxwell, R.L. Kinematics and Dynamics of Machinery. Prentice Hall, Inc. Englewood Cliffs, N.J., U.S.A. 1960

(13) Prentis, J.M. Dynamics of Mechanical Systems. Longman Group Ltd., Great Britain 1970

(14) Morrison, J.L.M. and Crossland, B. An introduction to the Mechanics of Machines. Longman Group Ltd., Great Britain. 1970

(15) Alexander, R.M. and Lawrence, K.L. Experimentally Determined Dynamic Strains in an Elastic Mechanism. Journal of Engineering for Industry, Trans. ASME 1974. Paper No. 74 - DET - 33

(16) Dubowsky, S., and Young, S.C. An Experimental and Analytical Study of Connection Forces in High-Speed Mechanisms. Journal of Engineering for Industry, Trans. ASME 1974. Paper No. 74 - DET - 72

(17) Singer, F.L. Strength of Materials (Second Edition). Harper and Row, Publishers. 1962

(18) Roark, R.J. Formulas for Stress and Strain. (Fourth Edition) McGraw-Hill Book Company 1965

(19) Holister, G.S. Experimental Stress Analysis. Cambridge University Press. 1967.

(20) Heywood, R.B. Designing Against Fatigue. Chapman and Hall Ltd., 1962

(21) Holowenko, A.R. Dynamics of Machinery. John Wiley & Sons. Inc. 1963

(22) Hinkle, R.T. Kinematics of Machines. Prentice-Hall, Inc. Englewood Cliffs, N.J., U.S.A. 1953

(23) Rayevskii, N.P. The Measurement of Mechanical Parameters in Machines. Pergamon Press. Ltd., 1965

(24) Greenwood, J.M. Stresses in the Reed and Weft Needle Arm of a Weaving Loom. Final Year Honours Project. May 1974. University of Durham. Department of Engineering Science.

(25) Imam, I., and Sandor, G.N. High-Speed Mechanicsm Design - A General Analytical Approach. Journal of Engineering for Industry. Trans. ASME. May 1975. Paper No. 74 - DET - 50

(26) Faires, V.M. Design of Machine Elements (4th Edition). Macmillan Co. 1962, U.S.A.

$n = 2500 rpm$
$\omega_2 = 261.66\ rad/sec$
$V_A = 2.87 m/s$
$V_C = V_B = 0.62 m/s$
$V_{BA} = 3.08 m/s$

$\omega_3 = \frac{V_{BA}}{BA} = 73.33\ rad/sec$
$\omega_4 = \frac{V_B}{BO_2} = 28.18\ rad/sec$
$V_D = 0.46 m/s$
$V_{DC} = 0.4 m/s$
$\omega_5 = \frac{0.4}{0.029} = 13.79\ rad/sec$

$A_A^t = 0$
$A_A^r = 753.12 m/s^2$
$A_{BA}^r = \omega_3^2 (AB) = 225.84 m/s^2$
$A_B^r = A_C^r = \omega_4^2 (BO_2) = 17.47 m/s^2$
$A_C^t = \alpha_4 (CO_2) = A_B^t = 1072.5 m/s^2$
[illegible]

$\alpha_3 = \frac{a_{BA}^t}{AB} = 7500\ rad/sec^2$
$\alpha_4 = \frac{a_B^t}{BO_2} = \frac{1072.5}{0.022} = 48750\ rad/sec^2$
$\alpha_5 = \frac{a_{DC}^t}{DC} = 8431.03\ rad/sec^2$